UNIVERSITÀ
DEGLI STUDI
FIRENZE

DOTTORATO DI RICERCA TOSCANO IN NEUROSCIENZE

CICLO XXXIII

COORDINATORE Prof.ssa Felicita Pedata

Non-invasive brain stimulation in Humans: from Image-guided targeting to clinical application

Settore Scientifico Disciplinare BIO/09

Dottorando
Dott. Mencarelli Lucia

Tutore
Prof. Rossi Simone

Coordinatore
Prof. Pedata Felicita

Anni 2017/2020

Ai miei nonni

Contents

SUMMARY

I started my Ph.D. in Neuroscience because I was fascinated by the possibility of modulating the brain activity through Non-Invasive Brain Stimulation (NIBS) techniques. My purpose was to help neurological and psychiatric patients to improve their symptoms and/or their cognitive deficits by using NIBS. Although I was really excited, I suddenly understood that it would have been a difficult and challenging path. NIBS techniques are complex, and their complete mechanisms of action are still not so clear. Moreover, before NIBS can be used clinically as a therapeutic tool, there are a lot of mechanisms and details that need to be understood and then gathered like a puzzle. This thesis should be considered as a journey, geographically begun in Siena 3 years ago and concluded in Boston, whereas scientifically it started reviewing the literature of NIBS, passed through the conceptualization of theoretical models, and ended with the application of these models in healthy subjects and patients with Alzheimer disorder. In particular, the project I have pursued during these three years aimed to investigate new approaches leveraging the combination of NIBS and neuroimaging techniques. In order to improve the safety and the applicability of these methods and obtain successful results in the field of clinical and experimental research, it has been crucial to adopt a multimodal way of thinking. Consequently, we have tried to highlight the potential of multimodal neuroimaging to personalize NIBS protocols through the research I am going to present in this thesis. I said “we” because obviously I would have never been able to pursue these goals and results without the help of my mentors (prof. Simone Rossi and Emiliano Santarnecchi) and all my colleagues.

This thesis is only a modest contribution to the current knowledge about the multimodal integration of neuroimaging and NIBS. Even though every chapter could be considered as an independent achievement, with its own introduction and discussion, they all share the same theoretical assumptions. For this reason, I decided to include a brief review of the literature about NIBS and neuroimaging techniques, as well as their integration, in Chapters 1 and 2, respectively. Since it is not possible to cover all the aspects in a Ph.D. thesis, I focused on the techniques used in the studies I have performed and described in the following chapters, i.e., Transcranial Magnetic Stimulation (TMS) and transcranial Electrical Stimulation (tES). Accordingly, in the first chapter, an overview of the technical aspects, the main protocols as well as the application in cognitive and clinical domains of these brain stimulation methods is provided. Moreover, an entire paragraph is

dedicated to the description of biophysical modeling, as an innovative tool useful not only for understanding the electric field (E-field) orientation and thus predicting the stimulation effects, but also to guide targeting of tES protocols. Modeling approaches for tES have matured over the last few years, now offering the possibility of generating subject-specific models of the E-field distribution in the brain for any electrode montage. Furthermore, optimization-based montage designs can be ideally suited to target single brain regions as well as brain networks, and the target maps can be produced based on functional data. This would allow the simultaneous stimulation of different brain areas belonging to the same or different networks, imitating a more natural cortical activation and thus offering a more efficient stimulation. For this reason, in the second Chapter the technical aspects of neuroimaging techniques (Magnetic Resonance Imaging (MRI) and Electroencephalography (EEG)) are described, focusing on Brain Networks. During the mid-2000s, neuroimaging analysis shifted from a focus on regional contributions to brain function to a broader network-level attention. With respect to this network-level approach, some studies showed that co-fluctuations during the resting-state largely reiterate patterns of activation during a task. Consequently, resting-state fMRI (rs-fMRI) has been implemented to delineate a whole-brain network's view of the brain's control architecture. Rs-fMRI allows the study of spontaneous fluctuations in the blood oxygen level-dependent (BOLD) signal in the absence of any explicit input or output, while subjects simply rest in the scanner. Finally, exemplifications of how neuroimaging techniques have been used in literature to predict and study the effects of NIBS are reported.

After the theoretical background, the remaining chapters (3rd, 4th, and 5th) explore the topic of the dissertation. In the third chapter, three different meta-analytic studies showing the neural substrate of a cognitive task (n-back task) in healthy controls and pathological conditions (studies 1 and 2 respectively), as well as the neural alteration in Disorder of Consciousness (DoC; study 3) are presented. These studies are three meta-analysis with the aim of showing different examples of neuroimaging and NIBS integration: at the end of each study, tES protocols using biophysical modeling based on the resulting fMRI maps are provided. In such a way, imaging-guided tES approaches, able to modulate not only the direct target region but the entire cortex taking advantage of network-to-network functional connectivity, are proposed. By mapping the functional network associated with a specific function, and by computing the corresponding multi-channels tES montages, these approaches also provide the spatial characteristics of the stimulation protocol able to modulate a specific cognitive function in healthy and clinical cohorts.

Considering all these advantages, the STUDY 1 aimed at investigating the neural correlates of one of the most studied cognitive function in Neuroscience, i.e., Working Memory (WM), as well as defining tES protocols based on its functional network. Nowadays, a lot of studies investigated the possibility to enhance WM performance in both healthy and clinical cohorts through NIBS. However, the broad literature in the field reported heterogeneous results caused by several factors as the different tasks used or the tES stimulation target selected. Most of these studies have indeed used the traditional two-electrodes montage targeting the right and left dorsolateral prefrontal cortex (dlPFC). Nevertheless, brain regions do not operate in isolation but interact with other regions through networks, which become the natural target of neuromodulatory interventions. In this study, we present a quantitative meta-analysis focusing on the underlying neural substrates upon which the n-back, one of the most commonly used task for WM assessment, is believed to rely on as highlighted by functional magnetic resonance imaging (fMRI) and positron emission tomography (PET) studies. Through the Activation Likelihood Estimate (ALE) statistical framework a set of task-specific activation maps, according to n-back difficulty, are generated. Our results confirm the known involvement of fronto-parietal areas across different types of n-back tasks, as well as the recruitment of subcortical structures, the cerebellum, and precuneus. Specific activations maps for four stimuli types, six presentation modalities, three WM loads, and their combination are provided and discussed, as well as the similarity between the n-back nodes and RSNs. Finally, based on the topography of the functional network associated to the n-back task, biophysical modeling of potential brain stimulation solutions suggests feasible targets for WM neuromodulation in healthy subjects.

WM deficits are present in several neurological, psychiatric, and neurodevelopmental disorders, thus making the full understanding of its neural correlates also in the clinical cohort a key aspect for the implementation of cognitive training interventions. The stimulation solutions suggested for healthy subjects may not be effective if used in patients with WM deficits. Therefore, in STUDY 2, we present a quantitative meta-analysis with the aim of investigating the neural activation during the n-back in patients with schizophrenia, depressive disorder, bipolar disorder, and Attention Deficit Hyperactivity Disorder (ADHD), highlighting similarities and differences in WM processing between patients and healthy controls and suggesting possible cognitive interventions aimed at reestablishing WM capacity in patients. Results indicate different brain activation patterns for each pathology compared to healthy controls, in the context of an overall less extensive activation in nodes of the fronto-parietal network as well as lack of activation in the subcortical, right

temporal lobe, and cerebellum areas. In particular, both bipolar and depressive disorder do not show activation in the bilateral dlPFC, and their parietal activation patterns are lateralized respectively on the left and right hemispheres. On the other hand, patients with ADHD show a lack of activation on the left parietal lobe, whereas schizophrenic patients show lower activity on the left prefrontal cortex. Implications for the design of cognitive enhancement interventions are discussed, including the definition of possible targets for non-invasive brain stimulation using imaging-guided biophysical modeling.

As widely discussed in the first chapter of this thesis, mapping the functional network associated with a specific cognitive function is not the only way to lead biophysical modeling. For example, by using rs-fcMRI seed as maps the information about the links between cortical and subcortical regions are provided, as well as information on how focal brain stimulation will propagate through networks, highlighting the perfect targets for stimulation (Fox, Buckner, et al., 2012; Fox, Halko, et al., 2012; Fox & Greicius, 2010). Such applications may be of interest for multiple pathologies usually characterized by network connectivity alteration, such as stroke, epilepsy, Parkinson's and Alzheimer's disease, and, as shown in STUDY 3, also for minimally conscious\vegetative state. Disorder of consciousness (DoC) refers to a group of clinical conditions that may emerge after brain injury, characterized by a varying degree of decrease in the level of consciousness that can last from days to years. An understanding of its neural correlates is crucial for the conceptualization and application of effective therapeutic interventions. In this study, we propose a quantitative meta-analysis with the aim of showing the neural substrate of DoC emerging from functional magnetic resonance (fMRI) and positron emission tomography (PET) studies. The relevant networks of resulting areas are mapped, allowing us to highlight similarities with RSNs and hypothesize potential therapeutic solutions leveraging network-targeted noninvasive brain stimulation. Results show that task-related activity is limited to temporal regions resembling the auditory cortex, whereas resting-state data reveal a diffuse decreased activation affecting two subgroups of cortical (angular gyrus, middle frontal gyrus) and subcortical (thalamus, cingulate cortex, caudate nucleus) regions. Clustering of their cortical functional connectivity projections identifies two main altered functional networks, related to decreased activity of (i) the Default Mode and Frontoparietal network, as well as (ii) Anterior Salience and Visual/Auditory networks. Based on the strength and topography of their connectivity profile, biophysical modeling of potential brain stimulation solutions suggests the first network as the most feasible target for neuromodulation in DoC patients.

Based on the meta-analytic studies conducted and described in the Third Chapter, it is clear the importance of using brain networks as target for neuromodulation instead of a single region. The possibility to noninvasively interact and selectively modulate the activity of networks would open to relevant applications in Neuroscience. Nowadays, the network neuromodulation approach has been investigated in few studies, confirming its feasibility, safety, and success from a physiological point of view, but no one has demonstrated their effects at the neuroimaging level so far. Therefore, in the fourth Chapter of this thesis, we propose a study showing for the first time the impact of network-targeted multichannel tDCS on intrinsic and network-to-network functional connectivity (STUDY 4). A novel approach for multichannel, network-targeted transcranial direct current stimulation (net-tDCS), optimized to increase the excitability of the sensorimotor network (SMN) while inducing cathodal modulation over prefrontal and parietal brain regions negatively correlated with the SMN, is tested. Using an MRI-compatible device, twenty healthy participants have received real and sham tDCS while at rest in the MRI scanner. Changes in functional connectivity (FC) during and after stimulation are evaluated, looking at intrinsic FC of the SMN and at the strength of negative connectivity between SMN and the rest of the brain. Standard, bifocal tDCS targeting left motor cortex (~C3) and right frontopolar (~Fp2) regions are tested as a control condition in a separate sample of healthy subjects to investigate the network-specificity of multichannel stimulation effects. Net- tDCS induce greater FC increase over the SMN compared to bifocal tDCS, during and after stimulation. Furthermore, analysis of the impact of net-tDCS on anticorrelated functional networks show an increase in the negative connectivity between SMN and prefrontal/parietal areas targeted by cathodal stimulation during/after real net-tDCS. Results suggest preliminary evidence of the possibility of manipulating distributed network connectivity patterns through net-tDCS, with potential relevance for the development of cognitive enhancement and therapeutic solutions.

Finally, during my experience abroad at Berenson Allen Center for Non-Invasive Brain Stimulation (Harvard Medical School - Boston), I had the opportunity to actively participate in a study aimed to investigate the feasibility and safety of multi-focal transcranial alternating current stimulation (tACS) delivered at 40 Hz for ten 1-hour-long sessions in patients with mild to moderate Alzheimer's disease (AD) (STUDY 5). In this case, we use modern approaches for multi-focal stimulation and combine T1-weighted MRI and amyloid-beta (Aβ) PET images to optimize the tACS intervention, targeting regions with maximal Aß burden. We decided to use the tACS instead of the heretofore used tDCS, based on the previous studies on animal model demonstrating the

decrease of amyloid-β plaques after the induction of gamma frequency through sensory stimulation or optogenetics (Iaccarino et al., 2016; Rajji, 2019). The induction of gamma oscillations also decreases inflammatory brain processes and leads to microglia-mediated clearance of Aß and tau depositions, with consequential cognitive benefits (Adaikkan et al., 2019; Iaccarino et al., 2016). Although these methods are limited to animal use, there is emerging evidence that gamma oscillations can be safely and noninvasively modulated by tACS, thus suggesting gamma-tACS as a potential therapeutic intervention for AD. Fifteen patients are assigned to three groups (n=5/per group): (i) 10 one-hour daily sessions of individualized tACS, primarily targeting frontal and temporal lobe areas, (ii) 10 or (iii) 20 one-hour sessions of bi-hemispheric temporal lobe tACS. EEG changes, global cognition, safety, and adverse effects are monitored/recorded daily. All patients have completed the study with no serious adverse events. Despite this is an ongoing study, and here a small sample size is presented, interesting results are reported. In particular, a cumulative increase in gamma power throughout tACS intervention in the regions predicted by biophysical modeling is shown. Additionally, as working memory is one of the cognitive functions that have been improved in healthy individuals throw gamma stimulation, the effects of the stimulation in the event-related activity registered during the n-back task is also explored. The results show a reduction of the P200 latency in the n-back task, indicative of faster working memory processing. Further, initial signs of declarative memory improvement, measured by Craft Story Recall Delayed, are detected. These findings show that daily gamma induction is feasible, well-tolerated, and safe in AD patients. Even though this is only a preliminary, still ongoing study, the results on 40 Hz tACS spatial and frequency specificity provide important suggestions for future clinical evaluation, although require a larger cohort.

In summary, the aims of this dissertation is to: i) give an overview of the current status on brain stimulation and neuroimaging methods, emphasizing the knowledge on biophysical modeling (Chapters 1 and 2); ii) demonstrate how neuroimaging and NIBS techniques can be combined in order to personalize stimulation protocols using meta-analyses studies, stressing the employment of innovative network stimulation able to imitate a more natural cortical activation compared to the standard tES protocols, offering a more accurate stimulation (Chapter 3, studies 1, 2 and 3); iii) validate the ability of network stimulation approach in modulating the intrinsic and network-to-network functional connectivity compared to the traditional bifocal stimulation on the sensorimotor network (Chapter 4, study 4); iv) prove the safety and feasibility of personalized

multifocal stimulation to optimize the gamma-tACS intervention targeting the regions with higher Aß burden in mild to moderate AD patients (Chapter 5, study 5).

This thesis ends with an overall conclusive remark. However, I hope my journey as a scientist will not end with this dissertation. Despite this thesis represents only a small contribution to the literature, to me it is the summary of three amazing years, and I am very grateful for the opportunities I had to grow as a scientist and as a person.

CHAPTER 1

TECHNICAL ASPECTS OF NON-INVASIVE BRAIN STIMULATION

Neuromodulation has been defined as a focused and reversible cerebral stimulation method, able to alter the communication between neurons and, consequently, to modify the human behavior sustained by that neurons in healthy and clinical population. To better understand how the neuromodulation techniques are born, we have to go back to the late eighteenth century when the Italian Luigi Galvani found the link between nervous tissue and electricity for the first time. Nevertheless, the most important finding in the history that led to the invention of the current neurostimulation systems is the discovery of electromagnetic induction by Michael Faraday in 1831. Electromagnetic induction is a process in which electricity converts into magnetism and vice versa. However, the first attempts to use Faraday's principles to alter brain activity were performed later in 1896 by Arsenne d'Arsonval and in 1910 by Silvano Thompson, not without difficulties and technical problems, partially solved only years later.

Currently, brain neuromodulation involves different neurostimulation techniques able to activate parts of nervous system with the aim of improving the quality of life in humans. Even though the neurostimulation can not substitute a pharmacological treatment, indeed usually is in support of it, several studies have demonstrated that these techniques can be successfully used as a therapeutic tool in psychiatry and neurology but also in cognitive neuroscience to study the functioning of the brain. The neurostimulation techniques can be classified as invasive, for example deep brain stimulation (DBS) used only with therapeutic purposes, or non-invasive, as transcranial magnetic stimulation (TMS) or transcranial electrical stimulation (tES), used also in healthy subjects. In this Chapter, the non-invasive brain stimulation (NIBS) will be further described. The term NIBS includes different methods aimed at inducing transient changes in brain activity and, in turn, altering behavioral performance, by means of electrical currents applied on the scalp. Over the last few years, these techniques, have become of major interest in the fields of neuropsychology and neurophysiology. Recent studies have already demonstrated their efficacy in terms of modulating neural activities (Ridding & Rothwell, 2007; Rossini & Rossi, 2007; Tatti et al., 2016; Valero-Cabré et al., 2017). Their applications in the motor, perceptual and cognitive

domains allowed researchers to make consistent steps forward to a better understanding of the neural substrates underlying different cerebral processes (see Miniussi et al., 2013 for a review). The principal reason of NIBS' growing interest may be related to their capacity of transiently modulating cerebral functions, possibly even improving performance in complex cognitive tasks (Evers et al., 2001; Klimesch et al., 2003; Nitsche & Paulus, 2000; Emiliano Santarnecchi et al., 2015; Töpper et al., 1998). These techniques have been largely used to investigate the neural basis of many cognitive and sensory-motor domains, as well as potential therapeutic interventions to restore physiological brain activity in psychiatric and neurological diseases (Lefaucheur et al., 2017; Ridding & Rothwell, 2007; Rossini & Rossi, 2007; Tatti et al., 2016; Valero-Cabré et al., 2017). However, the specific mechanisms of action have yet to be discovered and this is crucial to improve the outcome of neurostimulation therapies. Technical aspects such as the frequency, intensity, pulse shape, and electrodes combination are still heterogeneous between studies. One of the most debated problem is the brain stimulation target for various disorders: the conceptional framework of manipulating cortical excitability in human subjects has been obtained mainly from the motor cortex (M1) by combining NIBS and electrophysiological techniques. However, the online effect of NIBS techniques with a high spatial resolution is still unclear over other cortical areas. Nowadays, the concurrent combination of NIBS and fMRI allows tracing of alterations within the whole brain, during ongoing or immediately after stimulation, and this will be further explored in the second chapter of this thesis.

Two main classes of NIBS are currently applied for clinical and research purposes: TMS and tES. Here, a brief description of both techniques, covering their underlying mechanisms of action and the most validated protocols, have been provided.

1.1 Transcranial Magnetic Stimulation (TMS)

Firstly introduced by Barker and colleagues in 1985 (Barker et al., 1985), TMS is a non-invasive stimulation method based on Faraday's principle of magnetic induction. Through a magnetic coil (made of loops of wire) it is possible to generate a rapidly changing magnetic field perpendicular to coil plane, that induces an electric field parallel to the inner surface of the conductor that abruptly changes the excitability of the underlying neurons, making them to fire (Hallett, 2000; Kobayashi & Pascual-Leone, 2003; Rossi et al., 2020). This stimulation is restricted to the cortex because the current fall off rapidly with the distance to the magnetic stimulator coil (Barker, A. T., 1991). However, recent studies support the idea that the TMS can modify intracortical excitability

and activate distant cortical, subcortical, and spinal structures along with specific connections, for example by stimulating cortical areas that are known to be functionally connected to the targeted region. By modifying physical and biological parameters, such as magnetic pulse waveform, coil shape, as well as orientation, intensity, frequency and pattern of stimulation, TMS can generate different strengths and forms of electrical fields. Moreover, experimental procedure (e.g., coil orientation, on-line/off-line pulses discharge, respectively during or before a task) (Thut & Pascual-Leone, 2009); subject-related variables, including state-dependency (level of neural activity during stimulation), age and eventual pharmacological treatments (Miniussi et al., 2010; Rossini et al., 2010; Silvanto & Pascual-Leone, 2008) also impact on the efficacy of TMS.

TMS can be applied by means of several protocols including single pulses (single-pulse TMS), pairs of stimuli separated by variable intervals (paired-pulse TMS), or trains of repetitive stimuli at various frequencies (repetitive TMS or rTMS). When applied as a single-pulse stimulation (spTMS), TMS can depolarize neurons and evoke measurable effects, such as motor evoked potentials (MEPs) if applied over the motor cortex, or phosphenes after stimulating the visual cortex. Paired pulse stimulation (ppTMS) is mostly used to assess cortical excitability through a combination of conditioning stimulus (CS), test stimulus (TS) and inter stimulus interval (ISI). Finally, the repetitive TMS (rTMS) could be considered as the technological evolution of spTMS and consists of train of stimuli with a specific intensity and frequency. Introduced for the first time in the mid ‘90s, contrary to spTMS and ppTMS the effects of rTMS exceed the duration of the stimulation. According to the frequency of stimulation, rTMS induces after effects on cortical excitability, mainly impacting on synaptic efficiency, that may result in an inhibitory effect when delivered at low frequency (1 Hz or less) or an excitatory one, when delivered at high frequency stimulation (≥ 5 Hz) (Rossi et al., 2009). Long Term Depression (LTD) or Long-Term Potentiation (LTP) are the synaptic mechanisms invoked to explain such lasting effects (Cooke & Bliss, 2006). Recently, a new promising paradigm of rTMS has been introduced to produce long lasting effects in neuronal activity in a shorter time of intervention (i.e., few minutes): the theta burst stimulation (TBS). This technique uses bursts of high frequency stimulation (3 pulses at 50 Hz repeated at 200 ms intervals) to induce LTP, if applied intermittently (iTBS), or LTD, if applied continuously (cTBS) (Huang et al., 2005; Di Lazzaro et al., 2008). Accordingly to the model proposed by Huang and colleagues (2011), iTBS elicits LTP-like effects by keeping short-latency facilitation effects dominant on the inhibitory ones (Huang et al., 2011); whereas cTBS enhances longer-latency inhibitory effects resulting in LTD-like effects (Suppa et al., 2016). However, the direction of the

effect of TMS, inhibitory or excitatory, might also depend on the number of stimuli and the ISI, as showed by Gamboa et al., (2010). Moreover, the mechanisms underlying cortical excitability changes induced by TBS protocols are still debated: some authors refer to the modulation of NMDA receptors (Huang et al., 2005; Di Lazzaro et al., 2008), others to GABAergic receptors (Harrington & Hammond-Tooke, 2015; Thickbroom, 2007) whereas others hypothesize a modulation of the expression of transcription factors, such as nerve-growth-factor-induced protein A (NGFI-A) (Aydin-Abidin et al., 2008). Despite the misleading information about its specific mechanism of action, a large body of placebo-controlled evidence reports cognitive improvement after high frequency rTMS in healthy young adults and in patients with psychiatric/neurological diseases (Guse et al., 2010; Lefaucheur et al., 2017; Miniussi et al., 2010), obtaining also the approvement by the Food and Drug Administration (FDA) for the treatment of migraine and depression. TMS is indeed a safe technique, when it is performed following the TMS guidelines (Rossi et al., 2020). The most serious effect is the possible induction of epileptic seizures, especially in patients that had a pre-existing neurological disorder: a pre-screening of potential risk-factors is important.

1.2 Transcranial Electrical Stimulation (tES)

Transcranial Electrical Stimulation (tES) involves a series of techniques that conducting weak electrical currents (1-2 mA) through the scalp, can modulate firing properties of cortical neurons and ongoing rhythmic brain activity (Paulus, 2011; Ruffini et al., 2013). Conversely to TMS, tES uses subthreshold electrical currents and ground their potential on the capability of shifting intrinsic neuronal excitability rather than eliciting neuronal firing (Paulus, 2011; Radman et al., 2009). In the last years, the research involving tES (and its combination with other techniques) has been focused on depicting how the brain works by altering the operating point of neural networks. From a clinical point of view, tES has been applied in fibromyalgia, major depression without drug resistance and in addictions/cravings (with probable efficacy, Level B evidence; Lefaucheur et al., 2017), but many others are being developed, including epilepsy, chronic neuropathic pain, tinnitus, major depression with drug resistance, brain cancer, and cognitive remediation in neurodegeneration (Dell'Osso & Di Lorenzo, 2020). The electrical current is usually conveyed through at least two surface electrodes of different polarities, soaked with saline water or electroconductive gel, applied to the subject's scalp and linked to a current-controlled waveform generator. Despite tES has the advantage of being portable, relatively cheap and not painful, its

application in the clinical setting is still under debate because of its poor spatial focality, mostly associated to the use of bipolar montages and big-sized sponges. However, recent development of tES allows the employment of multiple small electrodes and detailed, realistic electric field modeling generated by the montage in the individual brain. This provides useful information to customize electrode montages in order to reach higher spatial focality and to individualize research and clinical protocols, as better explained in the following paragraphs. Moreover, various tES protocols can be implemented by changing parameters such as shape, position, and numbers of electrodes, current waveform, frequency, duration of stimulation and number and timing of sessions. Furthermore, based on the waveform of the electrical current and its polarity, different non-invasive tES techniques can be applied: transcranial direct current stimulation (tDCS), transcranial alternating current stimulation (tACS) and transcranial random noise stimulation (tRNS) (Nitsche et al., 2008; Paulus, 2011; uffini et al., 2013), are deeply described in the following paragraphs.

1.2.1 Transcranial Direct Current Stimulation (tDCS)

Transcranial Direct Current Stimulation (tDCS) modulates spontaneous neuronal activity without causing a direct neuronal firing, through the application of low-amplitude (0.5-2 mA) electrical fields in the cortex (0.2-2 V/m, Ruffini et al., 2018). In particular, tDCS modifies the transmembrane neural potential and thus influences the level of excitability (Wagner et al., 2007), leading to an increase in glutamine and glutamate levels (Hunter et al., 2009) and/or decreasing γ-aminobutyric acid (GABA) concentrations (Bachtiar et al., 2015; Stagg et al., 2011). N-methyl-D-aspartate (NMDA) receptors-dependent mechanisms as well as and brain-derived neurotrophic factors (BDNF, Fritsch et al., 2010) also play a key role (Liebetanz et al., 2002; Nitsche et al., 2003). In this regard, tDCS has been often referred as a brain modulation technique instead of a brain stimulation technique. In tDCS constant currents are applied via two electrodes: an anode and a cathode. Generally, positioning the positively charged electrode (the anode) over the stimulation target causes enhancement of neural activity, whereas positioning the negatively charged electrode (the cathode) over the target reduces excitability. However, the excitatory effects might become inhibitory when the duration of stimulation is extended beyond about 20 minutes.

The first study combining tDCS with TMS investigated the modulation of primary motor cortex (M1) cortical excitability (Nitsche & Paulus, 2000), showing that tDCS induces polarity specific changes in the targeted neural population. These modifications have been observed to outlast the

stimulation time and they were even more robust offline than during current delivery. Its applicability also in cognitive domain has been proved by several studies (Brunoni et al., 2014; Galli et al., 2019; Hill et al., 2016; Miniussi et al., 2008). However, in this case the results are mixed: the use of different modality of stimulation (online or offline), different density and/or time of stimulation and distinct cognitive tasks, might be the cause of heterogeneity in results. Nevertheless, the majority of the study aimed to increase the high order cognitive functions, has used traditional two-electrode montage and has chosen dorsolateral Prefrontal Cortex (dlPFC) as stimulation target, positioning the anode over either the F3 (left dlPFC) or F4 (right dlPFC) regions on the scalp in accordance with the international 10–20 system for electrode placement (Herwig et al., 2003). For example, tDCS application on working memory (WM) has been proved in a lot of studies, with a focus mostly on dlPFC stimulation (Brunoni & Vanderhasselt, 2014; Fregni et al., 2005; Hoy et al., 2015). Despite all these studies proved the efficacy of this techniques on enhancing WM, a recent review found no statistical evidence to support strong changes in cognitive performance after a single session tDCS in healthy subjects (Horvath et al., 2015). We think this may be related to the stimulation target. Nowadays, it is well-known that brain regions do not operate in isolation but interact with other regions through networks: the relevance of considering the entire network as stimulation target, both for clinical and research purposes, is the core of this thesis and it will be deeply discussed in the following Chapters.

1.2.2 Transcranial Alternative Current Stimulation (tACS)

Differently from polarity-specific effects of tDCS, transcranial alternative current stimulation (tACS) holding the ability to directly influence cortical rhythms, represents a different approach to cognitive neuroenhancement (Santarnecchi et al., 2015). tACS can interact with ongoing brain oscillatory activity and modulate them in a frequency-specific way (Thut & Miniussi, 2009), contributing to better understand the functional meaning of cortical rhythms. The mechanisms of action of tACS have been studied through intracranial recordings in animals (Battleday et al., 2014; Fröhlich & McCormick, 2010; Krause et al., 2019; Ozen et al., 2010), supporting the idea that tACS locks endogenous oscillations to its frequency and phase, leading to an increase in power. In particular, the alternating current delivered through tACS continuously shifts between positive and negative electric fields (Tavakoli & Yun, 2017), inducing shifting in the transmembrane potential, alternating depolarizing and hyperpolarizing effects, and allowing the entrainment of intrinsic brain oscillations thanks to its sinusoidal waveform (Antal & Paulus, 2013; Paulus, 2011). In a few

words, cortical populations start to oscillate at the same natural frequency as the one delivered by tACS, with a greater amplitude as per the resonance phenomenon (Paulus, 2011). tACS can be delivered at every EEG frequency (0.1–80 Hz) and in the so called "ripple" range (140 Hz) (Moliadze et al., 2010). Superimposed polarity, frequency, phase and intensity are the major parameters defining the effects of stimulation.

Considering that several human cognitive functions show specific patterns of brain oscillatory activity, determined by the synchronous neuronal firing across different spatial and temporal scales, the engagement of oscillatory activity through tACS could lead to a greater control of brain activity and corresponding behavior. The efficacy of tACS in modulating cortical excitability as well as in improving basic higher-cognitive functions has been showed in a wide range of studies (Chaieb et al., 2011; Feurra et al., 2011, 2013, 2016; Kanai et al., 2008, 2010; Pozdniakov et al., 2019; Shpektor et al., 2017; Wach et al., 2013). At electrophysiological level, the efficacy of tACS can be evaluated through the induced changes in EEG spectral power and phase-coherence induction on stimulated areas and networks (Roh et al., 2014). Nowadays, it is still not possible to record the electrophysiological response to tACS online, due to the high signal tACS artifact on EEG, however, offline EEG-tACS paradigms recording pre- and post-stimulus EEG have been successfully applied on healthy subjects (see e.g., Castellano et al., 2017).

1.2.3 Transcranial Random Noise Stimulation (tRNS)

Transcranial random noise stimulation (tRNS) is the youngest in the tES family, developed for the first time in 2008 by Terney. He found the possibility of using a random noise stimulation to increase cortical excitability through electrical patterns produced at a random frequency over a broad spectrum (0.1–640Hz; Terney et al., 2008). By the repeated opening of sodium channels (Chaieb et al., 2015; Terney et al., 2008), this technique induces long-term potentiation of cortical plasticity. However, the effective mechanism of action of this method is still under debate and some studies hypnotized that tRNS could use stochastic resonance (Miniussi et al., 2013), according to which weak signals can be amplified by the addition of noise (McDonnell & Abbott, 2009). Considering this explanation, random noise added to subthreshold neural oscillations in the brain would result in a summation of the two currents strong enough to exceed the threshold.

As recently demonstrated, tRNS can increase or decrease the excitability at different intensity range (Moliadze et al., 2012; Moret et al., 2019), however few studies have investigated the effects of tRNS in modifying EEG response so far. Mostly of the studies available in literature

focused in analyzing the effect of tRNS on a simple motor or sensory tasks (Fertonani et al., 2010; Terney et al., 2008), or on high cognitive function, as arithmetic skills and calculation (Pasqualotto, 2016; Popescu et al., 2016; Snowball et al., 2013). In patients, tRNS has been successfully applied to decrease pain in multiple sclerosis (Palm et al., 2016) and motor cortex excitability in Parkinson's disease (Stephani et al., 2011), as well as to reduce depressive symptoms (Chan et al., 2012) and to improve negative symptoms in schizophrenia (Palm et al., 2013). Despite the propagation of studies demonstrating the effects of tRNS on cognitive functions, only few studies have examined its fundamental principle and the impact of the various stimulation parameters on results (for a comprehensive review see Krause & Cohen Kadosh, 2014), condemning it to be the least tES technique used in clinical rehabilitation.

1.3 Pros and Cons of NIBS

As summarized in the previous sections, neurostimulation techniques are increasingly considered as a treatment option for numerous neurological and psychological disorders. TES and TMS allow to better understand the brain mechanism behind cognitive functions and their non-invasiveness might be beneficial, especially from a patient's point of view. However, their efficacy as long-lasting brain enhancers is still doubtful. Some studies reported long-term enhancement (lasting up to 1 month) after single session as well as after multisessions, especially when the stimulation was coupled with training (Hsu et al., 2015; Jones et al., 2015; Zimerman et al., 2013). On the other hand, invasive stimulation techniques (as Deep Brain Stimulation (DBS), Vagus Nerve Stimulation (VNS), Electroconvulsive Therapy (ECT)) require only a single surgical procedure, and the stimulation will continue for the duration of the battery lifetime without additional interventions for the patient. Moreover, the invasive brain stimulations have higher spatial resolution compared to NIBS, but the possible side effects make these interventions still disadvantageous.

A common limitation of NIBS in both diagnostic and therapeutic approaches is the restriction of the direct effects of respective interventions to only superficial cortical targets. This might be partially overcome by network stimulation approaches. As recently pointed out by Fox and collaborators (2014), the effect of NIBS extends in the brain along the functional network that includes the target region (Fox et al., 2014). This should allow to indirectly reach deeper brain regions through NIBS and achieve similar results with invasive and non-invasive techniques. Nowadays, NIBS techniques need further exploration for both therapeutic effect and research application, more detailed knowledge about the mechanism of action may be helpful in order to

indicate the best candidate for specific types of neurostimulation. Moreover, since the concept that the brain is organized in networks is accepted in the international scientific scene, also the optimization of the stimulation protocol should follow this concept. Highly customizable interventions on the base of the subjects' specific anatomy or functional connectivity could provide higher efficacy and adaptability and could increase the number of positive outcomes. The effects of fMRI-guided NIBS protocols are discussed in this thesis in the following Chapters.

1.4 Optimization of tES Electrodes Montages

Optimizing tES electrodes montages is particularly important in predicting the stimulation effects. Nowadays, tES electrodes montages are optimized on the assumption that the effects can be directly quantified from the measurement of the electric field (E-field) on the cortex and computational models of the brain (physics of electric fields and of their interaction with complex, active neuronal networks) are crucial in the development and optimization strategies for brain stimulation. Indeed, despite the availability of invasive methods to measure the E-field (in vivo techniques), the only non-invasive method helpful to predict the E-field distribution in the brain with a high spatial resolution is numerical modeling of Maxwell's equations in conductive media. Such computational models can predict E-field distribution in the human brain with reasonable accuracy, as the availability of recent measurements in-vivo confirms (Huang et al., 2017; Opitz et al., 2016). Several modeling methods for NIBS have been developed so far using ad hoc software (e.g., the commercial finite element model (FEM) software or the Simulation of Non-invasive Brain Stimulation (SimNIBS)). Even though this methodological approach is time-consuming and can improve the protocols' generalization problem, they are regularly developed for research applications enhancing the consistency and reproducibility of tES research (Miranda et al., 2018). Ruffini and colleagues (2014), for example, developed an optimization system called Stimweaver, working with a realistic head model derived from structural MRI images (Miranda et al., 2013; Ruffini et al., 2014) to calculate the tES electric field components rapidly from arbitrary EEG 10–20 montages. This modeling approach allows for fast calculation of electric field components normal and parallel to the grey matter and white matter surfaces. Moreover, it has also been combined with optimization algorithms to guide montage designs (electrode number and their locations) using a genetic algorithm. One of the most important input needed to optimize a tES montage is the target, which can be defined from various sources, as fMRI, EEG, positron emission, tomograpy (PET) and near-infrared spectroscopy (NIRS) (Shafi et al., 2012). These brain imaging techniques

can provide information for both clinical and research applications. In order to create more accurate E-field distributions and target specific regions or networks more efficiently, these optimization algorithms can be built using multichannel montages considering many small electrodes (Ruffini et al., 2009, 2013), as shown in the 3rd and 4th chapter of this thesis. Ruffini and colleagues (2014), comparing the bifocal to the multifocal montages targeting the same regions, noted that the multi-electrode solution better account for neutral effect target areas (Ruffini et al., 2014). Through image-guided targeting, the stimulation not only modulate the directly target region, but the entire cortex taking advantages of network-to-network functional connectivity. Additionally, by mapping the functional network associated with a specific function, and by computing the corresponding multi-channels tES montages, this approach would also provide the spatial characteristics of the stimulation protocol able to modulate a specific cognitive function in healthy and clinical cohorts (three examples of this application are provided in the Chapter 3).

Furthermore, more sophisticated models that combine the physical and physiological data of the individual brain in order to create a personalized computational model and design more refined personalized optimization protocols have been developed. The use of this personalized models based on individual scans, are crucial in specific cases (e.g., the case of damaged brains or skulls). In a study conducted in our laboratory, for example, we demonstrated that transcranial electrical stimulation (tES) allows to safely and noninvasively reduce intratumoral perfusion in humans by applying individualized multi-channel tES according to personalized biophysical modeling (Sprugnoli et al., 2019). In this case, a genetic algorithm considering the individual anatomical variability and the conductivity of different tumor tissues was used to identify a stimulation solution maximizing the induced electrical field over the solid tumor mass while minimally affecting the rest of the brain (Sprugnoli et al., 2019). Future implementations of personalized biophysical models may allow the prediction of structural/ functional brain changes induced by a given therapy, and combined with the incoming patient data, “correct” the therapeutic trajectory accordingly.

1.5 Biophysical Modeling

In this section a detailed description of the biophysical modeling used in the three studies presented in Chapter 3 is provided. For a general comprehension, an example based on the tES optimized montages for stimulation of the sensorimotor network by functional connectivity analysis is presented. The realistic head model used in the studies 1, 2 and 3 was built from a

structural T1-weighted MRI of the single-subject template Colin27 (Figure 1.1- a1). The 1 mm x 1mm x 1 mm resolution image was segmented into the main head tissues classes (Figure 1.1- a2) by using free software: the white-matter (WM) and grey-matter (GM) segmentations were obtained with FreeSurfer (https://surfer.nmr.mgh.harvard.edu), whereas cerebrospinal fluid (CSF), air filled sinuses, skull and scalp masks were obtained with MARS (Huang et al., 2013). The binary masks were combined into one 3D volume (Figure 1.1- a4) using custom Matlab scripts (r2018a) with Image Processing Toolbox and Iso2Mesh (Fang & Boas, 2009), which ensured that each tissue was surrounded by at least a 1 mm layer of another tissue and generated surfaces of all the tissues (Figure 1.1- a3). Sixty-four cylinders (1 cm radius 3 mm thickness) representing gelled PISTIM Ag/AgCl electrodes were placed in the scalp positions defined by the 10/10 EEG system, upon manual identification of the four fiducials (nasion, inion, left/right preauricular point) on the T1 image. The finite element volume mesh of the full head with electrodes (Figure 1.1- a5) was created using Iso2Mesh (Fang & Boas, 2009). The mesh comprised about 4.3 million tetrahedra. The mesh was then imported into Comsol (v5.3a) (http://www.comsol.com), where the tissues were assigned appropriate isotropic conductivities for the DC-low frequency range: 0.33, 0.008, 1.79, 0.40, 0.15 and 10-5 S/m respectively for the scalp, skull, CSF, GM, WM and air (Miranda et al., 2013). The electrodes were represented as isotropic homogeneous conductive media with conductivity of 4.0 S/m. Laplace's equation was solved for the electrostatic potential (V) using Lagrange second order finite elements. As boundary condition, floating potential was imposed at the surface of the electrodes, to ensure a constant current injection.

The E-field was obtained by taking the negative gradient of the potential. The E-field normal to the GM surface (En) was calculated for all the bipolar montages having Cz as a common cathode (-1 mA) and each of the other electrodes as the anode (+1 mA). These results were used as the input to the optimization algorithm (Ruffini et al., 2014), since the distribution of En for any montage involving these electrodes can be calculated as a linear combination of the bipolar unit-current En distributions multiplied by the electrode's current. The montage optimizations (Figure 1.1- c) were performed using the Stimweaver algorithm, as described in Ruffini et al. (2014). Under the assumption of the lambda-E-model [ref-lambda] for the interaction of the E-field with the neurons, the algorithm optimizes for the En component of the E-field. Positive/negative En values, directed towards/out-of the cortical surface, depolarize/hyperpolarize dendrites, soma and the axon terminal of pyramidal cells, thus modulating excitation. The best montage is found by minimizing the least squares difference between the weighted target En-map and the weighted

En-field distribution induced by the montage, which defines the objective function. Minimization is constrained by safety limits for the currents (maximum current per electrode of 2mA, and maximum total injected current of 4mA), and by the maximum number of stimulation electrodes in the device (N = 8 here). The last condition is imposed by using a genetic algorithm that searches in electrode space for the constrained solution that better approximates the optimization objective function, as described in Ruffini et al. (2014).

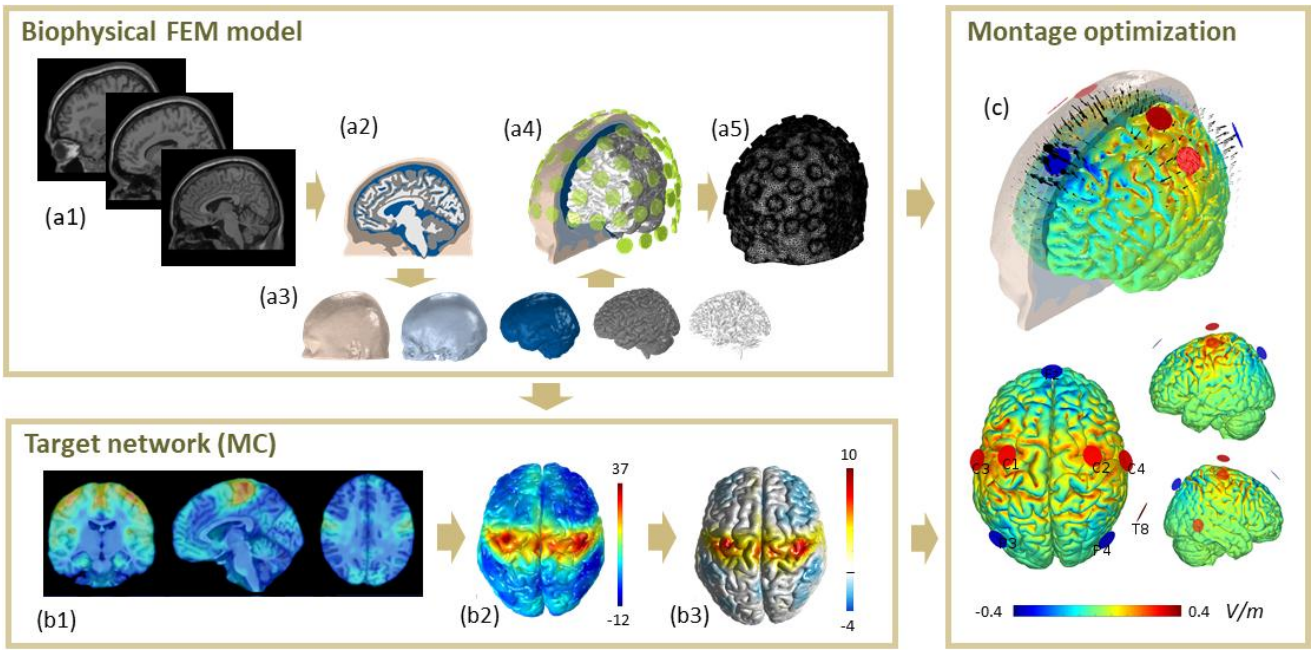

Figure 1.1. Biophysical head model, target map and multichannel tES optimized montages for stimulation of the motor cortex network by functional connectivity analysis.

BIOPHYSICAL FEM MODEL (a1-a5): the structural T1-weighted MRI (a1) of the template head (http://brainweb.bic.mni.mcgill.ca/brainweb) was segmented (a2) into the main tissue classes (scalp, skull, CSF and ventricles, grey matter, white matter); 3D surfaces of the tissues (a3) were created from the segmented volumes images and assembled into one head volume, where 64 1 cm-radius PISTIM electrodes were placed on the scalp according the 10-10 EEG system (a4). The tissues were assigned conductivity in the DC regime (scalp=0.33 S/m, skull=0.008 S/m, CSF and ventricles=1.79 S/m, GM=0.4 S/M, WM=0.13 S/m), and head model was meshed (a5) to calculate with finite elements the electric field induced on the cortex. **TARGET MAP** (b1-b3): the 3D image of the functional connectivity correlation (b1, in this example, the motor cortex network from Fisher et al. (2017) was remapped onto the cortical surface of the template brain (b2), and converted into a target map (b3) by linearly rescale and saturation of the values (the values in the scale are multiplied by the sign of E_n^{Target} to display excitatory and inhibitory areas). **MONTAGE OPTIMIZATION** (c1)**:** normal electric field (V/m) induced on the cortex of the reference head model by the best multielectrode solution targeting the map in (b3), as determined by the optimization algorithm (Ruffini et al., 2014). For this example, the solution involves 7 electrodes, delivering a total maximum current 4mA. Anodes are shown in red, cathodes in blue; arrows represent current density.

CHAPTER 2

NEUROIMAGING TO PREDICT AND STUDY THE EFFECTS OF NIBS

Neuroimaging is a broad term that encompasses multiple techniques to visualize anatomy or function within the central nervous system in vivo. In this chapter an introduction of two neuroimaging techniques has been provided: magnetic resonance imaging (MRI) and electroencephalography (EEG). In particular, how these techniques can be used to predict and study the effects of NIBS is emphasized.

2.1 Definition of MRI

Magnetic resonance imaging (MRI) represents a powerful and versatile method to safely and noninvasively measure several properties in the living brain. Through this technique is possible to capture images and consequently information about anatomy, neural activity and connectivity, as well as pathologies. Compared to other imaging methods (e.g., PET, MEG) MRI is more flexible: it can be used to manipulate and measure signal from the brain in several ways and it can acquire different type of images and information. In particular, there are three modalities that are the most commonly used in neuroimaging: structural, diffusion and functional imaging. In this chapter, the functional MRI (fMRI) will be described deeply, giving less space to the other modalities since they were not used for the purpose of this thesis.

Structural MRI. The structural imaging offers information about the characteristics of anatomical structures within the brain by finding their boundaries in the image. For example, through structural analysis is possible to understand if local gray matter is different between groups or in a way that relates to other parameters, as the NIBS treatment, but also to investigate the effect of disease or plasticity on specific anatomical structures. One of the most famous examples comes from a paper by Maguire and colleagues (2006) that showed the increased hippocampal region in the London taxi drivers (Maguire et al., 2006).

Diffusion MRI. The diffusion imaging provides information about microstructures and anatomical connectivity within the brain and spinal cord. This modality is useful for surgical planning since it delineates the path of connections, and it is currently the only way to study anatomical connectivity of the human brain in vivo.

Functional MRI. The functional imaging offers information about the neurons' activity in the brain that could be in relation to a specific task or stimuli, or to the spontaneous activity of participants' neurons. This method reveals an indirect measure of neuronal activity by measuring the changes in metabolic requirements related to neural activity. In particular it takes advantage of changing in the ratio between oxygenated and deoxygenated blood following the increase in neuronal activity. In fMRI there are two main research interests: investigating task-related activity using task-fMRI, and functional connectivity using resting-state fMRI (rs-fMRI). The task-fMRI paradigms allow to study a specific brain function during the presentation of certain tasks or stimuli used to trigger the phenomena under investigation. A very wide range of tasks can be used, from passive stimulation to cognitive tasks, in order to study the location and nature of brain activity from basic to high-level functions. In contrast to task-fMRI studies, resting-state functional connectivity studies examine BOLD fluctuations in the absence of any implicit input or output, in other words the spontaneous brain activity. Compared to task-fMRI, rs-fMRI has several practical and theoretical advantages, especially for clinical applications: significant rs-fMRI abnormalities have been identified across almost every neurological and psychiatric disorder (Fox & Greicius, 2010). The functional connectivity can be calculated considering the BOLD signal in specific regions of interests or by means of a data-driven approach such a spatial independent component analysis (ICA) that shows the presence of consistent resting state networks (RSNs) similar to the networks present during the activation (Damoiseaux et al., 2006; Smith et al., 2009). By studying specific RSNs, Fox and colleagues revealed for example that the default mode network (DMN) is always in anticorrelation with task-related networks (Fox et al., 2005, 2009). The function and the importance of studying RSNs will be discussed in the following paragraph.

There are some limitations of fMRI that need to be acknowledge. The most critical limit of fMRI is its relative low temporal resolution, because the hemodynamic response function is much slower than neural activity. Moreover, another critical limit is the Signal-to-Noise Ratio (SNR) usually solved with some acquisition and analysis trick that allow to maximize the signal in respect to noise. Furthermore, fMRI also does not presently provide information about whether connections are feedforward (ascending) or feedback (descending). Finally, there are limitations resulting from how the analysis are conducted and how the results are interpreted.

2.2 The Importance of Brain Networks

For several years, the studies in Neuroscience have been conducted considering the canonical separation between brain regions that, even though connected each other, performed their function in an independent manner. Recently, several studies have confirmed that our brain is not sector-based but it is organized in big functional structures that include several brain regions in constant interaction between each other. These macrostructures are called brain networks. The literature in the field suggests that large-scale networks trigger both integration and differentiation processes, essential for information processing. Moreover, also psychiatric, neurologic and neurodevelopmental disorders are characterized by network dysfunctions probably caused by abnormality in one isolated brain region that could produce alterations in the functionally connected brain networks (Fornito et al., 2015; Fox, Halko, et al., 2012). Considering these observations, networks are becoming the targets of therapeutic interventions (Ruffini et al., 2018). In order to study and identify networks activations during psychological and behavioral processes, neuroimaging represents the best tool in our possession. As discussed in the following paragraphs, neuroimaging methods in combination with NIBS techniques endorse a more comprehensive understanding of the network activity underlying both healthy human brain functions as well as connectivity changes associated with dysfunctional states. Depending on the neuroimaging modality, different aspects of NIBS-induced changes in brain activity can be captured.

2.2.1 Resting State Networks

One of the most important discovery in the field of neuroimaging is that our brain is never turned off but, instead, there is activity also during resting. The hypothesis of an 'always on brain' is not new but it has been detected by Berger through the electroencephalography (EEG). However, the more relevant neuroimaging studies come from the end of 90s century, when it was demonstrated that low frequency fluctuations (0.01–0.1 Hz) sampled on blood oxygenation level-dependent (BOLD) signal are phase-locked between many right and left-hemisphere symmetric functionally related cortices (i.e., bilateral motor cortex) in human subjects at rest (Biswal et al., 1995; Lowe et al., 2000). This temporal correlation of low frequency fluctuations was postulated to reflect functional connectivity between related brain regions (Biswal et al., 1995; Lowe et al., 2000). The demonstration that the correlation in low-frequency BOLD fluctuation reflects cortico-cortical connections came from a very interesting block-style fMRI experiment by Lowe and colleagues

(2000). In the subsequent years, many studies have following concluding that the low-frequency oscillations in human fMRI data have a small-world architecture that probably reflects underlying anatomical connectivity of the cortex and display spatial structure comparable to task-related activation (Achard et al., 2006; Beckmann et al., 2005; Cordes et al., 2000; De Luca et al., 2005; Hampson et al., 2002). The consistency, coherence and dynamicity of these low-frequency fluctuations in the BOLD signal across subjects has been studied through several analysis approach (region-of-interest cross-correlation (Cordes et al., 2000; Hampson et al., 2002; Lowe et al., 2000); seed-voxel based correlation analysis (Biswal et al., 1995); independent component analysis (ICA) (Beckmann et al., 2005; Calhoun et al., 2001; De Luca et al., 2005) and tensor probabilistic ICA (PICA) (Beckmann & Smith, 2005a; Damoiseaux et al., 2006)). All these studies have identified components that resemble functionally relevant cortical networks such as motor, visual and auditory cortical areas as well as the well-known default-mode network (DMN), usually activated in rest condition and deactivated during task (Fox et al., 2005). Moreover, negative correlations (anti-correlations) between regions with apparent opposing functional properties have also been observed (Fox et al., 2005).

Over the past decade, Neuroscience has made significant advances in understanding the circuits within the human brain and the interaction between regions and networks in healthy and pathological condition. Significant rs-fMRI abnormalities have been identified across almost every major neurological and psychiatric disease (for a review see Fox & Greicius, 2010). Nowadays, activity recorded during spontaneous rest using fMRI can be decomposed into separate but integrated resting state networks (RSNs) (Achard et al., 2006; Sporns, 2011) reflecting the activity within sensory (e.g., visual, motor, auditory) and associative brain regions related to high-order cognitive processes such as abstract reasoning, attention, language, and memory. In order to provide reference maps estimating the organization of the human cerebral cortex Yeo and colleagues (2011) explored cortical organization through resting-state functional connectivity in 1000 healthy subjects (Yeo et al., 2011). They concluded that different regions of the cerebral cortex display distinct characteristics and performed a fc-RSN ATLAS where brain areas have been grouped together in 7 or 17 RSNs based on their correlation. Recently, this ATLAS has been updated by Schaefer et al., (2018).

2.2.2 Task Related Brain Networks

Contrary to the resting-state studies, the studies aimed to investigate neural correlates of specific task or stimuli are usually block-design studies, where tasks blocks are alternated to rest blocks. Using this protocol, several studies so far have demonstrated that flashing visual stimuli are associated with increased activity in the visual cortex as well as auditory stimuli with increased activity in the auditory cortex. Moreover, considering attention-demanding cognitive tasks, two opposite brain responses are usually observed: frontal and parietal cortices exhibit activity increases (Cabeza & Nyberg, 2000; Corbetta et al., 2002), whereas posterior cingulate, medial and lateral parietal, and medial prefrontal cortex exhibit activity decreases (Gusnard et al., 2001; McKiernan et al., 2003; Shulman et al., 1997). This dichotomy demonstrated that there is an increased activity in regions whose function supports task execution and decreased activity in regions supporting unrelated or irrelevant processes. Going further, by examining both correlations and anticorrelations in spontaneous BOLD fluctuations associated with six predefined regions of interest, Fox and colleagues (2005) clarified that regions with similar task-related responses are correlated and these are usually in 'anticorrelation' with regions that have dissimilar task-related responses.

The most studied networks include the Default Mode Network (DMN), right and left Frontoparietal Network (FPN), Sensorimotor (SM), Limbic (LIM), Ventral Attention Network (VAN), Dorsal Attention Network (DAN) (Damoiseaux et al., 2006; Heuvel et al., 2009; Zuo et al., 2010). All these networks are related to different functions. For example, DAN allows the selection of sensory stimuli based on internal goals (goal-driven attention) and links them to motor responses. On the other hand, the VAN detects salient and behaviorally relevant stimuli in the environment, especially when unattended (stimulus-driven attention). These two networks dynamically interact during normal perception to determine where and what we attend to (Corbetta et al., 2008).

Despite each network plays a unique role in cognitive control, including its implementation, maintenance, and updating, the frontoparietal, cingulo-opercular, and salience networks works together for the same aim (Marek & Dosenbach, 2018). Thus, the cingulo-opercular network is more involved in the flexible control of goal-directed behavior while the frontoparietal network supports control initiation and provides flexibility by adjusting control in response to feedback. Because of the large degree of connectivity to several brain networks, the FPN is considered a functional hub, both globally and specifically in terms of distributed connectivity, able to rapidly and flexibly modulate other brain networks (Marek et al., 2015; Power et al., 2011, 2013).

Moreover, a significant positive correlation between functional integration of FPN and cognitive ability has been recently detected, showing that the strength of functional integration of the FPN and the rest of the brain is important for supporting high cognitive functions (Sheffield et al., 2015). The involvement of this network in high cognitive function as working memory will be deeply discussed in the 3rd Chapter of this thesis.

2.3 Combining fMRI and NIBS

NIBS and neuroimaging are complementary tools that can be combined to optimally study brain connectivity and manipulate brain networks (Fox, Halko, et al., 2012). NIBS can temporally modify the ongoing neural activity allowing the study of causal relationship between the stimulated cortical area and the underlying brain function or the main networks directly connected to it, suggesting information about brain connectivity. Despite its temporal resolution is inferior in comparison with EEG measures, its superior spatial resolution as well as the opportunity to monitor activity alterations across larger and deeper brain areas, including subcortical regions, represent important advantages (Siebner et al., 2009). Since the application of NIBS over a specific brain area can modulate not only neural activity in specific target region but also the evoked activity that propagates to anatomically and functionally interconnected regions, the combination of NIBS and fMRI allows the study of these dynamic network interactions. Combining fMRI with NIBS may be useful also for solving the already discussed targeting problem. By modulating the standard target regions onto individual subject anatomy (e.g., using anatomical MRI) or to individual functional activity (e.g., functional MRI), as well as by considering metabolic information (Positron Emission Tomography – PET), the stimulation protocols can be adapted to the specific aim of the intervention.

In general, NIBS and fMRI can be combined online or offline. In the offline protocols, it is possible to evaluate the functional connectivity changes due to one or several stimulation sessions (see e.g. Mantovani et al., 2020). On the other hand, the stimulation can be applied concurrently to fMRI acquisitions (online) with two aim: measuring the effect of stimulation on resting-state or evaluating the neural substrate of cognitive domain during the performance of cognitive tasks. The online effect of stimulation can be estimated through changes in the Cerebral Blood Flow (CBF) or BOLD signal, as well as in functional connectivity. Recently, Zheng and colleagues (2011) showed a significant increase of regional CBF in contralateral regions belonging to Sensorimotor Network (SMN) during the stimulation of the right motor cortex (Zheng et al., 2011). Later, other studies

confirmed the possibility to observe CBF modulation applying tDCS both on healthy (Baeken et al., 2017; Stagg et al., 2013) and clinical population (Hong et al., 2017), highlighting the advantages of using the combined approach tES-fMRI. Studying the online effects of tES on fMRI is also central for understanding the modulation of networks dynamics, as amply discussed in the 4th chapter of this thesis.

2.4 EEG

In contrast to metabolic measures (fMRI and PET), electrophysiological techniques, including magnetoencephalography (MEG) and electroencephalography (EEG), quantify physical phenomena directly produced by neural events, permitting to capture changes on a millisecond scale. Comparing EEG with MEG, the first appears less sensitive because of the phenomena called 'volume conduction': while the magnetic fields pass unimpeded through the meninges, the skull, and the scalp, the electric fields are affected by their differences in conductivity. However, MEG is less accessible, and it requires specialized installations, resulting in higher costs related to construction and maintenance. In contrast, EEG is portable and have a lower cost. For this reason, EEG is a highly informative and practical technique for studying brain activity in terms of brain oscillations (Baillet, 2017; Lopes da Silva, 2013). The EEG allows the recording of electrical activity within the brain, with an excellent temporal resolution, in spite of a limited spatial resolution, because of the relatively low number of electrodes. Moreover, other two main properties reduce the spatial resolution of its recordings: i) the electromagnetic fields decay exponentially with distance, consequently detecting fields generated by subcortical structures is unlikely; ii) electric fields with similar magnitude and opposite direction cancel out, constraining the sensitivity of EEG to dipoles produced radially to the skull. Additionally, estimating the exact position of the current sources remains a challenge in the field because many different configurations of dipoles could give rise to the same distribution of the EEG signal (Cohen, 2017).

The EEG is particularly able to capture the signal from the pyramidal neurons, organized in a way that the neighboring dendritic trees lie parallel to each other and orthogonal to the cortical surface. In literature two types of electrical activity within these cells are known: actions potentials and post-synaptic potentials. The first is induced when the transmembrane potential exceeds a threshold, at this moment the action potentials can travel along the neurons and the communication is possible, in particular the communication take place when the action potentials is propagated through synapses. When an action potential arrives at a synapse a postsynaptic

potential is generated if a threshold is exceeded. The action potential is then transferred to the postsynaptic neuron. The sum of the postsynaptic potentials can produce unidirectional current flow large enough to be picked up through the electrodes outside the brain. These currents can propagate to the scalp because the brain acts as a conductor. Therefore, the resulting EEG signal is the summation of the underlying sources.

EEG can be used to identify normal or pathological brain rhythms based on their amplitude and frequency. Brain oscillations can be observed at distinct spatial levels, ranging from neural circuits to brain networks, representing a common language shared by invasive, noninvasive and modeling studies. Additionally, through different type of analysis is possible to describe neural activity in a multidimensional framework, addressing the time and topographical distribution of brain rhythms, as well as their characteristics in terms of frequency, power, and phase (Cohen, 2017). The brain oscillations can be studied in humans during tasks and/or resting state. While recordings in resting state focus on the fundamental oscillatory profile of individuals, exploring differences in the frequency domain, task-related recordings explore changes in the brain activity elicited by an event. Recordings during cognitive tasks can be averaged across trials to observe changes in the brain oscillations in terms of time or time-frequency domain by calculating event-related perturbations (ERPs), and in terms of phase coherence by inter-trial phase coherence (ITPC) analysis (Delorme & Makeig, 2004). Different brain states and cognitive functions are associated to distinct frequency band: delta (1-4 hz) is the predominant band during sleep (Buzsáki & Draguhn, 2004), theta (4-7 hz) is prevalent during memory functions, and emotional regulations (Knyazev et al., 2009), alpha-band (8-13 hz) has been observed mainly during neural operations in the absence of sensory input and task-irrelevant brain areas (Palva & Palva, 2007) and beta band (14-35 hz) has been related to motor control and the maintenance of the status quo (Engel & Fries, 2010). Finally, a faster frequency band, known as gamma (35-100 hz), has been correlated with attention and sensory responses, as well as with the regulation of spike timing and synchrony of neural activity during memory formation (Bouyer et al., 1981; Cardin et al., 2009; Kemere et al., 2013). Representing the main topic of the last chapter of this thesis, the following paragraph will provide a detailed description of gamma oscillations.

2.4.1 Gamma oscillations and cognition

The gamma oscillations encompass the rhythmic activity within the range of 35 to 100 Hz. So far, an increase in gamma frequency has been observed in tasks such as reading and subtraction

expectancy (Fitzgibbon et al., 2004), as well as during memory encoding in humans and mice (Colgin, 2016; Yamamoto et al., 2014) and during working memory (Chen et al., 2014). Due to lack of evidence supporting gamma as a clock-like temporal framework of brain function (Burns et al., 2011; Ray & Maunsell, 2011), the involvement of gamma frequency in neural activity has been debated for a long time. However, prediction of cognitive performance by gamma power changes have been showed through intracranial recordings, highlighting the functional role of gamma in cognition. Nevertheless, the neural substrates underlying this high-frequency activity are not clear yet. Early studies have suggested that these oscillations result from the summed activation of pyramidal neurons in different assemblies, discharging at different rhythms (Fitzgibbon et al., 2004). On the other hand, recently it has been proposed that this band arise from the activity of GABAergic neurons (Chen et al., 2014), in particular the parvalbumin-positive basket cells (Mably & Colgin, 2018). At the circuit level, two models have been used to define the production of gamma oscillations, the Interneuron Network Gamma (ING) model, and the pyramidal interneuron network gamma (PING) model (Gonzalez-Burgos & Lewis, 2012; Whittington et al., 2000). The ING model proposes that besides interneurons are driven by tonic excitation, their synchronization in gamma relies on the activity of reciprocally connected GABAergic neurons. On the other hand, the PING model proposed that this band depends on the interplay between pyramidal neurons and GABAergic neurons. Several studies in vitro and in vivo are in favor of the PING model (Gonzalez-Burgos & Lewis, 2012).

Because of the involvement of gamma oscillations in high cognitive tasks, several studies evaluated the possibility to modulate cognitive performance through gamma-tACS. Santarnecchi and colleagues demonstrated that tACS at γ frequency (40-80Hz) can modulate fluid intelligence (Santarnecchi et al., 2013), problem-solving ability (Santarnecchi et al., 2019) and visuospatial coordination (Santarnecchi, et al., 2017a). Moreover, other groups shown its efficacy also in boosting working memory performance measured as reaction time (Röhner et al., 2018) and as changes in d-prime (Alekseichuk et al., 2016; Hoy et al., 2015). The strong effect of gamma-tACS on cognitive functions makes this technique highly interesting for the application also on populations with psychiatric and neurological disorders. Several studies have indeed shown its applicability and efficacy on patients with dementia (McDermott et al., 2018; Prince et al., 2016), supporting the idea of improving the cognitive impairment in Alzherimer disease by targeting the gamma band (Iaccarino et al., 2016a; McDermott et al., 2018; Palop & Mucke, 2016). A more in-

depth explanation of this aspect and one application example will be provided in last chapter of this thesis.

2.5 Combining EEG and NIBS

By combining EEG with NIBS, the effect of a pulse applied to the cortex can be assessed by measuring the neuronal response in the EEG, and the amount of neurophysiological information that can be derived is higher compared to the combination of NIBS with electromyography (EMG). In particular, TMS-EEG is one of the most promising multimodal techniques able to investigate brain dynamics. The EEG response obtained after a single or multiple TMS pulses is called TMS-evoked potential (TEP) (Ilmoniemi et al., 1997) and it is usually a complex waveform time-locked to the TMS pulse that offers a measure of cortical excitability. Recently, the combination of TMS and EEG become of great interest in the field of Neuroscience to study causal communication between brain regions with a high temporal resolution, and to offer information about the mechanisms of effective connectivity (Friston et al., 1993; Massimini et al., 2005). Information derived from TEPs has shown to be valuable in the distinction of several pathologies but also to study cortical connectivity in healthy subjects (for a comprehensive review: Tremblay et al., 2019).
The combination of tES and EEG is also of great interest, especially for studying long-distance synchronization and modifications in oscillatory activity in an easy way. Numerous studies have indeed explored the effects of tES in the human brain (Herrmann et al., 2013; Thut et al., 2011), however, due to the high amplitude artifact in EEG recordings produced by tES, is not possible to study the online effect of stimulation. On the other hand, the effect of tES could be evaluated by comparing the offline EEG recordings before and after stimulation (Zaehle et al., 2010). Several studies have shown the possibility to enhance memory performance by using tES (Berryhill & Jones, 2012; Mulquiney et al., 2011), also suggesting the recruitment of brain oscillatory patterns in specific frequency bands. Zaehle and collaborators (2010), found the possibility to modulated working memory (WM) performance by altering the underlying oscillatory brain activity in a polarity-specific way: they observed an increase in performance and amplified oscillatory power in the theta and alpha bands after anodal tDCS over the left dlPFC. Moreover, numerous EEG and MEG studies have reported WM-related increases in oscillations in theta (3–8 Hz; Gevins et al., 1997; Jensen & Tesche, 2002; Khader et al., 2010; Maurer et al., 2015; Onton et al., 2005) and gamma frequency bands (>30 Hz; Honkanen et al., 2015; Howard et al., 2003; Roux et al., 2012; Vugt et al., 2018). Based on these physiological evidences, several works have recently

demonstrated that parietal (Feurra et al., 2016; Jaušovec & Jaušovec, 2014; Pahor & Jaušovec, 2018) or fronto-parietal (Polanía, Paulus, et al., 2011; Violante et al., 2017) theta-tACS is able to boost behavioural performance on WM tasks and to induce a frequency specific modulation in the EEG activity (Helfrich et al., 2014; Pahor & Jaušovec, 2018). These results confirmed the exclusive opportunity to causally link brain oscillations of a specific frequency range to cognitive processes through tES. Moreover, several offline tES studies observed that EEG effects can last for several minutes after the end of stimulation (Antal & Paulus, 2013; Zaehle et al., 2010).

In summary, the combination of NIBS with EEG allows the study of cortico-cortical excitability and functional connectivity. The high temporal resolution of the EEG enables tracking of the temporal sequence of communication between regions and, combined with NIBS, can identify effective (causal) connectivity patterns in the brain. Moreover, NIBS techniques can trigger oscillatory rhythms or modify ongoing oscillations, allowing the study of causal specificity of brain rhythms for distinct cognitive and motor functions or disfunctions (Thut & Miniussi, 2009). Thus, amplitude and latency of the ERPs (generated in response to somatosensory, visual, or auditory stimuli but also cognitive tasks) may provide information regarding activity modulation induced also by tES in specific cortical regions (Miniussi et al., 2013). Even though the possibility to entrain brain oscillations by tES allows researchers to causally explore the interaction between brain oscillations and manifested behavior, technical challenges need to be addressed in order to more in depth understand this causal link.

CHAPTER 3

META-ANALYSES AS TOOL FOR NETWORK MAPPING AND TARGETING NEUROMODULATION: APPLICATION ON COGNITIVE TASK AND CLINICAL POPULATION

3.1 STUDY 1: Stimuli, Presentation modality and load-specific brain activity patterns during n-back task[1]

Working memory (WM) is generally defined as the capacity to temporary maintain and manipulate goal-relevant information as well as to concurrently remember and process information over brief periods of time (Baddeley, 1992). Compared to short-term memory, WM allows to manipulate incoming information, thus not being limited to storage capacity (Baddeley et al., 1996). Due to its many plausible links with other high-order cognitive functions— such as fluid intelligence (Friedman et al., 2006), inhibition (Miyake et al., 2000), switching (Miyake et al., 2000) and attention (Maurizio Corbetta & Shulman, 2002)—a large number of studies has recently focused in understanding its mechanisms and neural correlates, not only in the context of cognitive neuroscience, but also in clinical psychology, cognitive rehabilitation medicine and within the field of cognitive enhancement in healthy subjects.

Studies in both healthy humans and clinical populations have highlighted a set of brain regions playing a relevant role during WM-related cognitive processing, with hundreds of studies being published so far. The complexity of WM has also led to a vast number of assessment tools being created, each one stressing a particular aspect of WM processing, e.g., WM capacity vs manipulation, processing of visual stimuli with or without emotional valence, processing of auditory stimuli vs verbal ones and so on. This has led to a consensus over which regions or brain lobe might broadly play a role in WM, but with little to no specificity when it comes to the neural substrates underlying specific WM tasks that might be deployed in neurorehabilitation protocols or become a target within non-invasive brain stimulation (NIBS) techniques. The most recent Activation Likelihood Estimate (ALE) meta-analysis (Rottschy et al., 2012) examined a total of 189

[1] A similar version of the present article has been recently published (Mencarelli, L., Neri, F., Momi, D., Menardi, A., Rossi, S., Rossi, A., & Santarnecchi, E. (2019). *Human brain mapping*, *40*(13), 3810-3831).

adult WM experiments employing a variety of WM tasks. The authors reported a highly consistent activation of a core WM network across task variants, relaying mostly on fronto-parietal regions, with some differentiations depending on the type of stimuli, contrasts and cognitive processes examined. However, due to the great variability in the WM tasks being examined, the relevant contribution of Rottschy et al. (2012) did not define the task-specific activation clusters, or maps.

Among the most used WM tasks, examples include the Digit Span task, the Sternberg task, the n-back task and delayed match-to-sample. The n-back task—first described by Kirchner (1958)— is however the most popular measure of WM used in functional magnetic resonance imaging (fMRI) studies, relying on the presentation of "rapidly, continuously changing information" to measure very short-term retention. In this task, participants are presented with a series of stimuli and are asked to indicate whether the current stimulus matches the stimulus presented n stimuli back in the series. The majority of fMRI studies using n-back paradigms has so far focused on the effects of task load or type of material (e.g., verbal vs. spatial) in adults (Owen et al., 2005) and confirmed the well-established fronto-parietal network of activation mentioned above. Indeed, both differences in stimuli's type (e.g., letters, numbers, faces, words, objects, images) and presentation modalities (visual, auditory, tactile) can be used to personalize a variety of features in n-back paradigms, reason for which fMRI studies can be informative in revealing which brain areas are more active for a specific condition, or if instead the activated WM network remains the same independently from changes in such features. Few studies have proven WM network activation to be material-independent (Nystrom et al., 2000; Owen et al., 2005; Ragland et al., 2002; Schumacher et al., 1996), with the opposite finding holding true for other studies: while maintaining a bilateral fronto-parietal activation, greater network activation has been reported to the left for verbal inputs, and to the right instead when subjects were presented with visuo-spatial material (Owen et al., 2005; Rottschy et al., 2012). The latest meta-analysis to date based on n-back task date back to 2005. Owen et al. (2005) examined 24 studies of n-back WM tasks manipulating either processes required for task performance (i.e., location/spatial- vs. identity/non-spatial-monitoring) or stimulus material (i.e., verbal or non-verbal). This study originally showed for the first time the neural correlates active for a single WM task. However, in this meta-analysis only some neural activation related to several stimuli or presentation modality were presented: three activation maps ("identity verbal", "identity non-verbal" and "non-verbal location") and two comparison maps ("verbal vs non-verbal" and "identity vs location").

A detailed knowledge of the pool of regions upon which a specific task or, in this case, a particular stimulus used in an n-back paradigm mostly relies on, becomes crucial in the field of rehabilitation. Consider the case of WM cognitive training: if a patient has a lesion on the left hemisphere and he/she presents a WM deficit, it would be important to implement a cognitive training capable of stressing that area or the efficiency of surrounding healthy tissue, maximizing the rehabilitation. In addition, several neuroimaging studies have shown an increase in activity at the neural level over specific regions, such as the bilateral prefrontal and parietal cortices, as a function of processing load (Jonides et al., 1997; Owen et al., 2005; Rottschy et al., 2012). The notion of pivotal brain areas for a given task comes therefore of great interest, with strong clinical and rehabilitative implications. The creation of well-defined maps based on established task-specific clusters of activity would allow to selectively stimulate such areas, possibly through the implementation of non-invasive brain stimulation (NIBS) approaches, aiming to provide better cognitive training interventions and to overall increase individuals' quality of life. Furthermore, the ability to modulate brain activity in a completely non-invasive way has always been one of the greatest challenges in cognitive neuroscience, leading NIBS interventions to become among of the most used approaches in recent years.

Due to the aforementioned rationale, we hereby aim to present a quantitative meta-analysis of the n-back literature available to date, summarizing published experimental work involving task-fMRI and PET data. The Activation Likelihood Estimate (ALE) statistical framework (Eickhoff et al., 2009, 2012) was implemented in providing readers with a state-of-the art update on activation maps along a general to specific gradient of WM n-back paradigm characterization. In addition, a clear differentiation of the role played by the regions activated during WM tasks with respect to existing resting-state networks (RSN)(Biswal et al., 2010) is not yet available. To provide this information, we compare each n-back map with those representing different RSNs (e.g., attention, executive control, language, sensorimotor, visual and auditory processing). Results offer a still unexplored perspective and overview of the link between n-back related brain activity and brain connectivity in humans. Moreover, we provide some examples of network-guided targeting for tES based on the ALE maps, using biophysical modeling.

3.1.1 METHODS

Literature search

Potentially relevant articles were retrieved by performing a search on PubMed and Google Scholar databases without temporal restrictions. The following terms "Working Memory", "WM", “Working Memory Task”, "Memory", "Short-term Memory" were individually combined with "Functional Magnetic Resonance Imaging", "Position Emission Tomography" and their acronyms. References from the retrieved material were examined for relevant publications too. In the second step of the literature examination, we selected only the studies that used the n-back as task and following the abstract screening of every resulted article published before June 2018, a total of 152 studies were selected and analyzed (Figure 3.1). We intentionally excluded (i) studies involving patients with organic illnesses, pathological neurological exam, psychiatric conditions or history of drug abuse, (ii) studies discussing magic ideation, (iii) review papers, (iv) studies not mentioning any of the keywords in their abstract unless they cite specific n-back tasks, (v) studies not reporting fMRI/PET activations coordinates in MNI or Talairach space, (vi) studies not reporting activation foci in table format or reporting statistical values without corresponding coordinates, (vii) studies that used predefined Regions of Interest (ROIs), (viii) studies not using classic n-back tasks, define as those where subjects must respond when the stimulus presented is the same as the stimulus presented *n* times before, (ix) studies that used placebo or pharmacological therapies, (x) studies with only one subject, (xi) studies reporting results obtain with Small Volume Correction (SVC). The final selection comprised 85 studies reporting either fMRI or PET findings. For each study, the following information were retrieved: (i) number of participants, (ii) mean age, (iii) experimental design, (iv) cognitive task specifics, (v) main results. Data of the specific activation foci were collected and included in a quantitative Activation Likelihood Estimation (ALE) analysis for the identification of brain regions most commonly reported as involved in n-back tasks.

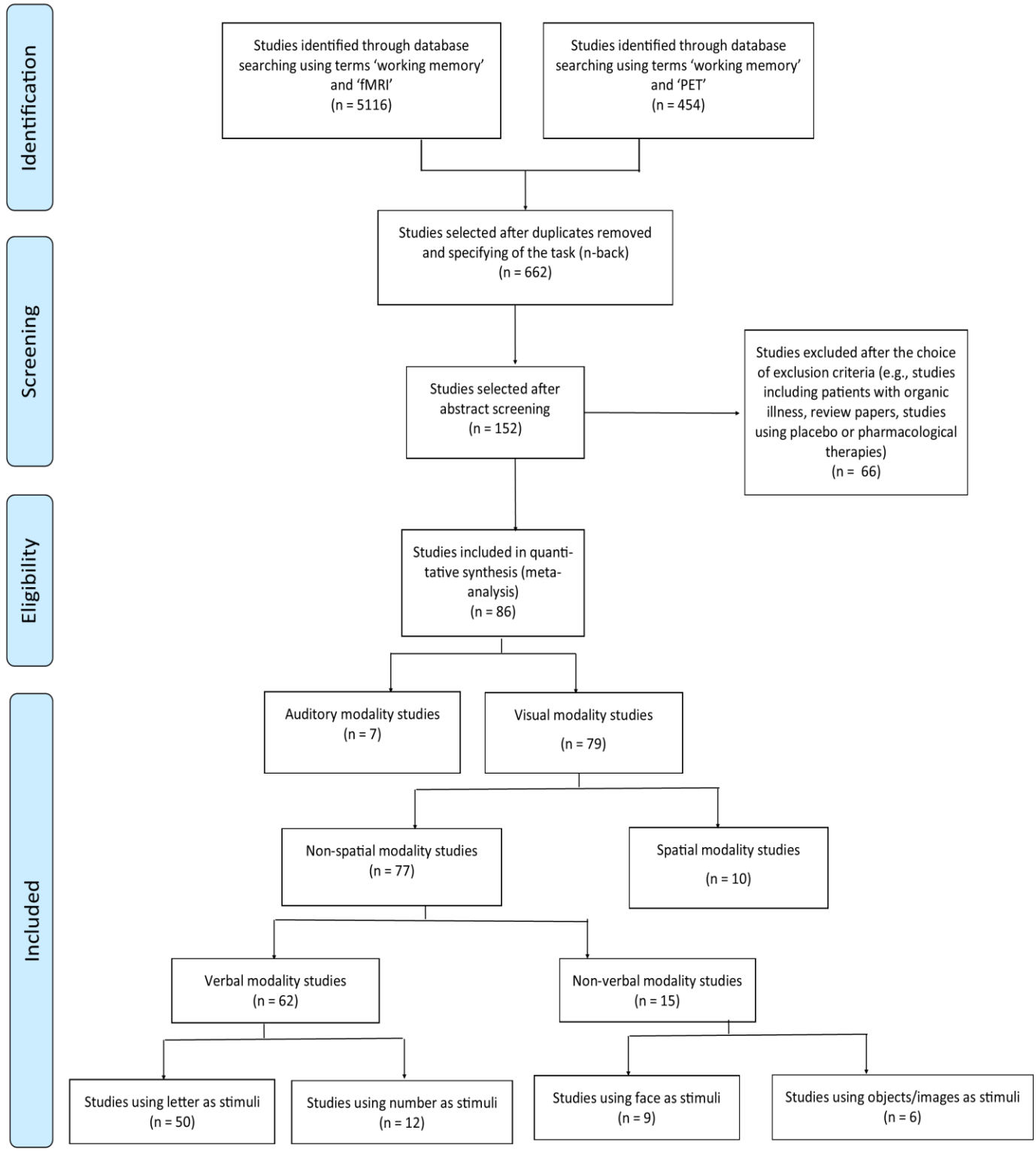

Figure 3.1. A detailed overview of literature search performed is shown.

N-back maps

Different maps were created, carefully inspecting each manuscript and extracting activation foci from tables referring to the contrast of interest. A (1) global "WM" map was obtained including all the coordinates referring to n-back tasks, regardless of presentation modality and stimulus type. We created (2) three maps of WM load containing all experiments that contrasted a high load n-back condition with a low load n-back condition (e.g., 3 back vs 1 back tasks). Both (3) "visual" and (4) "auditory" n-back maps were computed from studies using visual or auditory presentation modalities; words, letters, numbers, faces, objects and images are examples of the most commonly displayed visual stimuli within former studies. Moreover (5) “spatial” and (6) “non-spatial” n-back maps were computed from studies using spatial designs (e.g., *“judge whether if the current position of the box is the same or n position before the current position”)* or non-spatial design (e.g., *“judge whether if the current number is the same of n numbers before the current number”*). In addition, (7) “verbal” and (8) “non-verbal” maps were also created, in which we included all studies with a non-spatial design that have used stimuli like letters, numbers or any other type of stimuli requiring a stimulus-dependent semantic process (verbal WM); or non-verbal stimuli like faces, objects, images (non-verbal WM). For “verbal” and “non-verbal” maps, we produced a set of sub-maps, one for each type of stimuli used: (9) “letters”, (10) “numbers”, (11) “faces” and (12) “objects/images” maps. Finally, (12) we have realized a map revealing the neural deactivation during the n-back task.

ALE maps computation

The quantitative evaluation of spatial PET and fMRI patterns was carried out using the activation likelihood estimate (ALE) technique implemented in the GingerALE software v2.3.2 (www.brainmap.org) (Eickhoff et al., 2009, 2012). The method yields a statistical map that indicates the set of significant voxels while considering the magnitude of the effect, the number of studies and the number of participants in each study.

First, lists of coordinates were carefully checked for duplication of data across publications, in order to avoid artefactual inflation of a given foci significance. Differences in coordinate spaces (MNI vs. Talairach space) between experiments were accounted for by transforming coordinates reported in Talairach space into MNI coordinates through the tal2mni algorithm implemented in GingerALE. The reported foci of activation for each study were modeled as Gaussian distributions and merged into a single 3D volume. Equally-weighted coordinates were used to form estimates of

the probability of activation for each voxel in the brain, using an estimation of the inter-subject and inter-study variability usually observed in neuroimaging experiments, rather than applying a priori full-width half maximum (FWHM) kernel. Therefore, the number of participants in each study influenced the spatial extent of the Gaussian function used. We first modeled the probability of activation over all studies at each spatial point in the brain, returning localized "activation likelihood estimates" or ALE values. Values were then compared to a null distribution created from simulated datasets with randomly placed foci to identify significantly activated clusters (permutations test= 1000 run). Corrections based on false-discovery rate (FDR) at the cluster-level and voxel-level family-wise error (FWE) estimation (Eickhoff et al., 2012) were applied. In details, cluster correction for multiple comparisons with a $p<0.001$ threshold for cluster-formation and a $p<0.05$ for cluster-level inference were set. All values were chosen based on their common use in similar meta-analyses and algorithm tests (Eickhoff et al., 2012; Turkeltaub et al., 2012).

Contrast images were created from the subtraction of each pair of ALE maps, together with a map showing their statistically significant overlap. Given that the resulting subtraction image has the major drawback of not considering the differences in the dataset sizes between the two original maps, GingerALE's simulated data of the pooled foci datasets— obtained by randomly dividing the pooled data into two new groupings of the same size as the original datasets— were considered. An ALE image is hereby created for each new dataset, then subtracted from the other and compared to the original data. ALE maps were visualized using MRICronGL on an MNI standard brain. The same analysis has been computed in the Studies 2 and 3 of this Chapter.

Anatomic-functional characterization of WM load maps

For the specific contrasts examining the impact of WM load on n-back activation maps topography, an additional analysis was carried out to investigate the anatomo-functional profile of clusters characterizing the highest load conditions (i.e., 3-back). Specifically, the anatomo-functional anterior cingulate cortex (ACC) parcellation by Neubert et al. (Neubert et al., 2015) and the anatomo-functional cerebellar parcellation by Buckner et al. (Buckner et al., 2011) were used. We imported each WM-load map in MATLAB (The Mathworks, Release 2016b) and computed their quantitative overlap.

Overlap between n-back and resting-state fMRI networks

Shirer et al. (2012) defined 14 non-overlapping maps representing distinct resting state networks: dorsal and ventral default mode (vDMN, dDMN), dorsal and ventral attention (AN), anterior and posterior salience (AS, PS), right and left executive control (RECN, LECN), language (LANG), basal ganglia (BG), high and primary visual (HVIS, PVIS), precuneus (PREC), somatosensory (SM) and auditory (AUD) networks (Shirer et al., 2012). Within the present study, we decided to further estimate how much— in terms of percentage of voxels— each n-back map was found to overlap with Shirer's RSNs.

Biophysical model

The biophysical model has been obtained as described in the Chapter 1 (Figure 1.1). In this case, we use as target the activation maps resulting from the ALE computation, instead that the functional connectivity map described in the 'Biophysical modeling' paragraph (pag. 22). In particular, considering the difficulty to reach subcortical regions through NIBS, for these optimizations we decided to focus on the cortical nodes, thus implementing the optimization for the bilateral frontal and parietal areas resulting from the 'global' WM map.

3.1.2 RESULTS

Ale Maps

A total of 152 studies were retrieved and examined. Nevertheless, only 85 of them were found to match our inclusion criteria and were ultimately entered in the analysis (a more detailed overview of the literature search is reported in Figure 3.1). A complete list of the included studies, reporting the types of the n-back tasks examined, the stimuli used, their presentation modalities, the references (MNI or Talairach) and their relative transformation type, as well as the number of foci and imaging techniques (e.g., fMRI, PET), are reported in Table 3.1. Moreover, information about sample size, gender and age, acquisition parameters (e.g., MRI scanner, TR, TE, FA) and the neuroimaging software used for fMRI/PET data analysis are shown for each paper in Table 3.2.

In the following section, tables and figures for each n-back map are reported. A discussion about the role of each specific node is provided in the Discussion section of the manuscript.

Table 3.1. List of studies considered in this meta-analysis. For each type of the n-back task examined, the levels of task difficulty, the type of stimulus used, the modality of stimuli presentation, the type of references and their transformation modalities, the number of foci and the imaging modality are listed.

Paper	N-Back	Modality	Task Type	Stimuli Type	Contrast	Reference	Foci	Imaging Modality	Reference Transformation
Alain et al 2010	1,2	Auditory	Spatial	Sounds	2back>1back	TAL	13	fMRI	TAL NATIVE
Awh et al 1996	2	Visual	Identity	Letters	2back>control	TAL	12	PET	TAL NATIVE
Bartova et al 2015	0,2	Visual	Identity	Numbers	2back>0back	TAL	10	fMRI	TAL NATIVE
Beneventi et al 2007	0,1,2	Visual	Identity	Schematic Faces	Global	TAL	21	fMRI	TAL NATIVE
Binder et al 2006	0,2	Visual	Identity	Letters	2back>0back	MNI	19	fMRI	BRETT
Binder et al 2006	0,2	Visual	Identity	Shapes	2back>0back	MNI	17	fMRI	BRETT
Bleich-Cohen et al 2014	0,2	Visual	Identity	Numbers	2back>0back	TAL	9	fMRI	TAL NATIVE
Blockland et al 2011	0,2	Visual	Spatial	Numbers	2back>0back	MNI	32	fMRI	MNI NATIVE
Brahmbhatt et al 2010	0,1,2	Visual	Identity	Letters	Global	TAL	7	fMRI	TAL NATIVE
Braver et al 1997	0,1,2,3	Visual	Identity	Letters	Global	TAL	12	fMRI	TAL NATIVE
Cader et al 2006	0,1,2,3	Visual	Identity	Letters	2back>1back	MNI	8	fMRI	MNI NATIVE
Cader et al 2006	0,1,2,3	Visual	Identity	Letters	3back>1back	MNI	8	fMRI	MNI NATIVE
Callicot et al 1999	0,1,2,3	Visual	Identity	Numbers	Global	TAL	18	fMRI	TAL NATIVE
Campanella et al 2013	0,2	Visual	Identity	Numbers	2back>0back	MNI	6	fMRI	MNI NATIVE
Carlson et al 1998	0,1,2	Visual	Spatial	Shapes	1back>0back	TAL	17	fMRI	TAL NATIVE
Carlson et al 1998	0,1,2	Visual	Spatial	Shapes	2back>0back	TAL	28	fMRI	TAL NATIVE
Carlson et al 1998	0,1,2	Visual	Spatial	Shapes	2back>1back	TAL	26	fMRI	TAL NATIVE
Caseras et al 2006	0,1,2,3	Visual	Identity	Letters	Global	TAL	10	fMRI	TAL NATIVE
Cerasa et al 2008	0,2	Visual	Spatial	Pictures	2back>0back	TAL	16	fMRI	TAL NATIVE
Choo et al 2005	0,1,2,3	Visual	Identity	Letters	Global	TAL	8	fMRI	TAL NATIVE
Cohen et al 1997	0,1,2,3	Visual	Identity	Letters	Global	TAL	27	fMRI	TAL NATIVE
Dade et al 2001	0,2	Visual	Identity	Faces	2back>0back	TAL	24	PET	TAL NATIVE
Dell'Osso et al 2015	0,2,3	Visual	Identity	Letters	Global	MNI	14	fMRI	MNI NATIVE
Dima et al 2014	0,1,2,3	Visual	Identity	Letters	1back>0back	MNI	5	fMRI	MNI NATIVE
Dima et al 2014	0,1,2,3	Visual	Identity	Letters	2back>0back	MNI	8	fMRI	MNI NATIVE
Dima et al 2014	0,1,2,3	Visual	Identity	Letters	3back>0back	MNI	10	fMRI	MNI NATIVE
Drapier et al 2008	0,1,2,3	Visual	Identity	Letters	1back>0back	TAL	4	fMRI	TAL NATIVE
Drapier et al 2008	0,1,2,3	Visual	Identity	Letters	2back>0back	TAL	6	fMRI	TAL NATIVE
Drapier et al 2008	0,1,2,3	Visual	Identity	Letters	3back>0back	TAL	7	fMRI	TAL NATIVE
Druzgal et al 2001	0,1,2	Visual	Identity	Faces	Global	TAL	12	fMRI	TAL NATIVE
Duggirala et al 2016	0,2	Visual	Identity	Faces	2back>0back	MNI	15	fMRI	MNI NATIVE
Duggirala et al 2016	0,2	Visual	Identity	Objects	2back>0back	MNI	13	fMRI	MNI NATIVE
Duggirala et al 2016	0,2	Visual	Identity	Words	2back>0back	MNI	19	fMRI	MNI NATIVE
Elzinga et al 2006	0,1,2,3	Visual	Identity	Letters	Global	TAL	21	fMRI	TAL NATIVE
Fonville et al 2015	0,1,2,3	Visual	Identity	Letters	Global	MNI	26	fMRI	MNI NATIVE
Fonville et al 2015	0,1,2,3	Visual	Identity	Letters	2back	MNI	22	fMRI	MNI NATIVE
Fonville et al 2015	0,1,2,3	Visual	Identity	Letters	3back	MNI	24	fMRI	MNI NATIVE
Forn et al 2007	0,2	Auditory	Identity	Letters	2back	TAL	10	fMRI	TAL NATIVE
Frangou et al 2008	0,1,2,3	Visual	Identity	Letters	Global	TAL	11	fMRI	TAL NATIVE
Fusar-Poli et al 2010	0,1,2	Visual	Identity	Letters	Global	MNI	16	fMRI	MNI NATIVE
Garrett et al 2011	0,1,2	Visual	Identity	Letters	1back>0back	TAL	12	fMRI	MNI NATIVE
Garrett et al 2011	0,1,2	Visual	Identity	Letters	2back>0back	TAL	11	fMRI	MNI NATIVE
Georgiou-Karistianis et al 2013	0,1,2	Visual	Identity	Numbers	1back>0back	MNI	38	fMRI	MNI NATIVE
Gropman et al 2013	1,2	Visual	Identity	Letters	2back>1back	TAL	41	fMRI	tAL NATIVE
Harvey et al 2005	0,1,2,3	Visual	Identity	Letters	Global	TAL	10	fMRI	TAL NATIVE
Huang et al 2016	0,1,2	Visual	Spatial	Shapes	1back>0back	TAL	5	fMRI	TAL NATIVE
Huang et al 2016	0,1,2	Visual	Spatial	Shapes	2back>1back	TAL	10	fMRI	TAL NATIVE
Jiang et al 2015	0,2	Visual	Spatial	Numbers	2back>0back	MNI	9	fMRI	MNI NATIVE
Jiang et al 2015	0,2	Visual	Spatial	Numbers	2back>0back	MNI	4	fMRI	MNI NATIVE
Jonides et al 1997	control task, 0,1,2,3	Visual	Identity	Letters	1back>control task	TAL	3	PET	TAL NATIVE
Jonides et al 1997	control task, 0,1,2,3	Visual	Identity	Letters	2back>control task	TAL	22	PET	TAL NATIVE
Jonides et al 1997	control task, 0,1,2,3	Visual	Identity	Letters	3back>control task	TAL	24	PET	TAL NATIVE
Kasahara et al 2011	1,2,3	Visual	Identity	Letters	Global	MNI	9	fMRI	MNI NATIVE
Kim et al 2002	2	Visual	Identity	english words	2back	TAL	9	PET	TAL NATIVE
Kim et al 2002	2	Visual	Identity	korean words	2back	TAL	6	PET	TAL NATIVE
Kim et al 2002	2	Visual	Identity	Shapes	2back	TAL	7	PET	TAL NATIVE
Kim et al 2003	0,2	Visual	Identity	Shapes	2back>0back	TAL	8	PET	TAL NATIVE
Kim et al 2006	2	Visual	Identity	Letters	2back	TAL	8	fMRI	TAL LANCASTER

Table 3.1. Continued.

Korsnes et al 2013	1,2	Visual	Identity	Numbers	2back>1back	MNI	18	fMRI	MNI NATIVE
Koshino et al 2008	0,1,2	Visual	Identity	Faces	Global	MNI	15	fMRI	MNI NATIVE
Kumari et al 2006	0,1,2	Visual	Spatial	Pictures	1back>0back	MNI	22	fMRI	BRETT
Kumari et al 2006	0,1,2	Visual	Spatial	Pictures	2back>0back	MNI	18	fMRI	BRETT
LaBar et al 1999	0,2	Visual	Identity	Letters	2back>0back	TAL	8	fMRI	TAL NATIVE
Lee et al 2013	1	Visual	Identity	Numbers	1back>rest	TAL	58	fMRI	TAL NATIVE
Li et al 2014	0,1,2	Visual	Identity	Letters	0back	MNI	7	fMRI	MNI NATIVE
Li et al 2014	0,1,2	Visual	Identity	Letters	1back	MNI	10	fMRI	MNI NATIVE
Li et al 2014	0,1,2	Visual	Identity	Letters	2back	MNI	18	fMRI	MNI NATIVE
Lim et al 2008	1	Visual	Identity	Korean words	1back>rest	TAL	5	fMRI	TAL NATIVE
Luo et al. 2014	0,2	Visual	Identity	Faces	2back>0back	MNI	12	fMRI	MNI NATIVE
Lythe et al 2012	0,1,2,3	Visual	Identity	Letters	Global	MNI	7	fMRI	MNI NATIVE
Marquand et al 2008	0,1,2,3	Visual	Identity	Letters	2back	TAL	19	fMRI	TAL NATIVE
Matsuo et al 2007	0,1,2	Visual	Identity	Numbers	1back>0back	TAL	4	fMRI	TAL NATIVE
Matsuo et al 2007	0,1,2	Visual	Identity	Numbers	2back>0back	TAL	2	fMRI	TAL NATIVE
Mattfeld et al 2016	0,1,2,3	Visual	Identity	Letters	3back>2>1>0back	TAL	6	fMRI	TAL NATIVE
Mcallister et al 1999	0,1,2	Auditory	Identity	Letters	1back>0back	TAL	5	fMRI	TAL NATIVE
Mcallister et al 1999	0,1,2	Auditory	Identity	Letters	2back>1back	TAL	2	fMRI	TAL NATIVE
Meisenzahl et al 2006	0,2	Visual	Identity	Letters	2back	TAL	20	fMRI	TAL NATIVE
Mendrek et al 2004	0,2	Visual	Identity	Letters	2back>0back	TAL	7	fMRI	TAL NATIVE
Mendrek et al 2004	0,2	Visual	Identity	Letters	2back>0back	TAL	12	fMRI	TAL NATIVE
Migo et al 2014	0,1,2	Visual	Identity	Letters	1back>0back	MNI	6	fMRI	MNI NATIVE
Migo et al 2014	0,1,2	Visual	Identity	Letters	2back>0back	MNI	8	fMRI	MNI NATIVE
Monks et al 2004	0,2	Visual	Identity	Letters	2back>0back	TAL	17	fMRI	TAL NATIVE
Nagel et al 2011	1,2,3	Visual	Identity	Letters	3back>1back	MNI	5	fMRI	MNI NATIVE
Nagel et al 2011	1,2,3	Visual	Identity	Letters	3back>1back	MNI	3	fMRI	MNI NATIVE
Nebel et al 2005	1,2	Visual	Identity	Letters and Shape	1back>rest	TAL	10	fMRI	TAL NATIVE
Nebel et al 2005	1,2	Visual	Identity	Letters and Shape	2back>rest	TAL	30	fMRI	TAL NATIVE
Norbury et al 2013	0,1,2,3	Visual	Identity	Letters	Global	MNI	6	fMRI	MNI NATIVE
Nyberg et al 2009	1,2,3	Visual	Identity	Numbers	Global	TAL	28	fMRI	MNI NATIVE
Perlstein et al 2003	0,1,2	Visual	Identity	Letters	Global	TAL	9	fMRI	TAL NATIVE
Philip et al 2015	0,2	Visual	Identity	Letters	0back	TAL	7	fMRI	TAL NATIVE
Philip et al 2015	0,2	Visual	Identity	Letters	2back	TAL	11	fMRI	TAL NATIVE
Pomarol-Clotet et al 2012	1,2	Visual	Identity	Letters	2back>baseline	MNI	2	fMRI	MNI NATIVE
Qin et al 2009	0,2	Visual	Identity	Numbers	2back>0back	MNI	14	fMRI	MNI NATIVE
Ragland et al 2002	0,1,2	Visual	Identity	Letters	1back>0back	TAL	6	fMRI	TAL NATIVE
Ragland et al 2002	0,1,2	Visual	Identity	Letters	2back>0back	TAL	7	fMRI	TAL NATIVE
Ragland et al 2002	0,1,2	Visual	Identity	Letters	2back>1back	TAL	10	fMRI	TAL NATIVE
Ragland et al 2002	0,1,2	Visual	Identity	Pictures	1back>0back	TAL	5	fMRI	TAL NATIVE
Ragland et al 2002	0,1,2	Visual	Identity	Pictures	2back>0back	TAL	9	fMRI	TAL NATIVE
Ragland et al 2002	0,1,2	Visual	Identity	Pictures	2back>1back	TAL	6	fMRI	TAL NATIVE
Rama et al 2001	0,1,2	Auditory	Identity	Emotional Words	1back>0back	TAL	24	fMRI	TAL NATIVE
Rama et al 2001	0,1,2	Auditory	Identity	Emotional Words	2back>0back	TAL	32	fMRI	TAL NATIVE
Ricciardi et al 2006	1	Visual	Identity	Shapes	1back	TAL	44	fMRI	TAL NATIVE
Rodríguez-Cano et al 2014	1,2	Visual	Identity	Letters	1back>baseline	MNI	5	fMRI	TAL NATIVE
Rodríguez-Cano et al 2014	1,2	Visual	Identity	Letters	2back>baseline	MNI	1	fMRI	TAL NATIVE
Rodriguez-Jimenez et al 2009	2	Auditory	Identity	Letters	2back>control task	TAL	6	fMRI	BRETT
Sanchez-Carrion et al 2008	0,2,3	Visual	Identity	Numbers	2back>0back	MNI	16	fMRI	MNI NATIVE
Sanchez-Carrion et al 2008	0,2,3	Visual	Identity	Numbers	3back>0back	MNI	17	fMRI	MNI NATIVE
Sapara et al 2014	0,1,2	Visual	Spatial	Dots	1back>0back	MNI	18	fMRI	MNI NATIVE
Sapara et al 2014	0,1,2	Visual	Spatial	Dots	2back>0back	MNI	6	fMRI	MNI NATIVE
Scheuerecker et al 2008	0,2	Visual	Identity	Letters	2back>0back	MNI	8	fMRI	MNI NATIVE
Schmidt et al 2009	0,1,2,3	Visual	Identity	Letters	Global	TAL	14	fMRI	TAL NATIVE
Schumacher et al 1996	3	Visual	Identity	Letters	3back	TAL	12	PET	TAL NATIVE
Schumacher et al 1996	3	Auditory	Identity	Letters	3back	TAL	13	PET	TAL NATIVE
Seo et al 2012	0,2	Visual	Identity	Letters	2back>0back	MNI	19	fMRI	MNI NATIVE
Spreng et al 2014	2	Visual	Identity	Faces	2back>rest	MNI	18	fMRI	MNI NATIVE
Thomas et al 2005	2	Visual	Identity	Letters	2back	TAL	9	fMRI	TAL NATIVE
Thornton et al 2013	1,2	Visual	Identity	Faces	2back>1back	MNI	14	fMRI	MNI NATIVE
Trujillo et al 2015	0,1,2,3	Visual	Spatial	Dots	Global	MNI	18	fMRI	MNI NATIVE
Veltman et al 2003	0,1,2,3	Visual	Identity	Letters	Global	TAL	11	fMRI	TAL NATIVE
Walitt et al 2016	0,2	Visual	Identity	Letters	2back>0back	MNI	5	fMRI	MNI NATIVE
Yoo et al 2004	0,1,2	Visual	Identity	Letters	Global	TAL	16	fMRI	BRETT
Yoo et al 2004	0,1,2	Auditory	Identity	Letters	Global	TAL	23	fMRI	BRETT
Yoo et al 2005	2	Visual	Identity	Faces	2back	TAL	22	fMRI	TAL NATIVE
Ziemus et al 2007	0,2	Visual	Identity	Letters	2back>0back	TAL	15	fMRI	TAL NATIVE

Table 3.2. Details about considered studies. Sample size, gender and age of samples, fMRI/PET acquisition parameters and neuroimaging software used for data analysis are shown. TE= Echo Time; TR= Repetition Time; FA= Flip Angle.

Paper	Subjects	Sex (F)	Age (mean)	Acquisition Parameters				Neuroimaging Software
				Scanner Machine	*TE (ms)*	*TR (s)*	*FA*	
fMRI								
Alain et al 2010	28	15	26	3T Siemens Trio	30	2	70°	AFNI v.2.56a
Bartova et al 2015	42	25	25.3	3T Siemens Trio	42	2		AFNI
Beneventi et al 2007	12	6	25	1.5T Siemens Vision		6	50°	SPM99
Binder et al 2006	12	5	24.5	1.5T GE Signa	60	3	90°	SPM99
Binder et al 2006	12	5	24.5	1.5T GE Signa	60	3	90°	SPM99
Bleich-Cohen et al 2014	20	8	26.4	1.5T GE Sigma Horizon LX	55	3	90°	BrainVoyager 4.9
Blockland et al 2011	319	199	23.6	4T Bruker Medspec	30	2.1	90°	SPM5
Brahmbhatt et al 2010	35	8	20.5	1.5T Siemens Vision	50	3	90°	FIDL
Braver et al 1997	8	1	21.5	1.5T GE Signa	35	0.64	45°	AFNI
Cader et al 2006	16	15	37	3T	30	3		FEAT v.5
Cader et al 2006	16	15	37	3T	30	3		FEAT v.5
Callicot et al 1999	7	3	29.3	1.5T GE Signa	60	4	90°	SPM96
Campanella et al 2013	16	9	21.6	3T Philips Achieva	40	2.1	90°	SPM8
Carlson et al 1998	7	3	21.6	1.5T Siemens Vision	76	3.2	90°	XDS and MEDx
Carlson et al 1998	7	3	21.6	1.5T Siemens Vision	76	3.2	90°	XDS and MEDx
Carlson et al 1998	7	3	21.6	1.5T Siemens Vision	76	3.2	90°	XDS and MEDx
Caseras et al 2006	12	8	34.5	1.5T GE Excite	40	3		XBAM
Cerasa et al 2008	30	0	31	1.5T GE Signa	50	3	90°	SPM2
Choo et al 2005	12	9	21.8	3T Siemens Allegra		3		BrainVoyager 4.9
Cohen et al 1997	10	5	26	1.5T GE Signa	35	0.64	40°	AFNI
Dell'Osso et al 2015	27	15	29.4	3T Philips Achieva	35	2	90°	SPM8
Dima et al 2014	40	20	31.5	1.5T GE Signa	40	3	90°	SPM8
Dima et al 2014	40	20	31.5	1.5T GE Signa	40	3	90°	SPM8
Dima et al 2014	40	20	31.5	1.5T GE Signa	40	3	90°	SPM8
Drapier et al 2008	20	10	41.9	1.5T GE Signa	40	2	70°	XBAM
Drapier et al 2008	20	10	41.9	1.5T GE Signa	40	2	70°	XBAM
Drapier et al 2008	20	10	41.9	1.5T GE Signa	40	2	70°	XBAM
Druzgal et al 2001	9	4	24	1.5T GE Signa	50	2		SUN and Interactive Data Language
Duggirala et al 2016	50	22	23.6	3T Phillips Achieva	70	2	90°	SPM8
Duggirala et al 2016	50	22	23.6	3T Phillips Achieva	70	2	90°	SPM8
Duggirala et al 2016	50	22	23.6	3T Phillips Achieva	70	2	90°	SPM8
Elzinga et al 2006	14	14	34.6	1.5T Siemens AG	45	2.9		SPM2
Fonville et al 2015	149	103	20.5	3T GE Medical Systems	30	2	75°	SPM8
Fonville et al 2015	149	103	20.5	3T GE Medical Systems	30	2	75°	SPM8
Fonville et al 2015	149	103	20.5	3T GE Medical Systems	30	2	75°	SPM8
Forn et al 2007	10	5		1.5T GE Medical Systems	50	3		Brain Voyager QX
Frangou et al 2008	7		39	1.5T GE Neurovascular Sigma	40	3		Sun Microsystem and SPM99
Fusar-Poli et al 2010	34		25.5	1.5T GE Healthcare	40	2		SPM5
Garrett et al 2011	19	6	34.8	3T GE Signa	30	2	80°	SPM5
Garrett et al 2011	19	6	34.8	3T GE Signa	30	2	80°	SPM5
Georgiou-Karistianis et al 2013	23	16	42.5	1.5T Siemens AG	35	2.2	90°	SPM8
Gropman et al 2013	21	14	31.8	3T Siemens Trio	30	2.5	9°	SPM5
Harvey et al 2005	10	5	29	1.5T GE Signa	40	2	90°	SPM99
Huang et al 2016	18	12	43.1	1.5T Philips Medical Systems	45	2	90°	AFNI
Huang et al 2016	18	12	43.1	1.5T Philips Medical Systems	45	2	90°	AFNI
Jiang et al 2015	20	11	23.1	3T Siemens Trio	30	2	90°	SPM8
Jiang et al 2015	20	10	51.8	3T Siemens Trio	30	2	90°	SPM8
Kasahara et al 2011	9	5	31.9	3T Bruker MedSpec Avance S300	30	1.1	65°	SPM5
Kim et al 2006	12	3	34.4	3T Siemens Trio	17	4	90°	VoxBo and SPM99
Korsnes et al 2013	11	11	30.2	1.5T Siemens AG	60	3		SPM5
Koshino et al 2008	11	1	28.7	3T GE Medical Systems	18	1	70°	SPM99
Kumari et al 2006	13	0	33.3	1.5T GE Signa	40	3		SPM99
Kumari et al 2006	13	0	33.3	1.5T GE Signa	40	3		SPM99
LaBar et al 1999	11	4	32.6	1.5T Siemens AG	40	4.35	90°	SPM96
Lee et al 2013	14	5	64.8	3T Siemens Trio	30	3		AFNI
Li et al 2014	15	15	20.5	3T Siemens Trio	30	2	90°	SPM8
Li et al 2014	15	15	20.5	3T Siemens Trio	30	2	90°	SPM8
Li et al 2014	15	15	20.5	3T Siemens Trio	30	2	90°	SPM8
Lim et al 2008	12	7	68.8	1.5T Siemens Vision	60	3	90°	SPM2
Luo et al. 2014	22	0	23.1	3T Siemens Trio	25	2.18	80°	SPM8
Lythe et al 2012	20	0	26.7	1.5T GE Signa	40	3		SPM5
Marquand et al 2008	20	13	43.7	1.5T GE LX System	40	2		SPM5
Matsuo et al 2007	15	9	37.7	2T GE Prestige	45	2	90°	FSL
Matsuo et al 2007	15	9	37.7	2T GE Prestige	45	2	90°	FSL
Mattfeld et al 2016	17	6	28.7	3T Siemens Trio	30	2	90°	Nipype, Nipy, FSL, AFNI, FreeSurfer, ANTS and ART
Mcallister et al 1999	11	7	30.6	1.5T GE Signa	40	3		SPM96
Mcallister et al 1999	11	7	30.6	1.5T GE Signa	40	3		SPM96
Meisenzahl et al 2006	12	1	33.5	1.5T Siemens AG	0.6	60	90°	SPM99
Mendrek et al 2004	11			1.5T GE Signa	40	3	90°	SPM99
Mendrek et al 2004	12	3	27.7	1.5T GE Signa	40	3	90°	SPM99
Migo et al 2014	11	4	70.2	3T GE Medical Systems	30	2	75°	SPM8
Migo et al 2014	11	4	70.2	3T GE Medical Systems	30	2	75°	SPM8
Monks et al 2004	12	0	45.6	1.5T GE Signa	40	2.5	90°	locally written software previously validated

Table 3.2. Continued.

Nagel et al 2011	30	15	24.3	1.5T Siemens Vision	40	2.5	90°	FSL
Nagel et al 2011	30	15	63.5	1.5T Siemens Vision	40	2.5	90°	FSL
Nebel et al 2005	19	7	30.3	1.5T Siemens Sonata	45	3	90°	SPM99
Nebel et al 2005	17	11	26.4	1.5T Siemens Sonata	45	3	90°	SPM99
Norbury et al 2013	15	5	28.3	3T Siemens Trio	50	3	90°	FSL
Nyberg et al 2009	33	19	38.6	1.5T Philips Medical Systems	50	3	90°	SPM2
Perlstein et al 2003	15	6	36.4	1.5T GE Signa	35	2	80°	NIS
Philip et al 2015	13	9	30	3T Siemens Trio	28	2.5		AFNI
Philip et al 2015	13	9	30	3T Siemens Trio	28	2.5		AFNI
Pomarol-Clotet et al 2012	46	19	36.2	1.5T GE Signa	20	2	70°	FSL
Qin et al 2009	27	27	20.5	3T Siemens Trio	25	2.18	80°	SPM5
Ragland et al 2002	11	5	32.2	4T GE Signa	40	2	90°	MEDx 3.3 and SPM99
Ragland et al 2002	11	5	32.2	4T GE Signa	40	2	90°	MEDx 3.3 and SPM99
Ragland et al 2002	11	5	32.2	4T GE Signa	40	2	90°	MEDx 3.3 and SPM99
Ragland et al 2002	11	5	32.2	4T GE Signa	40	2	90°	MEDx 3.3 and SPM99
Ragland et al 2002	11	5	32.2	4T GE Signa	40	2	90°	MEDx 3.3 and SPM99
Ragland et al 2002	11	5	32.2	4T GE Signa	40	2	90°	MEDx 3.3 and SPM99
Rama et al 2001	8	8	23	1.5T Siemens Vision	70	3.55	90°	MEDx
Rama et al 2001	8	8	23	1.5T Siemens Vision	70	3.55	90°	MEDx
Ricciardi et al 2006	6	0	28	1.5T GE Signa	40	2.5	90°	AFNI
Rodríguez-Cano et al 2014	52	32	46.2	1.5T GE Signa	40	2	70°	FSL
Rodriguez-Jimenez et al 2009	13	6	30	1.5T GE Signa	40	3	90°	SPM5
Sanchez-Carrion et al 2008	14		24.2	1.5T GE Signa	40	2	90°	SPM2
Sanchez-Carrion et al 2008	14		24.2	1.5T GE Signa	40	2	90°	SPM2
Sapara et al 2014	20	5	31.9	1.5T GE Signa	40	3		SPM5
Sapara et al 2014	20	5	31.9	1.5T GE Signa	40	3		SPM5
Scheuerecker et al 2008	23	4	32.6	1.5T Siemens Vision	60	3	90°	SPM99
Schmidt et al 2009	46	21	33.7	1.5T GE Signa	40	3	90°	SPM2
Seo et al 2012	22	22	38.3	3T GE EXCITE	40	3		SPM5
Spreng et al 2014	36	19	22.3	3T GE Discovery MR750	25	2.5	80°	SPM8
Thomas et al 2005	16	5	37.6	3T Siemens Trio	30	2	90°	Brain Voyager 2000
Thornton et al 2013	14	9	22	3T Siemens Allegra	30	2	75°	SPM8
Trujillo et al 2015	35	15	56	3T GE Signa HDxt	30	2.1	80°	SPM8
Veltman et al 2003	22	15	22.7	1.5T Siemens Vision	60	3.48		SPM99
Walitt et al 2016	16	16	22.7	3T Siemens Trio	30	2.5	90°	SPM5
Yoo et al 2004	12	4	26.3	3T GE Signa Horizon	50	2.5	90°	SPM99
Yoo et al 2004	12	4	26.3	3T GE Signa Horizon	50	2.5	90°	SPM99
Yoo et al 2005	10	2	31.5	1.5T Siemens Vision	60	3	90°	SPM99
Ziemus et al 2007	9	3	44.2	1.5T Siemens Sonata	50	3.5	90°	SPM2
PET				*Scanner Machine*	*Resolution(mm)*	*Thickness (mm)*		
Awh et al 1996	9	9		Siemens ECAT EXACT	10	3.37		
Dade et al 2001	12	6	24.8	Siemens ECAT EXACT	4	4		
Jonides et al 1997	19			Siemens ECAT EXACT	10	3.37		
Jonides et al 1997	19			Siemens ECAT EXACT	10	3.37		
Jonides et al 1997	19			Siemens ECAT EXACT	10	3.37		
Kim et al 2002	14		24.8	Siemens ECAT EXACT	5.2	3.4		SPM99
Kim et al 2002	14		24.8	Siemens ECAT EXACT	5.2	3.4		SPM99
Kim et al 2002	14		24.8	Siemens ECAT EXACT	5.2	3.4		SPM99
Kim et al 2003	12		26.2	Siemens ECAT EXACT				SPM99
Schumacher et al 1996	8			Siemens ECAT EXACT	10	3.37		
Schumacher et al 1996	8			Siemens ECAT EXACT	10	3.37		

Working Memory Network

The resulting map and coordinates of the comprehensive set of activity patterns during n-back task execution are reported in Figure 3.2 and Table 3.3. The map includes 15 separate nodes highlighting a bilateral fronto-parietal distribution of activity. Moreover, additional contribution of regions in the left cerebellum, fusiform gyrus as well as in subcortical structures including the insula, claustrum, caudate and lentiform nucleus, are present.

Table 3.3. N-back nodes information. Volume, coordinates and corresponding Brodmann area, lobe, hemisphere and regional labels are reported for each cluster included in the ALE map for general n-back.

Cluster number	Volume (mm^3)	Weighted Center			Extrema Value	Extrema value coordinates			Brodmann Area	Hemisphere	Lobe	Label
		x	*y*	*z*		*x*	*y*	*z*				
1	20608	-41.2	11.6	34.6	0.089	-42	4	30	6	L	Frontal	Precentral Gyrus
					0.079	-28	2	54	6	L	Frontal	Middle Frontal Gyrus
					0.060	-46	26	30	9	L	Frontal	Middle Frontal Gyrus
					0.036	-52	14	4	44	L	Frontal	Precentral Gyrus
2	14288	-36.1	-51.1	46.2	0.128	-36	-50	44	40	L	Parietal	Inferior Parietal Lobule
					0.111	-42	-46	46	40	L	Parietal	Inferior Parietal Lobule
3	12968	1.6	19.2	46.4	0.116	4	20	46	6	R	Frontal	Medial Frontal Gyrus
					0.063	-4	10	58	6	L	Frontal	Medial Frontal Gyrus
4	11112	39.6	-52	45.8	0.138	44	-46	44	40	R	Parietal	Inferior Parietal Lobule
					0.072	34	-64	44	19	R	Parietal	Precuneus
5	9024	36.3	10.2	46.7	0.101	30	8	56	6	R	Frontal	Sub-gyral
					0.045	48	12	28	9	R	Frontal	Inferior Frontal Gyrus
6	7976	43.1	38.6	23	0.083	46	40	24	9	R	Frontal	Superior Frontal Gyrus
					0.077	44	32	30	9	R	Frontal	Middle Frontal Gyrus
					0.028	38	58	2	10	R	Frontal	Middle Frontal Gyrus
					0.027	40	58	-8	10	R	Frontal	Middle Frontal Gyrus
7	5456	-35.9	-62.5	-26.8	0.064	-30	-58	-34	.	L	Cerebellum	Cerebellar Tonsil
					0.037	-44	-66	-16	.	L	Cerebellum	Declive
					0.037	-46	-62	-14	37	L	Temporal	Fusiform Gyrus
8	5408	35.3	24.1	-4.2	0.134	34	24	-2	13	R	Sub-cortical	Insula
9	4920	-32.2	23.1	-3	0.109	-32	22	-2	.	L	Sub-cortical	Claustrum
10	3920	-15.5	-.4	8.8	0.069	-16	0	14	.	L	Sub-cortical	Caudate
					0.054	-16	0	2	.	L	Sub-cortical	Lentiform Nucleus
11	3904	-38.1	50.8	7.8	0.068	-38	52	10	10	L	Frontal	Middle Frontal Gyrus
12	3200	16.5	1.6	5.8	0.048	16	0	0	.	R	Sub-cortical	Lentiform Nucleus
					0.037	16	0	16	.	R	Sub-cortical	Caudate
13	2736	34.2	-62	-31.7	0.069	32	-62	-32	.	R	Cerebellum	.
					0.027	36	-68	-18	.	R	Cerebellum	Declive
14	2448	11.5	-64.9	54.9	0.048	8	-64	52	7	R	Parietal	Precuneus
					0.045	16	-66	60	7	R	Parietal	Precuneus
15	1664	-9	-65.8	51.9	0.040	-8	-68	48	7	L	Parietal	Precuneus
					0.035	-8	-62	54	7	L	Parietal	Precuneus

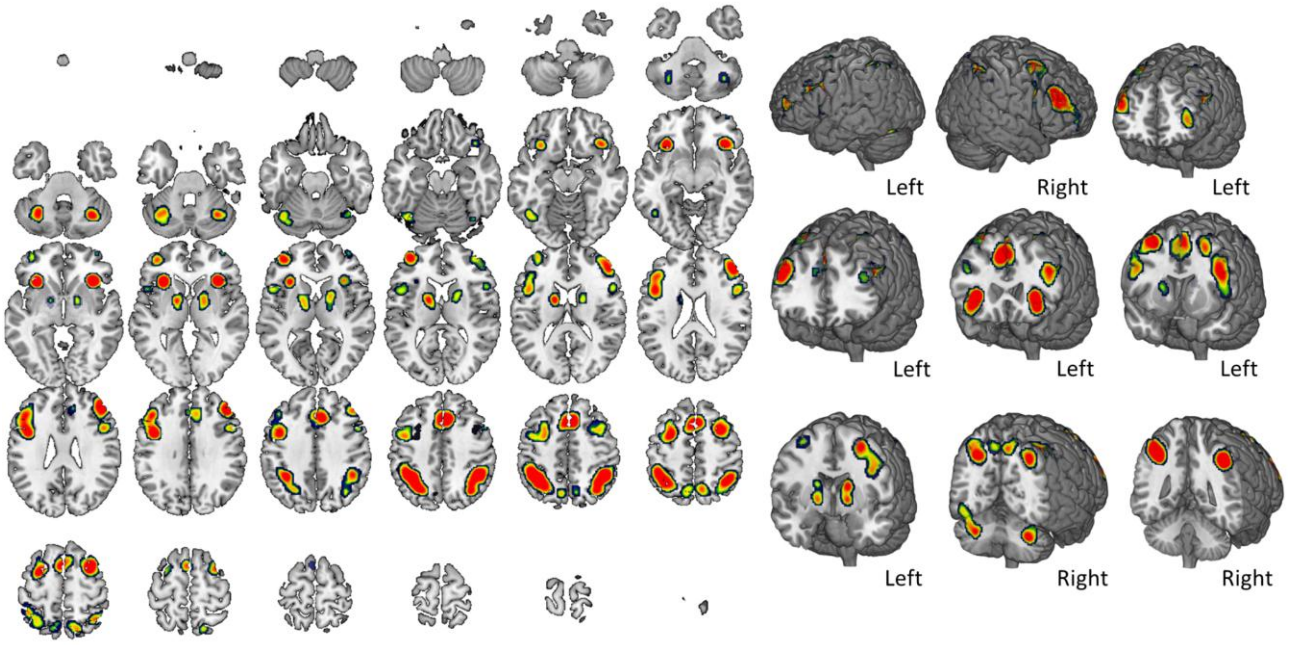

Figure 3.2. Brain activation during n-back task. The result of cluster-based statistics performed on the entire dataset of studies is shown. The map summarizes all 86 studies assessing n-back tasks considered in the meta-analysis, without distinction in material type or presentation modality. A complete set of coordinates for each cluster is available in Table 3.3.

N-back load

Activation patterns resulting from the contrasts between different n-back loads (high vs low) are reported in Figure 3.3A. The complete pool of studies was considered, without distinguishing in the nature of the stimuli presented across research efforts. Maps include different nodes of activation for different contrasts: the nodes for the contrast 3 vs 1 back are reported in green; 3 vs 2 back in blue and 2 vs 1 back in red color.

Anatomical and functional mapping

The difference between 3-back and 2/1-back maps highlighted clusters mostly located in the ACC and right cerebellum (Figure 3.3A). Significant clusters were mapped on the anatomo-functional cingulate parcellation by Neubert et al. (Neubert et al., 2015) and on the anatomo-functional cerebellar parcellation by Buckner et al. (Buckner et al., 2011). Significant nodes of interest in the 3 back vs 1 back map were found to overlap with 4 regions belonging to the aforementioned parcellation by Neubert (Figure 3.3B): i) area8m (shown in red), representing an area in the medial portion of the human superior frontal gyrus extending down to the paracingulate sulcus; ii) right

area 25 (shown in blue), i.e., the subgenual area; iii) right anterior rostral cingulate zone (RCZa) (shown in purple); vi) right posterior rostral cingulate zone (RCZp) (shown in cyan).

Of those, rostral regions have already proven to be implicated in learning and in the update of choices' value (Walton et al., 2004), as well as in cognitive control tasks (Picard & Strick, 1996).

The 3 vs 2 back contrast showed overlap with the same areas of the 3 vs 1 back map (8m, area 25, right RCZp) with the addition of left RCZp (shown in yellow) (Figure 3.3 C). For what concerns the difference between 2 back vs 1 back maps, a significant node of interest in the contrast was found to correspond with the crus I region of the cerebellar parcellation by Buckner (Figure 3.3 D).

To characterize the spontaneous functional connectivity of ACC and crus I, a seed-to-voxel analysis was run on a database of 1000 healthy participant from Yeo et al., 2011. Unthreshold functional connectivity maps are shown in Figure 3.3 B, C and D.

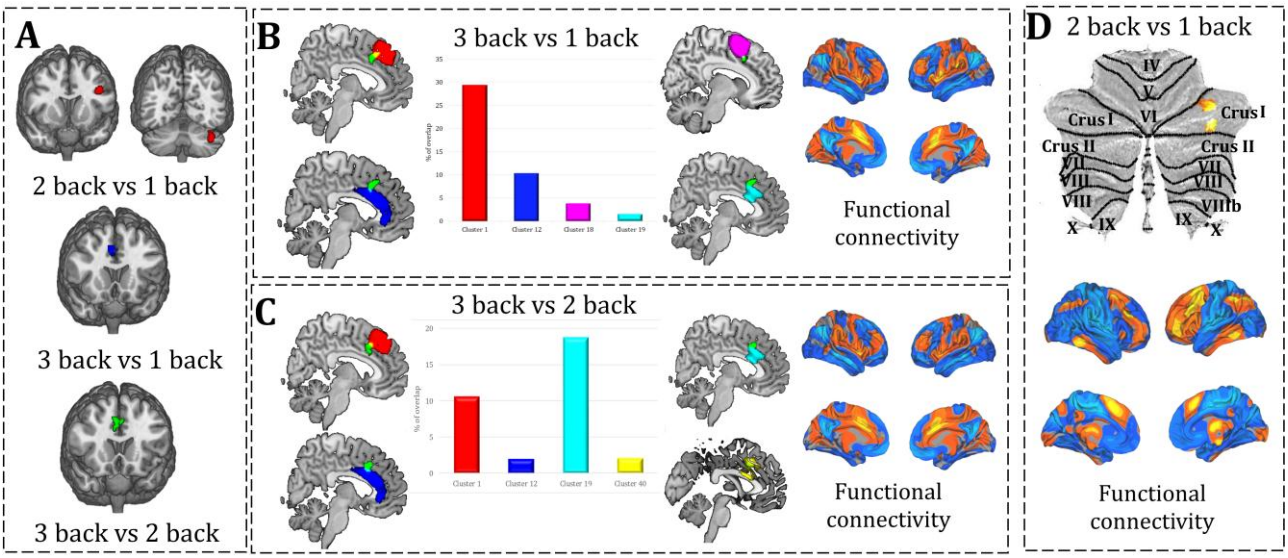

Figure 3.3. Anatomical and functional mapping of nodes resulting from contrast maps. (A) Cerebral and cerebellar nodes active as a function of task load as revealed by contrast maps. (B) and (C) Mapping of ACC activation (3 vs 1 back and 3 vs 2 back) and their respective overlap quantification for each cluster. Unthreshold maps of functional connectivity are shown to the right of each panel. (D) Mapping of cerebellar activation (2 back vs 1 back) and unthreshold maps of functional connectivity.

Verbal n-back

Figure 3.4 and Table 3.4 report neural activation patterns during verbal n-back tasks, without distinguishing between type of stimuli (letters, numbers or words). The map includes 21 clusters (i.e., nodes) of activation highlighting an involvement of the bilateral frontal and parietal cortices and of the cerebellum and of various other subcortical structures bilaterally.

Maps and coordinates of the activity patterns elicited during the performance of letters or numbers n-back tasks are shown in Figure 3.5 and 3.6 and Table 3.5 and 3.6. N-back tasks using letters as stimuli show a readily visible fronto-parietal activation, left lateralized over frontal structures. Moreover, an involvement of the bilateral cerebellum and subcortical structures is reported in the map. A right-lateralized activation of the thalamus is also observed, despite not being generally reported as a meaningful seed during verbal n-back tasks (Figure 3.4, Table 3.4).

For what concerns n-back tasks characterized by the visual presentation of numbers, 11 clusters of activity emerge (Table 3.6), involving mostly the parietal cortex bilaterally, the medial frontal cortex, the right and left insula and the anterior lobe of the cerebellum in both hemispheres (Figure 3.6).

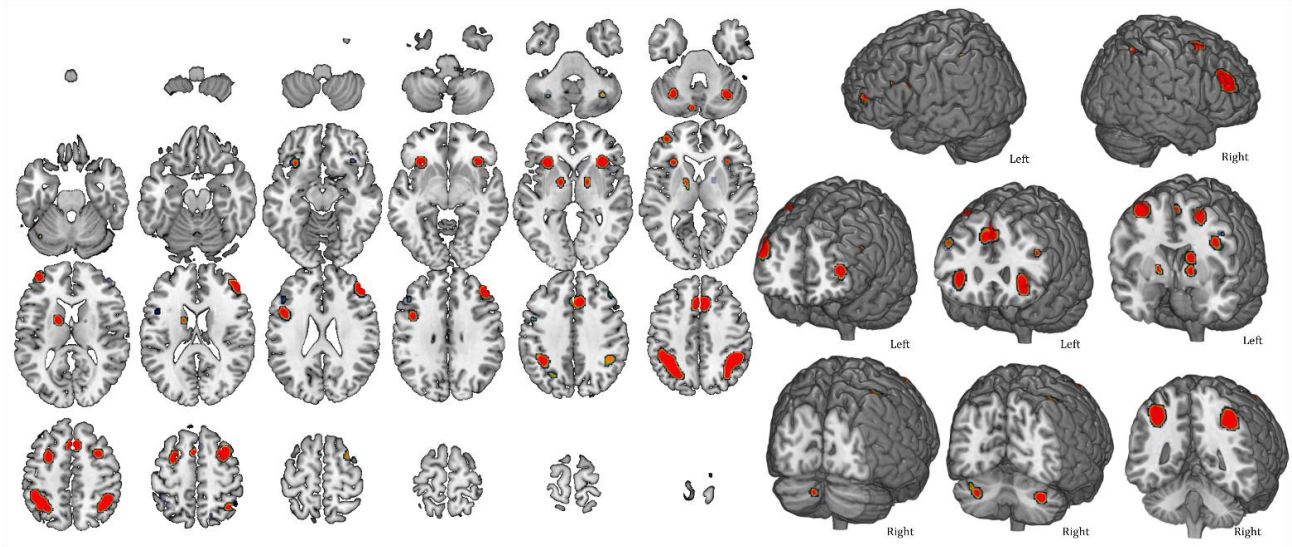

Figure 3.4. Areas of activation during verbal n-back tasks. The map refers to 62 verbal n-back studies in which stimuli (letters, numbers or words) were presented visually. A complete set of coordinates for each cluster is available in Table 3.4.

Table 3.4. Activity patterns in verbal n-back tasks. Volume, coordinates and corresponding Brodmann area, lobe, hemisphere and regional labels are reported for each cluster included in the ALE map for verbal n-back.

Cluster number	Volume (mm^3)	Weighted Center			Extrema Value	Extrema value coordinates			Brodmann Area	Hemisphere	Lobe	Label
		x	*y*	*z*		*x*	*y*	*z*				
1	6800	-36	-50	45.2	0.104	-36	-48	42	40	L	Parietal	Inferior Parietal Lobule
					0.063	-30	-58	44	39	L	Parietal	Angular Gyrus
2	5168	40.1	-49.7	45.7	0.111	44	-46	46	40	R	Parietal	Inferior Parietal Lobule
					0.046	34	-64	44	19	R	Parietal	Precuneus
3	4752	2.4	19.6	45.2	0.096	4	20	44	6	R	Frontal	Medial Frontal Gyrus
					0.043	-4	8	58	6	L	Frontal	Medial Frontal Gyrus
4	3568	45.1	37.9	25.7	0.064	46	40	24	9	R	Frontal	Superior Frontal Gyrus
					0.059	46	34	30	9	R	Frontal	Middle Frontal Gyrus
5	2376	31.2	8.3	56	0.083	30	8	56	6	R	Frontal	Sub-Gyral
6	2216	-32.2	23	-3.6	0.082	-32	22	-2	.	L	Sub-cortical	Claustrum
7	1880	34.2	23.8	-2	0.090	34	24	0	13	R	Sub-cortical	Insula
8	1632	-27.7	4.4	53.5	0.062	-28	2	54	6	L	Frontal	Middle Frontal Gyrus
9	1480	-44.8	8.5	27	0.052	-42	6	28	6	L	Frontal	Precentral Gyrus
10	1360	-16.1	.2	8.7	0.060	-16	0	14	.	L	Sub-cortical	Caudate
					0.052	-16	0	0	.	L	Sub-cortical	Lentiform Nucleus
11	944	-39.1	51.6	9.5	0.059	-40	52	10	46	L	Frontal	Middle Frontal Gyrus
12	792	33.2	-62.4	-33.5	0.057	34	-64	-34	.	R	Cerebellum	Cerebellar Tonsil
13	680	-32.1	-62	-32.8	0.046	-30	-62	-34	.	L	Cerebellum	Cerebellar Tonsil
14	328	16.3	0	.6	0.041	16	0	0	.	R	Sub-cortical	Lentiform Nucleus
15	192	-8.5	-78	-32	0.048	-8	-78	-32	.	L	Cerebellum	Pyramis
16	184	-47.5	25.4	27.9	0.037	-48	26	28	9	L	Frontal	Middle Frontal Gyrus
17	56	-48.3	2.3	38.9	0.033	-48	2	38	6	L	Frontal	Precentral Gyrus
18	24	16.7	0	15.3	0.035	16	0	16	.	R	Sub-cortical	Caudate
19	24	16	-65.3	58.7	0.033	16	-66	58	7	R	Parietal	Precuneus
20	8	0	-48	-22	0.033	0	-48	-22	.	L	Cerebellum	Cerebellar Lingual
21	8	-12	-66	54	0.033	-12	-66	54	7	L	Parietal	Precuneus

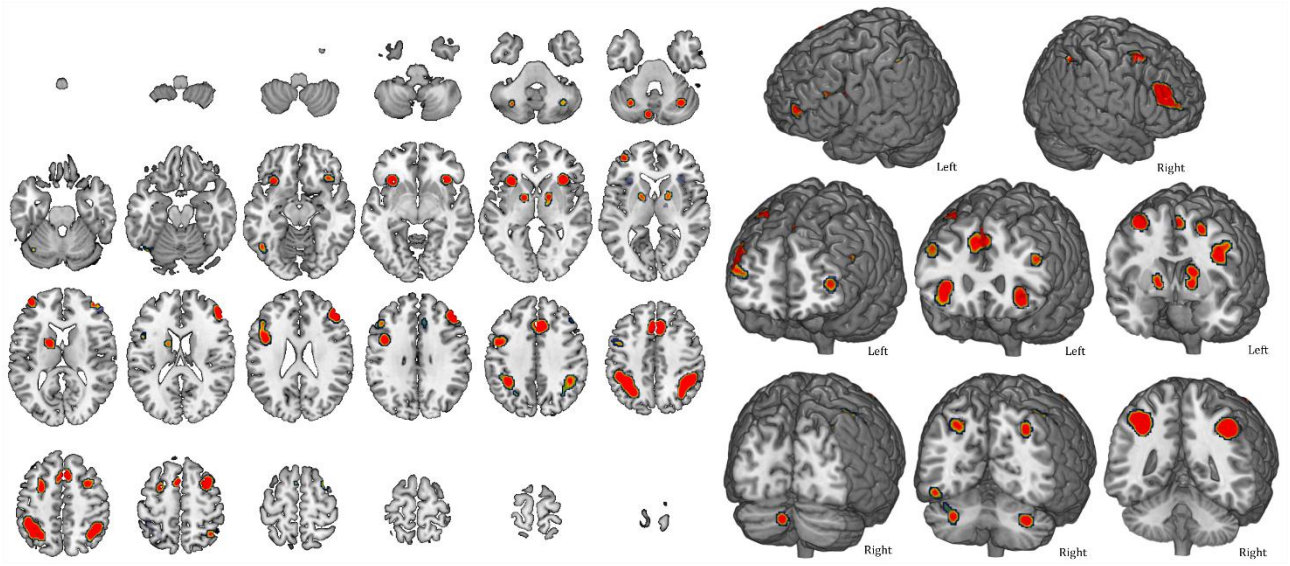

Figure 3.5. Average activity during letter n-back tasks. The map refers to studies that only used letters as stimuli (50). A complete set of coordinates for each cluster is available in Table 3.5.

Table 3.5. Activity patterns for letter n-back tasks. Volume, coordinates and corresponding Brodmann area, lobe, hemisphere and regional labels are reported for each cluster included in the ALE map for letter n-back.

Cluster number	Volume (mm^3)	Weighted Center			Extrema Value	Extrema value coordinates			Brodmann Area	Hemisphere	Lobe	Label
		x	*y*	*z*		*x*	*y*	*z*				
1	7920	-36.4	-49.09	45.35	0.086	-36	-48	42	40	L	Parietal	Inferior Parietal Lobule
					0.057	-44	-42	48	40	L	Parietal	Inferior Parietal Lobule
					0.049	-28	-58	46	7	L	Parietal	Superior Parietal Lobule
2	6616	2.19	19.92	44.69	0.076	4	20	44	6	R	Frontal	Medial Frontal Gyrus
					0.038	-4	10	56	6	L	Frontal	Medial Frontal Gyrus
3	6344	40.12	-50.39	45.26	0.077	44	-46	46	40	R	Parietal	Inferior Parietal Lobule
					0.052	36	-54	48	7	R	Parietal	Inferior Parietal Lobule
4	5032	45.14	38.44	24.49	0.062	46	40	24	9	R	Frontal	Superior Frontal Gyrus
					0.029	40	52	12	10	R	Frontal	Middle Frontal Gyrus
5	4080	-45.07	8.71	30.67	0.050	-42	6	28	6	L	Frontal	Precentral Gyrus
					0.033	-48	2	38	6	L	Frontal	Precentral Gyrus
					0.029	-46	26	28	9	L	Frontal	Middle Frontal Gyrus
6	2472	31.93	9.21	55.85	0.062	30	8	54	6	R	Frontal	Sub-Gyral
7	2440	-32.58	22.31	-5.41	0.073	-32	22	-4	.	L	Sub-cortical	Claustrum
8	2224	34.68	23.81	-3.85	0.066	34	24	-2	13	R	Sub-cortical	Insula
9	1816	-16.46	1.36	8.92	0.050	-16	2	14	.	L	Sub-cortical	Caudate
					0.044	-16	0	0	.	L	Sub-cortical	Lentiform Nucleus
10	1344	-27.12	4.54	52.5	0.048	-28	2	52	6	L	Frontal	Middle Frontal Gyrus
11	1160	-39.41	52.62	9.74	0.045	-40	52	10	46	L	Frontal	Middle Frontal Gyrus
12	824	15.57	.66	1.3	0.035	16	2	0	.	R	Sub-cortical	Lentiform Nucleus
					0.025	14	-6	0	.	R	Sub-cortical	Thalamus
13	720	32.83	-63.53	-33.84	0.045	32	-64	-34	.	R	Cerebellum	Cerebellar Tonsil
14	656	-31.93	-64.21	-33.44	0.037	-30	-64	-34	.	L	Cerebellum	Cerebellar Tonsil
					0.024	-38	-66	-26	.	L	Cerebellum	Tuber
15	568	-46.06	-63.51	-15.36	0.031	-46	-64	-16	37	L	Temporal	Fusiform Gyrus
16	480	-8.72	-78.15	-32.26	0.045	-8	-78	-32	.	L	Cerebellum	Pyramis

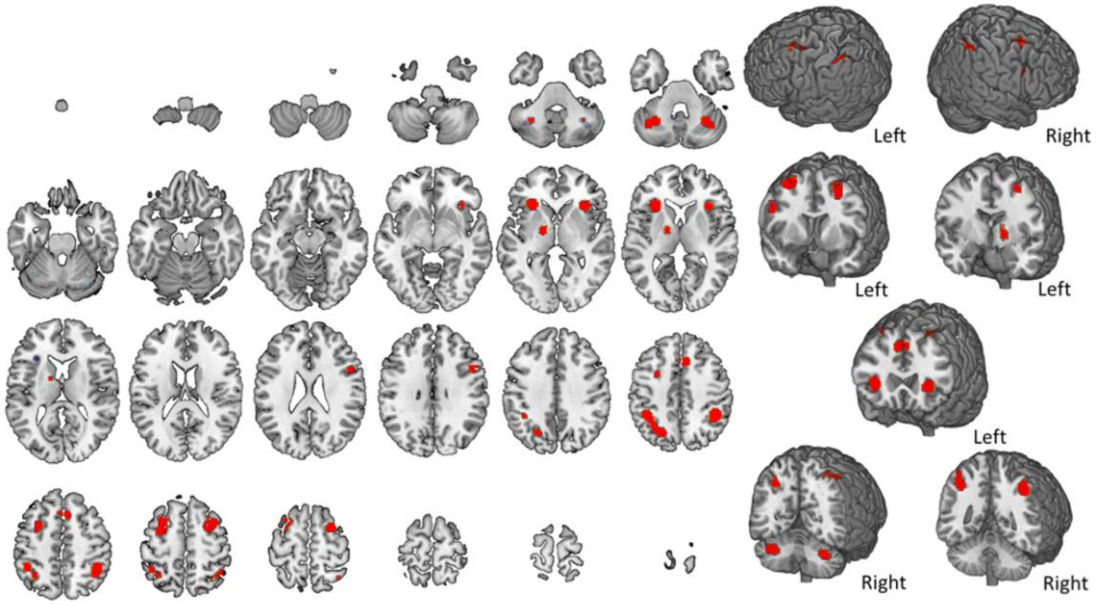

Figure 3.6. Brain activity during number n-back tasks. The map refers to 12 number n-back studies. A complete set of coordinates for each cluster is available in Table 3.6.

Table 3.6. Activity patterns in number n-back tasks. Volume, coordinates and corresponding Brodmann area, lobe, hemisphere and regional labels are reported for each cluster included in the ALE map for number n-back.

Cluster number	Volume (mm^3)	Weighted Center			Extrema Value	Extrema value coordinates			Brodmann Area	Hemisphere	Lobe	Label
		x	*y*	*z*		*x*	*y*	*z*				
1	3576	-34.8	-53.4	45.7	0.024	-40	-46	44	40	L	Parietal	Inferior Parietal Lobule
					0.023	-24	-66	42	7	L	Parietal	Precuneus
					0.016	-34	-54	54	7	L	Parietal	Superior Parietal Lobule
					0.015	-42	-48	58	40	L	Parietal	Inferior Parietal Lobule
2	2792	-29	5.6	55.3	0.023	-30	0	58	6	L	Frontal	Middle Frontal Gyrus
3	2664	41.3	-47.2	47.7	0.043	42	-44	46	40	R	Parietal	Inferior Parietal Lobule
					0.013	34	-58	60	7	R	Parietal	Superior Parietal Lobule
4	1928	28.2	6	57.8	0.028	28	4	58	6	R	Frontal	Sub-Gyral
5	1632	-30.5	24.6	3.1	0.027	-30	26	2	13	L	Sub-cortical	Insula
6	1328	33.9	23.7	.5	0.031	34	24	2	13	R	Sub-cortical	Insula
7	1264	-34.1	-59.4	-32.6	0.021	-32	-58	-32	.	L	Cerebellum	Anterior Lobe
8	1152	3.9	19.4	46.8	0.023	6	20	46	6	R	Frontal	Medial Frontal Gyrus
					0.013	-4	22	48	8	L	Frontal	Superior Frontal Gyrus
9	1064	32.3	-59.6	-32.3	0.023	30	-58	-32	.	R	Cerebellum	Anterior Lobe
10	816	49	11	28.7	0.017	50	10	28	9	R	Frontal	Inferior Frontal Gyrus
11	736	-16.6	-5.4	2.2	0.020	-18	-6	0	.	L	Sub-cortical	Lentiform Nucleus
					0.012	-16	0	12	.	L	Sub-cortical	Caudate

Visual – non-verbal n-back

Brain activity during non-verbal n-back tasks and their corresponding set of coordinates are reported in Figure 3.7 and Table 3.7. Studies ultimately considered in this section refer to those in which non-verbal stimuli (e.g., images, faces, objects) were visually presented during task execution. Figure 3.7 shows the results of 15 studies, without any distinction in material type. The map includes 9 nodes highlighting the involvement of the left frontal cortex, the inferior parietal lobule bilaterally and various subcortical structures, including the left insula and the right claustrum, right limbic structures— in particular the cingulate gyrus— and the left cerebellum. No active nodes were found over temporal lobe regions.

When the same studies were differentiated based on stimuli' s characteristics, two different maps and tables of coordinates emerged. Figure 3.8 and Table 3.8 refer to those studies in which faces were presented as stimuli. Six clusters (i.e., nodes) of activity over the left frontal and parietal cortices and subcortical structures (left insula and right claustrum mainly) are shown. Similarly to what is observed for the general non-verbal map, no activity in the temporal lobe is reported during face n-back tasks.

Figure 3.9 and Table 3.9 refer instead to those studies in which object or images were used as stimuli. The resulting map shows 6 activation clusters, involving the frontal cortex bilaterally, the left parietal cortex— in particular the inferior parietal lobule—, various subcortical structures

bilaterally and the right cingulate gyrus. Neither the cerebellum nor the temporal lobe showed an involvement within this type of task stimuli.

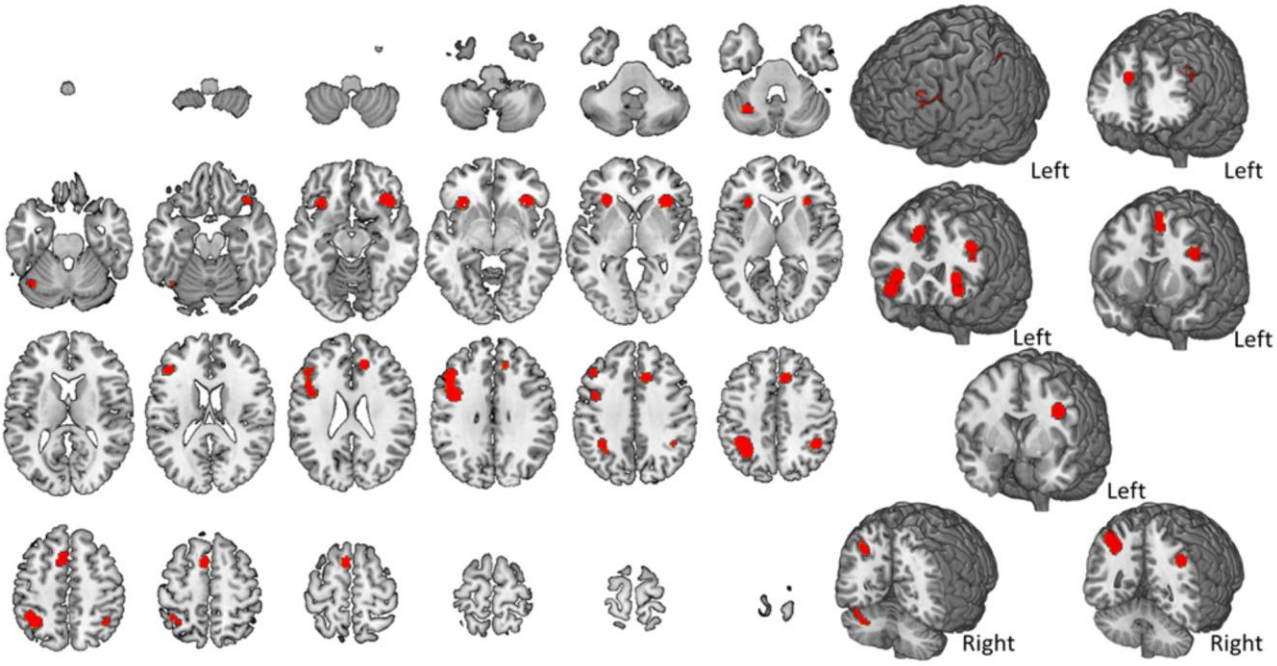

Figure 3.7. Average activity during visual- non verbal n-back tasks. The map refers to 15 studies relying on non-verbal n-back tasks where stimuli (faces, objects, images) were presented visually. A complete set of coordinates for each cluster is available in Table 3.7.

Table 3.7. Activity patterns for visual- non-verbal n-back tasks. Volume, coordinates and corresponding Brodmann area, lobe, hemisphere and regional labels are reported for each cluster included in the ALE map for non-verbal n-back.

Cluster number	Volume (mm^3)	Weighted Center			Extrema Value	Extrema value coordinates			Brodmann Area	Hemisphere	Lobe	Label
		x	*y*	*z*		*x*	*y*	*z*				
1	4216	-44.2	15.2	29.9	0.029	-42	4	32	6	L	Frontal	Precentral Gyrus
					0.023	-46	24	32	9	L	Frontal	Middle Frontal Gyrus
					0.022	-44	28	34	9	L	Frontal	Precentral Gyrus
					0.017	-44	30	20	46	L	Frontal	Middle Frontal Gyrus
2	3800	-35.6	-50.8	45.9	0.029	-34	-52	44	40	L	Parietal	Inferior Parietal Lobule
					0.023	-40	-48	50	40	L	Parietal	Inferior Parietal Lobule
3	3208	35	25.4	-6.4	0.037	32	24	0	.	R	Sub-cortical	Claustrum
					0.022	40	24	-14	47	R	Frontal	Inferior Frontal Gyrus
4	2072	-31.7	24.1	-4.6	0.024	-34	22	-10	47	L	Frontal	Inferior Frontal Gyrus
					0.021	-30	26	2	13	L	Sub-cortical	Insula
5	2008	-6.3	12.6	54.7	0.023	-6	16	50	6	L	Frontal	Superior Frontal Gyrus
					0.019	-6	10	62	6	L	Frontal	Medial Frontal Gyrus
6	1120	10.2	22.3	41	0.021	12	22	40	32	R	Limbic	Cingulate Gyrus
7	1032	41.2	-48.8	44.3	0.022	42	-48	44	40	R	Parietal	Inferior Parietal Lobule
8	728	-35.9	-61.8	-28.3	0.014	-40	-62	-24	.	L	Cerebellum	Declive
					0.014	-36	-62	-30	.	L	Cerebellum	.
9	632	12.5	35.9	25.9	0.020	12	36	26	32	R	Limbic	Cingulate Gyrus

.

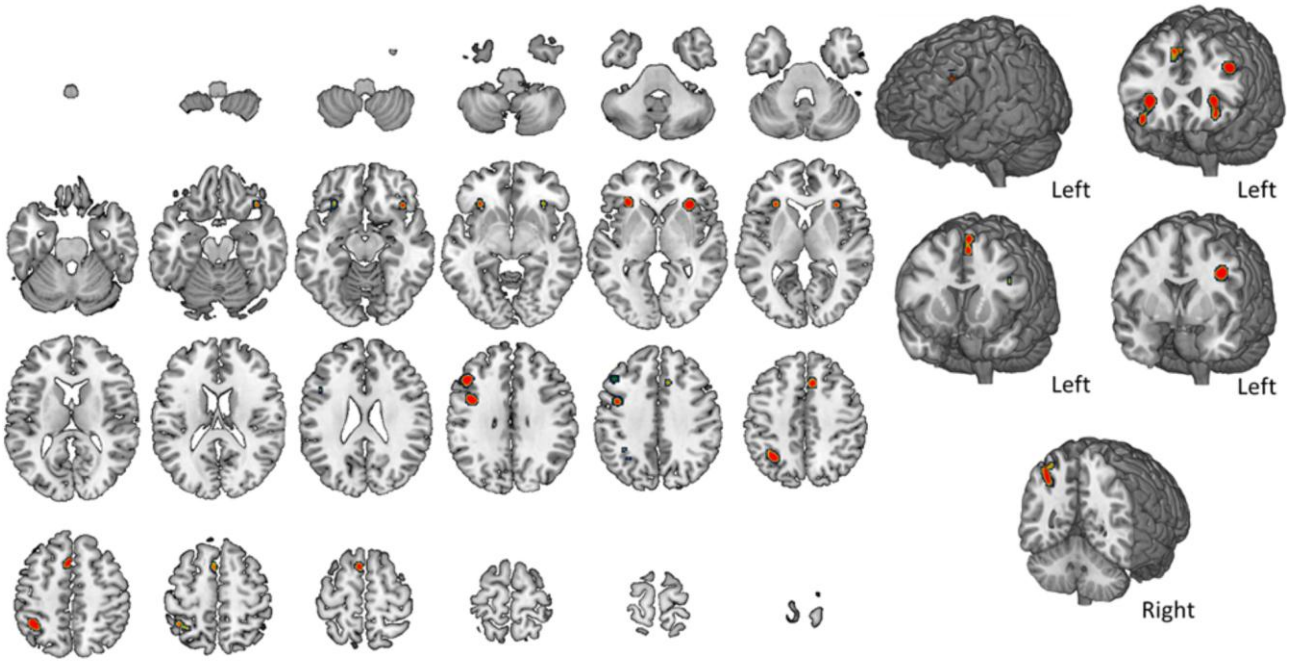

Figure 3.8. Brain activity during face n-back tasks. The map summarizes findings from 9 studies. A complete set of coordinates for each cluster is available in Table 3.8.

Table 3.8. Activation patterns for face n-back tasks. Volume, coordinates and corresponding Brodmann area, lobe, hemisphere and regional labels are reported for each cluster included in the ALE map for face n-back.

Cluster number	Volume (mm^3)	Weighted Center			Extrema Value	Extrema value coordinates			Brodmann Area	Hemisphere	Lobe	Label
		x	*y*	*z*		*x*	*y*	*z*				
1	1768	0	16.8	51.3	0.015	-4	16	52	6	L	Frontal	Superior Frontal Gyrus
					0.013	-6	12	64	6	L	Frontal	Medial Frontal Gyrus
					0.013	8	22	44	6	R	Frontal	Medial Frontal Gyrus
2	1752	-36.3	-51.9	48	0.018	-40	-48	52	40	L	Parietal	Inferior Parietal Lobule
					0.016	-32	-58	42	39	L	Parietal	Angular Gyrus
					0.010	-36	-48	38	40	L	Parietal	Supramarginal Gyrus
					0.010	-32	-52	58	7	L	Parietal	Superior Parietal Lobule
3	1328	33.2	25.2	-3.6	0.023	32	26	2	.	R	Sub-cortical	Claustrum
					0.013	38	24	-16	47	R	Frontal	Inferior Frontal Gyrus
4	1064	-31.4	26.8	-2.3	0.017	-30	28	2	13	L	Sub-cortical	Insula
					0.012	-32	26	-10	47	L	Frontal	Inferior Frontal Gyrus
5	928	-41.8	3.6	32.7	0.017	-42	2	34	6	L	Frontal	Precentral Gyrus
6	832	-45.8	24.3	31.8	0.018	-46	26	32	9	L	Frontal	Middle Frontal Gyrus
					0.010	-46	14	26	9	L	Frontal	Inferior Frontal Gyrus

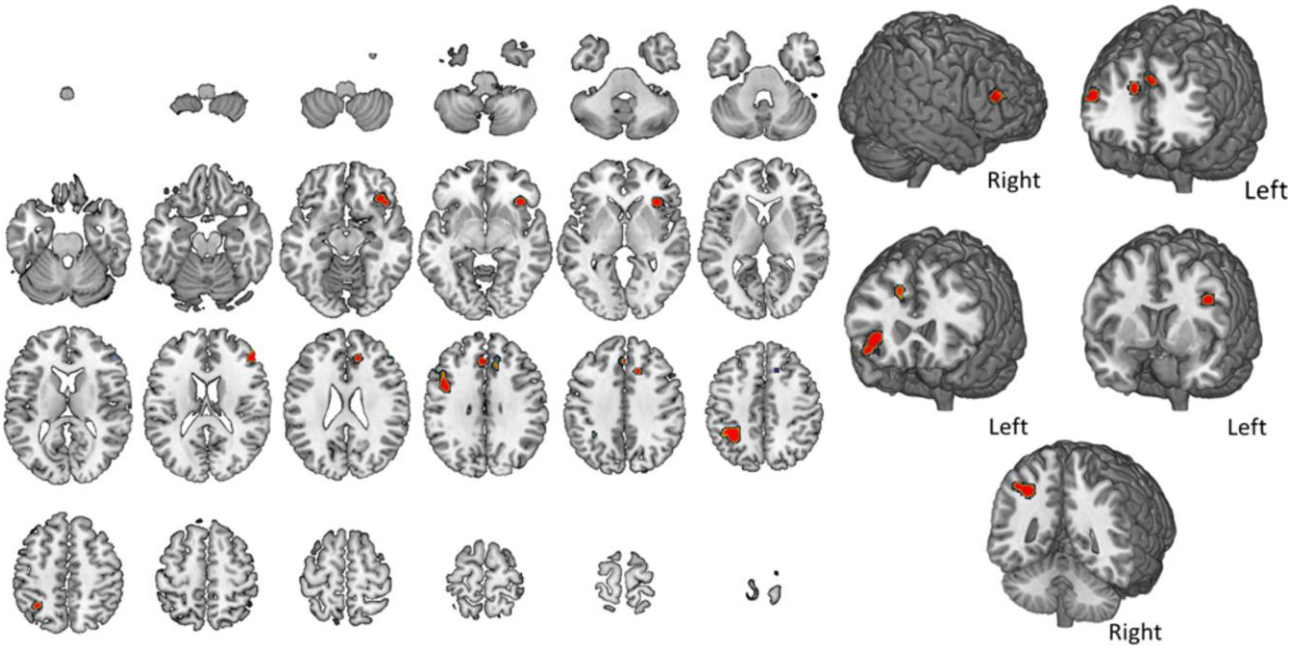

Figure 3.9. Average of the activity during objects/images n-back. The map summarizes findings from 6 studies. A complete set of coordinates for each cluster is available in Table 3.9.

Table 3.9. Activity patterns for objects/images n-back tasks. Volume, coordinates and corresponding Brodmann area, lobe, hemisphere and regional labels are reported for each cluster included in the ALE map for objects/images n-back.

Cluster number	Volume (mm^3)	Weighted Center			Extrema Value	Extrema value coordinates			Brodmann Area	Hemisphere	Lobe	Label
		x	*y*	*z*		*x*	*y*	*z*				
1	1952	-34.3	-48.7	44.4	0.019	-32	-50	44	40	L	Parietal	Inferior Parietal Lobule
					0.012	-44	-48	46	40	L	Parietal	Inferior Parietal Lobule
2	1664	36.5	25.6	-6.9	0.018	34	24	-2	13	R	Sub-cortical	Insula
					0.012	38	30	-12	47	R	Frontal	Inferior Frontal Gyrus
					0.012	42	24	-12	47	R	Sub-cortical	Extra-Nuclear
3	904	-44.5	8	30.6	0.014	-44	6	30	9	L	Frontal	Inferior Frontal Gyrus
					0.011	-46	20	30	9	L	Frontal	Inferior Frontal Gyrus
4	864	12.3	30.1	30.8	0.013	12	36	26	32	R	Limbic	Cingulate Gyrus
					0.012	14	22	38	32	R	Limbic	Cingulate Gyrus
5	792	48.1	37.7	18.1	0.014	48	36	18	46	R	Frontal	Middle Frontal Gyrus
6	688	-2.6	33	33.2	0.015	-4	34	32	6	L	Frontal	Medial Frontal Gyrus

Spatial n-back

Studies characterized by the spatial presentation of stimuli were selected and their results displayed (Figure 3.10). Spatial n-back requires to monitor the location of dots within a diamond shaped box on the screen at a given delay from the original occurrence (0-, 1-, or 2-back)(Kumari et al., 2006). Coordinates of brain activity for this type of task are shown in Table 3.10. A great involvement of the parietal cortex bilaterally and of the bilateral frontal regions, right cingulate

gyrus and right insula are shown. Neither the cerebellum nor the temporal lobe showed an involvement in this type of task.

Auditory n-back

Map and coordinates of the activity patterns elicited during the performance of auditory n-back tasks are shown in Figure 3.11 and Table 3.11. The distinction is hereby made based on presentation modality, rather than on stimuli's type, such as that only studies characterized by the auditory presentation of stimuli were considered in this section. The map includes 5 separate nodes highlighting the involvement of left frontal regions and of the parietal lobe bilaterally, aided by the co-activation of the right cingulate gyrus and left insula. Both the cerebellum and the temporal lobe failed to show an involvement in this type of task.

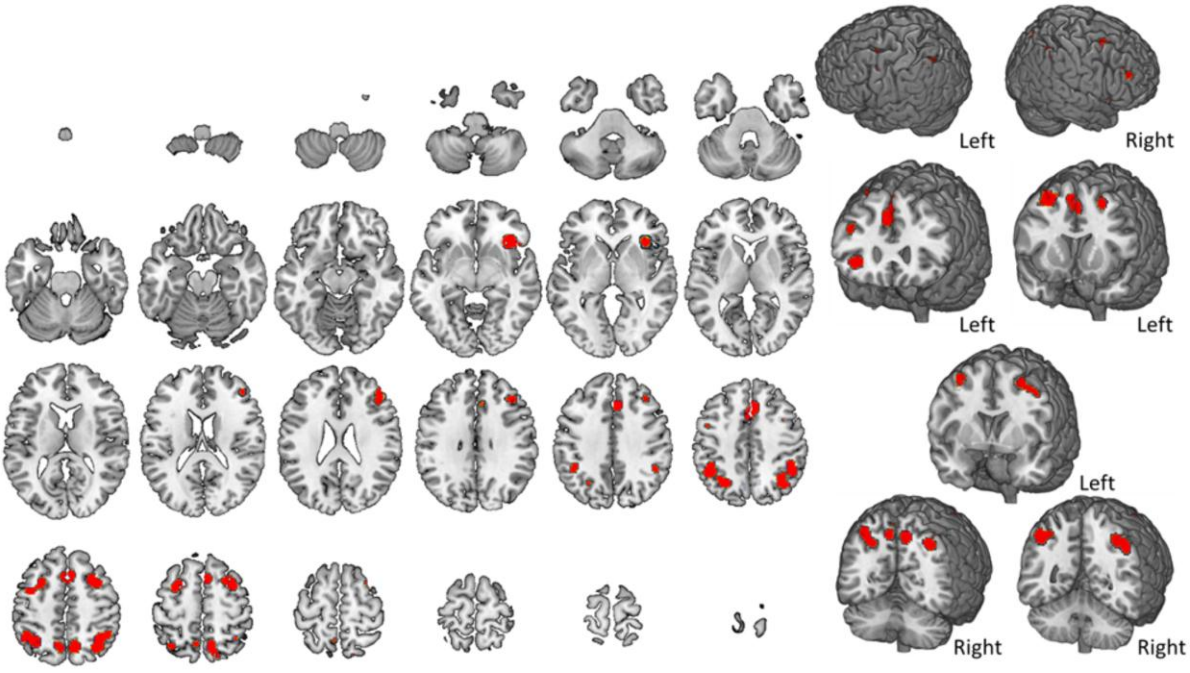

Figure 3.10. Brain activity during spatial n-back tasks. The map summarizes findings from 9 studies. A complete set of coordinates for each cluster is available in Table 3.10.

Table 3.10. Spatial n-back activation foci. Volume, coordinates and corresponding Brodmann area, lobe, hemisphere and regional labels are reported for each cluster included in the ALE map for spatial n-back.

Cluster number	Volume (mm^3)	Weighted Center			Extrema Value	Extrema value coordinates			Brodmann Area	Hemisphere	Lobe	Label
		x	*y*	*z*		*x*	*y*	*z*				
1	3784	39.2	-54	46.8	0.028	36	-54	50	7	R	Parietal	Inferior Parietal Lobule
					0.022	34	-64	48	19	R	Parietal	Precuneus
					0.020	46	-48	44	40	R	Parietal	Inferior Parietal Lobule
2	3656	-38.3	-53.8	45.9	0.028	-44	-48	44	40	L	Parietal	Inferior Parietal Lobule
					0.021	-28	-62	42	7	L	Parietal	Precuneus
					0.019	-34	-56	50	7	L	Parietal	Inferior Parietal Lobule
3	3272	2.5	18.4	46.2	0.024	0	16	48	32	L	Frontal	Medial Frontal Gyrus
					0.024	4	14	54	6	R	Frontal	Superior Frontal Gyrus
					0.022	4	24	38	32	R	Limbic	Cingulate Gyrus
4	2280	29.8	10	53.6	0.030	28	12	52	6	R	Frontal	Sub-Gyral
5	1760	36.8	23.6	-5.1	0.029	36	24	-6	13	R	Sub-cortical	Insula
					0.014	46	20	-6	.	R	Sub-cortical	Insula
6	1632	-31	5.3	52.9	0.024	-28	6	54	6	L	Frontal	Sub-Gyral
					0.015	-40	0	50	6	L	Frontal	Middle Frontal Gyrus
7	1544	9.8	-63.8	52.9	0.027	10	-62	52	7	R	Parietal	Precuneus
					0.017	14	-72	58	7	R	Parietal	Precuneus
8	1408	41.1	34.4	26.8	0.018	44	40	22	9	R	Frontal	Middle Frontal Gyrus
					0.016	42	30	26	9	R	Frontal	Middle Frontal Gyrus
9	752	-7.9	-62	51.6	0.016	-8	-60	54	7	L	Parietal	Precuneus
					0.014	-8	-66	48	7	L	Parietal	Precuneus

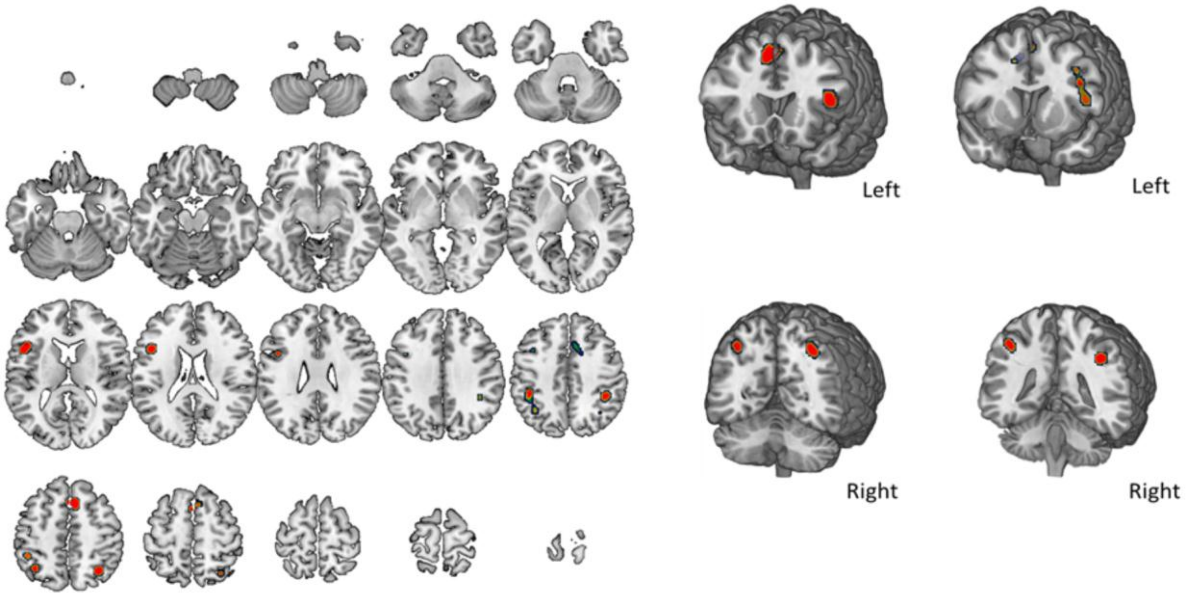

Figure 3.11. Areas of activity during auditory n-back task. The map refers to 7 auditory n-back studies. A complete set of coordinates for each cluster is available in Table 3.11.

Table 3.11. Auditory n-back activation foci. Volume, coordinates and corresponding Brodmann area, lobe, hemisphere and regional labels are reported for each cluster included in the ALE map for auditory n-back.

Cluster number	Volume (mm^3)	Weighted Center			Extrema Value	Extrema value coordinates			Brodmann Area	Hemisphere	Lobe	Label
		x	*y*	*z*		*x*	*y*	*z*				
1	1936	4.2	17.7	50.8	0.017	6	20	50	6	R	Frontal	Superior Frontal Gyrus
					0.016	2	20	50	6	L	Frontal	Superior Frontal Gyrus
					0.010	-2	12	56	6	L	Frontal	Superior Frontal Gyrus
					0.008	14	8	44	24	R	Limbic	Cingulate Gyrus
2	1736	-46	14.1	18.1	0.015	-46	16	16	13	L	Sub-cortical	Insula
					0.010	-44	8	28	9	L	Frontal	Inferior Frontal Gyrus
					0.008	-40	10	40	9	L	Frontal	Precentral Gyrus
3	1480	-40.6	-47.1	46.1	0.013	-36	-58	48	39	L	Parietal	Inferior Parietal Lobule
					0.012	-44	-42	46	40	L	Parietal	Inferior Parietal Lobule
4	872	31.5	-60.5	51.2	0.013	32	-60	50	7	R	Parietal	Superior Parietal Lobule
					0.013	30	-62	54	7	R	Parietal	Superior Parietal Lobule
5	680	39.8	-41.2	40.4	0.015	40	-42	40	40	R	Parietal	Inferior Parietal Lobule

N-back and resting state networks

The overlap between RSNs and n-back maps is presented in Figure 3.12. For the general n-back map, an overlap equal to the 42% of voxels is observed. For what concerns the stimuli-dependent maps, verbal letter n-back was found to entail a 43% of overlap, compared to the 28.9% reported for the non-verbal map. The greatest overlap is however observed for spatial maps, reaching a 66.1% of overlap. For what concerns the auditory n-back map, a 39.4% of overlap is reported. At the single RSN-level, the greatest overlap is shown in respect with the Dorsal Attention Network (DAN) for all n-back maps considered, showing a percentage of overlap higher than any other network (Figure 3.12 B). The overlap between n-back regions and the DAN nodes appears especially over the parietal lobes and left frontal lobe. For the general n-back task, an overlap is observed with the Ventral Default (4%) and right (7,7%) and left (7,6%) Executive Control networks as well. A certain degree of superimposition of the same networks with the spatial n-back map results respectively in an 11,4%, 12,2% and 7,8% of overlap. Results of the overlaps for the verbal letter n-back task also show a considerable involvement of the right (7,8%) and left (6,8%) Executive Control network. On the other hand, both the auditory and visual maps show a considerable sharing of voxels only with the DAN.

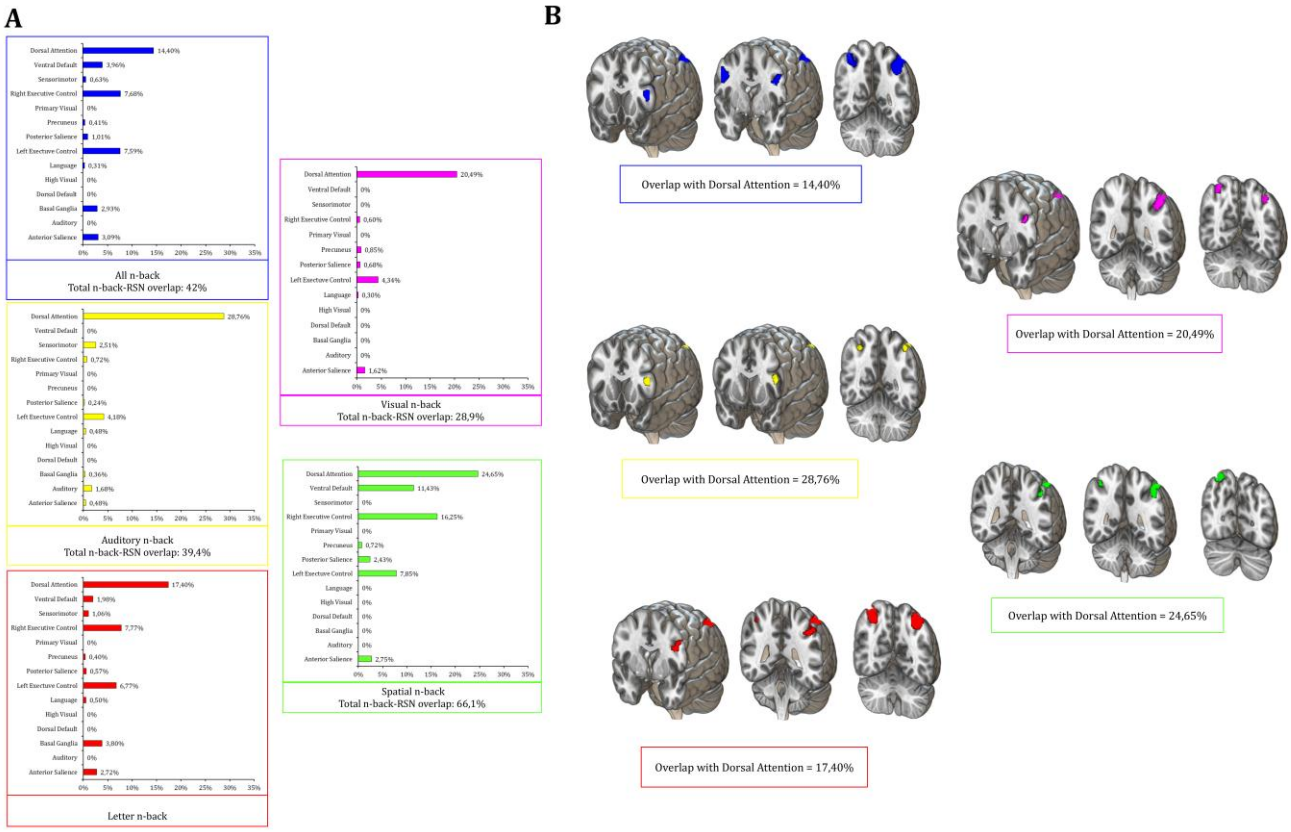

Figure 3.12. Overlaps between n-back maps and RSNs. Panel A shows the total percentage of overlap between ALE maps for each n-back task and the surface representation of RSNs according to Shirer et al. (2012). All resulting maps show greater correlation between n-back tasks and the DAN, compared to other RSNs. Specific overlap percentages are reported in Panel B.

Neural deactivations during the n-back task

Evaluating the studies showing the coordinates of deactivation during the n-back task in their results, we collected 15 papers that used verbal (stimuli: letters/numbers) or face n-back task. From this database we extracted the activation and deactivation coordinates, and we computed the ALE map, as we did for all the other maps (for a detailed description see paragraph 'ALE maps computation'). The results are shown in Figure 3.13 (panel A) and Table 3.12, without distinguishing between stimuli type. The map includes 8 activation nodes highlighting a bilateral fronto-parietal distribution and 5 nodes of deactivation, in particular in the bilateral temporal lobe and the posterior cingulate cortex. Moreover, to characterize the spontaneous functional connectivity of the activation and deactivation nodes, a seed-to-voxel analysis was run on a database of 1000 healthy participant (Yeo et al., 2011). This analysis shows a strong positive

connectivity profile between activation nodes and the DAN (Figure 3.13, panel B), and between deactivation nodes and the DMN (Figure 3.13, panel C).

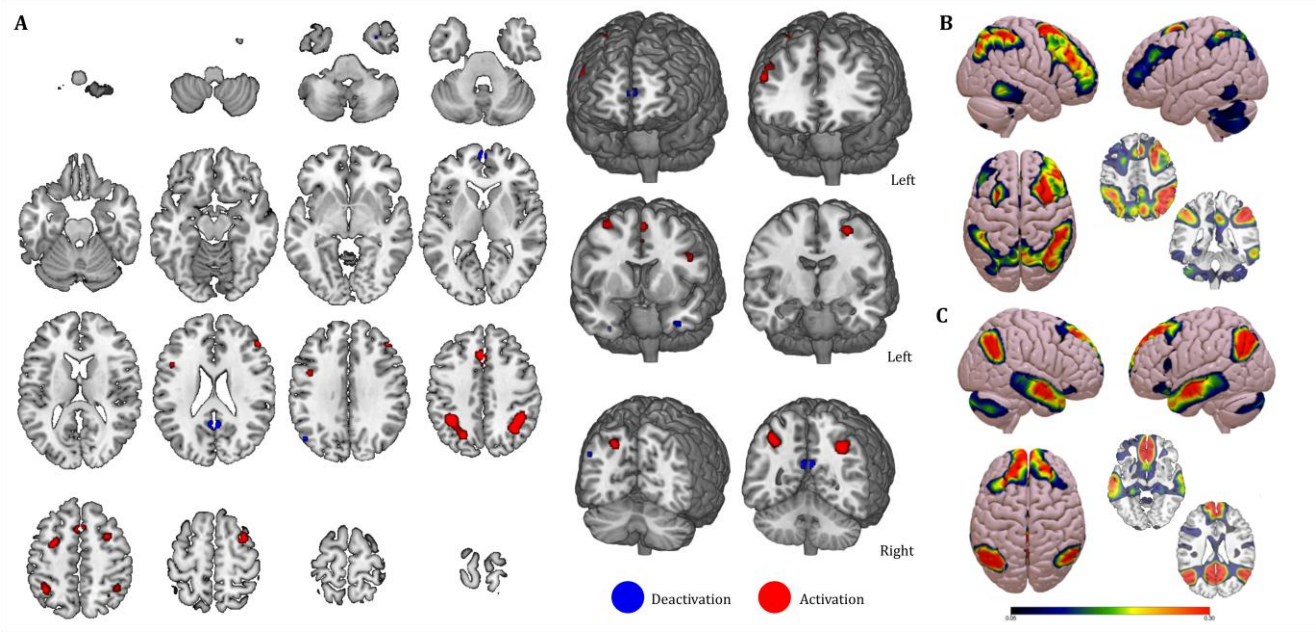

Figure 3.13. Increase and decrease during the n-back task. (A) Activation (red) and deactivation (blue) nodes resulting from the analysis conducted on 15 articles. (B) and (C) Functional connectivity maps for the activation and deactivation nodes respectively.

Table 3.12. Volume, coordinates and corresponding Brodmann are, lobe, hemisphere and regional labels are reported for each cluster included in the ALE map for the increase and the decrease of neural activity during the n-back task.

Cluster number	Volume (mm^3)	Weighted Center			Extrema Value	Extrema value coordinates			Brodmann Area	Hemisphere	Lobe	Label
		x	*y*	*z*		*x*	*y*	*z*				
Deactivation												
1	576	-.4	-53.4	22.9	0.035	-2	-54	22	23	L	Sub-cortical	Posterior Cingulate
2	304	-1.5	59.6	5.7	0.029	-2	60	6	10	L	Frontal	Medial Frontal Gyrus
3	64	-34	5.2	-36.8	0.025	-34	6	-36	38	L	Temporal	Superior Temporal Gyrus
4	64	-49	-69	31	0.026	-50	-68	32	39	L	Temporal	Middle Temporal Gyrus
5	16	30	6	-41	0.025	30	6	-40	38	R	Temporal	Superior Temporal Gyrus
Activation												
1	2640	37.55	-51.73	43.53	0.036	40	-48	44	40	R	Parietal	Inferior Parietal Lobule
					0.031	34	-58	44	19	R	Parietal	Precuneus
2	2504	-33.85	-52.44	44.04	0.037	-36	-48	42	40	L	Parietal	Inferior Parietal Lobule
					0.024	-22	-66	42	7	L	Parietal	Precuneus
3	1096	30.98	6.58	56.2	0.030	30	6	56	6	R	Frontal	Sub-Gyral
4	720	-2.97	21.94	42.66	0.024	-4	24	44	6	L	Frontal	Medial Frontal Gyrus
5	600	-44.5	6.3	29.98	0.019	-46	2	36	6	L	Frontal	Precentral Gyrus
					0.018	-42	6	30	6	L	Frontal	Precentral Gyrus
					0.017	-48	14	22	9	L	Frontal	Inferior Frontal Gyrus
6	504	-.94	15.17	52.91	0.022	-2	14	54	6	L	Frontal	Superior Frontal Gyrus
7	408	46.44	35.75	25.84	0.020	48	36	22	9	R	Frontal	Middle Frontal Gyrus
					0.017	44	34	34	9	R	Frontal	Middle Frontal Gyrus
8	408	-28.53	.25	51.65	0.020	-28	0	52	6	L	Frontal	Middle Frontal Gyrus

Biophysical Modeling Results

The optimal multichannel montages to target the network mainly involved during the n-back task on a MRI-derived realistic head model can be determined by optimization algorithms. Detailed information about these methods are reported in Chapter 1.

Figure 3.14 reports the results of multichannel tES montage optimization to promote the activation of the regions located in the fronto-parietal cortices. We performed four different optimizations, one for each node of the fronto-parietal network. These optimizations can be used for stimulating a single area or can be combined to obtain a network-stimulation approach. As demonstrated in this study, depending on the stimuli, presentation modality and contrast different brain activity can be revealed, so the possibility to personalize the tES optimization based on the experiments' own needs it is crucial, but still not available in literature. Offering different optimization montages, we want to cover this gap.

The signed weight map used for the four optimizations is shown in Figure 3.14 (axial view in the middle). For the stimulation optimizations we set a: 2 mA max current per electrode and 2 mA max total injected current. The positions of the electrodes were picked from a pool of 64 electrodes. The algorithm limited the montages to 4-channels, for each optimization. Considering the tES guideline and recommendation, declaring that the max total injected current in the brain should not exceed the 4 mA, a maximum of two optimization montages shown here can be combined. Despite all the stimulation optimizations yielded a total injected current of 2 mA, the average normal electric field (nE) for the nodes in the left hemisphere is lower than for those in the right hemisphere. The nE-field distribution in these optimizations is shown in Figure 3.14.

In detail the montage for the node 1 comprehends C1: -560uA, C5: 481uA, CP3: 1518uA, CP5: -1439uA (quality of solution (WCC): 0.47); for the node 2: F5: 1268uA, FC5: 732uA, FCZ: -501uA, FT7: -1499uA (quality of solution (WCC): 0.54); for the node 3: AF4: 448uA, F4: 1552uA, FT8: -835uA, FZ: -1165uA (quality of solution (WCC): 0.6); and for the node 4: CP4: 2000uA, CP6: -1348uA, PO4: -260uA, Cz: -392uA (quality of solution (WCC): 0.6).

Given the current constraints, these solutions represent the best fit of the En to the target maps obtained from FC correlation values, with an average value of En field of 0.066 v/m (range: 0.056-0.079). Results suggest that biophysical optimization of fronto-parietal nodes on the right hemisphere achieves stronger e-fields compared to left hemisphere on average, therefore suggesting the former as the most suitable target for stimulation during the n-back task.

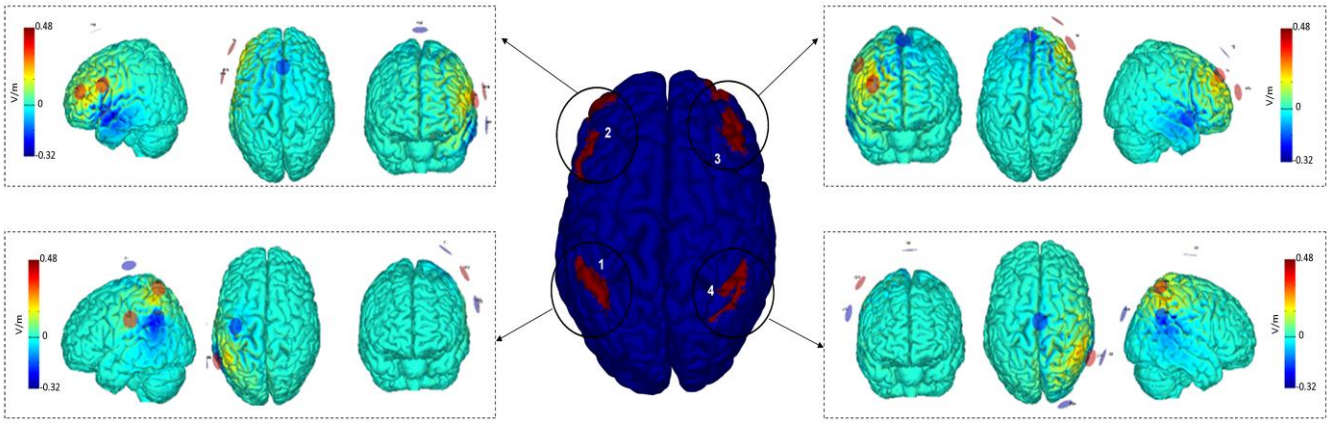

Figure 3.14. Multichannel tES optimized montages. Optimized montages for each node (1-4) of the bilateral fronto-parietal network involved during the execution of the n-back task, as shown in the axial view (in the middle). These solutions can be used for stimulating a single area or can be combined to obtain a network-stimulation approach. All the optimizations involve 4 electrodes, delivering a total maximum current of 2 mA. Anodes are shown in red, cathodes in blue. The bars represent the nE field (V/m) for each montage.

3.1.3 DISCUSSION

In the present meta-analysis, we reviewed studies reporting fMRI or PET findings during n-back task execution, aiming to create a set of available to download activation maps, specifically ideated to depict stimuli- and modality-dependent activation patterns. In the following paragraphs, we will discuss the functional role of the retrieved core regions for each n-back task being examined, as well as of the observed overlap between n-back related brain regions and resting state networks related to executive control, salience and attention. We will then discuss possible future functional and clinical applications, with a particular focus on neurostimulation driven by the results obtained from biophysical modeling optimization, and cognitive enhancement programs in healthy subjects.

Core regions in n-back tasks

Congruent with the literature in the field, a fronto-parietal network involvement underlying WM task execution, including n-back performance, was promptly confirmed in our ALE maps. Previous investigations (Owen et al., 2005; Rottschy et al., 2012) have reported a bilateral activation of a fronto-parietal network and have described the dorsolateral prefrontal cortex (dlPFC) as the area playing a key role in the monitoring of the incoming information (Bagherzadeh et al., 2016;

Brunoni & Vanderhasselt, 2014; D'Esposito et al., 1998; Owen, 1997; Owen et al., 2005). DLPFC is known to be involved in the updating of goal representations based on contextual information and task related demands (Barch et al., 2003; D'Esposito et al., 1995, 2000), as well as in maintaining comprehensive representations by encoding task relevant rules and associated responses, stimulus features and conflictual information (Mansouri et al., 2009). However, differently from previous working memory studies, we did not find a material-dependant activation of dlPFC. Opposite to what we expected, a strong involvement of parietal cortices in verbal n-back task was instead noticed, which has been previously merely described during short term storage of verbal material (Jonides et al., 1998; Miyauchi et al., 2016). Nevertheless, the inferior parietal lobule (IPL) is known to underlie many higher order functions, including numerical judgments and arithmetic (Göbel & Rushworth, 2004; Hubbard et al., 2005), reading (Turkeltaub et al., 2002), and semantic processing (Chou et al., 2006; Raposo et al., 2006). Moreover, this area seems to be involved in the maintenance of goal-directed attention (Corbetta & Shulman, 2002), in action observation (Buccino et al., 2001), and visual presentation of graspable objects (Chao & Martin, 2000). IPL is further known to be split into two cytoarchitecturally distinct areas: Brodmann's area 40 in the supramarginal gyrus and Brodmann's area 39 in the angular gyrus. Phonological processing, short-term memory, and phonemes sequencing have been reported to engage the former (Gelfand & Bookheimer, 2003; Jacquemot et al., 2003; Paulesu et al., 1993), while the latter are involved in some reading-related tasks (e.g., understanding of the relationship among different characters)(Inui et al., 1998). Despite few studies reporting an activation of IPL linked to spatial tasks (Cieslik et al., 2010), we failed to prove any stimuli-driven specificity of this area, leading us to favour its involvement more as that of a general aid during n-back task execution.

Activations outside the fronto-parietal network

Taken together, the fronto-parietal network activation during n-back task execution does not come surprising. However, many other regions including sub-cortical areas, the cerebellum and the bilateral precuneus also come at hand and require further investigation.

The bilateral activation of the anterior insula during WM tasks has already been reported by previous studies (Rottschy et al., 2012; Wager & Smith, 2003), opposite to those who have claimed greater activation over frontal areas located between the mid-ventrolateral frontal operculum and the insula, but not of the insula itself (Owen et al., 2005). Here, a lateralized activation of the right insula emerged within all n-back modalities, perhaps in line with its proposed role in the regulation

of the interaction between the ventral and dorsal attentional systems in mediating general arousal levels (environmentally driven) and selective attentional mechanisms (task driven) to ensure optimal performance execution (Eckert et al., 2009).

The role of the bilateral precuneus within a wide range of high-order cognitive functions is proposed by several studies (Cavanna & Trimble, 2006), like its involvement in episodic and semantic retrieval tasks (Shallice et al., 1994). This could explain the activation of precuneus bilaterally in the general n-back map, considering the importance in maintaining and retrieving information during n-back task.

Finally, a focus of activation in the bilateral cerebellum is shown. Embracing modern brain activity models, in which all brain areas must be considered functioning as an ensemble, rather than as a fragmented collection of isolated regions and abilities, the cerebellum itself might no longer be considered only in its role within motor functions, but rather as entailing a cognitive role too. Indeed both neuroimaging studies on cognitive domain and evidences from patients with cerebellar cognitive affective syndrome, reported the involvement of cerebellum in executive functions, including working memory, planning and abstract reasoning, as well as in spatial cognition (Schmahmann & Sherman, 1998). For this reason the cerebellar functions within the working memory task have been consistently studied and an explanation has been proposed by Marvel and Desmond (Marvel & Desmond, 2010): they suggested that working memory is supported by cerebellum through the engagement of inner speech mechanism. This could support working memory creating traces that facilitate the processing of new information (Ackermann, 2008; Ravizza et al., 2004). Within the n-back task frame, it might underlie both motor planning and the strategic recruitment of regions (Koziol et al., 2014).

Neural activity and task load

When considering load effects, a similar activation in fronto-parietal areas is found for all contrasts, with the added engagement of both ACC and right cerebellum as a function of task load. Both areas have already been mentioned as associated with increased difficulty in memory tasks (Haxby et al., 2000). Moreover, the anatomical mapping of the cerebellar activation is observed to specifically overlap with the crus I cerebellar parcellation by Buckner, previously reported as devoted to cognitive control— including working memory—and as part of the default network (Buckner et al., 2011; Stoodley & Schmahmann, 2009). Crus I projections to the prefrontal cortex and cingulate gyrus and the concurrent positive association between ACC, frontal areas and the

cerebellum itself (Buckner et al., 2011) might justify the involvement of such areas in memory performances.

Brain activity in verbal n-back tasks

The resulting map from all studies using verbal material is not found to differ much from the generic n-back task map, as observed in Figure 3.4. The fronto-parietal network remains the central core of activity, with the addition of the precuneus, as well as cerebellar and subcortical structures bilaterally. Differently from what we expected based on previous findings (D'Esposito et al., 1998; Nystrom et al., 2000), we did not observed a striking left lateralization in the prefrontal areas, particularly in Broca's area (Brodmann's areas 44/45), but a more distributed brain activation during verbal n-back tasks. The dissociation between the neural areas involved in storage and rehearsal has been amply discussed in literature and, probably, this effect is a consequence of this dissociation. Indeed, Awh and colleagues (1996) have revealed through a PET study a different model of brain activation for these two components of verbal working memory (Awh et al., 1996): when rehearsal-based activation was detracted from the activation due to storage and rehearsal together, some of the anterior brain activation (including Broca's area) was subtracted, while the posterior parietal regions remained active. In line with neuropsychological evidence (Smith & Jonides, 1997) inferior parietal areas were implicated in storage, whereas inferior frontal areas were implicated in rehearsal, and Broca's area may be important for articulatory processes involved in recoding visual material but not for maintenance of serial order per se (Henson et al., 2000).

Rather, greater activity is reported in the left parietal area, in the supramarginal and angular gyri of IPL (Brodmann's areas 39/40). In the field of visual word recognition studies, the supramarginal gyrus has been reported as particularly active when participants are focused on words' sound, whereas the angular gyrus is mostly related to words' meaning (Démonet et al., 1994; Devlin et al., 2006; Mummery et al., 1998). Besides being involved in the convergence of visual, auditory and somatosensory information, both regions appear involved in language comprehension, together with Wernicke's area (Kim et al., 2011). The central role of parietal areas for WM storage capacity was moreover demonstrated by a recent transcranial alternating current stimulation (tACS) study that provided the first causal relation between theta activity and n-back task (Jaušovec & Jaušovec, 2014).

Although in a recent meta-analysis by Rottschy et al. (2012) greater recruitment of the left inferior frontal gyrus (IFG) was observed for verbal tasks, in our study we did not find an activation for this area on the left, but rather on the right. The divergence in the results might be due to Rottshy et al. (2012) considering a greater variance of WM tasks, not limited to the n-back paradigm solely.
When entering in the specifics of the type of stimuli being presented during n-back paradigms, the resulting map of activity for letter n-back studies is identical as for the general verbal n-back, whereas few differences appear for numerically-based n-back tasks. In the latter, is observed a more consistent activation of the bilateral parietal cortex compared to frontal areas.

Brain activity in visual n-back tasks

Visual n-back tasks refer to those paradigms in which non-verbal visual stimuli, such as objects, images and faces, are presented. The map of brain activity for this type of task confirms once again the core role of the fronto-parietal network. However, differently from verbal n-back tasks, greater recruitment of the left frontal area is observed, in line with the lateralization hypothesis according to which there are a left lateralization for verbal as well as visual stimuli, probably because there is a left hemispheric bias for identity n-back task, not for a specific stimulus (D'Esposito et al., 1998).
For object n-back, our results reveal greater activity over the right limbic structures, in particular the anterior cingulate gyrus. Several functional neuroimaging studies have associated greater ACC activity with the execution of various high-order functional tasks, such as Go-No go tasks (Schulz et al., 2011), theory of mind scenarios (Kobayashi et al., 2008) and high-load working memory tasks (Haxby et al., 2000). Moreover, Smith and Jonides (1999) have described ACC as implicated in the temporary storage and manipulation of information and in the resolution of cognitive conflicts. However, the most plausible explanation for the activity of this area in image n-back tasks might be that of its role in the judgment of the pleasantness/averseness of stimuli (Lindgren et al., 2012). Indeed, coactivation of ACC with orbitofrontal structures is typically found when emotional stimuli are presented (Miller & Cohen, 2001), and could be that the emotional valence of the stimuli themselves—when no controlled for—triggers the reported activity.

Overlap between n-back task network and RSN

From the first fMRI study aimed at analysing brain activation during WM task, the role of fronto-parietal network has been suggested and further confirmed by the present meta-analysis. The

fronto-parietal network includes a set of regions that are implicated in a variety of executive functions, including inhibition, attentional switching, mental rotation and fluid intelligence. Recently, the research effort has shifted its focus from single areas to the study of well-interconnected networks that interact with each other's and ensure functioning of the individual. The increased awareness on brain cohesiveness has led to an interest being drawn in exploring the possible relationship between n-back derived brain networks and resting state networks. Indeed, our results suggest a higher degree of superimposition between n-back regions and DAN, as opposed to other networks like the Salience, Language and Sensorimotor networks. The synergy between WM and other functions such as attention has been postulated (Shipstead et al., 2015), but—to our knowledge—quantitative functional overlap has not been described before. The relevant role of attention during a working memory task needs to be considered and might explain the observed strong DAN component, together with the executive control component. A similar overlap has been recently identified for fluid intelligence (Santarnecchi, et al., 2017 b,c), a function highly correlated with WM (Friedman et al., 2006). The overlap observed with those RSNs confirms the strong correlation between executive functions— like working memory and attention— even across presentation modalities, such as echoic stimuli presentation.

Human functional evidences recognize four main regions as underlying DAN activity: the intraparietal sulcus, the superior parietal lobule, the superior and inferior precentral sulci and the middle temporal area (Fox et al., 2005; Yeo et al., 2011). The distinction between dorsal and ventral attention networks relates back to the work of Corbetta & Shulman (2002), who first proposed the former as involved in mediating top-down guided voluntary allocation of attention, whilst the latter detects salient and behaviourally relevant stimuli, in particular when unattended. Moreover, several neuroimaging studies have proved DAN to be modulated during search and detection processes (Corbetta et al., 1995; Shulman et al., 2001). This might explain the reported overlap between DAN and n-back networks, where the manipulation and maintenance of the incoming information represents a core aspect. Nevertheless, future work investigating the contribution of DAN in working memory tasks, in particular n-back tasks, is needed to improve our understanding of the functional interactions across different RSNs and n-back networks. Our knowledge of the interplay between attention, memory and other cognitive abilities would greatly benefit from such studies, driving relevant possible future implementations at both the research and clinical level.

Functional connectivity profile in neural activation and deactivation

Neural activation patterns during the n-back task has been amply discussed. However, for a more in-depth understanding of the neural activity pattern during this specific working memory task, deactivation patterns are also highly relevant and should be considered. To our knowledge, even though previous studies have reported deactivation coordinates for single analysis, we are the first to provide an ALE map showing the neural deactivation during the n-back task, revealing a significant decrease in BOLD response of posterior cingulate cortex as well as frontal and temporal regions during task execution. As expected, the functional connectivity profile of such ALE nodes highly resembles the topography of the DMN. This network includes the posterior cingulate cortex (PCC), medial prefrontal cortex (mPFC), middle frontal regions, lateral parietal and medial temporal regions, and is believed to be involved in introspection and background processing (Andrews-Hanna et al., 2014; Fox et al., 2005; Raichle et al., 2001; Sheline et al., 2009).

In line with the "deactivation of the DMN", we identified a high resemblance between the connectivity profile of regions activated during N-back processing and the DAN. Interestingly, the interplay between these two networks has been suggested as a major candidate biomarker for normal and pathological aging (Spreng et al., 2016; Spreng & Schacter, 2012) and has been correlated with cognition in healthy young participants (Santarnecchi, et al., 2017b,c). A clear overlap with DMN and DAN can suggest the modulation of their interplay as a candidate target for brain stimulation interventions based on Transcranial Magnetic Stimulation (TMS) and transcranial Electrical Stimulation (tES) able to modulate network-level activity and elicit cognitive enhancement (Ruffini et al., 2018; Santarnecchi, Momi, et al., 2018).

Potential brain stimulation solutions

Currently, a lot of studies investigated the possibility to enhance WM performance using NIBS, however reporting heterogeneous results. The causes could be held in several factors as the different tasks used or the stimulation target selected. The majority of these studies have indeed used the traditional two-electrode montage targeting the right and left dorsolateral prefrontal cortices (dlPFC), positioning the anode over either the F3 (left dlPFC) or F4 (right dlPFC) regions on the scalp in accordance with the international 10–20 system for electrode placement (Herwig et al., 2003). Nevertheless, our results support the idea that brain regions do not operate in isolation but interact with other regions through networks and that, based on the stimuli, presentation modality and load of the task used, the neural correlates could differ. Based on these results, we

performed the biophysical modeling of potential brain stimulation solutions suggesting feasible targets for WM neuromodulation in healthy subjects. Despite our ALE results have shown an involvement also of subcortical areas during the n-back task, we decided to focus the biophysical modeling on the cortical areas, as these are the more activated during the task execution, but also the regions most reachable by NIBS. Moreover, we decided to run different optimization for each cortical node (frontal and parietal bilaterally), giving the possibility to combined them and to suit the best stimulation based on different requirements. Finally, our biophysical modeling suggests the right hemisphere as the best target for the stimulation, since the montages created for targeting these regions induce stronger effects.

Future studies could investigate biophysical modeling and tES montage optimizations considering as target the functional connectivity map of these nodes, focusing the stimulation both on the positive and negative correlated areas and indirectly target subcortical regions (as shown in the Study 3).

Limitations of the study and future direction

Our ALE maps allow us to know which areas are more active for a specific condition of n-back task, and whether the WM network might be modified as a function of n-back change in its specifics. Few studies reported WM network activation to be material-independent (Owen et al., 2005; Ragland et al., 2002), with the opposite holding true for other evidences. Although we consider the results of our meta-analysis as accurate as possible given the status of the literature, there are some publication biases that should be evaluated. For example, based on a recent simulation study (Eickhoff et al., 2016), it is known that the results of a meta-analysis with a low number of papers could be driven by few experiments. A limited number of studies is available for specific n-back maps (e.g., number, face, object n-back). These results should be interpreted carefully. Moreover, considering that we included in the analysis also studies evaluating brain activity during n-back task in older healthy subjects, the WM decline in aging by investigating age-related changes in concordant patterns of brain activation during n-back task could have been evaluated. The growing literature on the neuroscience of cognitive aging has indeed suggested that there are some reliable age-related differences in the form of both decreases and increases of brain activity in old adults compared to their younger counterparts in several cognitive domains, including WM (Grady et al., 1998). Recently, a meta-analysis of the n-back task across the adult lifespan showed that young, middle-aged and older subjects share concordance in the engagement of parietal and

cingulate cortices, as well as the insula, claustrum, and cerebellum (Yaple et al., 2019). On the other hand, prefrontal cortex is more engaged in young subjects compared to middle-aged adults, but absent in older adults, suggesting a gradual linear decline in concordance of prefrontal cortex engagement. However, even though several middle-aged and older adults are included in our analysis, the sample size is not consistent to verify differences in lifespan in different domains (e.g., visual/verbal/spatial n-back), because mostly of the studies on middled-age/older subjects used verbal n-back task.

Future studies should consider tES montage optimizations in order to achieve a more accurate targeting of the fronto-parietal network and evaluate their effectiveness for cognitive enhancement in healthy subjects. WM deficits characterize also many psychiatric, neurodegenerative and neurodevelopmental disorders, including depression, schizophrenia, Alzheimer's and Parkinson's diseases, ADHD and the Autistic spectrum disorder. The Study 2 aimed to characterize the n-back activation profile of specific patient populations, also looking at differences between conditions and their network-level representations, will be presented in the following paragraphs.

3.2 STUDY 2: Common and Specific Brain Activations During N-back task in Psychiatric and Neurodevelopmental Disorders

As already described in the previous study, Working Memory (WM) plays an important role in many forms of complex cognitive functions constantly permeating our daily life. WM capacity deterioration pervades many psychiatric and neurodegenerative disorders as, for example, Bipolar Disorder (Latalova et al., 2011; Thompson et al., 2007), Alzheimer's and Parkinson's disease (Baddeley et al., 1991), as well as in neurodevelopmental disorders like the Attention Deficit Hyperactivity Disorder (ADHD) and Autistic Spectrum Disorder (ASD) (Martinussen et al., 2005; Williams et al., 2005). Therefore, studying the neural substrate of WM has become crucial also in patients in order to identify overlap and/or differences and tailor pathology—specific cognitive interventions aimed at restoring WM capacity.

A recent meta-analysis, studying functional magnetic resonance imaging (fMRI) activity on patients with ADHD (McCarthy et al., 2014), showed a significantly lower frontal lobe activity compared to control during three different tasks (Go/No-go, N-back, and Stroop task). However, the authors did not find significant differences in dorsolateral prefrontal cortex (dlPFC) activation between experimental and control groups, replicating the results previously reported by Hart and collegues (2013) during an inhibition task (Hart et al., 2013). On the other hand, an altered activity in dlPFC has been underlined in patients with the psychiatric disorder compared to healthy controls and this is usually associated with a deficit of the anterior part of the cingulate cortex (ACC) and thalamus. As several studies proved, this lower functional connectivity between ACC and thalamus could be the neural substrate of several deficits in attention, memory, and executive functions typically associated with psychiatric disorders (Argyelan et al., 2014; Latalova et al., 2011; Motter et al., 2016; Weinberger et al., 1986).

Tasks engaging WM typically require participants to hold and manipulate temporary information (Baddeley, 1992; Shallice, 1988). The n-back task is the most popular measure of WM used in functional magnetic resonance imaging (fMRI) studies also because this paradigm requires several working memory processes, including maintenance, monitoring, updating, and manipulation of retained information (Cohen et al., 1997), therefore being the most complete task to study WM neural substrate. Moreover, the n-back task is commonly used in pathology because of its flexibility to different presentation modality (visual or auditory), stimuli (letters, numbers, images,

etc..), and load (1, 2, 3 n-back), allowing to set the complexity based on patients' efforts and to avoid learning effects. The neural correlates of the n-back task in healthy subjects are well characterized and involved the bilateral fronto-parietal activation as well as the concurrent activation in the subcortical areas as the bilateral insula, the bilateral cerebellum, and the precuneus as shown in the previous study (Mencarelli et al., 2019). Considering the clinical population, meta-analyses showing neural correlates of different WM tasks have been already published (Cremaschi et al., 2013; McCarthy et al., 2014; Minzenberg et al., 2009; Müller et al., 2017). However, no studies have specifically investigated brain activity of clinical population during n-back task so far.

In an attempt to produce an overview of the neural correlates of n-back performance in patients with psychiatric or neurodevelopment disorders, we present a systematic quantitative meta-analysis of fMRI and Positron Emission Tomography (PET) data collected during n-back processing. We included and analyzed 36 studies within the Activation Likelihood Estimate (ALE) analytic framework (Eickhoff et al., 2009, 2012). Separated meta-analytic maps were created for patients with schizophrenia (SZ), depressive disorder (DD), bipolar disorder (BD), and ADHD. Based on previous sparse literature, we hypothesized a decreased activation in the dlPFC in psychiatric disorders, and a less extensive activation in nodes of the fronto-parietal network in patients compared to healthy controls. Moreover, considering that depressive and bipolar disorders are both mood disorders and some studies have already shown their resting-state functional connectivity similarity, we hypothesized an analogous pattern of activation for these two maps. Additionally, we investigated the qualitative overlap between these activation maps and the previously presented ALE maps in healthy subjects, underlying similarities and differences between pathological and healthy brains in the WM domain. Finally, using biophysical modeling possible targets for future tES studies for rehabilitation and cognitive enhancement purposes has been proposed. Considering the relevance of WM in high cognitive functions, its enhancement could resonate also in other cognitive domains and improve patients' quality of life.

3.2.1 MATERIAL AND METHODS

Literature search

Articles were collected by performing a search on the PubMed database without temporal restrictions. The following terms "N-back task", "Working Memory Task", were individually

combined with "Functional Magnetic Resonance Imaging", "Position Emission Tomography" and their acronyms and with “Schizophrenia”, “Depression”, “Depressive Disorder”, “Bipolar disorder”, “ADHD”, “Parkinson”, Alzheimer”, “MCI”, “Mild Cognitive Impairment” and “Multiple Sclerosis”. References from the collected material were also examined for relevant publications. Following the abstract screening of every resulted article published before October 2019, we evaluated a total of 169 studies (Figure 3.15), narrowing them to 36 final studies. We excluded (i) review papers, (ii) studies not mentioning any of the keywords in their abstract, (iii) studies not reporting fMRI/PET activations coordinates in MNI or Talairach space, (iv) studies not reporting activation foci in table format or reporting statistical values without corresponding coordinates, (v) studies that used predefined Regions of Interest (ROIs), (vi) studies that used small volume correction (SVC), (vii) studies not using classic n-back tasks (defined as ones where subjects must respond when the stimulus presented is the same as the stimulus presented *n* times before), (viii) studies that used a placebo or pharmacological therapies, (ix) studies with only one subject and (x) studies that did not report separate brain activation between healthy and pathological condition. We also excluded studies that considered patients with multiple sclerosis, MCI, Alzheimer’s, and Parkinson’s disease because the total number of papers that matched our inclusion criteria was unsatisfied. The complete list of the included studies is reported in Table 3.12, indicating the: (i) name of the first author, (ii) number of participants, (iii) experimental design, (iv) task specifics, (v) references (MNI or Talairach), (vi) the number of foci and (vii) imaging modality (e.g., fMRI, PET). Data of the specific activation foci were collected and included in a quantitative Activation Likelihood Estimation (ALE) analysis for the identification of brain regions involved in n-back tasks in psychiatric and neurodevelopment disorders. In particular, four different maps were created focusing on: (i) Schizophrenia, (ii) Depressive Disorder, (iii) Bipolar disorder, and (iv) ADHD.

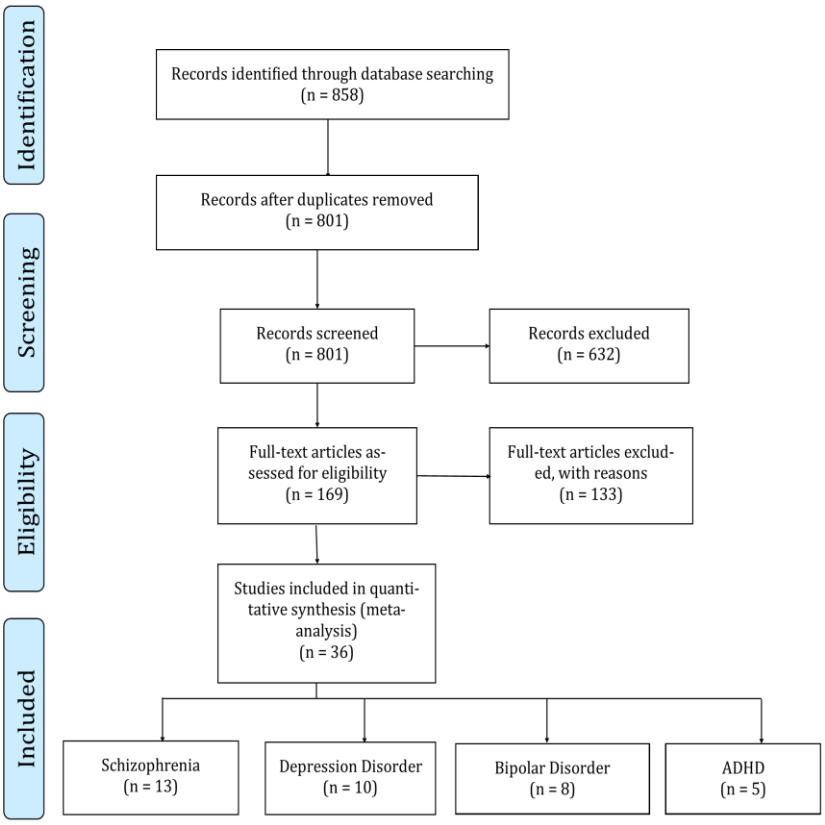

Figure 3.15 Literature search for the identification of relevant publications included in the ALE metanalysis (from Liberati et al., 2009).

Paper	Subjects	N-Back	Modality	Task Type	Stimuli Type	Contrast	Reference	Foci	Imaging Modality
Schizophrenia									
Jiang et al 2015	20	0,2	Visual	Spatial	Numbers/ Position Numbers	2back>0back	MNI	10	fMRI
Kim et al 2003	12	0,2	Visual	Identity	Geometric Figures	2back>0back	TAL	7	PET
Kumari et al 2006	12	0,1,2	Visual	Spatial	Dots	1back>0back	MNI	6	fMRI
Mendrek et al 2004	12	0,2	Visual	Identity	Letters	2back>0back	TAL	13	fMRI
Meyer-Linderberg et al 2001	13	0,2	Visual	Identity	Numbers	2back>0back	TAL	10	PET
Nielsen et al 2017	17	0,2	Visual	Identity	Letters	2back>0back	MNI	29	fMRI
Perlstein et al 2003	16	0,1,2	Visual	Identity	Letters	Global	TAL	9	fMRI
Perlstein et al 2001	17	0,1,2	Visual	Identity	Letters	Global	TAL	12	fMRI
Royer et al 2009	18	0,2	Visual	Identity	Numbers	2back>0back	TAL	21	fMRI
Sapara et al 2014	18	0,1,2	Visual	Spatial	Dots	1back>rest	MNI	7	fMRI
Sapara et al 2014	18	0,1,2	Visual	Spatial	Dots	2back>rest	MNI	13	fMRI
Sapara et al 2014	18	0,1,2	Visual	Spatial	Dots	1back>0back	MNI	7	fMRI
Sapara et al 2014	18	0,1,2	Visual	Spatial	Dots	2back>0back	MNI	9	fMRI
Sapara et al 2014	14	0,1,2	Visual	Spatial	Dots	1back>rest	MNI	12	fMRI
Sapara et al 2014	14	0,1,2	Visual	Spatial	Dots	2back>rest	MNI	10	fMRI
Scheuerecker et al 2008	23	0,2	Visual	Identity	Letters	2back>0back	TAL	7	fMRI
Wu et al 2017	45	0,2	Visual	Identity	Numbers	2back>0back	MNI	5	fMRI
Yoo et al 2005	10	2	Visual	Identity	Faces	2back	TAL	17	fMRI
Depression									
Bartova et al 2015	78	0,2	Visual	Identity	Numbers	2back>0back	TAL	10	fMRI
Fitzgerald et al 2008	13	1,2	Visual	Identity	Letters	2back>0back	TAL	20	fMRI
Garrett et al 2011	16	0,1,2	Visual	Identity	Letters	1back>0back	TAL	13	fMRI
Garrett et al 2011	16	0,1,2	Visual	Identity	Letters	2back>0back	TAL	15	fMRI
Garrett et al 2011	15	0,1,2	Visual	Identity	Letters	1back>0back	TAL	21	fMRI
Garrett et al 2011	15	0,1,2	Visual	Identity	Letters	2back>0back	TAL	5	fMRI
Harvey et al 2005	10	0,1,2,3	Visual	Identity	Letters	Global	TAL	8	fMRI
Korsnes et al 2013	22	1,2	Visual	Identity	Numbers	2back>1back	MNI	12	fMRI
Marquand et al 2008	20	0,1,2,3	Visual	Identity	Letters	2back	TAL	18	fMRI
Matsuo et al 2007	15	0,1,2	Visual	Identity	Numbers	1back>0back	TAL	3	fMRI
Matsuo et al 2007	15	0,1,2	Visual	Identity	Numbers	2back>0back	TAL	3	fMRI
Matsuo et al 2007	15	0,1,2	Visual	Identity	Numbers	2back>1back	TAL	7	fMRI
Rodríguez-Cano et al 2014	26	1,2	Visual	Identity	Letters	2back>1back	TAL	9	fMRI
Rodríguez-Cano et al 2017	26	0,1,2	Visual	Identity	Letters	1back>0back	MNI	4	fMRI
Rodríguez-Cano et al 2017	26	0,1,2	Visual	Identity	Letters	2back>0back	MNI	3	fMRI
Schoning et al 2009	28	0,1,2	Visual	Identity	Letters	2back>0back	MNI	13	fMRI
Schoning et al 2009	28	0,1,2	Visual	Identity	Letters	2back>1back	MNI	28	fMRI
Bipolar Disorder									
Alonso-Lana et al 2016	27	1,2	Visual	Identity	Letters	1back>baseline	MNI	7	fMRI
Alonso-Lana et al 2016	27	1,2	Visual	Identity	Letters	2back>baseline	MNI	1	fMRI
Alonso-Lana et al 2016	27	1,2	Visual	Identity	Letters	2back>1back	MNI	1	fMRI
Alonso-Lana et al 2016	23	1,2	Visual	Identity	Letters	1back>baseline	MNI	3	fMRI
Alonso-Lana et al 2016	23	1,2	Visual	Identity	Letters	2back>baseline	MNI	1	fMRI
Alonso-Lana et al 2016	23	1,2	Visual	Identity	Letters	2back>1back	MNI	3	fMRI
Dell'Osso et al 2015	28	0,2,3	Visual	Identity	Letters	Global	MNI	7	fMRI
Drapier et al 2008	20	0,1,2,3	Visual	Identity	Letters	1back	TAL	5	fMRI
Drapier et al 2008	20	0,1,2,3	Visual	Identity	Letters	2back	TAL	6	fMRI
Drapier et al 2008	20	0,1,2,3	Visual	Identity	Letters	3back	TAL	4	fMRI
Frangou et al 2008	7	0,1,2,3	Visual	Identity	Letters	Global	TAL	15	fMRI
Haldane et al 2008	8	0,1,2,3	Visual	Identity	Letters	Global	TAL	7	fMRI
Monks et al 2004	12	0,2	Visual	Identity	Letters	2back>0back	TAL	16	fMRI
Pomarol-Clotet et al 2012	29	1,2	Visual	Identity	Letters	Global	MNI	7	fMRI
Rodríguez-Cano et al 2017	26	0,1,2	Visual	Identity	Letters	1back>0back	MNI	3	fMRI
Rodríguez-Cano et al 2017	26	0,1,2	Visual	Identity	Letters	2back>0back	MNI	2	fMRI
ADHD									
Bedard et al 2014	24	0,1,2	Visual	Spatial	Dots	1back>0back	MNI	8	fMRI
Bedard et al 2014	24	0,1,2	Visual	Spatial	Dots	2back>0back	MNI	9	fMRI
Li et al 2014	33	2	Visual	Identity	Images	2back	TAL	6	fMRI
Massat et al 2012	19	0,2	Visual	Identity	Numbers	2back>0back	MNI	16	fMRI
Mattfeld et al 2016	16	0,1,2,3	Visual	Identity	Letters	Global	TAL	10	fMRI
Mattfeld et al 2016	17	0,1,2,3	Visual	Identity	Letters	Global	TAL	7	fMRI
Valera et al 2005	20	0,2	Visual	Identity	Letters	2back>0back	MNI	9	fMRI

Table 3.12 List of studies considered in this meta-analysis. For each study, the number of subjects, the levels of n-back task difficulty, the type of stimulus used, the modality of stimuli presentation, the type of references, the number of foci, and the imaging modality are listed.

ALE maps computation

The quantitative evaluation of spatial PET and fMRI patterns was carried out using the activation likelihood estimate (ALE) technique implemented in the GingerALE software v. 3.0 (www.brainmap.org) (Eickhoff et al., 2009, 2012). The method used is the same already described for the Study 1. For an overall comprehension, see 'ALE maps computation' paragraph of the first study (pages 42-43).

Qualitative meta-analysis comparison

Data acquired from our previously published ALE maps in healthy subjects (Mencarelli et al., 2019), also described in the Study 1, have been used for this meta-analysis for comparing healthy and pathological brain activity during n-back task. Even though the available ALE database involved 10 maps (e.g., maps based on stimuli or presentation modality used during n-back task), here we focused on the identification of a more general overlap between healthy and pathological subjects, therefore we used the general map (corresponding to the data shown in Figure 3.2 and Table 3.3 in Study 1). The results from this comparison should be evaluated carefully considering the differences in sample size used for different maps.

Biophysical modeling

The biophysical model has been obtained as described in the Chapter 1 (Figure 1.1). In this case, we use as target the activation maps resulting from the ALE computation, instead that the functional connectivity map described in the 'Biophysical modeling' paragraph (page 22).

3.2.2 RESULTS

Ale Maps

The results of the ALE meta-analysis include volumes representing the entire set of regions presented. In the following section, tables and figures describing n-back map for each pathology are shown. A discussion about the role of each specific node is also provided in the Discussion section.

N-back task activation profile in Schizophrenia

Figure 3.16 and Table 3.13 present the resulting map and coordinates of the comprehensive set of activity patterns in patients with the schizophrenic disorder during the execution of n-back task. The map includes 8 separate nodes showing a right fronto-parietal distribution of activation. Moreover, there are additional contributions of regions in the left cerebellum, left superior parietal lobule, and temporal structures including the fusiform gyrus (Figure 3.16 A). A qualitative overlap between brain activity during n-back task in SZ patients and healthy subjects (as shown in Study 1) is reported in Figure 3.16 B.

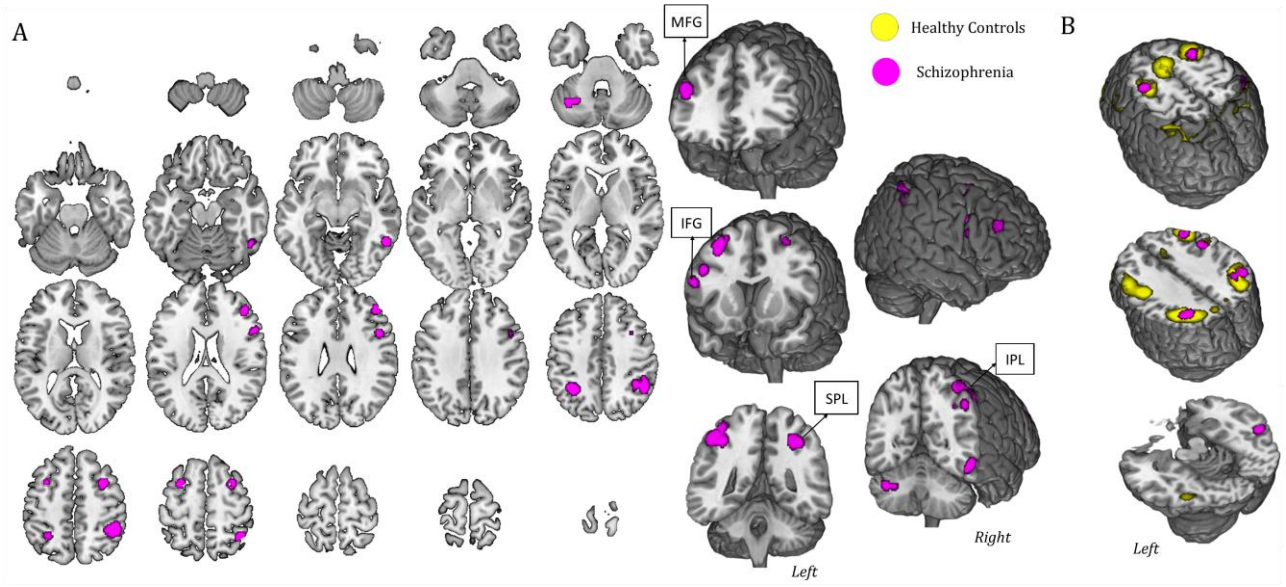

Figure 3.16. N-back task in SZ patients. (A) The map refers to 13 studies in which n-back task was performed by SZ patients. A complete set of coordinates for each cluster is available in Table 3.13. (B) Some significant slides of the brain activation overlap between healthy subjects (yellow) and SZ patients (pink) are shown.

Table 3.13. Activity patterns for n-back tasks in SZ patients. Volume, coordinates and corresponding Brodmann area, lobe, hemisphere and regional labels are reported for each cluster included in the ALE map.

Cluster number	Volume (mm^3)	Weighted Center			Extrema Value	Extrema value coordinates			Brodmann Area	Hemisphere	Lobe	Label
		x	*y*	*z*		*x*	*y*	*z*				
1	4000	43.2	-47.1	48.8	0.023	48	-46	48	40	R	Parietal	Inferior Parietal Lobule
					0.022	38	-52	58	7	R	Parietal	Superior Parietal Lobule
					0.021	40	-46	48	40	R	Parietal	Inferior Parietal Lobule
					0.012	36	-54	40	39	R	Parietal	Angular Gyrus
2	1552	-32.2	-51.5	44.6	0.023	-30	-52	46	7	L	Parietal	Superior Parietal Lobule
3	1512	30.9	7.6	52.8	0.018	32	8	52	6	R	Frontal	Sub-Gyral
4	1176	42.9	36.9	24.1	0.022	42	36	24	9	R	Frontal	Middle Frontal Gyrus
5	1152	48.7	11.6	26.2	0.019	46	10	30	9	R	Frontal	Inferior Frontal Gyrus
					0.015	54	14	20	9	R	Frontal	Inferior Frontal Gyrus
6	904	53.2	-52.6	-12.1	0.021	54	-52	-12	37	R	Temporal	Fusiform Gyrus
7	904	-30.6	8.2	55.3	0.019	-32	8	54	6	L	Frontal	Middle Frontal Gyrus
8	720	-35.4	-60.8	-32.9	0.017	-38	-62	-32	.	L	Cerebellum	Tuber
					0.014	-28	-60	-34	.	L	Cerebellum	Cerebellar Tonsil

Activation patterns in depressive disorder

Figure 3.17 and Table 3.14 report neural activation patterns during n-back tasks in patients with depressive disorder (DD). The map includes 5 clusters (i.e., nodes) of activation underlining an involvement of the bilateral frontal cortices, the right parietal cortex, and the middle temporal gyrus. All the articles included in this analysis used verbal stimuli (numbers or letters) in the n-back task. A qualitative overlap between brain activity during n-back task in DD and healthy subjects (as shown Study 1) is depicted in Figure 3.17 B.

Table 3.14. Activity patterns for n-back tasks in patients with depressive disorder. Volume, coordinates and corresponding Brodmann area, lobe, hemisphere and regional labels are reported for each cluster included in the ALE map.

Cluster number	Volume (mm^3)	Weighted Center			Extrema Value	Extrema value coordinates			Brodmann Area	Hemisphere	Lobe	Label
		x	*y*	*z*		*x*	*y*	*z*				
1	664	2.77	20.11	47.07	0.02515911	2	20	46	6	L	Frontal	Medial Frontal Gyrus
2	480	37.31	-58.65	44.29	0.02127223	38	-58	44	39	R	Parietal	Angular Gyrus
3	296	49.37	-40.74	48.74	0.021600092	50	-40	48	40	R	Parietal	Inferior Parietal Lobule
4	288	9.67	37.58	38.71	0.020535074	10	38	38	8	R	Frontal	Medial Frontal Gyrus
5	96	35.01	-56.32	32.35	0.01752005	36	-56	32	39	R	Temporal	Middle Temporal Gyrus

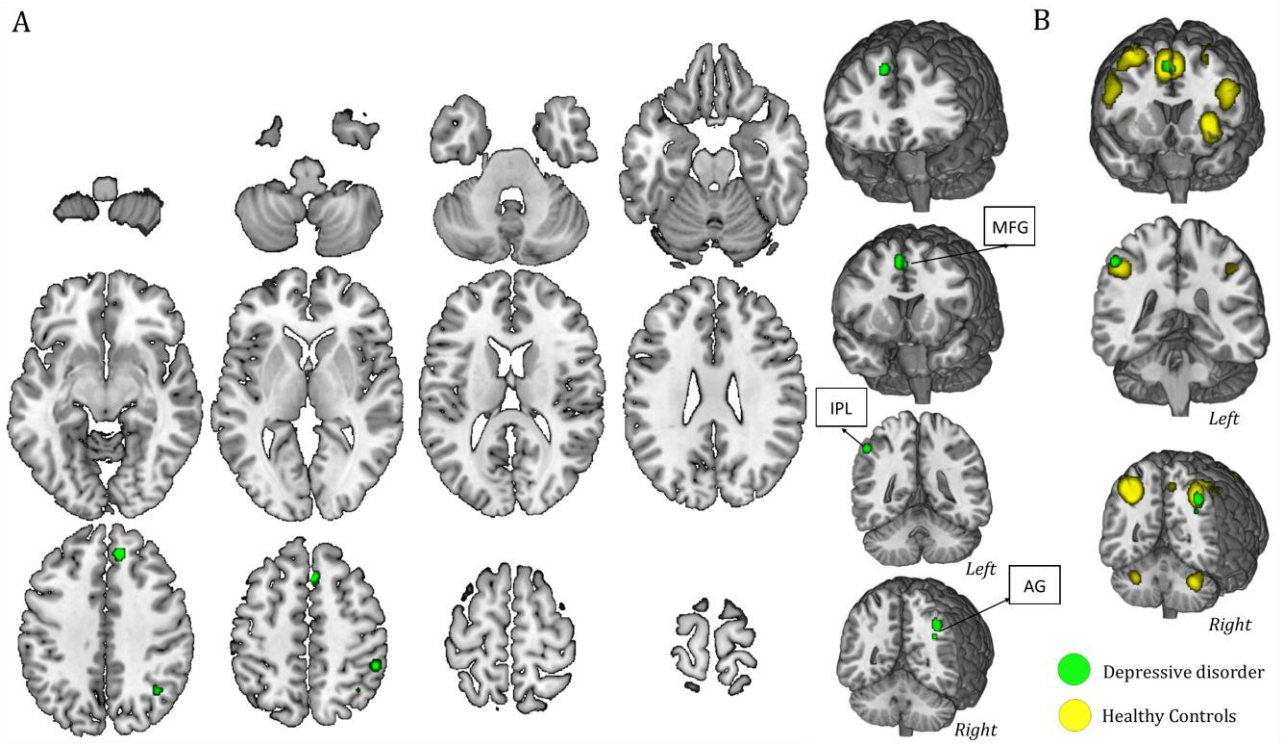

Figure 3.17. Depressive Disorder and n-back task. (A) The map refers to a set of studies that analyzed neural substrate during n-back task in patients with depressive disorder (10). A complete set of coordinates for each cluster is available in Table 3.14. (B) Qualitative overlap with the healthy subjects' map (in yellow) is presented.

Activation patterns in Bipolar disorder

Figure 3.18 and Table 3.15 show the map and coordinates of activity patterns elicited during the performance of the n-back tasks in patients with bipolar disorder (BD). The map includes 3 clusters (i.e., nodes) of activation showing a left lateralization of activation in the fronto-parietal areas and in the subcortical structures. All the articles included in this analysis used letters as stimuli in the n-back task. A qualitative overlap between brain activity during n-back task in BD and healthy subjects (as shown in Study 1) is reported in Figure 3.18 B.

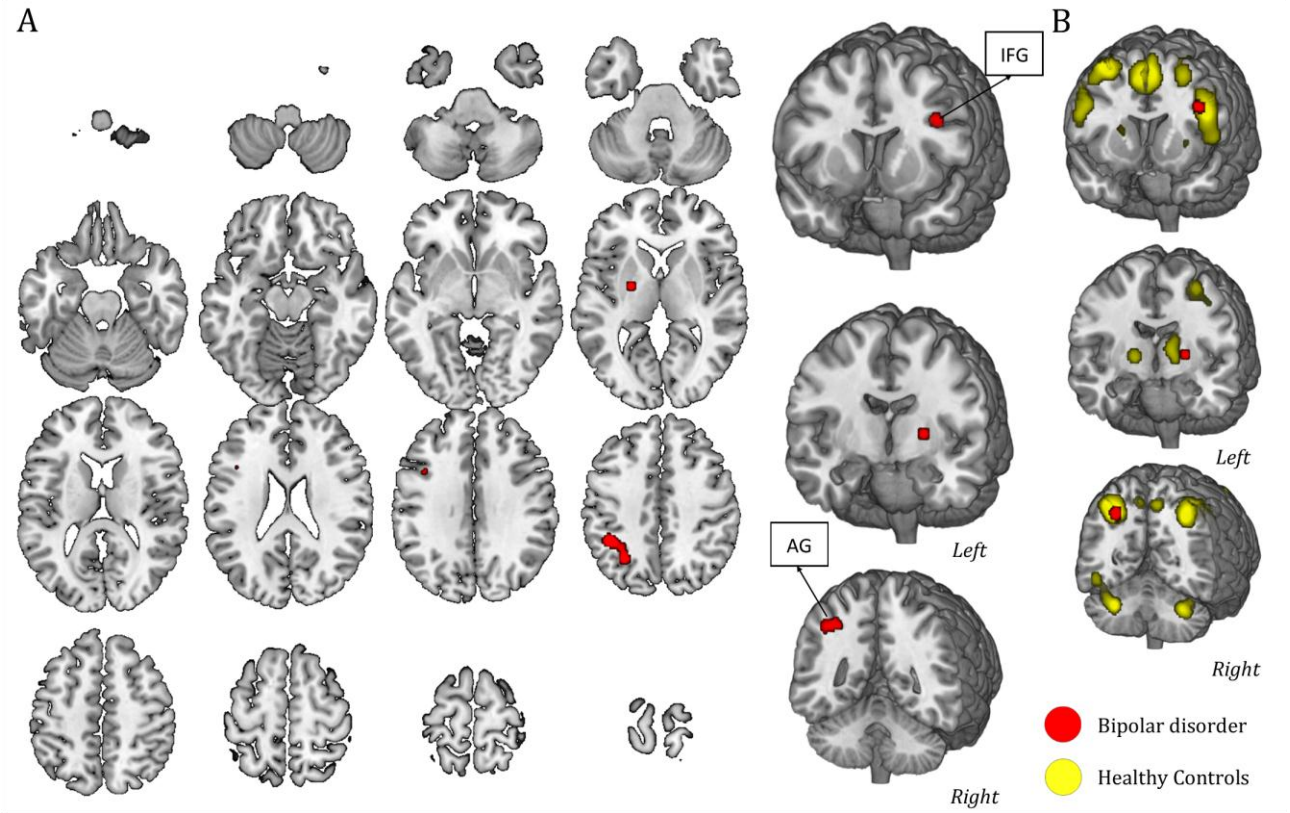

Figure 3.18. N-back task in patients with bipolar disorder. The map refers to 8 studies in which n-back task was performed by patients with bipolar disorder. A complete set of coordinates for each cluster is available in Table 3.15. (B) Significant slides of the qualitative overlap with the healthy subjects' map (in yellow) are reported.

Table 3.15. Neural substrate of the n-back tasks in patients with bipolar disorder. Volume, coordinates and corresponding Brodmann area, lobe, hemisphere and regional labels are reported for each cluster included in the ALE map.

Cluster number	Volume (mm^3)	Weighted Center			Extrema Value	Extrema value coordinates			Brodmann Area	Hemisphere	Lobe	Label
		x	*y*	*z*		*x*	*y*	*z*				
1	1632	-34.79	-50.99	43.45	0.024	-42	-44	42	40	L	Parietal	Supramarginal Gyrus
					0.019	-30	-58	44	39	L	Parietal	Angular Gyrus
2	376	-41.05	12.05	28.13	0.017	-40	12	28	9	L	Frontal	Inferior Frontal Gyrus
3	152	-24	-6	4	0.018	-24	-6	4	.	L	Sub-lobar	Lentiform Nucleus

Activation patterns in ADHD

Figure 3.19 and Table 3.16 report brain activity in patients with ADHD during n-back tasks and their corresponding set of coordinates. The map includes 7 clusters (i.e., nodes) of activation highlighting a bilateral involvement of the frontal areas, the right parietal areas, as well as the right subcortical structures and the right cerebellum. No active nodes were found over temporal

regions. A qualitative overlap between brain activity during n-back task in patients with ADHD and healthy subjects (as shown in Study 1) is illustrated in Figure 3.19 B.

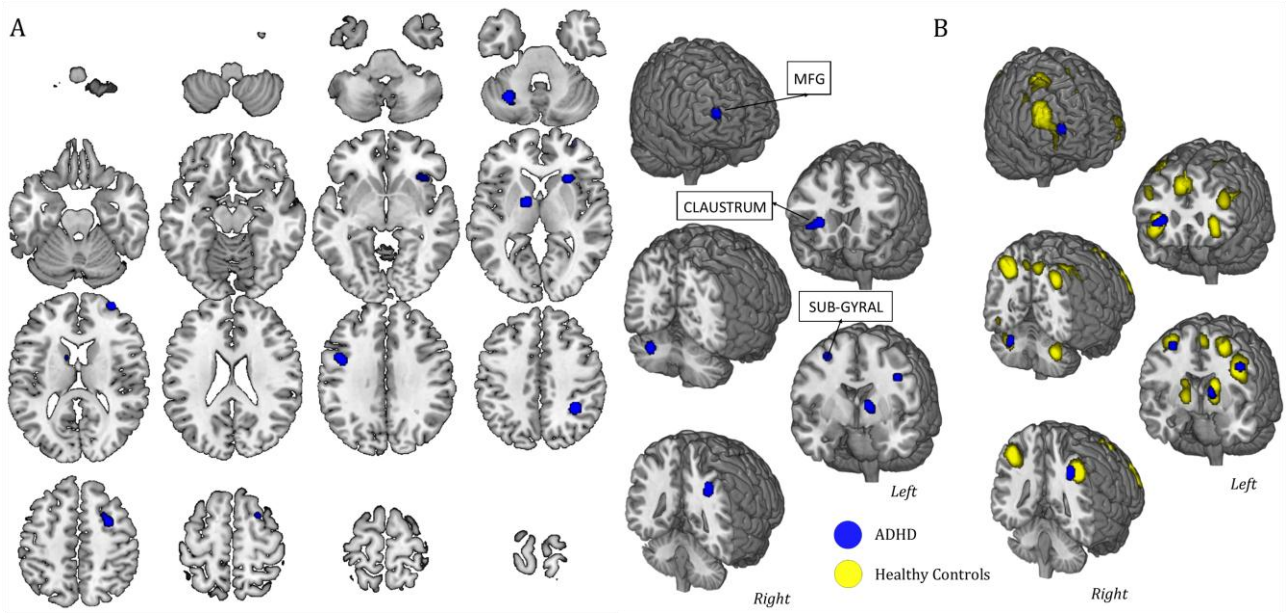

Figure 3.19. Brain activation pattern in patients with ADHD. (A) The map refers to 5 studies in which n-back task was performed by patients with ADHD. A complete set of coordinates for each cluster is available in Table 5. (B) Qualitative overlap with the healthy subjects' map (yellow) is shown.

Table 3.16. Pattern of activation during the n-back tasks in patients with ADHD. Volume, coordinates and corresponding Brodmann area, lobe, hemisphere and regional labels are reported for each cluster included in the ALE map.

Cluster number	Volume (mm^3)	Weighted Center			Extrema Value	Extrema value coordinates			Brodmann Area	Hemisphere	Lobe	Label
		x	*y*	*z*		*x*	*y*	*z*				
1	1112	33.3	-47.1	41.7	0.020	34	-46	42	7	R	Parietal	Precuneus
2	1040	29.7	22.1	.4	0.015	28	22	2	.	R	Sub-cortical	Claustrum
3	1032	-30.4	-61.1	-32	0.017	-32	-60	-32	.	L	Cerebellum	.
4	848	32	58	10.7	0.017	32	58	10	10	R	Frontal	Middle Frontal Gyrus
5	840	-13.5	-2.2	6	0.014	-14	-2	6	.	L	Sub-cortical	Lentiform Nucleus
6	760	27.9	5	53.6	0.014	30	4	54	6	R	Frontal	Sub-Gyral
					0.009	24	10	60	6	R	Frontal	Sub-Gyral
7	696	-44.6	3.4	34	0.014	-44	2	34	6	L	Frontal	Precentral Gyrus

Functional overlap between the different disorders and healthy subjects

The resulting map for the overall pattern of activation during n-back tasks in different disorders and healthy subjects is reported in Figure 3.20. The figure shows the involvement of the left

cerebellum as well as of the right frontal cortex only for ADHD and Schizophrenia, whereas the involvement of subcortical structures is especially marked in ADHD. Bilateral activation of parietal areas is more visible in patients with schizophrenia. Conversely, patients with other disorders showed lateralization in right (ADHD and DD) or left (BD) parietal regions. All these pieces of evidence overlap with the healthy subject map (in yellow). However, activity in the right subcortical areas (e.g., insula, claustrum, caudate) as well as in the right cerebellum is specifically shown in healthy people and none of the other pathological groups considered. Temporal activation on the left hemisphere is also typically observed in healthy subjects, whereas SZ and DD patients have a similar contribution only on the right temporal cortex. On the other hand, BD and ADHD do not show any temporal activation during the n-back task. Considering the bilateral parietal and frontal areas, neural activations are spatially similar between healthy and pathological cohorts, but they are wider in healthy subjects.

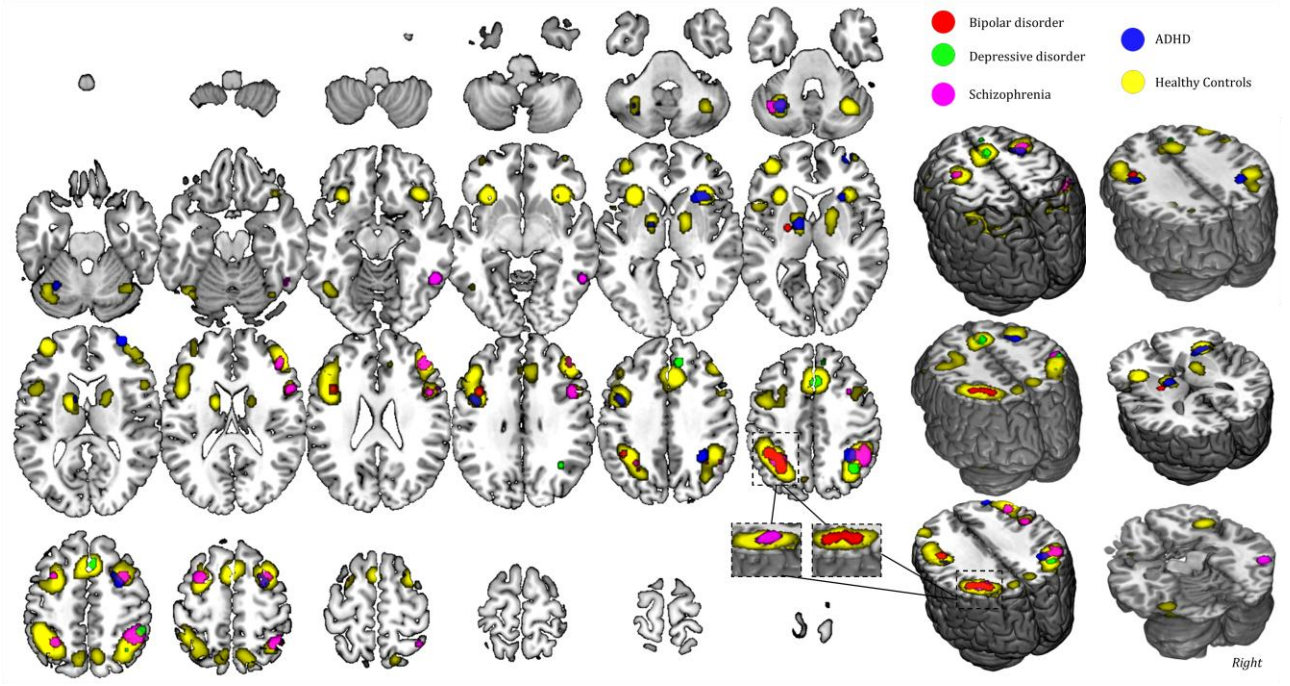

Figure 3.20. Overlap between pathologies and healthy subjects. The map shows a qualitative overlap of activation during n-back task between the four pathologies considered in this study and the general healthy map corresponding to the data shown in Study 1. The map is shown on a template brain in MNI space. MNI= Montreal Neurologic Institute.

Biophysical Modeling Results

The results of this metanalysis, pin down the most relevant regions of increased activity during the performance of n-back task in psychiatric and neurodevelopmental disorders. Therefore, they also provide relevant details to inform future targeted non-invasive brain stimulation interventions aimed to improve WM performance in the different clinical cohorts, as summarized in Figure 3.21. In particular, we suggest two possible approaches: i) restoring missing activations, thus stimulating areas that are activated in healthy subjects but not in the clinical cohort; ii) boosting the existing activations, thus modulating areas still active during the n-back task in patients. Following the latter approach, we also computed biophysical modeling to obtain the optimal multichannel montages targeting the main clusters involved during the n-back task in the clinical cohorts considered. Detailed information about this method are reported in Chapter 1.

Figure 3.22 reports the results of multichannel tES montage optimizations promoting the activation of the regions still active during the n-back task in the cohort of patients considered. We performed four different optimizations, one for each clinical group, targeting the two or three clusters easily reachable by tES and with the higher extrema values as reported by GingerALE maps (see the corresponding tables for each coordinate). The weighted maps used for the four optimizations are shown in Figure 3.22 (A-D). For the stimulation optimizations we set a: 2mA max current per electrode and 4 mA max total injected current, following the tES recommendation guidelines. The positions of the electrodes are picked from a pool of 64 electrodes. The algorithm limits the montages to 8-channels, for each optimization. In detail the montage for Schizophrenia comprehends F4: 1700μA, F6: -1700μA, C1: -500μA, CP3: -600μA, CP6: -600μA; P1: 1150μA; P2: 1150μa, P6: -600μA (Figure 3.22 A); for Depressive disorder: F2: -550μA, FC1: 1200μA, FCZ: 2000μA, FC2: -2000μA, C3: -650μA, CP2: 200μA, CP6: -800μA; P4: 600μA (Figure 3.22 B); for Bipolar disorder: FC5: -1350μA, FC3: 1750μA, FC1: -150μA, C3: 100μA, CP5: -1500μA, CP1: 1500μA, P3: 650μA, Pz: -1000μA (Figure 3.22 C); and for ADHD: Cz: -1200μA, AFz: 500μA, AF8: -500μA, F2: 1300μa, F8: -1200μA, CPz: 200μA, CP4: 2000 μA, P2: -1100 μA (Figure 3.22 D). Given the current constraints, these solutions represent the best fit of the normal E-field to the target maps obtained from the ALE meta-analysis. However, these montages are only suggestions based on our ALE maps, clinical experience and the limitations we used in performing the biophysical modeling. The same analysis can be performed considering other constraints or NIBS methods as, for

example, the transcranial alternate current stimulation (tACS) including also the wave shape as additional information.

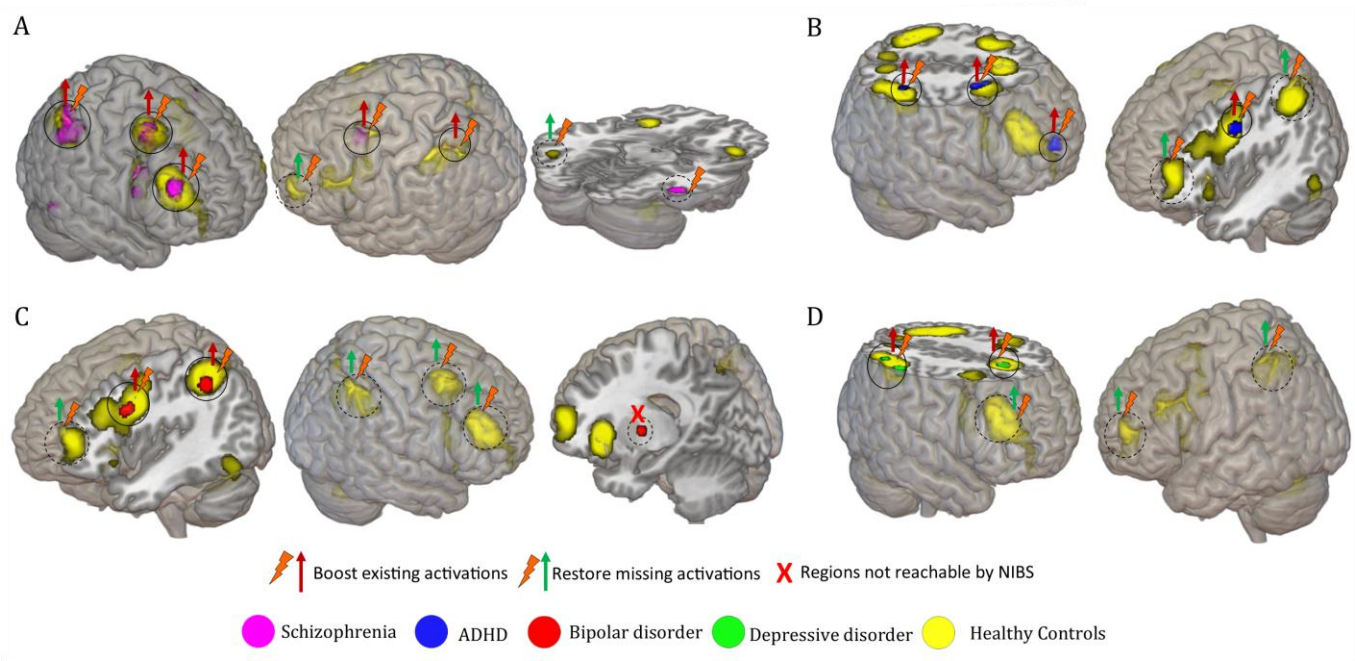

Figure 3.21. Possible targets for NIBS. Cortical regions that could be used as targets for NIBS are shown. Areas of overlap between healthy subjects and patients are highlighted with continuous line circles and red arrows, whereas areas that show activation only in the healthy subjects' map are underlined by dashed line circles and green arrows. Subcortical regions are depicted with an X since they are not accessible directly through NIBS. Areas of non-overlap with healthy subjects' map could be an expression of compensatory mechanisms or dysfunctional activity, future investigation should be conducted to detect the stimulation polarity (inhibitory or excitatory). (A) SZ; (B) ADHD; (C) BD; (D) DD.

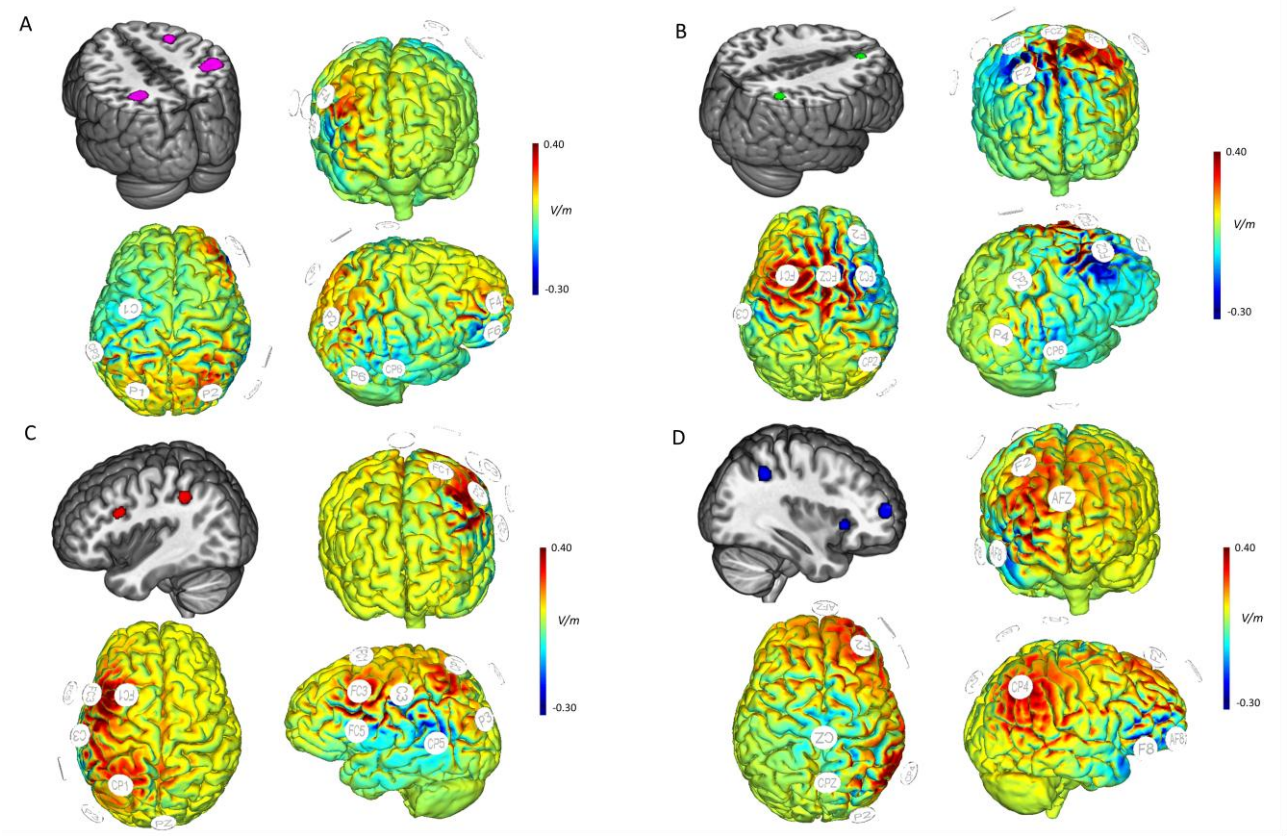

Figure 3.22. tES Optimization montages for each clinical cohort. Stimulation montages aimed at boosting the nodes still active during the n-back task in (A) SZ; (B) DD; (C) BD; (D) ADHD are shown. All the optimizations involve 8 electrodes, delivering a total maximum current of 2 mA each electrode (4mA in total). The weighted map, and the nE-field (V/m) for each montage are presented.

3.2.3 DISCUSSION

We showed a set of specific maps representing the neural substrate of n-back task in patients with schizophrenia, depressive and bipolar disorders, and ADHD. In the following paragraphs, we will discuss the functional role of the resulting core regions for each examined disorder, as well as the observed overlap with maps previously computed in healthy subjects (as shown in the Study 1). Finally, we will discuss the utility of different activation patterns for planning neurostimulation and cognitive enhancement interventions.

Core Regions in Schizophrenia

Frontal hypoactivation during cognitive training in SZ patients, compared to healthy subjects, has been consistent observed in the literature (Glahn et al., 2005; Minzenberg et al., 2009) as well as

the functional connectivity modulation in the fronto-temporal (Crossley et al., 2009), default mode network (Zhang et al., 2013) and fronto-parietal networks (Deserno et al., 2012; Nielsen et al., 2017). Particularly, the bilateral fronto-parietal networks have been associated with n-back task in healthy subjects (Mencarelli et al., 2019) and, the lack of neural activity in this network in SZ patients has been usually linked to their low ability in WM tasks. Nevertheless, the ALE map resulting from the present study shows a neural activity pattern similar to the control subjects (as shown in Figure 3.16B). The fronto-parietal network is activated during n-back task even in SZ patients, although with strong lateralization on the right hemisphere. Therefore, differently from the previous meta-analysis on SZ patients (Glahn et al., 2005; Minzenberg et al., 2009), we did not find a total absence of activation in the frontal lobe, but only a reduced activity in left frontal areas. Moreover, Glahn et al. (2005) underlined also increased activation in the anterior cingulate cortex (ACC) and left frontal pole regions in SZ patients during the n-back task. The authors suggested that abnormal activation patterns are not restricted to dlPFC, despite reduced activation of this region is consistently reported in SZ patients. However, our results are not in line with their observations because we did not find activity on ACC. The hypothesis that ACC increases its activity during the cognitive task in SZ patients due to hypoactivation on the frontal areas cannot be supported by our results, that instead revealed the opposite. Our findings partly sustain the guided activation model formulated by Miller and Cohen (2001). This model affirms that the concurrent activation of dlPFC and ACC is needed for the right allocation of additional control over the task that necessitates it. In SZ patients the absence of activity in ACC during a task that requires a high attentional control (like n-back task) may be the cause of their poor cognitive performance not only concerning the task but also in many daily life activities.

The activation in the left cerebellum may be considered an unexpected result, because it was not previously described in another meta-analysis, despite it is in line with activity related to n-back task in healthy subjects. Indeed, as previously explained by Marvel and Desmond, working memory tasks could be supported by the cerebellum through the engagement of inner speech mechanism (Marvel & Desmond, 2010). Moreover, the development of inhibitory control seems to be mediated by the functional maturation of fronto-cerebellar neural pathways (Rubia et al., 2007). This, together with the hypothesis that only the inferior frontal gyrus (IFG) could be specialized for the interplay with cerebellar areas for inhibitory control (Picazio et al., 2016), could support the role of the cerebellum in SZ patients while performing n-back task and, more generally, in the cognitive domain.

N-back and Depressive Disorder

Several neuroimaging studies have been conducted while patients with DD were performing WM paradigms, showing that their WM impairments could be mediated by the aberrant activity in related brain areas as the prefrontal, parietal, temporal, cerebellar, and subcortical regions (Harvey et al., 2005; Vasic et al., 2009; Walter et al., 2007). However, these studies reported contrasting findings: some studies described increased activation of the dlPFC and/or ventrolateral prefrontal cortex (vlPFC) in patients compared to controls (Harvey et al., 2005; Matsuo et al., 2007; Walter et al., 2007), while others observed decreased activity in the same areas (Goethals et al., 2005; Kerestes et al., 2012; Pu et al., 2011), additionally null findings have also been shown from other studies (Barch et al., 2003; Rose et al., 2006; Sandström et al., 2012). Recent meta-analyses also showed heterogenic results, probably because they collected cognitive and emotional experiments, while others focused only on one specific aspect (Müller et al., 2017; Wang et al., 2015), and also our results stand back to the previous findings. Differently from Wang et al., (2015), we did not find a specific prefrontal hyperactivation during WM processing in the left dlPFC and vlPFC. However, as we focused the meta-analysis on a single WM task (n-back), different results compared to other meta-analyses were expected. In particular, we showed an involvement of the left and right medial frontal gyrus and of the right parietal and temporal areas that have been already reported as involved in the n-back paradigm in healthy controls (Mencarelli et al., 2019; Figure 3.17 B). The inferior parietal cortex (BA 40) and the angular gyrus (BA39) play an important role in maintaining temporal information and switching attention rapidly (Ravizza et al., 2004), as well as in preparing for a forthcoming given task (Sohn et al., 2000). Moreover, in line with our results, an increase in cerebral blood flow (CBF) on the right parietal cortex in patients with DD during a cognitive task has already been reported (Berman et al., 1993). On the other hand, the lack of activation in the bilateral dlPFC during n-back task may be associated with local hypometabolism (Baxter et al., 1989; Sackeim et al., 1990) and decreased CBF (Bench et al., 1992; Galynker et al., 1998), usually reported in patients with DD when compared to controls. However, some studies suggested that a good WM performance in patients with DD is associated with increased cortical activity while impaired performance is associated with a decrease in cortical activation. Even though this represents a crucial aspect of clinical trials, we could not investigate it in our study due to the insufficient number of studies collected.

Core regions in Bipolar Disorder

Several studies have demonstrated that cognitive impairment, involving executive function and long-term memory particularly (Robinson & Ferrier, 2006), is a common feature in patients with BD. Recent neuroimaging studies provided numerous evidences about brain functional correlates of cognitive deficits in BD. Focusing on WM deficit, they have shown an aberrant activity in the prefrontal, parietal, and temporal cortices during WM tasks. However, also in this case, the available specific literature is not extensive and the results are moderately heterogeneous: all the studies presented a mixed picture of hyperactivation and hypoactivation in brain regions that are traditionally involved in WM circuits including dlPFC, vlPFC as well as the parietal and temporal cortices (Adler et al., 2004; Frangou et al., 2008; Monks et al., 2004; Thermenos et al., 2010). However, our results, focusing on n-back task only, showed a parietal as well as a subcortical activation, in line with the neural pattern showed in healthy subjects, even though with less extensive activity in BD. Unexpectedly, we found a left hemisphere lateralization in BD, that has been never reported so far. Such inconsistency could be the result of the balance between homogeneity and robustness: in this work we decided to focus on brain activity in BD during n-back task, complying with the criteria of homogeneity but, due to the limited literature available so far, we did not completely observe the criteria of robustness (Müller et al., 2018). Nevertheless, this evidence should be interpreted carefully since the results of a meta-analysis with a low number of papers could be driven by few experiments (Eickhoff et al., 2016). Moreover, other potential confounding factors, as different pharmacological treatments and clinical variables used within the considered studies, could also have driven the results.

Additionally, as hypothesized, both bipolar and depressive disorder did not show activation in the dlPFC. Several neuroimaging evidence has shown a similar pattern of brain abnormalities between mood disorders, with the involvement of the prefrontal cortex, the limbic system (e.g. the amygdala), the ventral striatum, the insula, and the hippocampus (Arnone et al., 2012; Bora et al., 2012; Delvecchio et al., 2012; Selvaraj et al., 2012). This has been confirmed also by other neuroimaging modalities, underling for example that depression and bipolar disorder are characterized by abnormalities in white matter tracts of the genu of the corpus callosum that connect the two hemispheres of the prefrontal cortex implicated in mood regulation (Wise et al., 2016). However, looking at the parietal activation, the two mood disorders showed an opposite pattern: lateralization on the left hemisphere has been shown for BD, whereas lateralization on the right hemisphere has been found for DD. These findings may support the idea that failure in

the engaging bilateral fronto-parietal network in mood disorders represents the core of cognitive impairment; this hypothesis should be verified in future studies.

Brain activity in patients with ADHD

The main behavioral features in ADHD are inattention and impulsivity that, as a collateral effect, lead to executive function impairment. In order to understand if this impairment could be directly linked to functional changes within specific brain regions, several studies have run WM tasks during fMRI in patients with ADHD. The current meta-analysis gathers all these studies in order to create a comprehensive activation map for the n-back task. As in healthy subjects, results in ADHD showed brain activity in frontal, parietal, subcortical, and cerebellar regions, although generally reduced. This result is in line with the literature in the field: several studies have already pointed out that participants with ADHD displayed hypoactivity compared to healthy controls in the right superior and middle frontal areas as well as in cerebellar, occipital, and parietal areas (Bayerl et al., 2010; Kobel et al., 2009; Mattfeld et al., 2016; McCarthy et al., 2014; Valera et al., 2005). Moreover, differently from the healthy controls, there is no activation in the left dlPFC and left parietal regions in patients with ADHD. The anomalous activity in the former has been already shown in a previous meta-analysis (McCarthy et al., 2014), and this is expected since dlPFC plays an important role in monitoring and updating the incoming information (Bagherzadeh et al., 2016; Brunoni and Vanderhasselt, 2014; D'Esposito et al., 1998; Owen, 1997; Owen et al., 2005), skills known to be impaired in ADHD. However, the dysfunctional activity in the left parietal cortex has never been pointed out in this clinical cohort. This area is involved in many higher-order functions and particularly in the maintenance of goal-directed attention (Corbetta & Shulman, 2002), and has an important role in the n-back task. However, the direct comparison between the neural activation in healthy subjects and patients with ADHD should be interpreted carefully, due to differences in the sample: in the study 1 all the studies performed on children or older adults have been excluded; while in the present meta-analysis, also studies that considered children or young adults in the sample have been included as ADHD is a neurodevelopmental disorder. Moreover, some neuroimaging studies have considered patients with ADHD as a whole group without differentiating between patients with and without working memory deficits, whereas other studies considered this difference. These latter studies highlighted that the impairment in the fronto-parietal network is mostly shown in patients with WM deficit (Mattfeld et al., 2016). Unfortunately, the small number of studies available did not allow us to investigate if there is a

direct link between the similarity in brain activation patterns between patients and healthy controls and WM performance.

Potential NIBS targets for Cognitive Enhancement

The present results shed light on the common and specific neural basis of n-back task in psychiatric and neurodevelopmental populations and suggest potential targets for TMS and tES neuromodulatory interventions (Bestmann et al., 2015; Santarnecchi et al., 2015; Tatti et al., 2016). Several non-invasive therapeutic applications have been proposed so far but with inconsistent results. In a recent review Hill et al., (2016) showed that anodal tDCS applied to a clinical population significantly improves accuracy for online, but not offline, WM tasks, and no effect was found on reaction times. The heterogeneity between studies could be ascribed to several factors, as, for example, current density and stimulation duration, but also to the stimulation target. Most of the studies investigating the effects of NIBS on WM performance have targeted the dlPFC, due to its strong involvement in WM tasks (for a comprehensive review see Hill et al., 2016). However, there are several WM tasks, and not all of them have the same neural substrate (e.g. backward digit span, dual task, visual pattern recall, visual working memory task; Cocchini et al., 2002; McCarthy et al., 1994; Salmon et al., 1996); also subjects' age may play a role in the responsiveness to NIBS for WM tasks, younger subjects reacting better than older ones (Feurra et al. 2016). Moreover, better results in terms of cognitive enhancement could be obtained using fMRI-guided targeting for NIBS increasing the accuracy of the treatment.

Considering the n-back task, several brain regions are implicated when the task is performed by healthy subjects, including frontal, parietal, and cerebellar areas (Mencarelli et al., 2019; Owen et al., 2005; Rottschy et al., 2012), however, dlPFC has been the most used target to boost n-back performance by NIBS. Nevertheless, this area could not be the best target for patients with WM deficits: the ideal parameters in one population may not be optimal in another. For instance, our results showed that schizophrenic patients mostly activate the right fronto-parietal network and left parietal cortex, whereas less activity has been shown in the left frontal cortex; on the other hand, patients with depressive disorder showed activation mostly on the right parietal cortex. In this case, the stimulation targets should be based on the patients' brain activity when a neuromodulation intervention is planned. Following our results, the possible approaches may aim to (i) improve the activity of nodes still active even in the presence of a pathological condition and working memory deficit, or (ii) reactivate nodes of the n-back network showing lack of activation

as compared to healthy controls (Figure 3.21). Following the first approach, we proposed different tES multichannel optimization using biophysical modeling (Figure 3.22). Future studies may investigate the effects of stimulation over these locations, covering additional therapeutic targets that have never been considered so far, as, for example, parietal and temporal cortices. Moreover, only single-site stimulation has been tested in patients with WM deficits so far. However, it is unlikely that this approach will produce a clinically meaningful whole brain effect and corresponding cognitive effects could be inconsistent between studies, as already pointed out in recent reviews (Hill et al., 2016; Hurley & Machado, 2018). Recently, multichannel stimulation devices have been developed, allowing the stimulation over multiple cortical sites using small and more focal electrodes, as the one we proposed here (Ruffini et al., 2018). These devices could provide an innovative alternative for potentially stimulating the entire WM network or functional MRI networks, as already proved in healthy (Brem et al., 2018; Fischer et al., 2017; Mencarelli et al., 2020; Neri et al., 2019; Polanía et al., 2012) and clinical (Dagan et al., 2018; Sprugnoli et al., 2019; Thibaut et al., 2017) cohorts. Moreover, future studies could analyze the functional connectivity profile of the ALE regions resulting from our meta-analysis, suggesting hypoactivation/hyperactivation of one or more networks in the clinical cohort and leading a more specific non-invasive brain stimulation intervention. Future studies could also consider the use of other techniques such as EEG and TMS-EEG, able to explore brain-behavior relationships (Daskalakis et al., 2012; Fitzgerald, 2010; Rogasch & Fitzgerald, 2013) and provide more information on temporal dynamics between networks as well as to characterize network-level individual brain dynamics (Ozdemir et al., 2020), useful for NIBS interventions (e.g. cc-PAS TMS, Di Lorenzo et al., 2018; Fiori et al., 2018; Koch, 2020; Nord et al., 2019; Veniero et al., 2013).

Finally, NIBS interventions are not the only ones useful in order to increase WM performance in patients with cognitive deficits. Several studies have already pointed out that specific memory training programs produce short-term effects but, unfortunately, do not generalize to other cognitive domains (for a comprehensive review see Melby-Lervåg & Hulme, 2013). Other studies reported the possibility to increase WM capacity through mindfulness meditation (Baranski & Was, 2018; Innes et al., 2017) or physical exercises (Hoffman et al., 2008; Kramer et al., 1999; Rand et al., 2010), but with inconsistent results. Moreover, numerous evidences suggest that the combination of two kinds of interventions, cognitive training and physical activity training, improves cognitive function in healthy older adults (for a comprehensive review see Jak, 2012). From this perspective also the combination of NIBS with cognitive interventions offers a

potentially powerful new approach for treating neuropsychiatric disorders, as recently reviewed by Sathappan et al., (2019). In this case, the timing of the NIBS is important since it could be applied online or offline for cognitive intervention. In particular, the functional engagement of a specific network during a cognitive task could simplify the long-term potentiation effects obtained with neuromodulation. Future studies could demonstrate the efficacy of WM training combined with MRI-guided targeted NIBS based on different clinical cohorts.

3.3 STUDY 3: Network Mapping of Connectivity Alterations in Disorder of Consciousness: Towards Targeted Neuromodulation[2]

Brain injury is one of the major causes of death and disability in the world (Langlois et al., 2006). As a consequence, several patients suffer from disorder of consciousness (DoC) (for specific statistics see Pisa et al., 2014), a condition that can be divided into four states: (i) coma (patients are not able to spontaneously open their eyes and to be awakened even with strong sensory stimulation; (Jellinger, 2009)), (ii) vegetative state/unresponsiveness wakefulness syndrome (VS/UWS; patients are able to stay awake spontaneously or after stimulation, but they have no awareness of themselves or of the environment; (Jennett & Plum, 1972; Laureys et al., 2010)), (iii) minimally conscious state (MCS; patients show some behavioral evidence of consciousness; (Giacino et al., 2002)) and (iv) patients emerging from MCS (EMCS; patients recover the ability to use objects in a functional manner, (Nakase-Thompson et al., 2004)). Patients may fluctuate between these different states until they fully recover consciousness, or may remain in a DoC state for years or permanently. Due to the strong impact of disease in patients and their caregivers, research aimed at improving diagnosis and therapies for patients with DoC is of great interest.

In the last years, consciousness has been defined as separated in two linearly correlated components: arousal and awareness (Zeman, 2001). Awareness can be divided in two distinct and negatively correlated networks: the 'external awareness' network, which includes bilateral fronto-temporo-parietal cortices, and the 'internal awareness' network, consisting of midline posterior cingulate cortex/precuneus and anterior cingulate/medial prefrontal cortices (Vanhaudenhuyse et al., 2011). In support of this hypothesis, several neuroimaging and electrophysiological studies showed the presence of a structural and functional disconnection between these brain areas in DoC patients (Bodart et al., 2017; Massimini et al., 2012; 2009). Specifically, deficits of cortico-subcortical (i.e., including the thalamus) and cortico-cortical connectivity have been proposed as one of the biological causes of DoC (Laureys & Tononi, 2011; Posner, 1994). Resting state fMRI (rs-fMRI) and PET studies suggest impaired inter-hemispheric connectivity in the 'external awareness' network (Vanhaudenhuyse et al., 2011), as well as in corticothalamic circuitry and the default

[2] A similar version of this article has been recently published (Mencarelli, L., Biagi, M. C., Salvador, R., Romanella, S., Ruffini, G., Rossi, S., & Santarnecchi, E. (2020). *Journal of clinical medicine*, *9*(3), 828).

mode network (DMN) in patients compared to healthy controls (Boly et al., 2009; Ovadia-Caro et al., 2012; Vanhaudenhuyse et al., 2010). Moreover, a decrease in functional MRI resting state low frequency fluctuations and regional voxel homogeneity (Tsai et al., 2014) has been shown in DMN regions in patients with DoC. Historically, the DMN has been associated with conscious and self-related cognitive processes (Buckner & Vincent, 2007; Raichle et al., 2001) such as inner or task-unrelated thoughts (McKiernan et al., 2006) and self-reflection (Ingvar, 1979), with a progressive decrease in the functional connectivity (FC) of DMN regions alongside the spectrum of consciousness (Boly et al., 2009; Demertzi et al., 2014; Huang et al., 2014; Norton et al., 2012; Vanhaudenhuyse et al., 2010).

Until now, both pharmacological and non-pharmacological therapies for DoC have been proposed, with several contrasting results. Non-pharmacological interventions (reviewed in Ragazzoni et al., 2017) are divided in invasive (deep brain stimulation or vagal nerve stimulation) and non-invasive approaches (e.g., transcranial direct current stimulation -tDCS-, repetitive transcranial magnetic stimulation -rTMS-, transcutaneous auricular vagal nerve stimulation, low intensity focused ultrasound pulse and sensory stimulation program). Recent literature reviews (Bourdillon et al., 2019; Thibaut et al., 2019) support the hypothesis that Non-Invasive Brain Stimulation (NIBS) is more successful than other therapies, but, considering the few evidence available to date, these techniques are not yet officially recommended by clinical consensus groups. In particular, the dorsolateral prefrontal cortex (dlPFC) was identified as a better target for tDCS compared to precuneus and motor cortex, due to its involvement in cortico-subcortical network and to its strong connection with thalamus and striatum, which is impaired in DoC according to the mesocircuit fronto-parietal model (Giacino et al., 2014). However, only two studies on tDCS provided class II evidence (Thibaut et al., 2019) and only in MCS patients, whereas for VS patients none of these approaches have provided group-level effects yet (Cincotta et al., 2015; Mancuso et al., 2017).

Although new therapeutic approaches seem to be beneficial for patients with DoC, the optimization of procedures and parameters should be the goal of future studies. So far, the stimulation target in patients with DoC has been chosen based on anatomical and physiopathological models. However, several neuroimaging studies revealed the disconnection between different brain networks in DoC (‘external awareness’ and ‘internal awareness’ networks), and also found that brain regions do not operate in isolation but rather continuously interact with each other (Fox et al., 2005; Fox, Halko, et al., 2012; Sheffield & Barch, 2016).

Therefore, network targeting is becoming the main goal of neuromodulatory interventions and should be used in patients with DoC. Several studies already showed the possibility to target an entire network by means of non-invasive brain stimulation (NIBS; Dmochowski et al., 2011; Miranda et al., 2013; Ruffini et al., 2014). In particular, Ruffini et al. (2014) developed an algorithm for the optimization of multielectrode tES that uses subject's data (fMRI, PET, EEG or other data) to optimize personalized stimulation protocols in terms of electrodes position and stimulation intensity. This approach is applicable to all tES modalities (e.g., tACS, tDCS, tRNS) and had already been implemented successfully in healthy subjects (Brem et al., 2018; Fischer et al., 2017; Neri et al., 2019) and patients (Dagan et al., 2018; Sprugnoli et al., 2019; Thibaut et al., 2017).

In this study we present a quantitative meta-analysis with the aim of localizing the brain regions usually displaying altered activity both during external stimulation and at rest in patients with DoC, summarizing the fMRI and PET literature available to date. Network mapping was performed on brain regions resulting from the metanalysis, pinning down the most relevant networks altered in DoC patients and providing relevant details to inform future personalized tES solutions.

3.3.1 MATERIAL AND METHODS

Literature search

The literature search was carried out using PubMed and Google Scholar databases without temporal limitations. The following terms "Disorder of Consciousness", "DoC", "vegetative state", "minimally conscious state", "unresponsive wakefulness syndrome" were individually combined with "Functional Magnetic Resonance Imaging", "Position Emission Tomography" and their acronyms. Following careful abstract screening of every resulted article published before February 2020, a total of 40 studies were chosen and scrutinized (Figure 3.23). We intentionally excluded (i) review papers, (ii) studies not mentioning any of the keywords in the abstract, (iii) studies not reporting fMRI/PET activations coordinates in MNI or Talairach space, (iv) studies not reporting activation foci in table format or reporting statistical values without corresponding coordinates, (v) studies that used predefined Regions of Interest (ROIs), (vi) studies reporting results obtained with Small Volume Correction (SVC), (vii) studies not in English language. The final selection included 17 studies reporting either fMRI or PET findings. For each study, the following information were retrieved: (i) number of participants, (ii) etiology; (iii) sex, (vi) mean age, (v) contrast, (vi) reference, (vii) foci, (viii) imaging modality. Moreover, for task-related experiments we also

included the following information: task category, modality, and task type (Table 3.17). In particular, the etiology of patients considered in these studies is heterogeneous: traumatic brain injury (TBI), anoxic brain injury, cerebrovascular accident, hypoxic ischemic brain injury, hypoglycemia, subarachnoid hemorrhage, encephalitis, cardiopulmonary arrest, occlusion basilar artery, intoxication, stroke, cardiac arrest, and aneurysm. Due to the limited literature, we decided to consider any cause of DoC, not just TBI. Moreover, the number of subjects for each study ranges from case report (Fernández-Espejo et al., 2010; Monti et al., 2013), to large simple size (n=27) (Demertzi et al., 2014; Marino et al., 2017). The majority of the patients are male (225 on 341 total subjects), mean age is 44. Specific activation foci were collected and included in a quantitative Activation Likelihood Estimation (ALE) analysis for the identification of brain regions most commonly reported as involved in DoC.

Two separate maps were created: (i) a task-based map including all the coordinates referring to fMRI/PET activations during specific tasks (6 studies; Fernández-Espejo et al., 2010; Laureys et al., 2000; Liang et al., 2014; Marino et al., 2017; Monti et al., 2013; Owen et al., 2002), and (ii) a resting-state map considering all the coordinates referring to neural deactivation in DoC patients compared to healthy controls (11 studies; Bruno et al., 2010; Bruno et al., 2012; Demertzi et al., 2014; He et al., 2014; Kim et al., 2010, 2013; Koenig et al., 2014; Nakayama, 2006; Norton et al., 2012; Soddu et al., 2016; Thibaut et al., 2012). Furthermore, when selecting data for the resting state ALE map, we divided fMRI/PET activations data for VS (including Unresponsive Wakefulness Syndrome, UWS) and MCS patients, resulting into two distinct maps. Activation foci were extracted separately for MCS and VS/UWS patients for each study. Studies in which DoC patients were combined (e.g., VS and MCS) without reporting separate information for each condition were excluded from the analysis. Patients defined as in 'coma', were considered as in "VS" for the analysis. The final selection included 4 studies for MCS (Bruno et al., 2012; Kim et al., 2013; Nakayama, 2006; Thibaut et al., 2012) and 7 studies for VS (Bruno et al., 2010; Kim et al., 2010; Koenig et al., 2014; Nakayama, 2006; Norton et al., 2012; Soddu et al., 2016; Thibaut et al., 2012). Given the limited number of studies focusing on each specific condition, more in-depth analysis was not feasible, therefore results must be considered exploratory in nature. Data on Locked-In Syndrome (LIS) and Emerging Minimally Conscious State (EMCS) were not included in the analysis due to very limited literature.

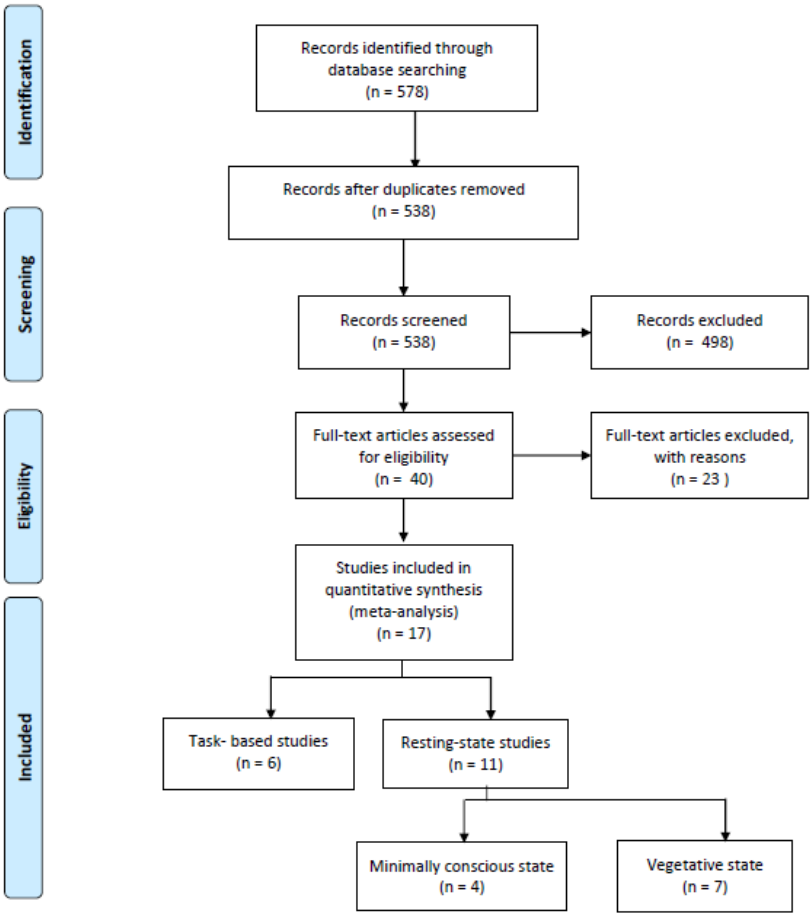

Figure 3.23. Literature search for the identification of relevant publications included in the ALE metanalysis (from Liberati et al., 2009).

Table 3.17 List of studies considered in the meta-analysis. Sample size, etiology of DoC, gender and age of sample, reference space, number of foci, imaging modality and experimental conditions are shown. Additional information about the specific experimental paradigm are reported for task-based studies. Patients labeled as in a "coma" were relabeled as VS; studies specifically comparing LIS and EMCS patients were not included in the analysis due to small sample size.

Paper	Subjects	Etiology	Sex (F)	Age (mean)	Reference	Foci	Imaging Modality	Contrast	Task category	Modality	Task Type
Task-based studies											
Fernández-Espejo et al., 2010	1 UWS	TBI	0	48	MNI	2	fMRI	For>back; listen>silence	passive	auditory	sentences listening
Liang et al., 2014	5 (2UWS, 3 MCS)	TBI	2	42.8	MNI	10;6;11;4	fMRI	listen>rest; Navigation>rest; counting>rest; face>rest	active and passive	auditory	spoken sentenses and motor/mental imagery
Monti et al., 2013	1 MCS	TBI	---	---	MNI	33	fMRI	no contrast	passive	auditory	visual stimulation
Owen et al., 2002	3 UWS	acute febrile illness; TBI; cardiorespiratory arrest	3	28	MNI	8	PET	visual stimulation; familiar face perception; speech perception	passive	visual and auditory	visual stimulation
Marino et al., 2017	50 (23 UWS, 27 MCS)	TBI, anoxic brain injury; cerebro-vascular accident		50	MNI	12	fMRI	no contrast	passive	auditory	sentences listening
Laureys et al., 2000	5 UWS	hypoxic origin	3	44	TAL	4;8	PET	no contrast; DOC<HC	passive	auditory	click
Resting-State Studies											
Bruno et al., 2010	10 UWS	cronic post-anoxic enephalopathy	2	44.3	MNI	16	PET	DOC<HC			
Bruno et al., 2012	27 MCS	anoxia; TBI; subarachnoid hemorrhage; encephalitis; hypoglycemia; cerebro-vascular accident	10	45	MNI	40	PET	DOC<HC			
Demertzi et al., 2013	53 (5coma, 24 UWS, 24 MCS)	brain insult	23	50	MNI	50	fMRI	DOC<HC			
He et al., 2014	12 (9 UWS, 3MCS)	TBI; cerebro-vascular accident; anoxic brain injury	4	44.7	MNI	8;8	fMRI	DOC<HC; DOC>HC			
Kim et al., 2010	12 UWS	anoxic brain injury	5	41.7	MNI	4;3	PET	DOC<HC; DOC>HC			
Kim et al., 2013	17 MCS	hypoxic-ischemic brain injury	8	40.5	MNI	16;5	PET	DOC<HC; DOC>HC			
Koenig et al., 2014	17 coma	cardio-pulmunary arrest	3	55	TAL	3	fMRI	DOC<HC			
Nakayama et al., 2006	30 (17 UWS, 13 MCS)	TBI	11	30	TAL	13;10	PET	DOC<HC			
Norton et al., 2012	13 (11 irreversible coma, 2 reversible coma)	cardiac arrest	5	66.3	MNI	16	fMRI	DOC<HC			
Soddu et al., 2016	15 (11 UWS, 4 LIS)	anoxia; cerebro-vascular accident; TBI; hypoglycemia; occlusion basilar artery	10	45	TAL	17	PET/fMRI	DOC<HC			
Thibault et al., 2012	70 (24 UWS, 28 MCS, 10 EMCS,8LIS)	TBI; cardiac arrest; stroke; intoxication; anoxia; hydrocephali; meningitis encephalopathy; aneurysm	27	43.9	MNI	8;4	PET	DOC<HC			

ALE maps computation

The quantitative evaluation of spatial PET and fMRI patterns was carried out using the activation likelihood estimate (ALE) technique implemented in the GingerALE software v. 3.0 (www.brainmap.org) (Eickhoff et al., 2009, 2012). The method used is the same already described for the study 1. For an overall comprehension, see 'ALE maps computation' paragraph of the first study.

Neuroimaging analysis

MRI dataset

In order to perform network mapping, a fMRI dataset collected at Beth Israel Deaconess Medical Center was used. The dataset included 187 healthy participants (mean age 29 years, range 21 to 49, SD = 12; mean education 15 years, range 11 to 23, SD = 3). Neuroimaging data were acquired

on a 3.0 T General Electric (GE Medical Solutions, Erlangen, Germany). For each subject, a three-dimensional T1-weighted MPRAGE image was acquired in the axial plane (TR/TE 2500/3.5ms; 192 slices; slice thickness 1mm; flip angle 8°; voxel size 1.0×1.0×1.0mm). Resting-state fMRI data were collected using T2-weighted BOLD images (TR/TE 2500/30ms; 38 interleaved slices; slice thickness 3mm; 260 volumes; flip angle 80°; voxel size 3.0×3.0×3.0 mm). Participants were asked to maintain their eyes opened in the scanner while fixating a cross-hair without focusing on any topic.

fMRI Preprocessing

Preprocessing of the functional images was carried out using SPM8 (Wellcome Department of Cognitive Neurology, Institute of Neurology, University College London; http://www.fil.ion.ucl.ac.uk/spm/) within the MATLAB scientific computing environment (http://www.mathworks.com, MathWorks, MA, USA). The first five volumes of functional images were discarded for each subject to allow for steady-state magnetization. EPI images were then stripped of skull and other non-cerebral tissues, slice-timed using interleaved descending acquisition, manually realigned, and subsequently resliced. Structural images were co-registered to the mean volume of functional images and subsequently segmented using the NewSegment routine in SPM8. A Hidden Markov Random Field model was applied in order to remove isolated voxels. Moreover, to obtain a more accurate spatial normalization we applied the SPM8 DARTEL (Diffeomorphic Anatomical Registration Through Exponential Lie algebra) module, creating a customized gray matter template from all subjects' segmented images (Ashburner, 2007). A nonlinear normalization procedure to the Montreal Neurological Institute (MNI) template brain, and voxel resampling to an isotropic 3x3x3 mm voxel size, were then applied. We removed linear trends to reduce the possible influence of the rising temperature of the MRI scanner. All functional volumes were band-pass filtered between 0.01 and 0.08 Hz to reduce low-frequency drifts. Finally, we controlled the potential contribution of nuisance sources of variability to grey matter BOLD time courses by regressing out the head motion parameters as well as the signal derived from four regions of interest (ROIs) placed in the white matter and cerebro-spinal fluid. This approach has been shown to significantly enhance within-subject and test-retest reliability (Behzadi et al., 2007).

Seed-based functional connectivity

To characterize the functional connectivity pattern of each region resulting from the ALE metanalysis, a seed-based connectivity analysis was conducted by extracting the average BOLD

time course from all the voxels included in a given resting-state map (e.g., altered rs-fMRI connectivity in MCS patients). Subsequently, we correlated the signal from each map with the remaining voxels in the rest of the brain, resulting in a 3D weighted volume where each voxel value represents the correlation coefficient between its BOLD activity and that of the seed map of interest. Results were computed applying a voxel-level threshold ($p < 0.001$, false discovery rate -FDR- corrected) and cluster size correction ($p < 0.001$, family-wise error -FWE- corrected).

Clustering Analysis

Given the different significant regions identified by the ALE analysis, the presence of similar connectivity alterations was also tested by comparing their respective seed-based connectivity maps via a functional clustering algorithm (Matlab 2016b, The Mathworks). The algorithm identified similarity in the cortico-subcortical functional maps derived from each ALE region, assigning them to N clusters based on their profile (accounting for both topography and sign of connectivity values). The analysis allowed to reduce the number of potential networks altered in DoC, allowing to focus on identifying and testing possible tES solutions to enhance connectivity in patients.

Similarity index

Once the main functional connectivity clusters were identified, the functional maps belonging to the same cluster were averaged together, resulting in one main whole-brain connectivity map depicting a major Network altered in DoC. In order to characterize the functional profile of each resulting Network, functional labeling was performed by looking at the spatial similarity of each Network map and those of known RSNs using a weighted variant of the DICE coefficient (weighted Dice Coefficient, wDC) (Dice, 1945). RSNs were defined following the parcellation scheme by Shirer et al., (2012), reporting 12 non-overlapping maps of different networks: default mode (DMN), right and left executive control (RECN, LECN), dorsal attention (DAN), anterior and posterior salience (AS, PS), basal ganglia (BG), language (LANG), high and primary visual (HVIS, PVIS), auditory (AUD), and somatosensory (SM) (Shirer et al., 2012). Over the last 15 years, different research groups applied various approaches for extracting and labeling RSNs. In this study, we considered the AS as the network including bilateral insula (mostly referring to its anterior part) and dorsal anterior cingulate cortex (dACC). However, according to the work by Dosenbach et al., (2007), the same network, with the inclusion of two anterior frontal regions corresponding to

Brodmann area 9/10, is known as the cingulo-opercular network (Dosenbach et al., 2007). The same applies to the LECN and RECN, indicating two lateralized networks resembling the fronto-parietal control network as originally described by the same group (Dosenbach et al., 2007, 2008). Both definitions, with the additional distinction of a left and right component in Shirer et al. (2012), refer to a network involved in cognitive control, with a specific involvement in control initiation, flexibility, and modulation of response to feedback. Also, the AN identified here reflects the ventral and dorsal attention network proposed by Corbetta et al. (2008), with no differentiation between a dorsal (including bilateral parietal lobe, frontal eye fields and, to a lesser degree, parieto-occipital regions) and a ventral part (i.e., more frontal, including regions of the inferior and middle frontal gyrus) (Corbetta et al., 2008). Moreover, we decided to group together vDMN, dDMN, and precuneus in a single network (DMN). Finally, another classification has been proposed by Yeo et al. (2011), including multiple labeling solutions acknowledging the existence of 7 or up to 17 resting-state fMRI networks. The main difference with respect to the work by Shirer et al. (2012) concerns the labeling of a subset of prefrontal regions, classified as part of the FPCN by Yeo et al. (2011) instead of AN (Shirer et al., 2012; Yeo et al., 2011).

Importantly, the comparison of weighted, unthresholded connectivity maps for each DoC Network and RSN map at the single voxel level requires considering not only spatial similarity, but also similarity of connectivity sign (i.e., positive and negative connectivity). Therefore, the similarity index was obtained by computing the product of each voxel's value across two maps (e.g., voxel j in the DoC and DMN maps), resulting in a map where positive values represent voxels with the same sign in both maps (i.e., positive connectivity in both DoC and DMN), while negative ones represent opposite signs (i.e., positive connectivity value in voxel j in DoC, negative in DMN). As a result, the magnitude of the similarity index represents the similarity of connectivity strength in any two given maps (expressed as wDC). This procedure allowed to identify similar connectivity profiles between the main Networks altered in DoC (as resulting from functional clustering of regions showing altered activity during fMRI or PET imaging) and known RSNs, thus providing insight about the function and meaning of Networks altered in DoC.

Biophysical modeling

The biophysical model has been obtained as described in Chapter 1 (Figure 1.1). Moreover, considering that in this study functional connectivity images has been used as targets for the

modeling, we included here an additional description reporting how these maps have been used in order to obtain the best result.

Functional connectivity volume images were converted into target networks for the optimization algorithm following a procedure already applied to the motor cortex network. The FC correlation coefficient values t in the image (Figure 1.1- b1) are mapped onto the cortical surface of the reference brain (http://brainweb.bic.mni.mcgill.ca/brainweb), after registration to a common space (Figure 1.1- b2) (MNI). Since we aim at promoting the activation (excitation) of the positively correlated areas and the inhibition of negatively correlated ones, regions with positive t were assigned positive target electric field E_n^{Target}= 0.25 V/m (excitatory), while regions with negative t were assigned to negative E_n^{Target} = -0.25 V/m (inhibitory). The target network map for the optimization (Figure 1.1- b3) is created by applying different thresholds to ignore low and emphasize high correlation, and by linearly rescaling the t-values into weights w (from 0 to 10). Note that, in order to reflect the absolute correlation strength, the values are saturated to different maximum weights wmax: higher wmax maximum weight is assigned to the regions with higher maximum absolute correlation |tmax|.

3.3.2 RESULTS

ALE Meta-analysis

The results of the ALE meta-analysis are available for download as a nifti. nii volumetric file at (www.tmslab.org/santalab.php). The maps include network-level volumes representing the entire set of regions presented in the following paragraphs. Detailed information on the anatomical localization of each significant regions and the relative statistics is reported in dedicated figures and tables. A more in-depth discussion about the meaning of the patterns identified, as well as the role of specific regions, is provided in the discussion section.

Task-based map

The resulting map and coordinates of the neural activity patterns during active or passive tasks execution are reported in Table 3.18 and Figure 3.24 A. The map includes 2 regions showing a very specific activation of the bilateral temporal lobes (BA 41, MNI coordinates of main clusters: x= -52, y= -30, z= 10; x= 46, y= -28, z= 12), without contribution of any other region.

Table 3.18. Brain activity pattern in task-based map. Coordinates, extrema value, and corresponding Brodmann area, lobe, hemisphere, and regional labels are reported for each region included in the ALE map.

Region number	Extrema value coordinates			Extrema Value	Brodmann Area	Hemisphere	Lobe	Label
	x	*y*	*z*					
1	-52	-30	10	0.013	41	L	Temporal	Superior Temporal Gyrus
1	-44	-30	10	0.010	41	L	Temporal	Superior Temporal Gyrus
2	46	-28	12	0.013	41	R	Temporal	Trasverse Temporal Gyrus
2	50	-20	10	0.010	41	R	Temporal	Trasverse Temporal Gyrus

Resting-state maps

Figure 3.24 B and Table 3.19 show the pattern of deactivation in patients with DoC during resting state compared to healthy subjects. Results on the entire sample of DoC patients include 6 separate regions highlighting the involvement of cortical areas (frontal and parietal areas in particular: BA 6 and BA 39, MNI coordinates of main regions: x= -36, y= 6, z= 54; x= -44, y= -70, z= 40) and subcortical regions (e.g., cingulate gyrus; BA 31; MNI coordinates of main regions: x= 0, y= -36, z= 32; caudate; MNI coordinates of main regions: x= 14, y= 14, z= 8; and thalamus; MNI coordinates of main regions: x= 8, y= -16, z= 6). Similarities and differences in resting-state connectivity of MCS and VS patients are also shown (Figure 3.25, Table 3.20), specifically referring to regions of decreased fMRI activity in DoC patients. Major connectivity alterations are visible in the thalamus for both VS and MCS. Interestingly, MCS patients present alteration of more anterior subcortical structures (i.e., right and left caudate nuclei), whereas VS patients display significant decrease in connectivity in more posterior structures (i.e., posterior cingulate cortex).

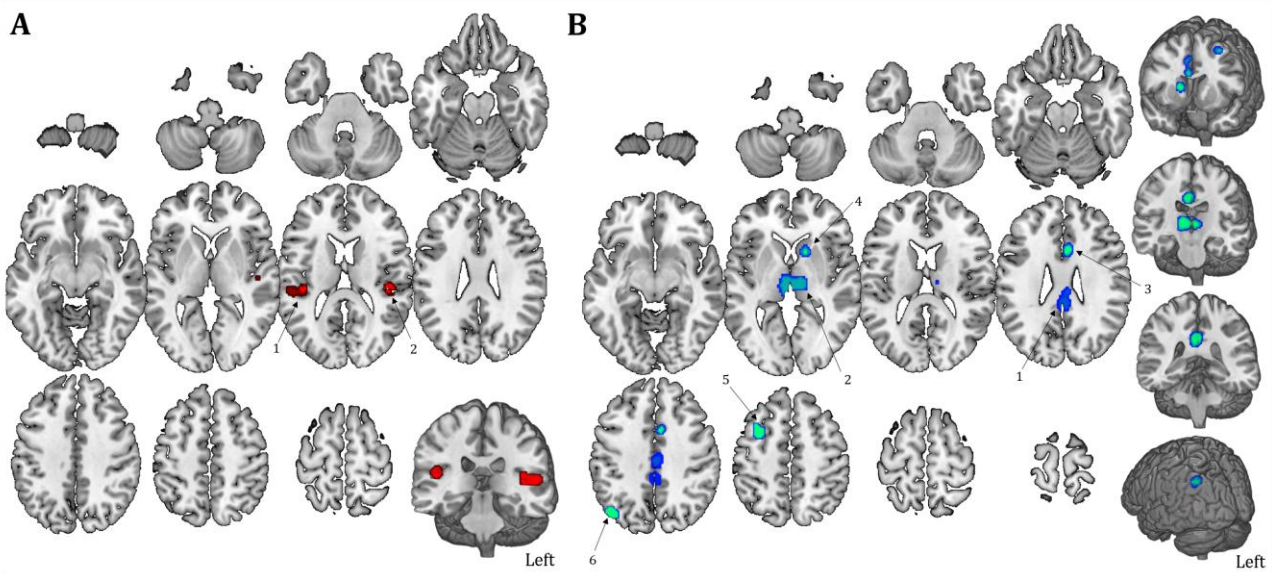

Figure 3.24. Task- and resting state- related activation map. (A) Temporal lobes are strongly activated when DoC patients performed a task (in red). (B) Brain hypoactivation in both internal and external awareness networks in patients compared to healthy controls during rs-fMRI is shown (blue). The ALE regions numbers are reported.

Table 3.19. Brain activity pattern in resting-state map. Coordinates, extrema value and corresponding Brodmann area, lobe, hemisphere and regional labels are reported for each region included in the ALE map.

Region number	Extrema value coordinates			Extrema Value	Brodmann Area	Hemisphere	Lobe	Label
	x	*y*	*z*					
1	0	-36	32	0.034	31	L	Limbic	Cingulate Gyrus
1	2	-20	36	0.029	24	L	Limbic	Cingulate Gyrus
2	8	-16	6	0.031	.	R	Sub-lobar	Thalamus
2	-4	-14	6	0.024	.	L	Sub-lobar	Thalamus
3	4	12	24	0.018	24	R	Limbic	Cingulate Gyrus
3	4	8	42	0.013	24	R	Limbic	Cingulate Gyrus
4	14	14	8	0.026	.	R	Sub-lobar	Caudate
5	-32	6	54	0.020	6	L	Frontal	Middle Frontal Gyrus
6	-44	-70	40	0.021	39	L	Parietal	Angular Gyrus

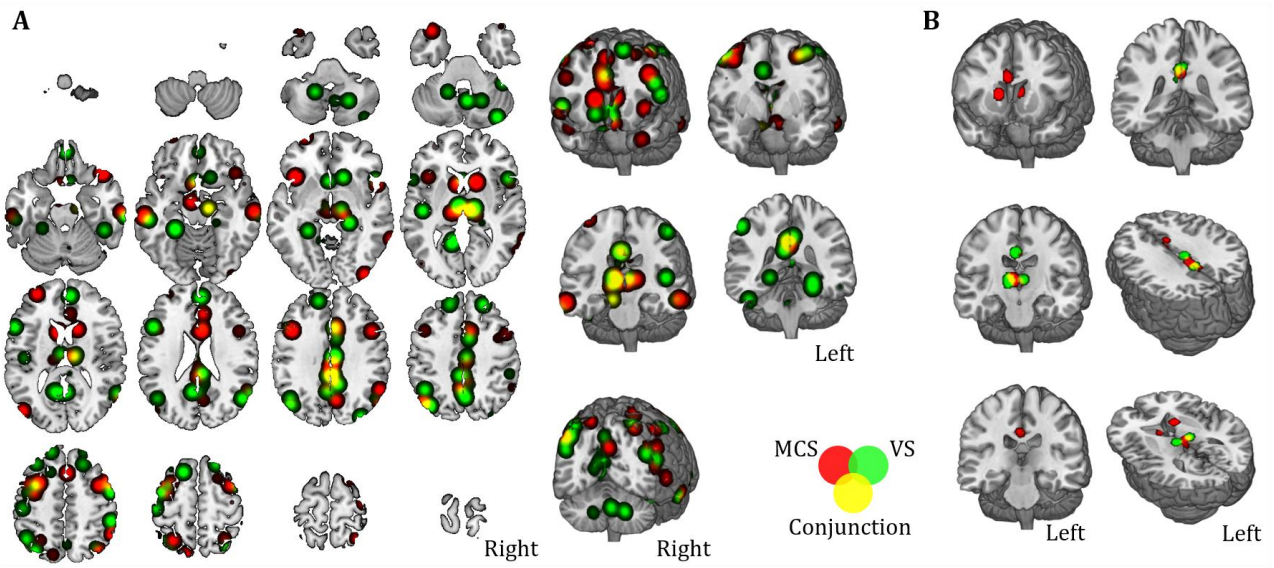

Figure 3.25. Similarities and differences between MCS and VS. Brain hypoactivation during resting state is shown for MCS (red) and VS patients (green), as well as for overlapping regions (yellow). The map shows the qualitative overlap without any statistical threshold (panel A), as well as with a family-wise error (FWE) correction both at cluster level and voxel level ($p<0.001$ for cluster-formation; $p<0.05$ for cluster-level inference, panel B).

Table 3.20. Activity patterns during rs-fMRI in MCS and VS patients. Coordinates, extrema value and corresponding Brodmann area, lobe, hemisphere, and regional labels are reported for each region included in the ALE map.

Region number	Extrema value coordinates			Extrema Value	Brodmann Area	Hemisphere	Lobe	Label
	x	y	z					
MCS patients								
1	0	-36	32	0.022	31	L	Limbic	Cingulate Gyrus
2	4	-18	6	0.017	.	R	Sub-lobar	Thalamus
3	4	12	24	0.017	24	R	Limbic	Cingulate Gyrus
4	14	14	8	0.023	.	R	Sub-lobar	Caudate
5	-8	12	10	0.021	.	L	Sub-lobar	Caudate
VS patients								
1	10	-18	4	0.019	.	R	Sub-lobar	Thalamus
2	0	-38	34	0.015	31	L	Limbic	Cingulate Gyrus
2	4	-36	24	0.008	23	R	Limbic	Posterior Cingulate
3	4	-16	34	0.019	23	R	Limbic	Cingulate Gyrus
4	-6	-14	6	0.019	.	L	Sub-lobar	Thalamus

Functional connectivity mapping

In order to better illustrate the spontaneous functional connectivity of the regions resulting from the resting-state map, a seed-based analysis was run on a database of 187 healthy subject previously collected at Beth Israel Deaconess Medical Center (BIDMC) in Boston (MA, USA). Figure 3.26 shows the functional connectivity mapping of each region separately. In particular, the functional connectivity profile between the only two cortical regions identified at the ALE analysis (region #5 and #6) and the posterior cingulate gyrus (region #1) resemble the DMN and FPN, while the functional connectivity of subcortical areas, thalamus (region #2), anterior cingulate gyrus (region #3) and caudate nuclei (region #4), resembles the anterior and posterior salience networks (AS, PS).

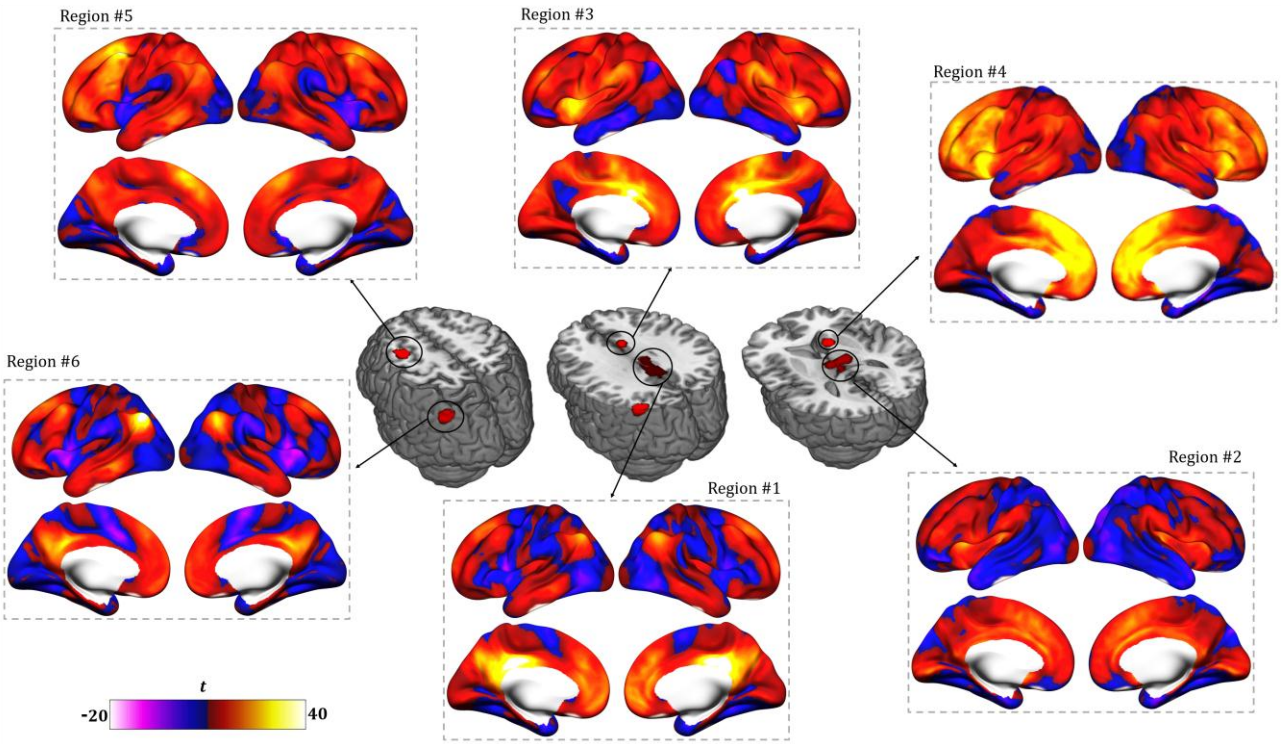

Figure 3.26. Network mapping. Positive and negative functional connectivity profile for each ALE region is shown. Surface representation underlies the high similarity between the FC of regions #1, #5 and #6 and between the FC of regions #2, #3 and #4.

Furthermore, as shown in Figure 3.27A, clustering analysis ($p < 0.05$, FDR correction at single voxel level; $p < 0.05$ NBS correction at whole network level) reveals a quantitative estimate of the positive connectivity between cortical nodes (middle frontal gyrus and angular gyrus) and the posterior cingulate gyrus, as well as a positive correlation among the three subcortical nodes

(thalamus, caudate nuclei and anterior cingulate gyrus). As expected, the functional clustering algorithm grouped the six maps into two main clusters (Cluster #1 and #2) resembling cortical nodes in the first one and subcortical structures in the second one (Figure 3.27A). The resulting two connectivity maps obtained by averaging the connectivity maps of cortical and subcortical regions separately displayed different topography (Network #1 and #2 hereafter; Figure 3.27B).

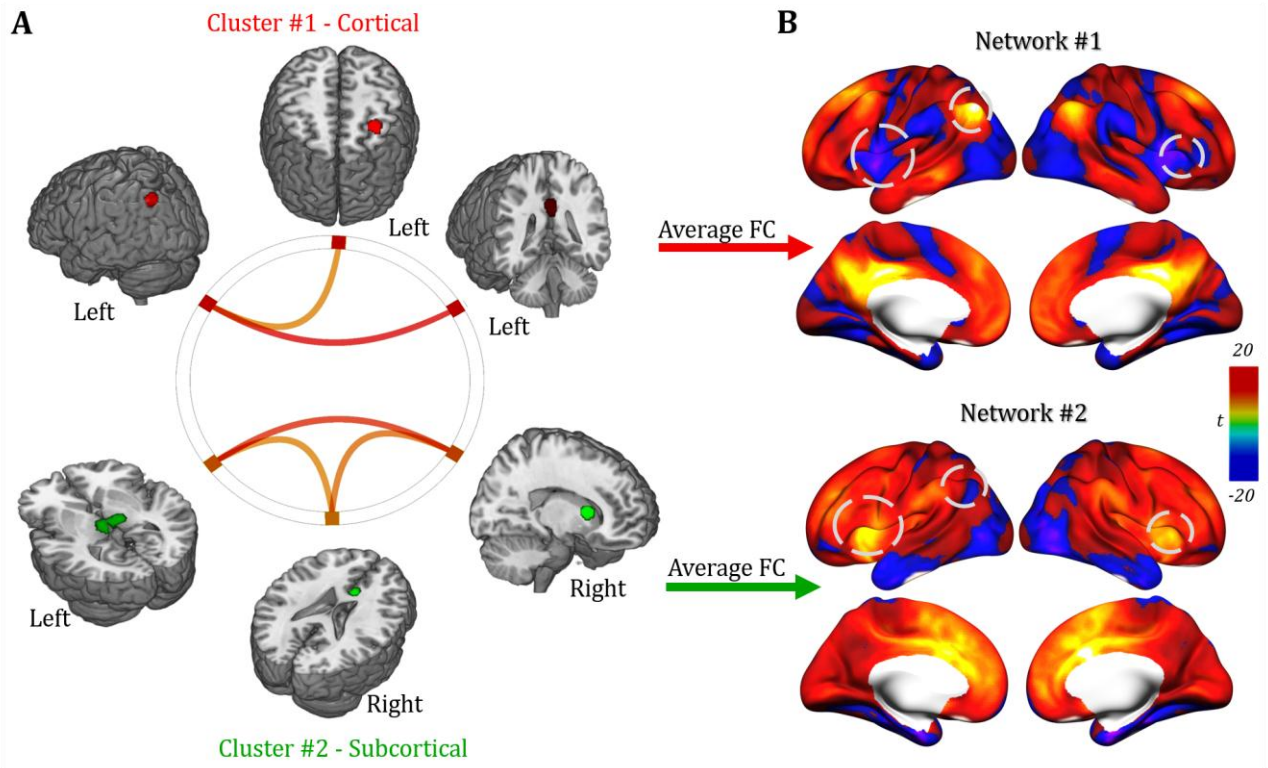

Figure 3.27. Cluster mapping. (A) A strong similarity within the functional connectivity profile of cortical regions (Cluster #1, red) and subcortical regions (Cluster #2, green) was highlighted by the functional clustering analysis. (B) Resulting average functional connectivity maps characterizing cortical and subcortical clusters (Networks #1 and #2) shows similar topography in the anterior prefrontal cortex but partially negatively correlated profiles in parietal and ventrolateral prefrontal cortices (dashed circles).

DoC Networks and RSNs

Cortical and subcortical maps for multiple RSNs were computed in order to provide a qualitative comparison with DoC Network #1 and #2. As shown in Figure 3.28, a qualitative spatial similarity analysis suggests Network #1 as mostly resembling the right and left Fronto-Parietal Control Networks (FPCN), given its strong activation in prefrontal and parietal areas, as well as the DMN due to high connectivity in the precuneus. The FPCN is usually associated to cognitive control with

a specific involvement in control initiation, flexibility and modulation of response, whereas DMN is mostly involved in self-related and internal control. The similarity between Network #1 and these two cognitive networks led us to label Network #1 as a 'Cognitive' network altered in DoC. Network #2, instead, showed high similarity with the anterior salience (AS) and basal ganglia (BG) networks, suggesting more specific matching in ventrolateral prefrontal and parietal cortices. These two networks are involved in top–down control over sensory and limbic regions, as well as in the integration of external sensory information with internal emotional and bodily states (Menon & Uddin, 2010; Uddin, 2015). Because of the similarity between Network #2 and RSNs involved in salience and sensory perception, we labeled Network #2 as 'Sensory/Salience'.

Quantitative similarity analysis confirmed the pattern (Figure 3.29), while also underlining a similarity between Network #1 and the Language Network (LANG), as well as between Network #2, DMN and Auditory Network (AUD). Interestingly, the two networks display a complementary pattern in term of their loading on known RSNs, further confirming the different nature of the two separate clusters identified via functional clustering of ALE regions.

Additionally, the same analysis performed by splitting MCS and VS connectivity maps shows a similar pattern for both groups and mostly comparable to Network #1 – Cognitive (Figure 3.30).

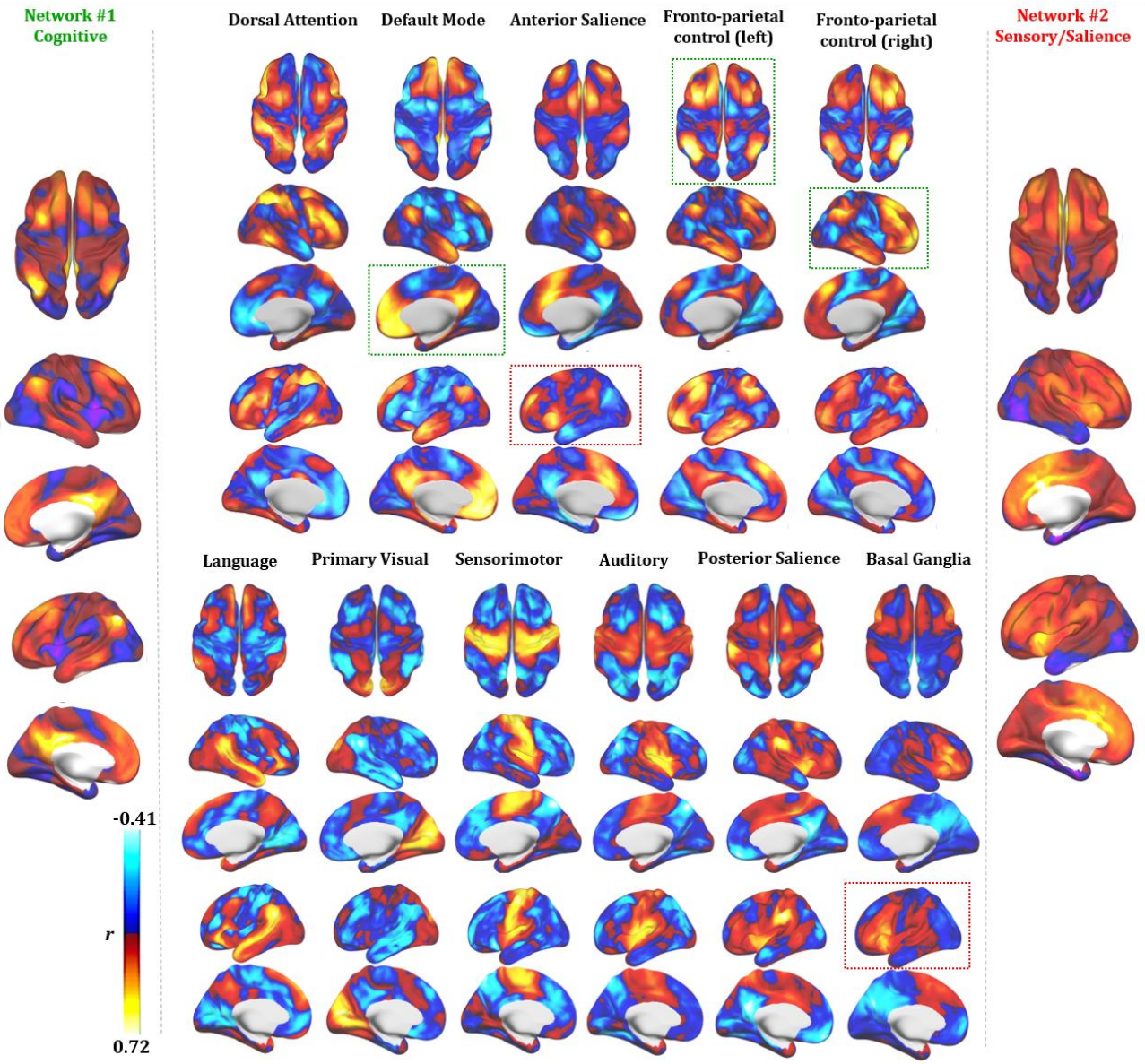

Figure 3.28. Functional connectivity profile of the two identified DoC networks. A visual comparison of seed-based connectivity maps for DoC networks (Network #1 and #2) and major RSNs is shown. Red and blue colors represent the intensity and polarity of connectivity between each network and the rest of the brain. At the qualitative level, Network #1 (cognitive) resembles the Fronto-parietal Control Network (right and left) and DMN are highlighted (green dotted lines). Qualitative similarity is also present for Network #2 (sensory/salience) and Anterior Salience and Basal Ganglia Networks (red dotted lines). Connectivity is expressed as correlation coefficient between the average BOLD signal extracted from each map and that of any other voxel in the brain.

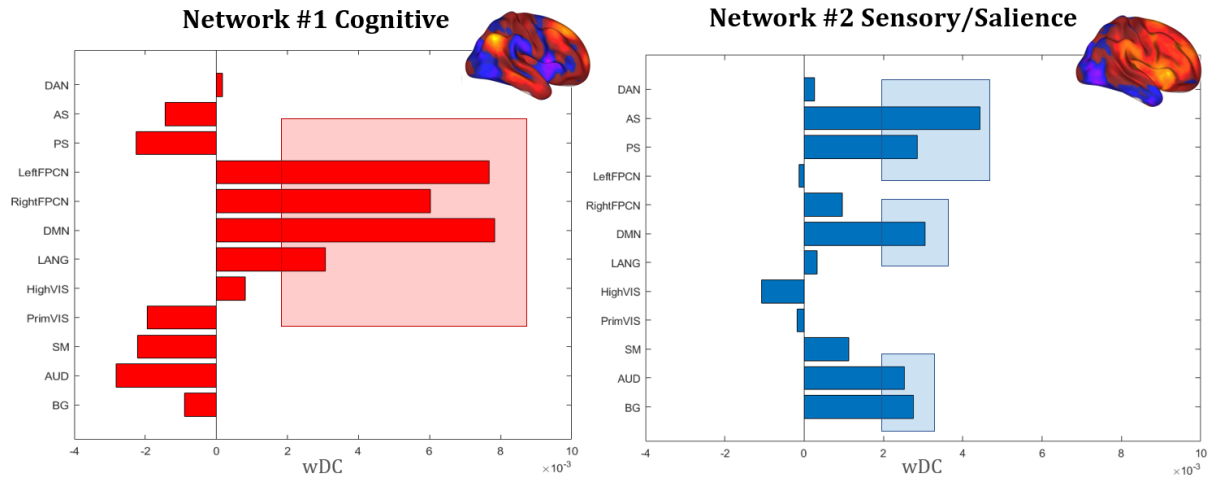

Figure 3.29. Similarity coefficient. Weighted DICE Coefficients (wDC) for every RSN are shown, confirming the higher similarity between Network #1 and DMN, left and right FPCN and LANG, as well as the dissimilarity in connectivity profile with AS, PS, Auditory, Visual and Somatomotor networks. The opposite pattern was identified for Network #2, showing higher similarity for networks involved in sensory perception (AUD, SM, BG) and salience (AS, PS). Red and blue rectangles underline the higher significant overlap between RSNs and DoC Networks. Note: default mode network (DMN), right and left fronto-parietal control networks (right and left FPCN); dorsal attention network (DAN), anterior and posterior salience networks (AS, PS), basal ganglia network (BG); language network (LANG); high and primary visual networks (HighVIS, PrimVIS); precuneus network (Precuneus); auditory network (AUD); somatosensory network (SM).

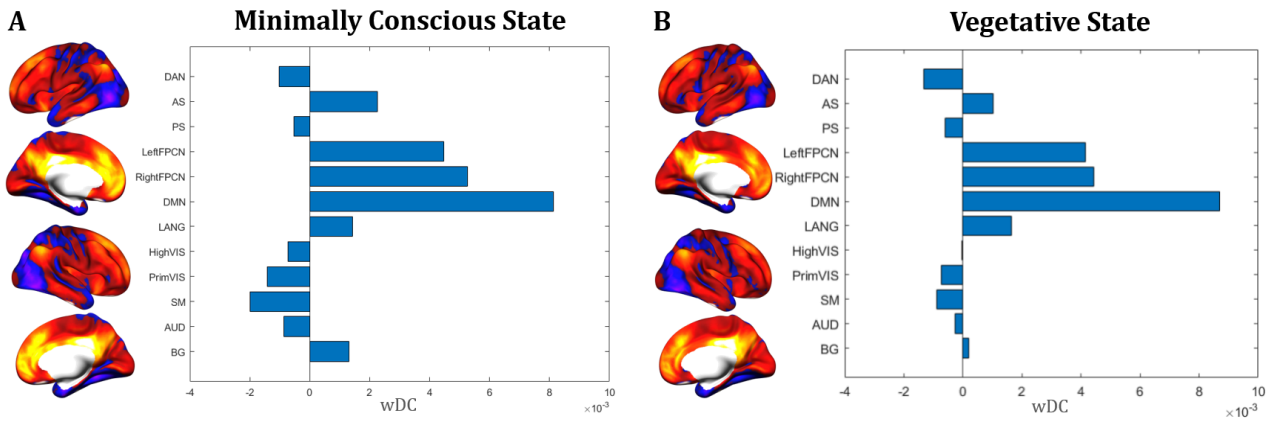

Figure 3.30. MCS and VS and RSNs. The functional connectivity profile and the similarity coefficient with RSNs is shown separately for MCS (A) and VS (B). Similar network profile was identified for both MCS and VS patients, with major overlap with DMN and FPCN as shown for Network #1.

Biophysical Modeling Results

The optimal multichannel montages to target the aforementioned networks on a MRI-derived realistic head model can be determined by optimization algorithms. These algorithms require the creation of a signed target map out of the network, indicating the importance of each network area in the optimization, as well as the desired stimulation effect (excitation/inhibition). Detailed information about these methods are reported on Chapter 1.

Figure 3.31 shows the result of multichannel tES montage optimization to promote the activation of positively correlated FC areas in DoC patients. The signed weight maps used for the two optimizations are shown in Figure 3.31 (panel b) for Network #1- Cognitive (left) and Network #2- Sensory/Salience (right). Since for both networks the maximum negative correlation values r are, in absolute, lower than the maximum positive ones (for Network #1 rmin=-0.118; rmax= 0.982; for Network #2 rmin=-0.102; rmax= 0.839), we assigned a maximum weight of wmin =5 to the areas to inhibit, and a maximum weight of wmax =10 to the areas to excite.

For Network #1, values of $r>0.4$ and $r<-0.06$ were clipped to wmax and wmin respectively; values $|r|<0.045$ were considered not significant to target and set to no-stimulation with low weight w0 = 2. For the Network #2, we mapped $r>0.15$ to wmax, $r<-0.04$ to wmin, and $|r|<0.02$ to w0. For both networks, intermediate negative correlation values were linearly rescaled between w0 and wmin, positive ones between w0 and wmax. As we observe, the maps thus created represent a reasonable translation of the cortical FC correlation information in terms of the target network, as they retain and emphasize only the areas with the strongest positive and negative correlation, with consistent significance. In particular, we observe that for Network #2, the FC correlation between cortical areas and seeds is much lower in the external surface than in the midsagittal region (Figure 3.31, panel A, right). However, since tES can induce higher En on the external cortex than on the internal surfaces, the weight map enhances the importance of the former as a target for the stimulation as the preferential venue to reach the deep cortical seed.

The optimized montages are shown in Figure 3.31 (panel c) for Network #1 and #2. Both montages involve 8 electrodes, delivering a total injected current of approximately 4mA (max current per electrode was limited to 2.0 mA). For Network #1, the montage comprehends C6: -831uA, CZ: -741uA, FC1: 759uA, FC5: -1054uA, FZ: 826uA, P3: 1576uA, P4: 837uA and PO3: -1372uA. For Network #2, it comprehends: AF3: 829uA, AF7: -1402uA, C1: -710uA, C6: 398uA, CP2: -1257uA, CZ: 1650uA, FT7: 1121uA and P7: -629uA. Given the current constraints, these solutions represent the best fit of the En to the target maps obtained from FC correlation values. Moreover, using only 8

electrodes, they reach respectively 95% and 89% of the optimal fit value using a full electrode cap with 64 channels. For Network #1, the optimized montage induces an average normal electric field on the correlated areas, set to excitation, of <En, ex>=0.014V/m and on the anticorrelated areas, set to inhibition, of <En, in>=-0.016 V/m. The montage for Network #2 induces <En, ex>=0.007 V/m on the areas set to excitation, and <En, in>=-0.003 V/m on the areas set to inhibition. Results suggest that biophysical optimization of Network #1 achieves stronger e-fields compared to Network #2 on average, therefore suggesting the former as the most suitable target for network stimulation in DoC.

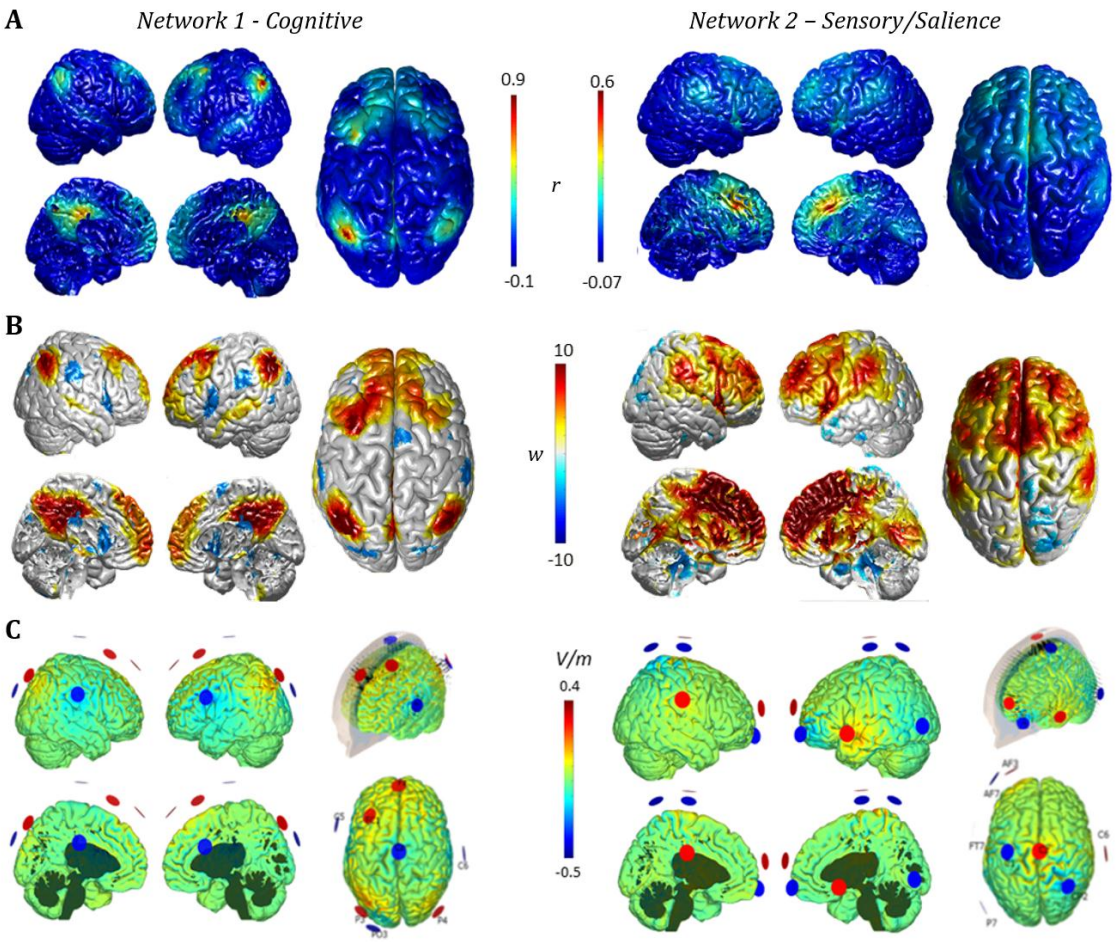

Figure 3.31. Multichannel tES optimized montages. (A) Functional connectivity profile for Network #1 and #2, mapped onto the cortical surface. (B) Weighted target maps for both networks. The values in the scale correspond to the weights multiplied by the sign of En target to display excitatory and inhibitory areas. For Network #1, correlation higher than 0.4 were assigned to excitation with maximum weight wmax=10, whereas lower than -0.06 were assigned inhibition with lower negative weight wmin=5. For Network #2, the threshold value for excitation was set to 0.15 and for inhibition to -0.04. (C) Optimized montages for Networks #1 and #2. Both solutions involve 8 electrodes, delivering a total maximum current of 4 mA. Anodes are shown in red, cathodes in blue; arrows represent current density.

3.3.3 DISCUSSION

In the present work, we reviewed all the studies reporting fMRI or PET activity in DoC patients, in order to provide a set of activation/deactivation maps related to both task-dependent or resting-state activity. We expanded these findings by mapping the functional connectivity profile of each identified region, and by calculating the similarity coefficient between resting-state networks altered in DoC patients and canonical RSNs maps. In the following paragraphs we discuss our results and their relevance for possible new therapeutic applications in DoC, including personalized transcranial electrical stimulation (tES) solutions.

Brain activations and deactivations in DoC

The brain activation pattern reported during tasks in DoC is mostly restricted to the bilateral temporal cortices, reflecting the use of passive auditory tasks during fMRI in most of the considered studies. The task materials and presentation modalities were various in the articles included in the meta-analysis. An example of active task during fMRI was: “imagine navigating your home” (Liang et al., 2014); whereas, during the passive task participants heard long spoken narrative regarding everyday events (Fernández-Espejo et al., 2010). Despite this dissimilarity, it was not possible to compute two different maps (active/passive task) since only one study used active task paradigm.

Differently from similar analysis done by Berlingeri et al. (2019), we did not find activity in bilateral orbito-frontal and frontal gyrus. However, our results are comparable with theirs when comparing results obtained with the same cluster correction approach, i.e., family wise error (FWE, see Table S2 in Berlingeri et al., 2019). As suggested by Müller et al., (2018), cluster-level FWE correction is the most reliable approach to control for false positives (Müller et al., 2018). Moreover, following the same recommendation, we also used a more conservative mask size compared to Berlingeri et al. (2019).

Looking at resting-state results, diminished activity in the posterior and anterior cingulate, thalamus, angular gyrus, and prefrontal cortex were found, in line with previous literature (Hannawi & Lindquist, 2015). Subcortical regions mostly matched with the internal awareness network, also defined as the network involved in mental processes (i.e., mind wandering, daydreaming, mental imagery) without the requirement of external stimuli (Vanhaudenhuyse et al., 2011). On the other hand, cortical regions (middle frontal gyrus and angular gyrus) resemble the external awareness network, typically involved in conscious perception of environmental

stimuli and in goal-directed behavior (Vanhaudenhuyse et al., 2011). Results also confirm the central role of thalamus in consciousness (Hannawi & Lindquist, 2015), as well as the necessary link between cortex and thalamus for conscious perception (Laureys et al., 2000; Schiff et al., 2007), with thalamic lesions classically leading to global loss of consciousness (Castaigne et al., 1981). Moreover, considering the analysis conducted separately for MCS and VS patients, the central role of the thalamus stands out again. As shown in Figure 3.26 and in line with a previous study (Hannawi & Lindquist, 2015), in VS patients both thalami seem less activated at rest, whereas in MCS patients only the right thalamus is impaired compared to healthy controls. Additionally, from a qualitative point of view the main difference between MCS and VS resides in a differential alteration of the internal network, with a more anterior impairment in MCS compared to a more posterior deactivation in VS patients. These results are also in line with a previous study by Vanhaudenhuyse et al. (2010) showing that only medial parietal regions are sensitive to differences in functional connectivity between MCS and VS (Vanhaudenhuyse et al., 2010).

Overall, during passive task a specific pattern of activity in the temporal lobe seems present, whereas reduced activity during rs-fMRI is observed mostly in subcortical structures of the internal network. However, a widespread reduction of activity in DoC patients compared to healthy controls is also visible in cortical areas (i.e., middle frontal gyrus and angular gyrus) of the external network (Vanhaudenhuyse et al., 2011).

Network mapping

The functional connectivity analysis conducted on ALE regions based on resting-state data shows the involvement of multiple functional networks possibly responsible for different clinical characteristics of DoC. Our results suggest that areas of hypoactivation in DoC patients belong to two main networks: Network #1, resembling networks related to high-order cognitive processing and executive functions (right and left FPCN) and Network #2, resembling networks involved in salience and sensory perception (AS and BG). Moreover, both networks display clear overlap with the DMN, as already pointed out by several studies (Hannawi & Lindquist, 2015; He et al., 2014; Vanhaudenhuyse et al., 2010).

In particular, quantitative similarity analysis between Network #1 and RSNs suggests higher similarity with right and left FPCN. These networks are mostly related to cognitive processes, such as control of attention allocation, abstract reasoning, and flexibility. Moreover, they are highly involved in fluid intelligence (Santarnecchi, et al., 2017b) and executive functions (updating,

switching and inhibition, Miyake et al., 2000) and play a relevant role in mediating the dynamic balance between DMN and DAN (Spreng et al., 2012). The impairment of areas strongly related to the FPCN in DoC patients was previously pointed out by Crone et al., (2013). Using graph-theory analysis of BOLD data, the authors reported that fronto-parietal network proprieties are altered in several regions associated with conscious processing. Additionally, the middle prefrontal cortex (a central hub in the FPCN) has been associated to emotional balance, response flexibility and self-knowing awareness, processes impaired in DoC patients.

Despite Network #2 presented less similarity with other RSNs compared to Network #1, we found an interesting resemblance with AS and PS networks. These networks are usually involved in monitoring and maintaining performance during a task (Botvinick et al., 2001, 2004), as well as play a role in cognitive control and error detection due to their involvement in top–down control over sensory (Crottaz-Herbette & Menon, 2006) and limbic regions (Etkin et al., 2006). Impairment in these networks could be driven by the loss of thalamic activity: anatomically the thalamus is well connected to the salience network since the interoceptive signals pass through the autonomic afferent nuclei and the thalamus before reaching the insula and then dispatched to other cortical areas of the salience network where signals are integrated and used to coordinate other large scale cortical networks (Uddin, 2015).

Moreover, the well-known similarity between both DoC networks and DMN is not surprising considering that the DMN has been linked to self-related and internal processes, such as stimulus-independent thoughts (McKiernan et al., 2006), mind-wandering (Mason et al., 2007), social cognition (Schilbach et al., 2008), introspection (Goldberg et al., 2006), monitoring of the 'mental self' (Lou et al., 2004) and integration of cognitive processes (Greicius et al., 2003)(for a review see: Buckner & DiNicola, 2019). The hypoactivity in brain areas that are functionally related to these networks could be linked to patients' deficit in perception of external stimuli, maybe not at primary level (since the task-based ALE map shows an activation in the temporal cortex probably related to auditory tasks), but in the connections between primary areas and associative cortices, responsible for cognitive behavior, motor planning, memory and higher cortical functions.

Finally, network mapping reveals very similar functional connectivity patterns between MCS and VS, with a main involvement of DMN and bilateral FPCN, as previously observed for Network #1. Unfortunately, due to the small number of available studies, our results are not strong enough to detect any significant difference in VS and MCS functional connectivity profile. Future studies should focus on exploring the potential for imaging biomarkers to differentiate VS and MCS

patient, also leveraging network-level alterations identified by means of combined TMS-EEG studies (Casarotto et al., 2016; Ozdemir et al., 2020; Ragazzoni et al., 2017).

Potential therapeutic interventions

An effective treatment for DoC has not been identified yet, and the clinical management of these patients remains very challenging. Invasive and non-invasive therapeutic interventions have been proposed with inconsistent results (Ragazzoni et al., 2017). For what concern noninvasive brain stimulation, several studies have shown the efficacy of tDCS over the dlPFC in improving patients' responsiveness to external stimuli both after single (Thibaut et al., 2014) and repeated stimulation sessions (Angelakis et al., 2014; Estraneo et al., 2017). Although available studies reported a beneficial tDCS effect in MCS compared to VS patients, even within MCS patients high variability in response to the treatment was present and any effect was not strong enough to impact patients' clinical status (Mancuso et al., 2017). Such heterogeneity may be explained by single site stimulation and therefore not able to produce a meaningful whole brain effect. Following this rationale, Thibault et al. (2017) stimulated the fronto-parietal network using tDCS. However, results showed that only 30% of MCS patients positively responded to stimulation. Crucially, in this study the stimulation targets were not chosen based on functional connectivity maps (Thibaut et al., 2017). In an attempt to move the field towards image-guided, network-based targeting for DoC, here we leveraged results of network mapping to test two tES montages designed to modulate cortical and subcortical regions identified via the ALE analysis. The approach considers functional connectivity maps as a target for stimulation montage optimization, selecting number and location of the electrodes as well as stimulation intensity according to weighted distribution of connectivity values. Such approach allows to indirectly target subcortical structure using transcranial cortical stimulation by leveraging cortical projections of deep structures, constituting a potential alternative for the treatment of pathologies currently addressed by DBS (Fox et al., 2014).

In the optimized montage solution proposed, and in agreement with the connectivity profiles of Network #1 and #2, lower priority has been assigned to the negative correlated areas than to the positive correlated ones. Therefore, stronger excitatory than inhibitory effect is expected for both target networks. The results indeed reveal that in both montages the electrodes delivering the highest currents are anodes, placed over the areas to excite: the parietal lobes for Network #1 are targeted by P3/P4, whereas the superior frontal gyrus for Network #2 is addressed by Cz and AF3.

However, the overall excitatory effect is larger than the inhibitory one only in Network #2, whereas in Network #1 the two effects are comparable. Moreover, both excitatory and inhibitory effects are stronger in Network #1 than in Network #2. These differences result from the combination of head anatomy and current constraints with network topology. In Network #2, a large portion of highly relevant areas to be excited lies on the midsagittal cortex, which is rather difficult to reach with scalp electrodes due to the limited penetration depth of the current. In Network #1, instead, important patches are also located on the lateral cortex, where, with the current less attenuated, the excitatory effect can be higher. On the other hand, negative correlated areas lie only on the cortical surface, and they are larger and have slightly higher (negative) weight in Network #1 than in Network #2. Consequently, the inhibiting electric field on the negative correlated areas is larger for Network #1.

In short, the montage created for targeting Network #1 induces stronger effects, with a good balance between excitation and inhibition. This montage solution could help in reaching deep brain structures by stimulating multiple cortical areas functionally connected to DMN and FPCN, whereas the solution proposed for targeting Network #2 seems to be less efficient possibly due to the fact that subcortical regions altered in DoC do not display a strong functional correlation with cortical structures.

Limitations of the study and future directions

The aim of this study was to show the brain activation/deactivation pattern typically involved in DoC patients during task-evoked activity or resting state, and the similarity of these nodes to known RSNs. Even though we consider our ALE maps the most accurate representation of available literature, potential publication biases should be considered. Based on a recent study (Müller et al., 2018), the importance of finding a balance between homogeneity and power has to be considered. ALE maps based on a small number of studies are more affected by studies heterogeneity (Eickhoff et al., 2016), while at the same time focusing on a specific topic/task (and therefore a smaller number of studies) is also important to provide specific contribution to the field of interest. In this work we decided to focus on alterations of brain activity in DoC as a whole, complying with the criteria of homogeneity and including patients with DoC of any cause. Unfortunately, due to the limited literature available so far, we could not create specific ALE maps for every source of DoC, which should remain the ultimate goal of this type of work.

Moreover, a crucial missing element in our analysis is a characterization of the increase in neural activity observed in DoC compared to healthy controls. However, the number of studies reporting this information is very limited and it is not possible to compute reliable ALE maps. Future studies should investigate this aspect, in order to understand whether the increased brain activity in DoC could represent a compensatory mechanism and possibly an alternative therapeutic target.

Additionally, a few methodological issues in the study of rs-fMRI connectivity in DoC patients should be considered. DoC patients often present severe and heterogeneous brain damage: anatomical defects alter FC estimation as well as confound estimation of current distribution during brain stimulation (Laakso et al., 2015). Moreover, group-level functional connectivity analysis is usually performed by normalizing individual MRI data to a reference space (e.g., MNI), inevitably losing spatial resolution and individual features. Even though the approach presented in our study is a valuable step forward in the direction of identifying pathology-specific NIBS montages, future studies should involve modeling of individual MRI-fMRI data and personalized NIBS solutions for each patient.

BRIEF SUMMARY

In the first two meta-analyses presented in the Chapter 3, we demonstrated how neuroimaging techniques can lead biophysical modeling aimed at improving the activity in brain nodes associated to a cognitive function, in this case the WM, using NIBS. On the other hand, in the third meta-analytic study we showed that also neural alterations and their functional connectivity profile can be useful to individualize biophysical modeling, hypothesizing potential therapeutic solution leveraging network-target NIBS. Even though with different foremost aims, these three meta-analyses point out an important statement: the non-invasive network stimulation, imitating a more natural cortical activation and offering a more accurate stimulation, could be more effective in modulating cognitive functions or specific neural state compared to the traditional bifocal stimulation. However, the network stimulation approach has been employed in few studies, and no evidence on his efficacy at neuroimaging level has been shown so far. Therefore, in the Study 4 we are going to propose the network stimulation approach to stimulate the whole sensorimotor network by using tDCS during the concurrent fMRI acquisition on healthy subjects. Although in the Chapter 3 we proposed network targeting for specific cognitive function (WM) and neural alterations (DoC), in here we firstly decide to test the network specificity of multichannel stimulation approach on a well-known brain area (M1) and its related network, the sensorimotor network. Demonstrating the possibility to induce functional effects on multiple network nodes at the same time by using network stimulation approach in healthy subjects, we then decided to use this technique in clinical population characterized by network-connectivity alterations (like AD) with cognitive enhancement purposes. Consequently, in the Study 5 we are going to show how to use the modern approach of personalized multifocal stimulation to optimize the tACS intervention targeting the regions with higher Aß burden in mild to moderate AD patients. Considering the recent evidence confirming the effect of gamma induction in promoting protection against neurodegeneration in mouse model of AD, here we propose 40 hz tACS as a potential therapeutic intervention for AD.

These two studies will be amply discussed in the following Chapters.

CHAPTER 4

STUDY 4: TARGETING BRAIN NETWORKS THROUGH NON-INVASIVE BRAIN STIMULATION: IMAPACT ON INTRINSIC AND NETWORK-TO-NETWORK FUNCTIONAL CONNECTIVITY[3]

Transcranial direct current stimulation (tDCS) is a non-invasive brain stimulation (NIBS) technique capable of influencing spontaneous neuronal activity by means of a decrease or increase of resting membrane potential of neuronal populations underneath, respectively, positively (i.e. anode) and negatively (cathode) charged scalp electrodes (Paulus, 2003) (Nitsche & Paulus, 2001). For instance, when applied to the motor system, tDCS has been found to increase corticomotor excitability —up to 90 minutes following stimulation (Nitsche & Paulus, 2001)— and to enhance motor performance in healthy individuals —up to 45 minutes after stimulation's cessation (van Asseldonk & Boonstra, 2016)—, possibly acting on cortical plasticity mechanisms (Antal, Terney, Poreisz, & Paulus, 2007; Boros, Poreisz, Münchau, Paulus, & Nitsche, 2008; Fritsch et al., 2010; Furubayashi et al., 2008; Nitsche & Paulus, 2000; Nitsche et al., 2005; Uy, Ridding, Hillier, Thompson, & Miles, 2003). Moreover, results from studies on clinical populations with motor deficits suggest tDCS as a promising neuromodulatory tool to restore motor function (Liew et al., 2014) (for a review see (Sánchez-Kuhn et al., 2017).

However, traditional tDCS approach employs a two-electrode montage with rather large rectangular electrodes. The poor focality and the risk of producing diffuse electric fields in the brain— which could exert unspecific cortical effects— represent a known downfall of tDCS (Miranda et al., 2013). Moreover, brain regions do not operate in isolation, but rather continuously interact with each other in well-organized cortical networks (Fischer et al., 2017; Fox et al., 2005; Sheffield & Barch, 2016), creating the need for tDCS solutions able to target brain networks. This becomes even more important when considering how alterations of such networks are also responsible for psychological and neurological deficits in almost any neurological or psychiatric condition (Drysdale et al., 2017; Fox, 2018; Fox, Buckner, White, Greicius, & Pascual-Leone, 2012; Sheffield & Barch, 2016).

[3] A similar version of this article has been recently published (Mencarelli, L., Menardi, A., Neri, F., Monti, L., Ruffini, G., Salvador, R., ... & Rossi, S. (2020). *Journal of Neuroscience Research*, *98*(10), 1843-1856).

Therefore, if brain networks are becoming the targets of neuromodulatory interventions, stimulation of a single brain region might no longer be sufficient. Recently, Fischer and colleagues (2017) tested a novel approach for multifocal network-targeted tDCS (net-tDCS) of the primary motor cortex (M1) and its associated resting-state fMRI network. The approach is based on the genetic algorithm already described in Chapter 1 (Ruffini, Fox, Ripolles, Miranda, & Pascual-Leone, 2014). By optimizing the net-tDCS solution on the basis of a resting-state functional connectivity map of the right hand representation on the left motor cortex, Fischer and colleagues (2017) investigated the impact of network-targeted tDCS on corticospinal excitability via combined TMS and electromyography (EMG). Net-tDCS induced approximately twice the increase in left M1 excitability over time (compared to traditional bifocal tDCS targeting left M1 and contralateral fronto-orbital region), with a concomitant increase in the excitability of the contralateral motor cortex (usually not induced by traditional tDCS applied solely over left M1). Results suggested the possibility of using network-targeted stimulation approaches to engage multiple nodes of a given network, possibly resulting in an overall greater modulatory effect (Ruffini et al., 2018). However, TMS-tDCS measurements do not entail the same specificity in assessing network-level changes compared to what can be achieved with combined tDCS-fMRI (Antal et al., 2011; Lindenberg et al., 2013; Meinzer et al., 2012, 2013; Polanía, Nitsche, et al., 2011; Zheng et al., 2011). Among the major advantages, simultaneous tDCS-fMRI allows to produce whole-brain data at high spatial resolution, uncovering changes in brain activity over both stimulated and not-stimulated region(s). Moreover, this allows to also look at changes in network-to-network dynamics, a relevant target for net-tDCS.

Here we attempted to replicate the findings previously reported by Fischer et al., (2017) by directly looking at changes in network dynamics during a concurrent tDCS-fMRI study. In particular, we tested the effects of net-tDCS on the activity of (i) a target resting-state fMRI network (i.e., the sensorimotor network, SMN), as well as (ii) on its negatively correlated regions in the prefrontal and parietal lobe. To do so, we collected resting-state functional connectivity BOLD MRI in two groups of ten healthy participants before, during and after tDCS using an MRI-compatible brain stimulation device. In the first group, a more canonical bifocal sponge-based tDCS targeting the left motor cortex was used. In the second group, the tDCS electrode placement was optimized to match the rs-fcMRI pattern of the right hand representation in the left motor cortex (M1), with anodal stimulation affecting bilateral motor cortices and cathodal stimulation eliciting maximal inhibition over prefrontal and parietal cortices as in Fischer et al. 2017 (see

Figure 4.1). By comparing the increase in functional connectivity over the SMN between these two groups we want to verify whether stimulating only one motor cortex (left) or the entire sensorimotor network would lead to different changes in FC. In particular, we hypothesized that (i) net-tDCS would elicit a stronger modulation of the SMN as a whole, i.e., a greater change in functional connectivity of both left/right motor cortices during as well as after stimulation compared to standard tDCS (which should selectively modulate only the left motor cortex, as previously found in Fisher et al., 2017). Moreover, in order to validate potential effect of net-tDCS over Network-to-Network dynamics, we compared the effect induced by real and sham net-tDCS on negative functional connectivity. In particular, we assumed that (ii) net-tDCS would also modulate the functional connectivity between SMN and its negatively correlated regions (resembling the fronto-parietal network -FPN-; Corbetta, 1998). Finally, given the different number and distribution of electrodes on the scalp for net-tDCS and bifocal tDCS, side/adverse effects and subjective feelings during both stimulation approaches were assessed after each session.

4.1 MATERIALS AND METHODS

Participants

Two groups of ten right handed healthy individuals (14 males and 6 females, age 26,3 ± 3,1), with normal neurological exam and no history of psychiatric disorders were recruited through flyers and online advertisement. Subjects with personal and family history of epilepsy were excluded, as well as those reporting recent migraine attacks. Each subject provided written informed consent. The study was approved by the Local Ethics Committee at Le Scotte Hospital and University of Siena School of Medicine (Siena, Italy; IRB protocol “APOLLO”).

Experimental paradigm

The subjects took part into two different experimental protocols: standard tDCS (8 males and 2 female, age 25,5 ± 3,5) and network targeted tDCS (net-tDCS hereafter; 6 males and 4 female, age 27,2 ± 2,5). Each condition consisted of two randomized experimental sessions, real-tDCS and sham-tDCS, held on separated days at least 1 week apart. Four resting-state fMRI were acquired in order to evaluate brain FC at different time points: before, during and after tDCS. In particular, the first resting state scan was computed as a baseline without the stimulation, the second and the third fMRI were computed concurrent to tDCS to evaluate “acute” and “cumulative” stimulation

effects, whereas the last one was used for evaluating tDCS after-effects. The experimental design is shown in Figure 4.1A. The duration of the experiment was approximately one hour per session. At the end of each study visit, a questionnaire evaluating possible side effects of stimulation was administered (Fertonani et al., 2010).

Brain Stimulation Device

tDCS was delivered by means of an MRI compatible Starstim hybrid EEG/tCS 8-channel neurostimulator system (Neuroelectrics, Barcelona, Spain). The device was connected via Bluetooth to a computer located outside the Faraday cage (Figure 4.1B). The stimulation protocol was created and monitored using the NIC 2.0 software (www.neuroelectrics.com/products/software/nic2/). MR-compatible electrodes consisting of conductive rubber electrodes were used (Figure 4.1B) and inserted in circular sponge sockets soaked with 15 ml of sterile sodium chloride solution (0.9%) for at least 10 minutes (MRI Sponstim, Neuroelectrics). The electrodes were positioned in a neoprene cap with 32 electrode positions corresponding to the 10/20 EEG system. The stimulator was connected to the MR-compatible electrodes by specially designed MR-compatible (non-ferrous and radio translucent) leads.

Standard tDCS protocol

Traditional tDCS was applied using a "standard" montage widely used in the tDCS literature (Lefaucheur et al., 2017), with the anode over the left M1 area (C3 in the 10/20 EEG-reference system) and the cathode over the right supraorbital area (Fp2) (Figure 4.1D). A current intensity equal to 2mA was delivered by means of 23 cm^2 round electrodes positioned inside saline-soaked sponges (Figure 4.1B). This montage is thought of activating the motor system with a major focus on left motor cortex. Given the nature of bifocal tDCS, a second electrode delivering cathodal stimulation needs to be placed on the scalp. In the case of bifocal tDCS for motor cortex stimulation, the cathode is usually placed over a "neutral" region (i.e., contralateral frontopolar region, Fp2), which implies the potential induction of two stimulation effects: a desired anodal –excitatory— stimulation over M1, and an unspecific cathodal –inhibitory— stimulation over the right frontopolar cortex, both potentially contributing to resulting changes in brain physiology and/or behaviour. Net-tDCS was thought of leveraging such limitation of canonical tDCS by systematically placing anodes and cathodes following fMRI-based patterns of positive and negative connectivity within/outside the motor system. This should lead to both a stronger

modulation of motor system's excitability compared to standard tDCS, as well as to the modulation of functionally relevant network-to-network dynamics between motor cortices and the rest of the brain via carefully tailored cathodal stimulation (see below).

Network-targeted tDCS optimization

As in Fischer et al. (2017), the target region for net-tDCS was based on the hand area representation of the left motor cortex (Figure 4.1C). The functional connectivity pattern of the hand area was calculated (Figure 4.1C); the coordinates of 5 largest clusters positively correlated with left M1 are: x= -42, y= -18, z= 62; x=50, y= -72, z= 2; x= 18, y= -82, z= 30; x=-10, y= -88, z= 36; x=-50, y= -74, z=8; whereas the coordinates of 5 largest clusters negatively correlated with left M1 are: x= 46, y= -46, z= 40; x=-40, y= 24, z= 32; x= -8, y= -78, z= -26; x=-30, y= 18, z= -6; x=-54, y= -54, z=-4. This pattern was used as input for the optimization of a genetic algorithm (Stimweaver algorithm; Ruffini et al., 2014) comparing thousands of multi-electrode montages including up to 8 stimulating electrodes located on any of the 32 positions of the 10/20 International EEG system, as already described in Chapter 1. Stimulation was performed using MRI compatible Sponstim electrodes (circular 1 cm radius, π cm^2 area sponges, Neuroelectrics), with a maximal current at any electrode of 2.0 mA, and a maximal total injected current of 4.0 mA across 8 electrodes (Figure 4.1D). Stimulation parameters were maintained within recommended safety parameters for transcranial electrical stimulation (tES) in humans (Lefaucheur et al., 2017). Anodal stimulation was delivered via five electrodes placed over the sensorimotor cortex bilaterally: specifically, C1 (872 uA), C2 (888 uA), C3 (1135 uA), C4 (922 uA), T8 (183 uA); —cathodal electrodes were placed over frontopolar and parietal areas, specifically Fz (-1843 uA), P3 (-1121 uA), P4 (-1036 uA) (Figure 4.1D).

Real-tDCS for both conditions was delivered for 22 mins, with periods of ramp-up/down of 30 secs, whereas sham-tDCS consisted of only 60 secs of stimulation at the beginning (ramp-up) and at the end (ramp-down) of the session. The impedance levels were kept below 10 kΩ throughout the stimulation sessions, thereby minimizing cutaneous sensations**.**

Biophysical modeling

Biophysical modeling has been computed as already described in Chapter 1. For this study two separate models were built, for standard and net-tDCS respectively. Distribution of current and

normal components of the generated electrical fields is reported for each montage in Figure 4.1 (C-D, for more details see Figure 1.1).

MRI data acquisition

Imaging was conducted on a Siemens Avanto scanner with a 12-channel head-coil (Siemens, USA). High-resolution T1-weighted anatomical images were obtained using a 3D-MPRAGE sequence (TR = 1880ms, TE = 3.38ms, TI = 1100ms, flip angle (FA) = 15°, number of slices = 176, thickness = 1mm, gap = 0mm, imaging matrix = 256 × 256, acquisition duration: 5 minutes). Functional MRI data were acquired before tDCS ("BASELINE"), during stimulation (mins 1'-8' of stimulation, "ACUTE"; mins 15'-22' of stimulation, "CUMULATIVE") and after stimulation ("AFTER"). Functional MRI images were acquire using standard echo-planar blood oxygenation level-dependent (BOLD) imaging (TR = 2000ms, TE = 20 ms, flip angle (FA) = 70°, number of slices = 37, thickness = 3.59mm, gap = 4.64mm, acquisition duration: 8,36''). Subjects were instructed not to focus their thoughts on any particular topic, do not cross their arms or legs and keep their eyes open. Arterial Spin Labeling (ASL) data were also acquired before and during tDCS; however, perfusion-related results are not discussed as part of the present manuscript.

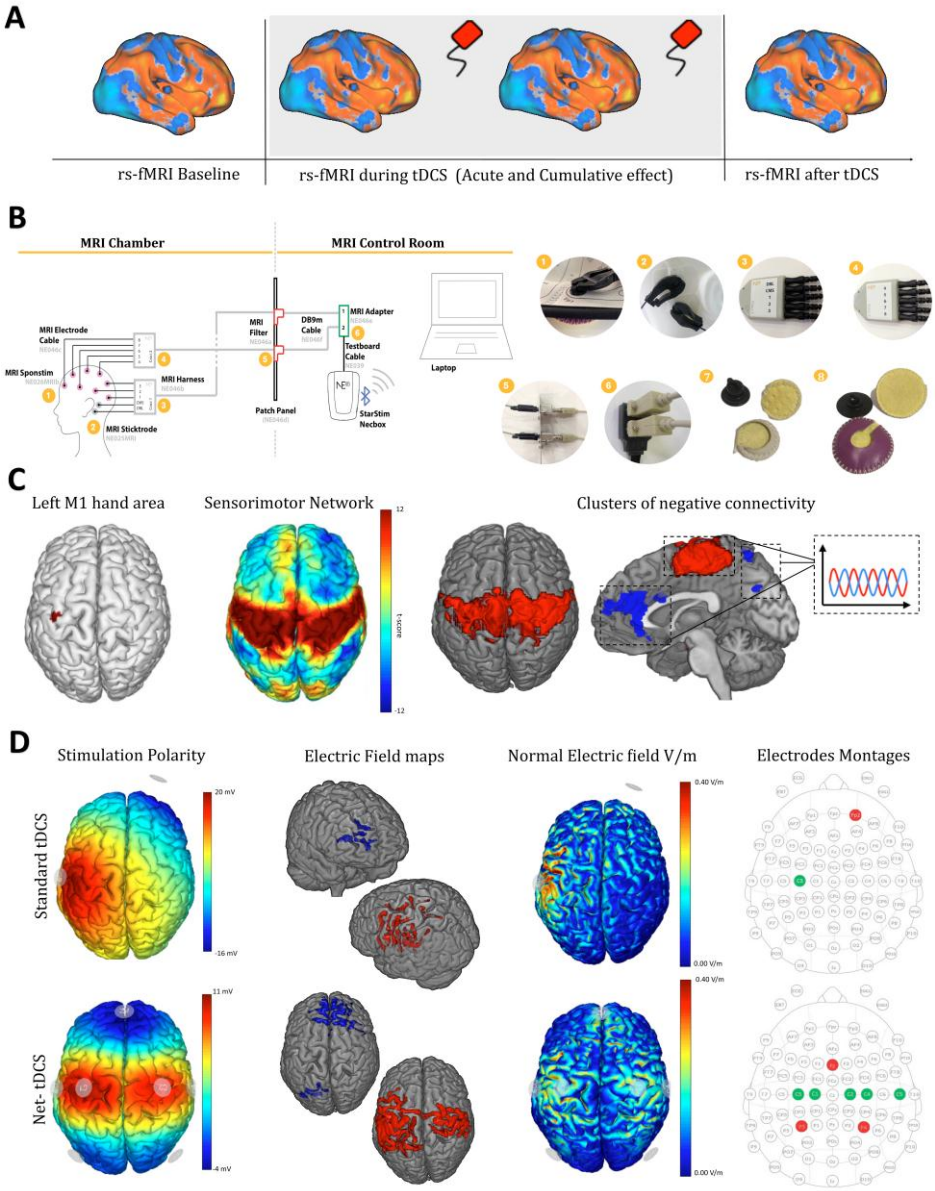

Figure 4.1. Experimental paradigm. (A) Overview of the tDCS-fMRI experimental session. (B) Schematic of multichannel stimulator MRI installation. (1) electrode in cap detail, (2) CMS/DRL mastoid electrodes for impedance check, (3) and (4) MRI compatible touchproof connector, (5) Patch panel connection, (6) Starstim cable adaptor. (www.neuroelectrics.com), MRI-compatible rubber electrodes used for (7) standard (5x5 cm) and (8) net-tDCS (1x1 cm). (C) The hand area of left M1 (targeted by standard tDCS) and areas positively and negatively connected to left M1, constituting the sensorimotor resting state network (targeted by net-tDCS), are reported. Clusters of negative connectivity to the SMN are shown. (D) For both standard and net-tDCS stimulation polarity, electric field maps >0.25V/m (red=anodal, blue=cathodal), normal electric field, and electrode positions (right; green anodes, red cathodes) are shown.

fMRI data preprocessing

fMRI data preprocessing and statistical analyses were carried out using SPM12 software (Statistical Parametric Mapping; www.fil.ion.ucl.ac.uk/spm/) and MATLAB 2013b (MathWorks, MA, USA) software. BOLD images underwent the following preprocessing steps: discarding of the first three volumes to allow for steady-state magnetization and stabilization of participant status; slice timing; realigning to correct for head motion; co-registration to structural images; segmentation; nonlinear normalization to the Montreal Neurological Institute (MNI) template brain; voxel resampling to an isotropic 3 × 3 × 3 mm voxel size; smoothing with an isotropic Gaussian kernel (full-width at half maximum, 8 mm). Structural images were co-registered to the mean volume of functional images and segmented using routines in SPM12. To obtain a more accurate spatial normalization, we created a customized grey-matter template from all subjects' segmented images. Briefly, this approach is based on the creation of a customized anatomical template built directly from participants T1-weighted images instead of the canonical one(s) provided by SPM (MNI template, ICBM 152, Montreal Neurological Institute). This allows a finer normalization into standard space and consequently avoids under- or overestimation of brain region volume. Linear trends were removed to reduce the influence of the rising temperature of the MRI scanner and all functional volumes were bandpass-filtered at 0.01 Hz < f < 0.08 Hz to reduce low-frequency drifts. Finally, an important issue for brain connectivity analysis is related to the deconvolution of potential confounding signals –mainly physiological high frequency respiratory and cardiac noise— from the grey matter voxels' BOLD time course. We decided to regress out potential confounding signals, like physiological high frequency respiratory and cardiac noise, from grey matter voxels' BOLD time course using the Compcorr algorithm (Whitfield-Gabrieli & Nieto-Castanon, 2012), in order to reduce artificial negative correlation and provide adequate filtering of the data.

Second-level analysis

Given the rationale of the study, changes in FC were expected on both left and right sensorimotor cortices, as well as on their negatively correlated regions during/after net-tDCS; instead, standard tDCS was expected to induce changes only on left sensorimotor cortices and right frontopolar regions. However, the two approaches generate electric fields of different intensity, shape, and polarity on the cortex, making it difficult to capture stimulation effects by implementing a single set of regions of interest (ROIs) defined anatomically. Therefore, we extracted individual RSNs for each participant using Independent Component Analysis (ICA)(Beckmann & Smith, 2005). Fifteen

components were obtained from subjects' resting data and visually inspected by three investigators. The SMN was chosen as seed to directly compare the effects of standard and network-targeted stimulation at whole-brain level. Additionally, the effect of tDCS in modulating the interaction between sensorimotor cortices and brain regions showing the highest negative functional connectivity was also investigated (Figure 4.1C). Specifically, these regions corresponded to a cluster of voxels mapping onto the anterior portion of the cingulate cortex (ACC hereafter) and the precuneus. In summary, FC analyses were focused on evaluating changes in local connectivity involving the sensorimotor cortices due to anodal stimulation, as well as changes in the negative connectivity between sensorimotor cortices and ACC/Precuneus as a measure of network-to-network connectivity.

Functional connectivity analysis

In order to verify our hypothesis, we implemented two different analysis. The first one, aimed to compare the modulation of FC induced by bifocal or net-tDCS at whole-brain level considering as seed the SMN identified via ICA. The second one, aimed at investigating the potential network effects of net-tDCS by looking at changes in connectivity between the motor system and its negatively correlated brain regions.

Whole Brain Functional connectivity modulation

Statistical analysis was carried out using the CONN (v.17f) toolbox and Matlab 2013b software (Mathworks, MA, USA). A repeated measure analyses of variance (rp-ANOVA) was carried out on the connectivity profile of the sensorimotor network identified via ICA. The model included factors 'Montage' (standard bifocal, network-targeted), 'Condition' (real, sham), and 'Time' (Baseline, Acute, Cumulative and After tDCS), as well as 'Montage X Condition X Time' interaction term. Age, gender and order of stimulation were included as covariates in all analyses. Results were computed applying a voxel-level threshold ($p< 0.001$ uncorrected) and cluster size correction ($p< 0.05$, false discovery rate -FDR- corrected).

Changes in Network-to-Network connectivity

To specifically investigate the effect of net-tDCS on network-to-network connectivity patterns involving the SMN, the following analysis was carried out for net-tDCS montage and was focused on the effects of the condition (real and sham) on negative correlation/connectivity in different time points (acute, cumulative and after). We initially run an ICA to define the SMN across subjects (data-driven, based on our sample) and then we identified the clusters of voxels showing the

significant (p< 0.001 uncorrected at voxel level; p< 0.05 FDR-corrected at cluster size) negative connectivity with the sensorimotor ICA component at baseline, for each session/condition. At this point we look at negative connectivity at whole-brain level, therefore not biasing the analysis towards a specific topology/topography. Then, we investigate the modulation of negative connectivity in these clusters, extracting significant connectivity values for each participant (p< 0.001 uncorrected at voxel level; p< 0.05 FDR-corrected at cluster size; r>3) at each time point (acute, cumulative and after tDCS). The values diverged by 2 or more standard deviation from the mean have been removed from the dataset. Finally, a repeated measure analyses of variance (rp-ANOVA) was carried out including the factor 'Condition' (active, sham), 'Time' (baseline, acute, cumulative, after), and the interaction 'Condition x Time'. Moreover, as exploratory analysis we compared FC values extracted for each time point with the FC value obtained at baseline separately for real and sham net-tDCS by means of paired t-tests (p< 0.05) using Statistical Package for Social Science (IBM SPSS Statistics 20) for Windows.

Subjective sensations

Given the different spatial distribution of the induced currents (due to the different number, location and size of the electrodes, with an overall higher total stimulation current intensity for multifocal stimulation equal to 4mA, compared to standard bifocal stimulation inducing 2mA), we used a self-report questionnaire (Fertonani et al., 2010) to collect information about subjective sensations during both standard bifocal and network-targeted stimulation, addressing commonly reported subjective feelings (e.g. tingling, pain, headache, etc..) that might be relevant for participant and operator blinding in future studies. We performed a rp-ANOVA testing the factor 'Condition' (real and sham), 'Montage' (standard bifocal and network targeted) and the interaction 'Condition x Montage' for each item of the questionnaire. Moreover, post-hoc analyses of simple main effects were performed using pairwise comparisons (p < 0.05) in SPSS 20.

4.2 RESULTS

Connectivity changes in the Sensorimotor network

The overall ANOVA model was significant ($F_{(2,158)}$= 4.25, p< 0.003), with a significant effect of *Montage* ($F_{(2,158)}$= 3.58, p< 0.007), as well as an effect of *Condition* ($F_{(2,158)}$= 2.62, p< 0.012) and *Time* ($F_{(2,158)}$= 3.71, p< 0.002). A significant Montage X Condition X Time interaction was found ($F_{(2,158)}$= 2.36, p< 0.025), therefore post-hoc comparisons of interest were run to understand the

specific acute, cumulative and after effects of net-tDCS. Similar to what observed using cortico-spinal excitability in the previous study by Fischer et al 2017, a significant increase in intrinsic FC of the sensorimotor ICA component (i.e. increased positive connectivity in both motor cortices) was observed both during (ACUTE: $t_{(158)}$= 9.86, p< 0.03; CUMULATIVE: $t_{(158)}$= 25.81, p< 0.006)(Figure 4.2 A and B) and immediately after real net-tDCS (AFTER: $t_{(158)}$= 36.14, p< 0.002, Figure 4.2C), compared to standard tDCS. On the other hand, no significant results have been showed comparing the effects of sham conditions (net-tDCS and standard montages) at the same time windows (all p>0.05). MNI coordinates of each significant cluster are reported in Table 4.1.

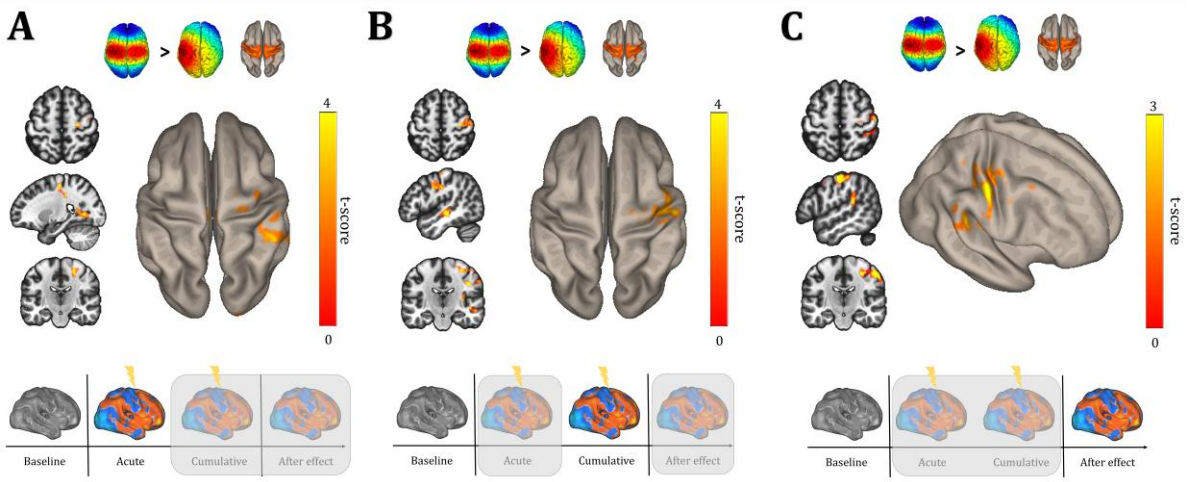

Figure 4.2. Functional connectivity results. Results of the contrasts between standard and net-tDCS for the sensorimotor ICA component are shown for each time point relative to baseline: Acute (A; minute 1-8); Cumulative (B; minute 15-22) and After (C) tDCS effect. The images, displayed in neurological convention, shown an increase of functional connectivity in the left part of SMN during and after net-tDCS compared to baseline and compared to the standard tDCS group. Axial, coronal and sagittal views are shown.

Table 4.1. ICA connectivity results. MNI coordinates, cluster size and localization of significant clusters displaying increased connectivity for net-tDCS compared to bifocal tDCS, both during and after stimulation

Time point	MNI			Size (voxel)	*Peak* p-uncorrected	Cluster p-FDR	Location/Label		
	x	*y*	*z*				Voxel	Hemisphere	Area
ACUTE									
	8	24	4	1699	.00001	.005	409	RL	Subcallosal cortex
							164	RL	Cingulate gyrus
							126	R	Paracingulate gyrus
							105	R	Caudate
							85	RL	Frontomedial cortex
							26	L	Paracingulate gyrus
							21	L	Frontoorbital cortex
	24	-64	2	1610	.0003	.005	214	R	Lingual gyrus
							205	R	Intracalcarine cortex
							115	R	Tempooccipital Fusiform cortex
							89	L	Lingual gyrus
							66	R	Occipital pole
							57	R	Middle Temporal gyrus
							52	R	Cerebellum
							36	R	Middle Temporal gyrus
							32	RL	Precuneus
							27	L	Occipital Fusiform gyrus
							24	R	Inferior Temporal gyrus
	10	-24	38	1243	.00002	.01	207	R	Supramarginal gyrus
							175	R	Precentral gyrus
							165	RL	Cingulate gyrus
							64	R	Supramarginal gyrus
							20	R	Angular gyrus
CUMULATIVE									
	42	16	36	2503	.00005	.0003	605	R	Precentral gyrus
							335	R	Postcentral gyrus
							285	R	Middle Temporal Gyrus
							108	R	Insular Cortex
							65	R	Parietal operculum
							59	R	Superior Temporal gyrus
							30	R	Heschl's gyrus
							29	R	Supramarginal gyrus
AFTER									
	30	-20	50	783	.00009	.03	419	R	Postcentral gyrus
							114	R	Precentral gyrus
							58	R	Supramarginal gyrus
							28	R	Superior Parietal lobule

.

Effect on network-to-network connectivity

A significant effect of *Condition* ($F_{(1,9)}$= 5.24; p= 0. 048) was observed, whereas no significant results was depicted for *Time* ($F_{(3,27)}$= 1.70; p= 0.19) and for *Condition x Time* interaction ($F_{(3,27)}$= 1.16; p= 0. 34). In order to investigate these results in detail and for a qualitative perspective, we conducted several paired t-tests (p< 0.05) evaluating the differences in all time points (acute, cumulative and after) between the two conditions (active and sham). The results showed a significant increase of the negative connectivity between SMN and ACC/Precuneus for real net-tDCS in all time points when compared to acute sham tDCS (Acute: $t_{(9)}$= 2.11, p= 0,032; Cumulative: $t_{(9)}$= 2.93, p= 0,008; After: $t_{(9)}$= 1.93, p= 0,043; see Figure 4.3). All the other contrasts reported no significant results (all p> 0.08).

Moreover, the exploratory analysis conducted separately for real and sham net-tDCS comparing FC values extracted for each time point to baseline showed an increase of negative connectivity

both during (ACUTE and CUMULATIVE) and AFTER stimulation only for real tDCS (respectively, ACUTE: $t_{(9)}$=-2.28, p= 0.024; CUMULATIVE: $t_{(9)}$=-2.09, p= 0.033; AFTER: $t_{(9)}$=-2.20, p= 0.027; % increase in FC for real net-tDCS with respect to baseline: ACUTE: 12%; CUMULATIVE: 15%; AFTER: 11%). Conversely, the connectivity between SMN and its negatively correlated clusters was not significantly different during or after sham net-tDCS (respectively, ACUTE: $t_{(9)}$= 1.29, p= 0.11; CUMULATIVE: $t_{(9)}$=-0.45, p= 0. 33; AFTER: $t_{(9)}$= 0.014, p= 0.49; % increase in FC for sham net-tDCS with respect to baseline: ACUTE: -0.8%; CUMULATIVE: 2%; AFTER: -0.1%) (Figure 4.3).

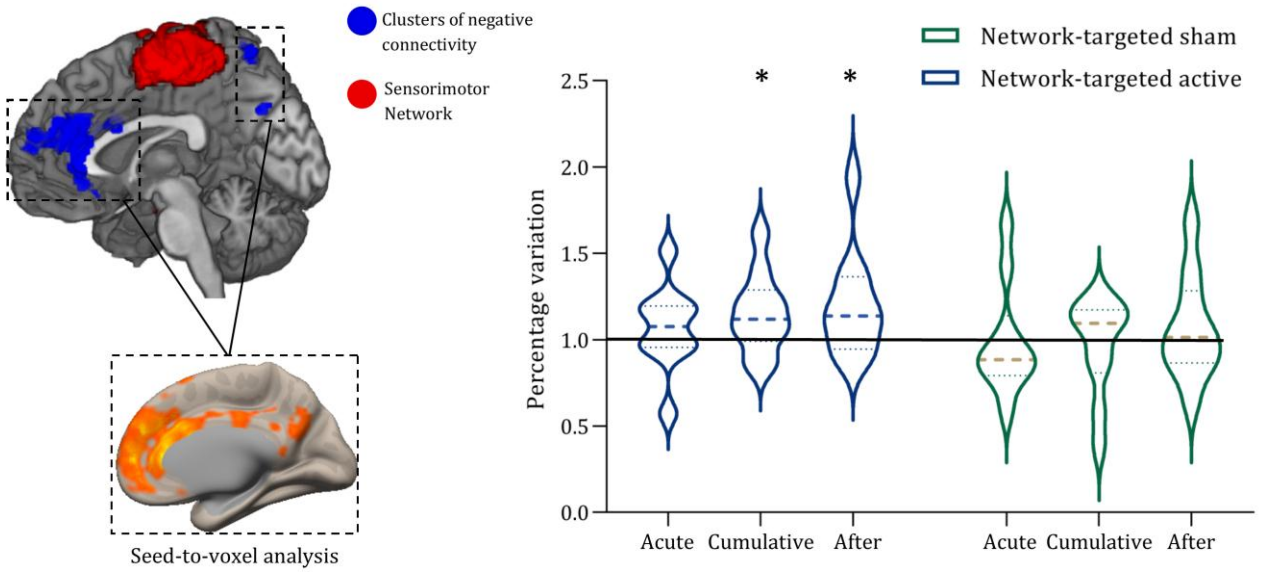

Figure 4.3. Modulation of network-to-network connectivity. The acute, cumulative and after effect of stimulation on the negative FC is shown for net-tDCS. The plot represents the change in FC as compared to baseline (1 =100% baseline) at each time point (Acute, Cumulative and After; e.g. 1.1 equals to 10% increase in FC compared to baseline), for both real and sham net-tDCS. Negatively correlated regions targeted by cathodal stimulation (ACC and Precuneus) are shown. * identifies timing in which the modulation of negative FC is significative different between conditions (p< 0.05), whereas ^ shows the significant effect of real net-tDCS in different time points compared to baseline.

Induced subjective sensations

Neither side-effects nor adverse effects were reported during or after stimulation, confirming the safety profile of both standard and net-tDCS. The reported subjective sensations were not significantly different between stimulation modalities, as showed by the ANOVAs results. In

particular, no significant effect was observed for Headache (*Montage*: $F_{(1,9)}$= 1.80; *p*= 0. 21; *Condition*: $F_{(1,9)}$= 0.31; *p*= 0.59; *Montage x Condition*: $F_{(1,9)}$= 3.85; *p*= 0.08); Scalp pain (*Montage*: $F_{(1,9)}$= 1.55; *p*= 0. 24; *Condition*: $F_{(1,9)}$= 0.10; *p*= 0.76; *Montage x Condition*: $F_{(1,9)}$= 3.46; *p*= 0.09); Scalp burn (*Montage*: $F_{(1,9)}$= 0.10; *p*= 0. 76; *Condition*: $F_{(1,9)}$= 0.00; *p*= 1; *Montage x Condition*: $F_{(1,9)}$= 0.23; *p*= 0.64); Sensation under the electrodes (*Montage*: $F_{(1,9)}$= 0.03; *p*= 0. 86; *Condition*: $F_{(1,9)}$= 0.80; *p*= 0.39; *Montage x Condition*: $F_{(1,9)}$= 3.12; *p*= 0.11); Sleepiness (*Montage*: $F_{(1,9)}$= 2.71; *p*= 0. 13; *Condition*: $F_{(1,9)}$= 0.37; *p*= 0.56; *Montage x Condition*: $F_{(1,9)}$= 0.37; *p*= 0.56); Trouble in concentrating (*Montage*: $F_{(1,9)}$= 2.44; *p*= 0.15; *Condition*: $F_{(1,9)}$= 2.25; *p*= 0.17; *Montage x Condition*: $F_{(1,9)}$= 0.00; *p*= 1); Change in mood (*Montage*: $F_{(1,9)}$= 0.79; *p*= 0.40; *Condition*: $F_{(1,9)}$= 0.31; *p*= 0.59; *Montage x Condition*: $F_{(1,9)}$= 3.86; *p*= 0.3). A significant effect of *Montage* ($F_{(1,9)}$= 7.36; *p*= 0.02) was observed for the item 'Skin redness', whereas no significant effects of Condition ($F_{(1,9)}$= 2.25; *p*= 0.17) and Condition x Montage ($F_{(1,9)}$= 2.25; *p*= 0.17) were observed. *Post-hoc* analysis conducted on this item on this item confirmed the higher skin redness after real standard stimulation ($t_{(9)}$= 2.23; *p*= 0.038) compared to the real net-tDCS. For the real conditions, higher scores were observed for (i) sleepiness (mostly imputed to the length of the study visits), (ii) tingling under the electrodes (usually reported at the beginning of stimulation and decreasing afterwards), and (iii) burning (mild, not reported as uncomfortable), but no one of this item resulted significant different compared to the sham conditions. Most commonly reported effects were headache, changes in mood, neck pain, scalp pain and trouble in concentrating. Individual scores are reported in Figure 4.4, mean and standard deviation (SD) for each item by condition and montage are shown in Table 4.2.

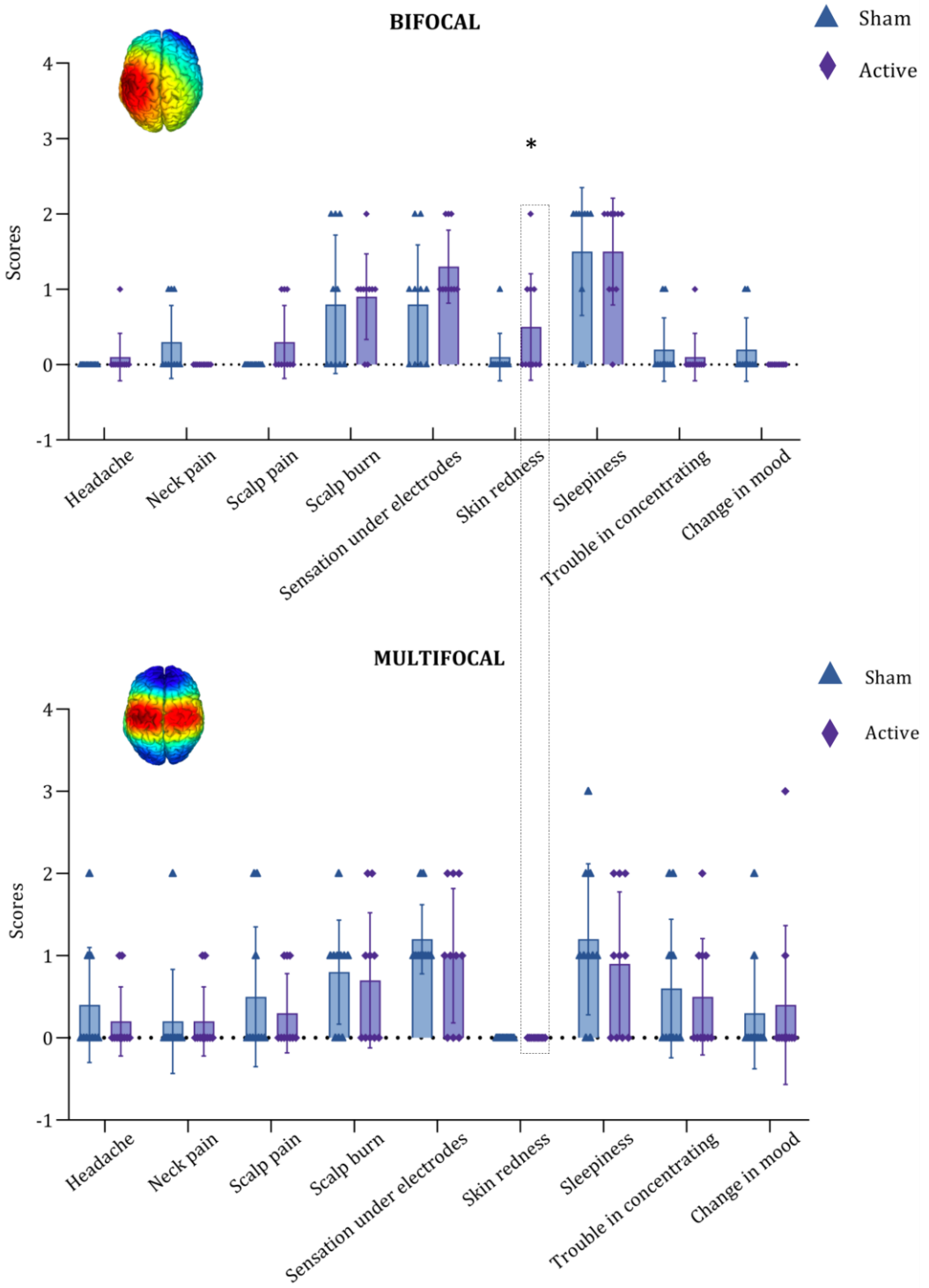

Figure 4.4. Side effects. Bars represent average subjective reports (Lickert scale: 0=none, 4=strong, adapted from Fertonani et al., 2010) for both standard bifocal and net-tDCS. Blue triangles and violet diamond represent the subjects' single value reported respectively for sham and real conditions. Error bars represent standard error of mean. * = $p < 0.05$.

Table 4.2. Mean and standard deviation (sd) for each subjective sensation reported trough a self-report questionnaire by conditions and montages.

	headcache	neck pain	scalp pain	scalp burn	sensation under the electrodes	skin redness	sleepiness	trouble in concentrating	change in mood
Bifocal tDCS REAL									
Mean	0,1	0	0,3	0,9	1,3	0,5	1,5	0,1	0
SD	0,316	0,000	0,483	0,568	0,483	0,707	0,707	0,316	0,000
Bifocal tDCS SHAM									
Mean	0	0,3	0	0,8	0,8	0,1	1,5	0,2	0,2
SD	0,000	0,483	0,000	0,919	0,789	0,316	0,850	0,422	0,422
Net-tDCS REAL									
Mean	0,2	0,2	0,3	0,7	1	0	0,9	0,5	0,4
SD	0,422	0,422	0,483	0,823	0,816	0,000	0,876	0,707	0,966
Net-tDCS SHAM									
Mean	0,4	0,2	0,5	0,8	1,2	0	1,2	0,6	0,3
SD	0,699	0,632	0,850	0,632	0,422	0,000	0,919	0,843	0,675

4.3 DISCUSSION

The aim of the study was to further explore previous findings reported by Fisher et al., (2017) using TMS-EMG (i.e., net-tDCS is able to modulate the entire SMN beyond the effect of canonical bifocal tDCS over left M1) using a concurrent tDCS-fMRI approach, by also investigating the feasibility, efficacy as well as safety of a tDCS solution optimized to engage a target RSN via multichannel stimulation. Moreover, the present study was designed to test the possibility of using net-tDCS to modulate not only local brain dynamics but also the interplay between the target networks and its negatively correlated brain regions/networks. Results suggest a stronger engagement of the bilateral sensorimotor areas during net-tDCS compared to bifocal tDCS. Furthermore, by conducting an exploratory analysis to have a qualitative overview of the effects of net-tDCS on network-to-network interaction, the results show its efficacy in amplifying the negative connectivity between the SMN and its negatively correlated brain regions targeted by

cathodal stimulation. However, due to the small sample size, this finding should be interpreted carefully and requires further validation. Findings might be relevant for the optimization of tDCS in clinical contexts, where alterations of network-to-network connectivity have been documented (e.g. see Zhou et al., 2010), as well as for cognitive enhancement purposes (Santarnecchi et al., 2017c; Spreng et al., 2016).

Modulation of Intrinsic functional connectivity

Modulation of M1 excitability via tDCS has been extensively used to enhance motor behaviour and motor learning (Nitsche et al., 2003; Reis et al., 2009), also exploring its potential in clinical and rehabilitative settings (Liew et al., 2014). Several studies have also investigated the impact of tDCS by combining TMS-EEG (Pellicciari et al., 2013; Romero Lauro et al., 2014; Varoli et al., 2018) or by means of neuroimaging measures (Amadi, Ilie, Johansen-Berg, & Stagg, 2014; Polanía, Paulus, & Nitsche, 2012b, 2012c; Sehm, Kipping, Schäfer, Villringer, & Ragert, 2013). Given the shift in focus towards network-based approaches for the study of human cognition (Santarnecchi et al., 2017b; Santarnecchi, Momi, et al., 2018; Santarnecchi, Sprugnoli, et al., 2018; Spreng et al., 2016; Pisoni et al., 2018) and more recently even for the diagnosis of neuropsychiatric conditions (Fox et al., 2014), we tested the impact of a tDCS montage optimized to concurrently modulate multiple nodes of the sensorimotor network (and its negatively correlated regions) instead of solely left M1. Using a multifocal tDCS solution previously tested by assessing corticospinal excitability (Fischer et al., 2017), here we document a greater modulation of functional connectivity involving both left and right M1 during net-tDCS compared to standard tDCS. Moreover, the effect on fMRI connectivity seemed present both during and after tDCS, similarly to what we observed in the previous investigation and to what has been reported for standard and high-density (HD) tDCS (Antal et al., 2011; Bikson et al., 2010; Dmochowski et al., 2011; Nitsche & Paulus, 2001). This suggests an interesting convergence between neurophysiological findings (i.e., Motor Evoked Potentials as measured via combined TMS and electromyography) and neuroimaging results related to net-tDCS.

Of note, changes in cortical excitability in one hemisphere could increase or decrease cortical excitability in the other hemisphere by means of interhemispheric connections, such that functional inhibition or excitation of contralateral homologous areas may occur at different times depending on the task at hand/brain state (Bloom & Hynd, 2005). When dealing specifically with the primary motor cortices, neurophysiological and neuroimaging research investigating

interhemispheric interactions have corroborated the idea of these two areas being negatively correlated when subjects perform a unimanual motor task (Ferbert et al., 1992; Kobayashi et al., 2003; Vines et al., 2006). The network-targeted solution investigated in the present study offers interesting opportunities to target a bilaterally distributed network, but it should be considered that this might only apply to a healthy brain stimulated at rest. Ad-hoc investigations are needed to adapt net-tDCS for applications in clinical populations with pathological interhemispheric imbalance or those with unilateral lesions in general (as showed in Chapter 1), for which a reduction of interhemispheric connections has been reported in favour of greater intrahemispheric cohesion (Siegel et al., 2016).

Effect on network-to-network connectivity

A growing body of literature suggests the importance of looking at alterations of brain networks, as well as network-to-network interactions, as potential biomarkers of neurological and psychiatric conditions. For instance, alterations of the interplay between the Default Mode Network (DMN) and Anterior Salience Network (AS) have been documented in both Alzheimer's Disease and Frontotemporal Dementia patients: however, while the former shows increased DMN-AS functional connectivity, the latter display the opposite pattern, even though both conditions shared a significant neuropathological substrate. This highlights the need for network-targeted interventions able to modulate such dysfunctional inter-networks dynamics. Moreover, the negative connectivity (or "anticorrelation") between brain networks has been also promoted as a crucial aspect of the functional organization of the human brain, with relevance for cognitive performance (Fox et al., 2005). For instance, recent reports have highlighted how the strength of the negative connectivity between regions of the dorsal attention network (DAN) and the DMN is among the best predictors of individual variability in intelligence levels (Santarnecchi et al., 2017c). Recent work by our group has shown the possibility to selectively modify resting-state fMRI network-to-network coupling by means of multi-site TMS using cortico-cortical paired associative stimulation (cc-PAS) (Santarnecchi, Momi, et al., 2018). However, the possibility to modulate inter-network dynamics by means of network-targeted tDCS has not been demonstrated yet. Here we show how a tDCS montage optimized to desynchronize the target network (SMN) and its negatively correlated nodes is partially able to increase the negative connectivity between networks. By systematically placing cathodal electrodes over frontal and parietal brain regions (i.e., Fz to target the medial prefrontal cortex and ACC; P3/P4 to target the left/right angular

gyrus), net-tDCS resulted in an amplified negative correlation between SMN, ACC and bilateral angular gyri, compared to the results obtained in the acute sham net-tDCS, but not in the other time points. The presented results originally suggest the opportunity of manipulating network-to-network functional connectivity patterns by means of optimized tDCS targeting both positively and negatively connected brain regions. Moreover, looking at active or sham stimulation alone, a significant trend in the increase of negative connectivity both during and after real net-tDCS compared to baseline was found, with no effect during sham stimulation. While this is suggestive of potential modulation of network-to-network connectivity, this finding should be interpreted carefully given the very limited sample size and high number of conditions/comparisons in the design.

Limitations and future directions

The first limitation is represented by the small sample size, which has had a significant impact on data analysis and our ability to draw firm conclusions about some findings, especially those related to modulation of negative connectivity. For these reasons, our study only represents a preliminary yet informative investigation on the potential of network-targeted tDCS for modulation of network dynamics as compared to bifocal tDCS. Another potential limitation is the higher current intensity induced by net-tDCS (4mA) compared to bifocal stimulation (2mA). In fact, given the nature of multichannel stimulation and the need to target multiple brain regions, net-tDCS is usually performed at higher stimulation intensity compared to standard tDCS, and through a higher number of scalp electrodes. Even though this might represent an advantage, electrodes' location and their corresponding current intensity actually increase the parameter space and potentially leads to suboptimal situations where not enough electrodes deliver sufficient stimulation to reach the brain transcranially. For instance, while in traditional tDCS current diffuses through a single anode injecting 2mA, in the current net-tDCS protocol anodal stimulation was delivered via 5 small electrodes with an average of 0.8 mA stimulation intensity per electrode (with values as low as 0.183mA for electrode T8 over the temporal lobe). Moreover, given the focus on the sensorimotor cortices/network, a smaller set of electrodes is used for stimulation of negatively correlated nodes (n=3), leading to one electrode delivering almost 2mA on a single location (Fz=-1843uA). Future optimizations may consider a fixed lower intensity bound (e.g., ensuring that each electrode deliver at least 0.5mA) and possibly more than 8 electrodes to guarantee higher spatial resolution. Although the orientation of the current flow across gyri and sulci (Lafon et al., 2017) is considered

in the biophysical modeling, our analysis was focused on the areas where stimulation is predominantly “anodal” or “cathodal”. Future study should develop a consistent method to look at the difference of the anodal or cathodal current flow in the gyri and sulci.

Furthermore, TMS-based MEPs should be collected before and after the fMRI-tDCS sessions to provide a comparison between electrophysiological and fMRI effects, also replicating findings from Fischer et al. (2017) and further looking for the predictive power of baseline cortical excitability over tDCS modulation of functional connectivity. Moreover, an additional limitation of rs-fMRI technique should be considered. Functional RSNs have been mostly studied through fMRI, with several investigations focused on fMRI-based connectivity dynamics within and across distributed brain networks. However, rs-fMRI is a low temporal resolution estimate of FC, unable to capture brain oscillatory rhythms reflective of actual neural activity (i.e. at millisecond timescale) (He et al., 2010). Only direct external manipulation of RSN activity may provide valuable information about fast-evolving interactions between RSNs. An increasing number of studies over the years have employed multimodal neuroimaging techniques to better understand the neural origins and spatial− temporal signatures of RSNs (Britz et al., 2010; Chang et al., 2013; Chen et al., 2008; Feige et al., 2017; Laufs, 2008; Liu et al., 2018; Sadaghiani et al., 2010; Tagliazucchi et al., 2012). For example, some studies examined the specificity of tDCS effects on brain connectivity by means of TMS-EEG, highlighting how the spread of tDCS effects follows structural brain connections when applied at rest (Romero Lauro et al., 2014), whereas spreading only to functionally relevant areas when tDCS is applied during task execution (Pisoni et al., 2018). Moreover, recent work by our group (Ozdemir et al., 2020) has revealed that is it possible to capture the same fMRI dynamics but with high temporal resolution by using network-guided TMS-EEG. Despite no consensus has been reached on the correlation between EEG spectral power features and dynamic functional connectivity profiles within or across specific RSNs, multifocal tES approaches could be helpful in investigating this link.

Future studies should also investigate other control conditions (e.g., inverse condition, extracephalic cathodal electrode) and the possibility of personalizing electrode montages (i.e., electrode number and intensity) based on individual brain anatomy (Tecchio et al., 2013) and fMRI network dynamics/topology, like recently shown in a similar network-target brain stimulation approach using personalized multi-coil TMS (Santarnecchi, Momi, et al., 2018).

CHAPTER 5

STUDY 5: Preliminary evidence of gamma induction on neural dynamics via tACS in patients with Alzheimer's disease

Gamma oscillations are rhythmic fluctuations in local field potentials (LFPs) encompassing a broad range of frequencies (35–100 Hz). The involvement of gamma oscillations in high cognitive tasks is a well-known concept in literature. An increase in gamma has been observed in tasks such as reading and subtraction expectancy; where each task elicited gamma oscillations with a distinct distribution (Fitzgibbon et al., 2004). Furthermore, gamma increases have been reported during working memory (Chen et al., 2014) and during memory encoding in humans and mice (Colgin, 2016; Yamamoto et al., 2014). In particular, there are evidence suggesting that gamma rhythms are involved in hippocampal memory processing (Buzsáki, 2015; Carr et al., 2011, 2012). Therefore, it is not surprising that some brain diseases characterized by memory impairments are linked to disorders in gamma rhythms (Mably & Colgin, 2018). Alzheimer's disease (AD) is characterized by a relative attenuation and dysregulation of gamma frequency and a shift from faster (e.g. gamma) to slower (e.g. theta) brain activity (Mably & Colgin, 2018). Current studies in AD indicate that amyloid-ß (Aß) oligomers cause dysfunction in parvalbumin-positive (PV+) and somatostatin-positive (SST+) interneurons, resulting in dysregulation of gamma oscillations and cognitive decline (Palop & Mucke, 2016; Palop & Mucke, 2010). These studies suggest that decreasing slow gamma disorders may be a promising new strategy for treatment of memory impairments in AD. Therefore, gamma induction could be highly beneficial in individuals with AD. So far, studies in animals revealed that the induction of gamma frequency through sensory stimulation or optogenetics reduces amyloid-β plaques (Iaccarino et al., 2016; Rajji, 2019). Moreover, optogenetic modulation of PV+ and SST+ interneurons restores gamma oscillations in murine models of AD (Adaikkan & Tsai, 2020). The induction of gamma oscillations also decreases inflammatory brain processes and leads to microglia-mediated clearance of Aß and tau depositions, and consequential cognitive benefits (Adaikkan et al., 2019; Iaccarino et al., 2016). Although the optogenetic method is limited to animal use, there is emerging evidence that gamma oscillations can be safely and noninvasively modulated by transcranial electrical stimulation (tES) in humans (Guerra et al., 2018; Santarnecchi et al., 2013; Santarnecchi et al., 2017a; Santarnecchi

et al., 2019). Furthermore, Naro and colleagues (2016) demonstrated that failure in responding to gamma-tACS correctly discriminated between MCI patients designated to convert into AD, showing that gamma-tACS could be a useful perturbation-based biomarker in predicting MCI to AD conversion (Naro et al., 2016). The modulation of gamma oscillation can be achieved by inducing spike-timing-dependent plasticity (STDP) via a multiple session of 40 Hz tACS. Successful gamma induction would be reflected as changes in both resting-state brain oscillations and in the evoked gamma during a cognitive task.

In this study the feasibility and safety of gamma induction via transcranial alternating current stimulation (tACS) have been investigated in patients with mild to moderate AD. A biophysical model targeting the region with maximal Aß burden by combining T1-weighted MRI and Aβ PET images has been optimized (Ruffini et al., 2014). This method leverages modern multi-focal stimulation solutions allowing for whole-scalp stimulation montages including up to 32 channels, promoting personalization of tACS treatment and greater spatial accuracy. In this case we propose a multifocal tACS protocols, instead of a net-tDCS as suggested in the Study 4, following the literature showing an effect of gamma stimulation, through sensory stimulation or optogenetics, in reducing amyloid-β plaques on AD's animal models. In particular, we hypothesized that the daily application of 40 Hz tACS would be firstly safe and well-tolerated, and secondly would increase gamma activity in resting-state EEG recordings and enhance the evoked gamma during the N-back task, measured as event-related synchronization.

5.1 MATERIALS AND METHODS

Study design

Fifteen individuals with a diagnosis of mild to moderate AD (median age = 76, range= 63-78; median MMSE = 25, range = 20-26; median ADAS-Cog = 17, range=15-19; APOE gene = 40% ε3/ε3, 33%ε4/ε4, 27%ε3/ε4; BDNF gene = 53% Val/Val, 33%Val/Met, 14% Met/Met) were assigned to three groups (n=5/per group) to receive: 10 sessions of right-hemispheric, unilateral tACS applied with a personalized electrode montage designed to target each patient's Aβ deposition as mapped by positron emission tomography (PET) (Group 1); or either 10 (Group 2) or 20 (Group 3) sessions of bi-hemispheric tACS targeting both temporal lobes (Figure 5.1). Sessions were conducted daily, Monday through Friday. All participants underwent a comprehensive neuroimaging assessment including brain magnetic resonance imaging (MRI), amyloid-β imaging with PET,

electroencephalogram (EEG) recording, Transcranial Magnetic Stimulation (TMS) combined with EEG, and neuropsychological assessment preceding and following tACS treatment. Saliva samples were collected and analyzed for brain-derived neurotrophic factor (BDNF) Val66Met, catechol-O-methyltransferase (COMT) Val158Met, and apolipoprotein E (APOE) e2, e3, e4 polymorphisms (Figure 5.1A). In this study, we present the results of only a part of this dataset, including the rs-EEG collected daily before and after every stimulation session, and the event-related potential response to the n-back task collected before and at the end of the entire treatment. Qualitative results on cognitive enhancement are also provided.

Participants were amyloid positive, completed at least until the 8th grade of education, did not have any history of intellectual disability, and were receiving a stable dose of medications for at least six weeks. The exclusion criteria included a history of migraines, neurological disorders other than dementia, major psychiatric disorders, as well as substance abuse or dependence.

This study was conducted following the Declaration of Helsinki and the International Ethical Guidelines for Biomedical Research Involving Human Subjects. This study was approved by the Beth Israel Deaconess Medical Center (BIDMC) Institutional Review Board, and informed consent from all participants was obtained before performing any research procedures. The data collection was performed under two IRB protocols registered separately on ClinicalTrials.gov (NCT03412604 and NCT03290326).

Safety and adverse event monitoring

Given the unprecedented nature of tACS application in AD, adverse events were collected during all the time of the experiment. All adverse events, regardless of attribution to tACS, PET, MRI, or EEG were collected and recorded using standard forms (Fertonani et al., 2015). Moreover, participants were asked in an open-ended way about the presence of any such events. Before and after each tACS daily visit, we administered an adverse event questionnaire. We also monitored cognitive effects with a rotation of three parallel versions of the Montreal Cognitive Assessment (MoCA). In the case of a 4-point or greater drop from the baseline MoCA, a neurological examination was conducted to assess the patient's condition (Milani et al., 2018).

Transcranial Alternating Current Stimulation (tACS)

TACS was delivered via a battery-driven current stimulator Starstim 32 (Neuroelectrics Barcelona, Cambridge) through surface 3.14 cm Ag/AgCl electrodes. The electrodes were placed into a

neoprene cap corresponding to the international 10/20 EEG system, with the Cz electrode position aligned to the vertex of the head. Gel was applied to optimize signal conductivity and lower impedance (Signa Gel, Parker Laboratories Inc.). For all daily sessions, we placed 32 electrodes on the scalp to record EEG before/after every tACS session, although only a subset was used to deliver tACS (Figure 5.1B). Stimulation frequency was set to 40 Hz and it was applied for 1 hour, preceded by 30 seconds ramp-up and followed by 30 seconds ramp-down intervals.

Biophysical modeling and montage optimization

Individualized tACS optimizations were conducted from the subject's own MRI and Aβ PET. The algorithm was constrained by safety parameters, in which the total injected current could not exceed 2 mA per electrode, consistent with the safety limits of the Starstim device. As an example, for one patient, the algorithm identified the optimal electrode configuration and amperage to be: AF4= -823µA, C6= 812µA, F8= 602µA, FP2= 1061µA, FZ= -318µA, P10= -444µA, T8= -1162µA, IZ= 271µA for a total injected current of 2746 µA and a maximum current any electrode of 1162 µA (quality of the solution weighted correlation coefficient (WCC): 0.54, and the ideal solution that minimized error relative to no intervention (ERNI) was (mV^2/m^2): -4151; for details about WCC and ERNI see Ruffini et al., 2014). Bi-hemispheric temporal lobe tACS montage was delivered by electrodes P7-P8-T7-T8 for the subjects of the Groups 2 and 3, considering these areas as the most affected by TAU proteins (Figure 5.1B). For all daily visits, tACS was applied for 60 minutes at an intensity of 2 mA, with a ramp up/down interval of 30 seconds. 40Hz stimulation frequency yielded 144000 cycles for every 60 minutes of stimulation.

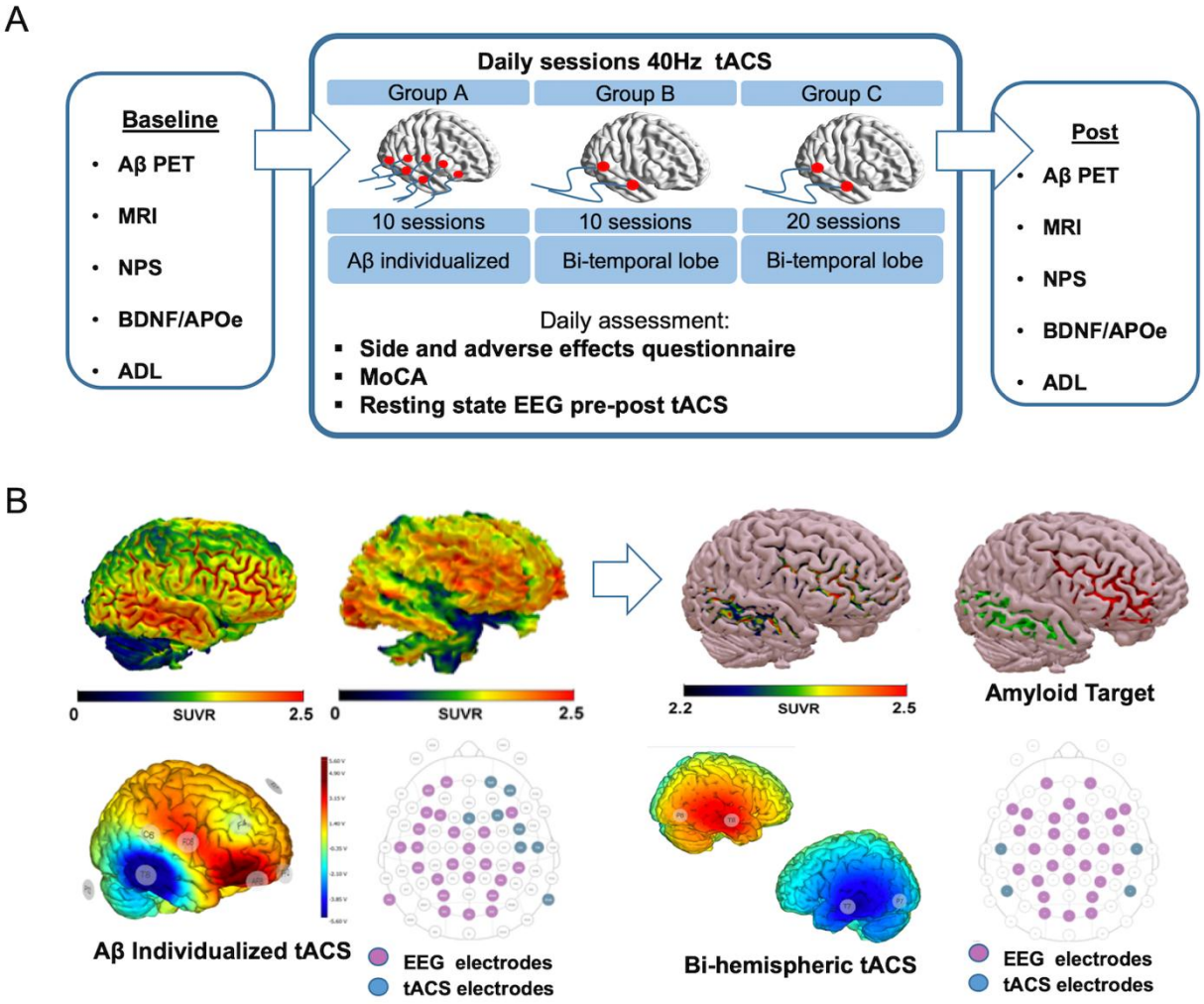

Figure 5.1. **Experimental design and tACS montages optimization**. A) Preceding and following tACS intervention, PET, MRI, EEG were recorded; Neuropsychological (NPS) and activities of daily living (ADL) assessments were conducted; saliva samples were analyzed for BDNF (rs6265) and COMT (rs4628) ValMet polymorphism and apolipoprotein E (APOe) e2, e3, e4 allele. During 40 Hz tACS daily intervention we monitored EEG and safety and adverse effects. B) We adopted two stimulation solutions, one targeting the subject's Aβ deposition (Group 1, on the left an example of one subject), and the other targeting bi-hemispheric temporal lobe (Groups 2 and 3), with target maps defined on Aβ PET, CT, and T1-weighted MRI data. For all daily sessions, we placed 32 electrodes on the scalp to record EEG, although only a subset of the electrodes was used to deliver tACS. For all daily visits, the stimulation was applied for 60 minutes with intensity of 2 mA, with a ramp up/down interval of 30 seconds. SUVR = standard uptake value ratio.

Scalp EEG Recordings

To monitor EEG resting-state dynamics throughout daily tACS visits intervention, whole scalp 32-channel EEG was recorded using standard 10-20 montage according to the 10-20 International System (Jasper, 1958), for 10 minutes immediately before and after 40 Hz tACS. Participants were instructed to stay relaxed, to reduce movement and consequent muscular contractions. EEG was acquired by Starstim 32 (Neuroelectrics Barcelona, Cambridge) and was recorded from 32 tES-compatible Ag/AgCl disk electrodes placed in: AF3, AF4, C1, C2, C3, C4, CP1, CP2, CP5, CP6, CZ, FC1, FC2, FC5, FC6, FP1, FP2, F3, F4, F7, F8, FZ, P3, P4, P7, P8, Pz, PO3, PO4, O1, O2, OZ. Recordings were online-referenced to the right mastoid at a sampling rate of 500 Hz and online filtered with a band-pass of 0.01–100 Hz. Electrode impedances were kept below 5 kΩ.

EEG signal was also recorded while patients were performing a 1-back task within one week before starting the stimulation sessions, as well as within one week after completing the treatment. In this case the Event-Related Potentials (ERPs) have been analyzed.

N-Back paradigm

Previous studies showed that mild cognitively impaired (MCI) and AD patients are compromised in working memory functioning (Baddeley et al., 1991; Missonnier et al., 2007). Further studies also identified specific electrophysiological alterations of ERP components. In particular, when performing the N-back task a marked delay of P200 latencies was found in MCI patients relative to control participants (López Zunini et al., 2016; Missonnier et al., 2007), indicative of delays in storage and retrieval stages of working memory. Therefore we administered the N-Back task (Kane et al., 2007; Owen et al., 2005) before and following tACS intervention with the hypothesis that daily applications of 40 Hz tACS would drive a reduction of the P200 delay.

Visual stimuli (letters) were presented using Presentation software (Neurobehavioral Systems, Inc., Albany, CA, USA), installed on a laptop PC (Dell Inc.). Stimuli were displayed on a 15-inch screen (refresh rate of 60 Hz). The sequence of the stimuli was pseudo-randomized. The visual material comprised capital letters from the alphabet (A, B, C, D, F, G, H, J). The onset time of each letter was of 1500 ms with an inter-trial interval of 3000 ms. The letters and fixation cross were presented in the middle of the screen on a light grey background. All letters were in black ink with a 54-point Arial font (Figure 5.2B). Participants received instructions about how to do the task, and then they practiced the task with the assistance of the investigator until they became familiar with the stimuli presentation and the response keys, and they were able to execute the task

autonomously. When ready, participants performed four blocks of 1-back task with 50 trials (40 distractors, 10 targets, for a total of 200 trials) while EEG was recorded with the Starstim Neurostimulator device.

Statistical analysis

Resting-state EEG analysis

Resting-state EEG has been analyzed using EEGLAB 14.1 (Delorme & Makeig, 2004) and Brainstorm, and customized scripts in the Matlab R2017b (MathWorks Inc.) environment. Specifically, recordings were band-pass and notch filtered, with high pass and low pass cut-off frequencies of 1 Hz and 70 Hz, respectively, and notch frequencies centered around 60 Hz. Then, the signal was visually inspected in order to remove bad electrodes or artifact not detectable by Independent Component Analysis (ICA). Finally, the ocular (e.g., blinks) and muscular components were isolated and subtracted using the ICA approach provided in EEGLAB 14.1, and the data has been re-reference to the average of the electrodes. Fast Fourier Transform (FFT) and Hilbert method were then used to measure spectral power (μV2/Hz) for each electrode site. Changes in power spectral densities (PSD) before and after the tACS were calculated, specifically absolute and relative power density values (μV2/Hz) were calculated within the delta (1-4 Hz), theta (4-7 Hz), alpha (8-13 Hz), beta (14-30 Hz), low gamma (35-45 Hz), narrow gamma (38-42 Hz) and high gamma bands (45-55 Hz) for each participant at each site. Relative power denotes the power in a frequency band as a percentage of the total power of the signal over the 1-55 Hz range.

We hypothesized that the repeated 1-hour daily stimulation might have a carry-over/additive effect on the EEG spectral dynamics and might also depend on other factors (e.g. a good/bad night of sleep). Therefore, we calculate a within visit index that we called ACUTE effect ($Visit_n$ post - $Visit_n$ pre/ $Visit_n$ pre * 100), a between visits index called the DELAYED effect ($Visit_n$+1 pre – $Visit_n$ post/ $Visit_n$ pre*100) and the sum of the two called TOTAL effect. The ACUTE, DELAYED and TOTAL effects for each daily tACS visit were determined across sessions for each participant and then averaged across participants. Finally, the grand average of ACUTE, DELAYED and TOTAL effects across all participants, all visits and all electrodes were calculated (Figure 5.2). From a statistic point of view, three separate one-way ANOVA were conducted to compare the effects of 40 Hz tACS on ACUTE, DELAYED and TOTAL effects in all EEG bands. Power changes were expressed as percentage relative power variations. Specifically, for each band we used this equation: Δ-power = (P-Post - P-Pre)/ P-Pre x 100, where Δ-power denotes the percentage relative variation of relative

powers, P-Pre and P-Post are the powers in the pre- and post-daily tACS, respectively. Note that a positive value of Δ-power means an increase in power and a negative one a decrease.

ERPs analysis

To isolate the ERPs from the ongoing EEG, the segments preceding and following each stimulus were extracted, applying a 30 Hz filter to visualize the ERP curves. A total of 200 trials for each subject have been detected. After discarding artifactual and error trials, we calculated the ERPs for each patient and then we calculated the grand average across all patients. Lastly, given that P200 component has been shown to be maximal over the frontal region we clustered the electrodes F3, Fz, and F4. In total at group level, 1353 out of 3000 trials were considered for the analysis, resulting from the correct responses to target and distractor. The time window of -500 to 900 ms relative to the stimulus presentation was analyzed, and the pre-onset average was subtracted from the post-onset signal (baseline correction). Independent components analysis (ICA) was used to extract blinking and eye movements within the data. Therefore, two-tailed paired sample t-test corrected for multiple comparisons were conducted to compare pre and post tACS ERPs.

5.2 RESULTS

Adverse events

All 15 patients completed the study and tolerated the tACS gamma induction intervention. The majority of patients reported mild adverse effects; one patient reported severe head pain and one reported hand tingling, however both effects were deemed unrelated to tACS application by the covering neurologist. All patients reported sensations that are commonly reported during the administration of other types of tES. The most frequently described sensations were a light burning sensation underneath the stimulation electrodes, tingling, itching, and mild headache induced by mechanical pressure from the stimulation cap (see Table 5.1). No serious adverse events were reported. Notably, less than 5% (9/200) of scheduled tACS visits were missed, indicating the low level of attrition and feasibility of the tACS gamma induction approach in AD (Table 5.2).

Table 5.1. Adverse events frequency, severity and attribution.

ID	GROUP	SENSATION			HEAD PAIN			VISUAL CHANGES			NERVOUSNESS			SCALP IRRITATION			NECK PAIN			EYE PAIN			TROUBLE CONCENTRATING			HAND TINGLING		
		F	S	A	F	S	A	F	S	A	F	S	A	F	S	A	F	S	A	F	S	A	F	S	A	F	S	A
1	1	1	1	5	1	1	4	2	2	4	2	1	2	2	1	5	-	-	-	-	-	-	-	-	-	-	-	-
2	1	1	1	5	-	-	-	2	1	4	-	-	-	2	2	5	-	-	-	-	-	-	-	-	-	-	-	-
3	1	2	1	5	-	-	-	2	1	4	-	-	-	2	1	5	1	1	5	2	1	3	-	-	-	-	-	-
4	1	2	1	5	2	1	5	-	-	-	-	-	-	-	-	-	-	-	-	-	-	-	-	-	-	-	-	-
5	1	2	1	5	-	-	-	2	1	4	-	-	-	2	1	5	-	-	-	-	-	-	2	1	4	-	-	-
6	2	2	1	5	-	-	-	2	1	4	-	-	-	-	-	-	-	-	-	-	-	-	-	-	-	2	1	4
7	2	1	1	5	-	-	-	-	-	-	-	-	-	-	-	-	-	-	-	-	-	-	-	-	-	-	-	-
8	2	1	1	5	2	1	5	1	1	4	-	-	-	1	1	5	-	-	-	-	-	-	-	-	-	-	-	-
9	2	1	2	5	2	1	3	1	1	2	-	-	-	2	1	5	2	1	5	-	-	-	-	-	-	-	-	-
10	2	-	-	-	-	-	-	-	-	-	-	-	-	-	-	-	-	-	-	-	-	-	-	-	-	-	-	-
11	3	1	1	5	2	3	5	2	1	4	-	-	-	1	1	5	1	1	5	-	-	-	-	-	-	-	-	-
12	3	-	-	-	-	-	-	-	-	-	-	-	-	-	-	-	-	-	-	-	-	-	-	-	-	-	-	-
13	3	-	-	-	-	-	-	-	-	-	-	-	-	-	-	-	-	-	-	-	-	-	-	-	-	-	-	-
14	3	-	-	-	-	-	-	-	-	-	-	-	-	-	-	-	-	-	-	-	-	-	-	-	-	-	-	-
15	3	-	-	-	-	-	-	-	-	-	-	-	-	-	-	-	-	-	-	-	-	-	-	-	-	-	-	-

F= frequency, 1-constant, 2-intermittent; S= severity, 1-mild, 2-moderate, 3-severe, 4-life threatening, 5-fatal; A= attribution, 1-unrelated, 2-unlikely, 3-possible, 4-probable, 5-definite

Table 5.2. tACS daily visits and missing visits.

ID	Group	1	2	3	4	5	6	7	8	9	10	11	12	13	14	15	16	17	18	19	20
1	1	✓	✓	✓	✓	✓	✓	✓	x	✓	x										
2	1	✓	✓	✓	✓	✓	✓	✓	✓	✓	✓										
3	1	✓	✓	✓	✓	✓	✓	✓	✓	✓	x										
4	1	✓	✓	✓	✓	✓	✓	✓	✓	✓	x										
5	1	✓	✓	✓	✓	✓	✓	✓	✓	✓	x										
6	2	✓	✓	✓	✓	✓	✓	✓	✓	✓	✓										
7	2	✓	✓	✓	✓	✓	✓	✓	✓	✓	✓										
8	2	✓	✓	✓	✓	✓	✓	✓	✓	✓	✓										
9	2	✓	✓	✓	✓	✓	✓	✓	✓	✓	✓										
10	2	✓	✓	✓	✓	✓	✓	✓	✓	✓	✓										
11	3	✓	✓	✓	✓	✓	✓	✓	✓	✓	✓	✓	✓	✓	✓	✓	✓	✓	✓	✓	✓
12	3	✓	✓	✓	✓	✓	✓	✓	✓	✓	✓	✓	✓	✓	✓	✓	✓	✓	✓	✓	x
13	3	✓	✓	✓	✓	✓	✓	✓	✓	✓	✓	✓	✓	✓	✓	✓	✓	✓	✓	✓	✓
14	3	✓	✓	✓	✓	✓	✓	✓	✓	✓	✓	✓	✓	✓	✓	✓	✓	✓	✓	✓	x
15	3	✓	✓	✓	✓	✓	✓	✓	✓	✓	✓	✓	✓	✓	✓	✓	✓	✓	x	x	x

✓= visit completed; x= visit missed; Group 1 = 10 sessions of right-hemispheric tACS target each patient's Aβ deposition map; Group 2 = 10 sessions bi-hemispheric tACS targeting both temporal lobes; Group 3 = 20 sessions bi-hemispheric tACS targeting both temporal lobes.

Effects of tACS gamma on power

Consistent with our hypothesis, EEG power spectral analysis of the TOTAL effect of tACS reveals that the gamma power increase is significantly greater compared to the other bands. Specifically, a one-way ANOVA revealed an effect of tACS on relative spectral power of all frequency band ($F_{(6,63)}$ = 5.01, p< 0.01). Post hoc analysis show that gamma power increase more than the power in other frequencies. In particular, a difference between gamma (M=12.61, SD=8.53) and theta (M=2.44, SD=2.21, $t_{(9)}$ = 3.80, p < 0.01), and alpha (M=5.37, SD=3.88, $t_{(9)}$ = 2.27, p < 0.01), and beta (M=3.94, SD=2.06, $t_{(9)}$ = 3.34, p < 0.01) was found (see Figure 5.2A). The effects of 40Hz tACS were greater for the gamma band (e.g., 35-60 Hz) than for activity in lower bands (e.g., theta, alpha, beta) supporting the predicted frequency specificity. Moreover, we performed a one-way ANOVA of the ACUTE effect ($F_{(6,63)}$ = 2.07, p = 0.06), and DELAYED effect ($F_{(6,63)}$ = 0.44, p = 0.8) (see Figure 5.2B), without finding any significant effect.

Effects of tACS montage

We tested the spatial specificity of the intervention by comparing the ACUTE relative power change in the gamma band (35-45 Hz). We compare bi-hemispheric temporal lobe and mono-hemispheric montages, as a proxy of stimulated brain regions, and central electrodes as control regions (Figure 5.2B). The bi-hemispheric temporal cluster comprises the same electrodes of the groups 2 and 3 montages (P8-T8-P7-T7). The mono-hemispheric cluster comprises common electrodes of group 1 montage (F2-FC2-FC6-F6-CP6). The central cluster includes CP1-CP2-Pz electrodes. For group 1 we found a difference between mono-hemispheric electrodes (M=11.36, SD=22.05) and central electrodes (M=-0.44, SD=6.86, $t_{(9)}$ = 2.02, p=0.03). For groups 2 and 3 we found a difference between bi-hemispheric temporal lobe (M=11.05, SD=22.15) and central electrodes (M=-2.67, SD=8.89, $t_{(19)}$ = 3.12, p=0.03). As shown in Figure 5.2B, results indicate a greater increase of gamma activity in the areas underneath tACS stimulation electrodes as predicted by the biophysical model E-field distribution (Figure 5.1B).

Effects of tACS number of sessions

For the bi-hemispheric temporal lobe stimulation (groups 2 and 3), we also examined the dose-response relation over two stimulation durations, 10 and 20 hours. For group 2 that received 10 visits we found no difference between temporal lobe (M=3.14, SD=14.04) and central electrodes (M=-0.44, SD=6.86, $t_{(9)}$ = 0.88, p=0.2). Also, for the first 10 visits of group 3 we found no difference

between (M=11.35, SD=17.49) and central electrodes (M=-0.44, SD=6.86, $t_{(9)}$ = 0.88, p=0.2). In contrast for group 3 we found a difference between temporal lobe (M=10.75, SD=14.04) and central electrodes (M=-4.91, SD=6.86, $t_{(9)}$ = -2.28, p=0.04) considering visits 11-20. These results suggest that longer tACS intervention might lead to a sustained increase of gamma, which might be in line with previous studies using other non-invasive brain stimulation techniques (D'Agata et al., 2016; Winker et al., 2020). We also found that the cumulative effect over time is characterized by a trend of peaked gamma around mid-week (see Figure 5.2B).

Effects of tACS on ERPs

In order to analyze the effects of tACS on ERPs during the N-Back task, we used a permutation paired t-test to compare ERPs pre and post tACS intervention. To correct for multiple comparison, we adopted FDR correction by the Benjamini-Hochberg step-up procedure. Paired sample t-test corrected for multiple comparisons shows a reduction of P200 latency after the intervention ($p< 0.05$), possibly indicative of faster working memory retrieval and storage phases. The shadowed area in the Figure 5.2C represents a significant difference in the P200 between pre and post tACS.

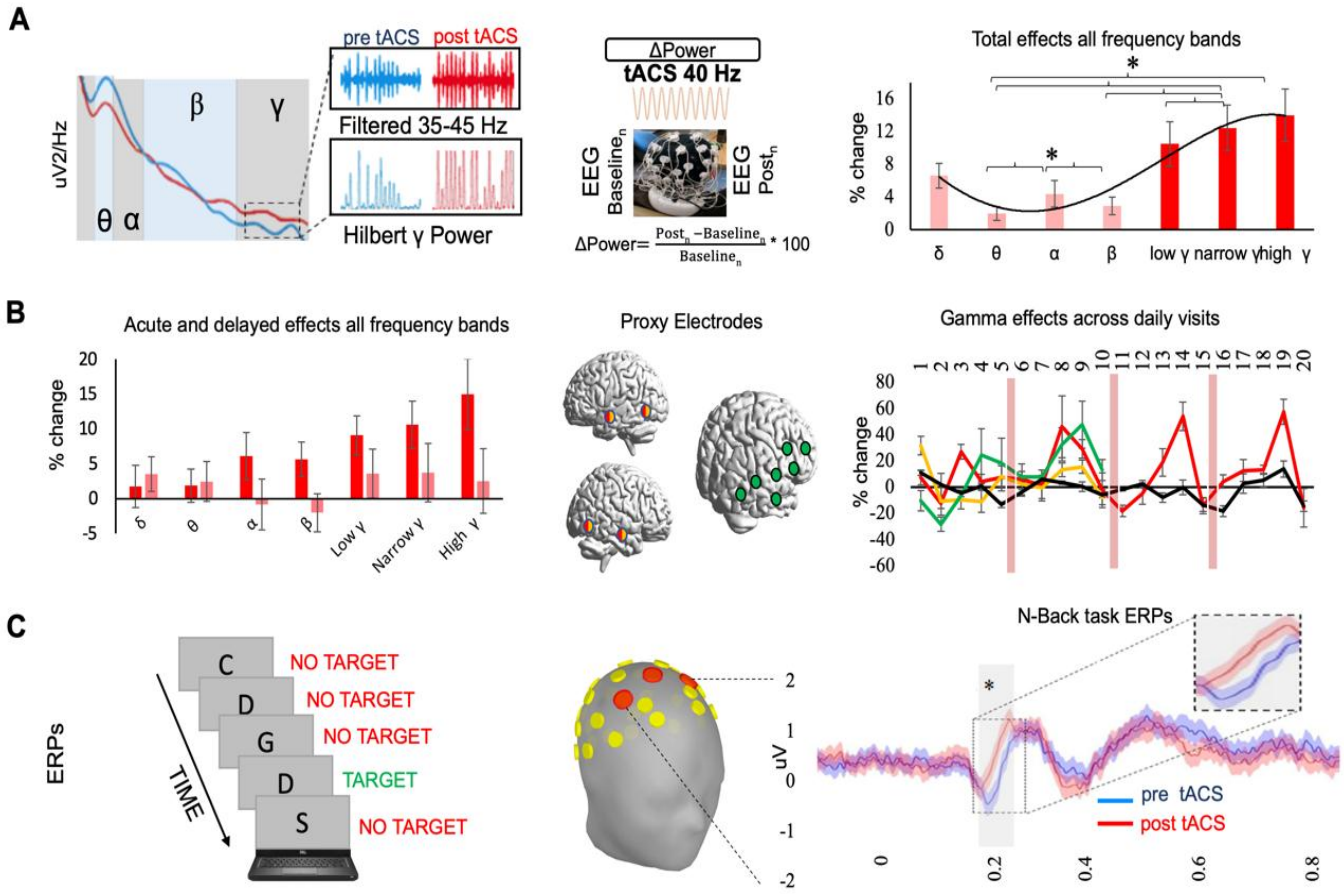

Figure 5.2. **EEG power spectral dynamics and event-related potentials (ERPs) are shown.** A) From left to right, a schematic illustration of gamma extraction by Hilbert transformation (bandpass filtered at 35-45 Hz, 1 minute before and after daily tACS. Clearly observable are more frequent gamma burst at T2 (after the intervention, red line) than at T1 (before the intervention, blue line). Schematic illustration of ΔPower calculation. Grand average of ΔPower TOTAL effect across all frequency bands and all visits: the effects of 40Hz tACS on gamma band (e.g., low γ 35-45, narrow γ 38-42 and high γ 45-60 Hz) are significantly greater than lower bands (e.g., theta, alpha, beta). B) Left: Grand average of ΔPower ACUTE (pre vs post tACS within session) and DELAYED (post vs pre tACS across sessions) effects across all frequency bands and all visits. Middle: schematic showing the position of the electrodes for group 1 (green) and groups 2 and 3 (orange, red). Right: differential results between the 3 groups across daily visits: green line for Group 1, orange and red lines respectively for Groups 2 and 3, black line for the control site. Positive values represent the percentage increase of gamma power (35-45 Hz) during the treatment and light red rectangles depict weekends during treatment. C) Schematic representation of N-back task and event-related potentials (ERPs) recorded during the N-Back task. Stimuli are presented while the EEG is being recorded. Frontal cluster average activity of the electrodes F3, Fz, and F4. P200 latency was found to be reduced after tACS intervention. Gray shadowed area represents a significant difference between pre (light blue line) and post (light red) tACS intervention. All data are shown as mean ± s.e.m. *p < 0.05.

Effects of tACS on cognitive tests

Given the short duration of tACS intervention, we did not expect substantial changes in cognition, therefore neuropsychological assessment was administered before and following the tACS intervention primarily to assess the safety of tACS intervention. Although no significative changes were found in any of the cognitive measures, our results suggest that some patients showed a tendency towards improvement in declarative memory and language tasks. We report some of the results here for completeness, but they should be considered explorative results. Global cognition, evaluated by ADAS-Cog remained stable (pre: M=18.27, SD=7.68; post: M=18.11, SD=7.69). Activities of daily living (ADL) were assessed by a questionnaire covering multiple aspects of everyday personal activities (e.g., eating, bathing, dressing, shopping, keeping appointments, etc.), and remains stable (pre: M=68.5, SD=4.68; post: M=68.3, SD=6.23). The majority of patients showed signs of improvement in declarative memory and language assessed by Craft Story Recall (CSR) Delayed, (pre: M=3.87, SD=3.36; post: M=4.93, SD=4.30; see Figure 5.3 for individual datapoints, x axis pre tACS and y axis post tACS). The language and memory improvement were supported by caregivers' feedback.

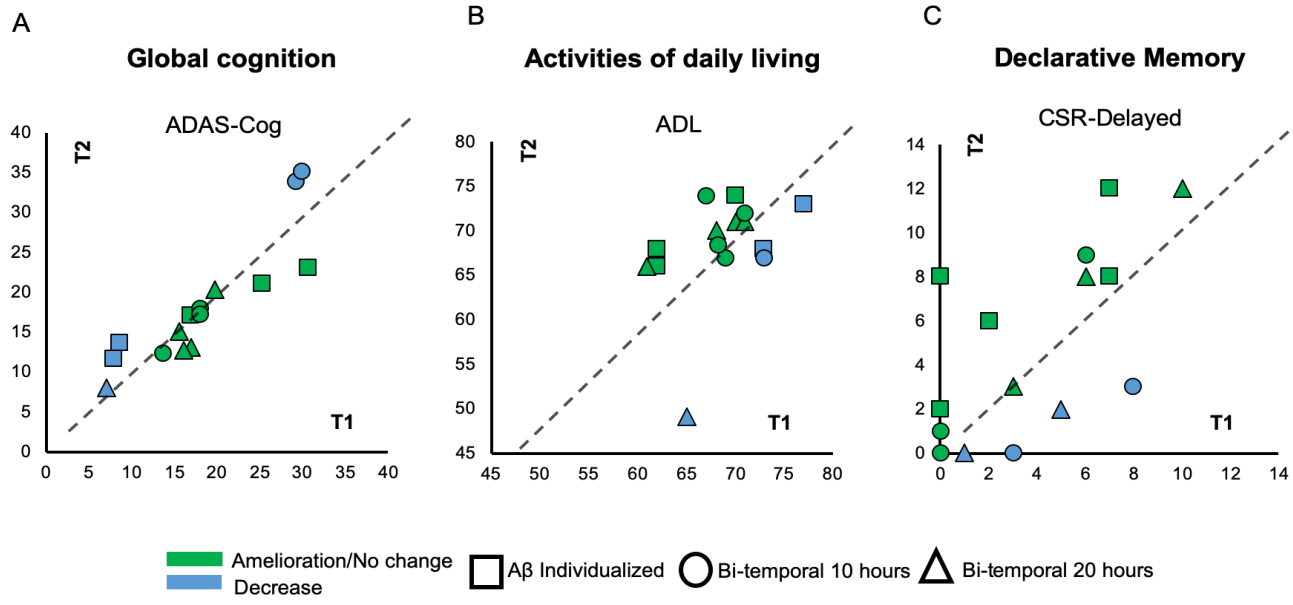

Figure 5.3. tACS effects on cognitive domain. A) changes in global cognition (ADAS-cog). B) activities of daily living (ADL). C) declarative memory (CSR-D). Legend: markers depict each patient, shapes are used to indicate the group: (i) square for Aβ Individualized, (ii) circle for bi-hemispheric temporal lobe 10 hours and (iii) triangle for bi-hemispheric temporal lobe 20 hours; colors indicate improvement or no change (green) and decline (blue) in performance after tACS gamma induction. These are exploratory results.

5.3 DISCUSSION

Despite the open-label nature of the present study, it constitutes a first-in-human translational trial of recent evidence on the effect of gamma-induction in promoting protection against neurodegeneration documented in mouse model of Alzheimer's Disease (AD) (Adaikkan & Tsai, 2020; Iaccarino et al., 2016). In patients with mild to moderate AD, we investigated the clinical, neurophysiological, and cognitive impact of multiple daily sessions of tACS to induce gamma oscillations. To our knowledge, this is the first study addressing the effects of 40Hz tACS on individuals with AD during a 10-days long intervention. This study proved the feasibility and safety of this procedure for the studied population. Going further, a key result of our non-invasive 40 Hz tACS gamma-induction protocol is the significant increase of gamma oscillations throughout the intervention. Beside significant frequency-specific effects on gamma oscillations, we also observed that tACS generate greater effects on the brain regions underneath stimulation electrodes, indicating spatial-specificity and efficacy of the targeting approach. Further, prolonged tACS treatment leads to a cumulative impact on gamma oscillations throughout the daily stimulation sessions, suggestive of a dose-response relation which highlights the need to further explore tACS as a treatment in follow-up studies. Moreover, we show a significant improvement in working memory processing revealed by a reduction of P200 latency normally associated with dementia-related cognitive decline. Finally, qualitative results of potential improvement in declarative memory, language, and activities of daily living have been reported.

Safety and feasibility

Although there is extensive evidence about the safety of tACS applied in healthy humans, we show for the first time that multiple sessions of gamma-tACS in AD are feasible, safe and well-tolerated. Normally, tACS is delivered for 10-20 minutes duration in a single session (Antal et al., 2017), whereas here we provide further support of the feasibility of multiple consecutive 1-hour daily sessions of 40Hz tACS in AD patients. Moreover, here we administered tACS via multiple electrodes adopting a multi-focal stimulation approach that allows for stimulation montages based on up to 32 stimulating channels, in contrast to the conventional two electrodes administration of tACS. We also included the careful stimulation design defined through MRI-based modeling of induced electric field, resulted in more realistic, individualized montages, which might become crucial when targeting Aβ in AD patients. Given the novelty of this stimulation approach, we continuously monitored adverse events throughout tACS intervention. We found that the majority

of patients reported only minor adverse events that are generally described also during standard short tACS –or tDCS/tRNS— protocols. For instance, mild itching, tingling, burning sensations under the stimulating electrodes, discomfort, and tiredness for the long protocol, which can be efficiently handled (e.g., by adding conductive gel, improving skin-electrode contact, etc.). The fact that no serious adverse events were reported is noteworthy since the prolonged exposure to tACS in a vulnerable clinical population such as AD is unprecedented.

Gamma induction, temporal and spatial specificity

Several studies have shown that gamma oscillations are decreased in AD (Palop & Mucke, 2016). Iaccarino and collaborators (2016), using mice model 5XFAD, investigated how AD affects gamma rhythms under the hypothesis that abnormal neuronal states play a key role in the symptoms of the disease. They found that reduced levels of gamma power in the hippocampus of 5xFAD mice preceded the accumulation of amyloid plaques and cognitive impairment (Iaccarino et al., 2016). Furthermore, the authors reported a reduction of Aβ levels after 1 hour of optogenetic stimulation or flickering light stimulation at 40Hz. This effect was related to the activation of GABAergic neurons, which in turn activated microglia, allowing for amyloid plaque depletion, improving behavior, and ultimately promoting protection from neurodegeneration (Adaikkan et al., 2019). These studies proved that optogenetic and multisensory stimulations are recognized methods for gamma-induction in animal models of AD (Adaikkan & Tsai, 2020; Cardin et al., 2009; Martorell et al., 2019; Sohal et al., 2009). Here we investigated non-invasive gamma-induction via tACS in AD patients, showing a significant increase of gamma oscillation throughout the intervention. Although there is accumulating evidence that tACS can be used to synchronize frequency-specific neuronal networks in healthy humans (Helfrich et al., 2014; Herrmann et al., 2013; Witkowski et al., 2016), we show for the first time that tACS produces a significant change in gamma oscillations in AD. Our results, indicating that 40 Hz tACS specifically upregulates fast oscillations in AD, are important considering that generalized EEG slowing is a hallmark of AD and correlates with cerebrospinal fluid (CSF) biomarkers and poorer cognitive outcome (Stomrud et al., 2010). Although the mechanisms underlying the after-effects of tACS are still subject of investigations, converging evidence from intracranial recordings in awake nonhuman primates suggests that tACS modulates spike timing activity of neurons in a frequency-specific manner (Alekseichuk et al., 2019; Krause et al., 2019). However, future studies that better clarify the mechanisms of tACS in humans and the potential application to clinical populations are needed.

Moreover, we investigated the effects of prolonged exposure to 40 Hz tACS by recording longitudinal EEG data during each daily session. We show that the repeated daily administration of tACS produced significantly greater effects over time (e.g., 20 vs 10 sessions), suggesting a cumulative effect of tACS on gamma oscillations. Earlier studies provide evidence of Hebbian-type neuroplasticity modifications of synaptic strength following repetitive daily application of other non-invasive brain stimulation techniques (e.g. rTMS and tDCS)(Huang et al., 2017; Koch et al., 2013; Revill et al., 2020). Our results extend current evidence demonstrating that also 40 Hz tACS yields an additive effect on gamma neural dynamics. Intriguingly, the cumulative tACS action is marked by a maximum gamma peak level around mid-week followed by a period where the effectiveness of tACS diminishes. Thus, the repeated exposure to 40 Hz tACS appears to cause a drop in the brain response to the stimulation around mid-week, probably caused by a mirrors habituation (Cohen et al., 1997; Rankin et al., 2009), in which the response to tACS decreases after repeated consecutive prolonged exposure.

Furthermore, to examine the spatial specificity of tACS intervention, we adopted two stimulation solutions, one targeting individual subject Aβ deposition (Group 1), and the other targeting Bi-hemispheric temporal lobe (Groups 2 and 3). Recent major technological developments presently enable individualized multi-electrode stimulation solutions based on modeling of current distribution to optimize the precision of tACS targeting (Fischer et al., 2017; Ruffini et al., 2014). We analyzed the differences between the proxy of stimulated regions and a group of central electrodes as control regions (Figure 5.2), showing that gamma increases more in the proximity of the stimulation electrodes as predicted by biophysical modeling, thus supporting spatial specificity. These results are important because they provide preliminary validation for targeting optimization integrating different imaging modalities in AD.

ERPs and Cognitive effects

For a physiological point of view, we showed a significant reduction of P200 latency in the n-back task after tACS gamma-induction. As well-known in literature, P200 expresses retrieval and storage phases in memory domain and it is significantly delayed in mild cognitive impairment (MCI) in contrast to healthy controls (López Zunini et al., 2016). Our observed changes indicate that tACS gamma-induction speeds up working memory processing in AD patients. Despite preliminary, these results showing initial signs of a potential effect of gamma-induction on cognitive processing are very encouraging. However, we can not exclude that the observed effect

is a consequence of the basic attentional levels' improvement or of the practice effects. Therefore, future investigations with sham-controlled designs are necessary to disentangle these novel findings.

The effects of tACS on cognitive domain has been investigated through an extensive neuropsychological battery. tACS gamma-induction did not significantly affect the tests, however we found interesting evidence of improved declarative memory in the CSR-Delayed Paraphrased. This result is especially salient because declarative memory is one of the most sensitive signs of memory loss in the early stages of AD. In this task, patients hear a brief story, each containing 25 informational bits, and were asked to recall as much as possible both immediately and after a 10 minute delay period using the same words (verbatim) or other similar words (paraphrased) (Craft et al., 1996). We found that 75% of patients improved in the paraphrased delayed recall after tACS gamma-induction (Figure 5.3). Even though these results should be interpreted carefully because only qualitative, they were mirrored by the subjective reporting of improvement in word finding and episodic memory by the patients' caregivers (e.g., "I noticed an improvement in word finding", "He remembered his appointments", etc.).

Limitations of the study and future directions

In this Chapter, I reported only the data results I had the opportunity to analyze during my period abroad in Boston. Surely, the main limitation of the results presented here is the lack of a control condition. However, this is an ongoing research, and the center in Boston is working on extending the sample and including a control group that will receive the sham protocol. This implementation will allow us to draw conclusion about whether the observed effect is caused by the 40 Hz stimulation and not by placebo effects or confounding variables. Future studies should also consider controlled sham designs leveraging novel solutions for placebo control (Neri et al., 2019). Within-subject study designs may also allow for comparison between sham and real tACS stimulation keeping a low variability in the data. Moreover, the small sample size limited the statistical power of our study. Using a larger sample size will increase the power to detect changes in event-related synchronization or desynchronization, as well as increase the signal to noise ratio in the EEG recordings during the N-back task. In order to better investigate the spatial localization of tACS, the higher density EEG montages could be useful considering the stimulation space specificity and the recordings spatial resolution, allowing the implementation of source reconstruction techniques to localize the stimulation effects more efficiently. Furthermore,

implementing MEG could improve the gamma oscillations' detection and localization. Such technique reliably measures gamma (Cheyne & Ferrari, 2013; Tan et al., 2016) and could increase the spatial resolution of recordings both by using a high number of sensors to quantify brain activity and by its immunity to volume conduction effects. Additionally, new techniques as oscillatory transcranial direct current stimulation (o-tDCS) and close loop tACS may be explored in the future. Finally, studies in animal models and humans found an association between sleep deprivation and Aβ protein burden (Mander et al., 2016; Shokri-Kojori et al., 2018). Furthermore, gamma oscillations have been reported during slow-wave sleep in intracranial EEG recordings (Valderrama et al., 2012). These findings, together with the possible capability of 40Hz stimulation to reduce amyloid-beta burden, encourage the study of the effects of 40Hz tACS during slow-wave sleep. Stimulation at this brain state could generate a stronger response regarding the state dependency of tACS effects.

CONCLUSIONS

The ambition of this dissertation was to discuss new applicative approaches of Non-Invasive Brain Stimulation (NIBS) combined with neuroimaging techniques, aimed at improving safety and applicability of these methods. For this purpose, various implementation of neuroimaging techniques to gain more understanding about the mechanism of action of NIBS has been discussed. Moreover, we highlighted the potentiality of neuroimaging to personalized NIBS protocols through the experiments presented as independent landmark, although strictly connected to one another. In particular, we started from theoretical assumptions useful to understand and explain the meaning of the disclosed studies, we presented three different meta-analysis showing how neuroimaging techniques can be used to lead biophysical modeling and personalize NIBS protocols, and we concluded with a validation of this methodology through the results of two different experiments implemented on healthy and AD patients.

In Chapters 1 and 2 an overview of the current options for brain stimulation and neuroimaging methods has been provided, mostly focusing on the techniques used (tDCS, tACS and fMRI). The emphasis has been placed on the possibility to integrate NIBS and neuroimaging techniques through biophysical modeling. Computational electric field modeling has shown that the individual brain geometry can substantially impact the strength and distribution of the NIBS-induced electric field. Individual head model can be derived from anatomical MRI data and segmented in different tissue types with specific conductivity value. However, instead of calculating the NIBS-induced electric field given the coil/electrodes positions and the subject-specific head model, an inverse method might be useful to calculate the optimal target for the stimulation, thus fMRI data can be useful for accurate, orientation specific conductivity mapping, and to lead the targeting of NIBS protocols. This targeting approach based on fMRI data have matured over the last few years, given now the possibility to target not only a single brain area, but also an entire RSN, offering a more precise stimulation. In Chapter 3, three different examples on how meta-analytic studies can be used to drive the targeting of NIBS through biophysical modeling have been presented. In the Study 1 we identified stimuli-, presentation modality- and contrast- dependent brain activity maps for n-back processing in humans. While providing insight on working memory processing in healthy subjects, the study aimed at informing also future neuroimaging investigations. For this purpose, based on the topography of the functional network associated to the n-back task,

biophysical modeling of potential brain stimulation solutions has been suggested. By unifying and guiding targets for future brain stimulation protocols on healthy subjects, the present work also intended to reduce the observed variability in the outcome of cognitive enhancement studies, that have used bilateral dlPFC as target, without considering the network-stimulation approach. However, the stimulation target suggested for healthy subjects may not be effective in patients with WM deficits. Therefore, in Study 2 similarities and differences in brain activity within neurodevelopmental and psychiatric populations during the n-back task have been revealed. As in the previous study, the aim was to provide information about neural bases in psychiatric and ADHD patients while performing the n-back task, offering a comparison to activation in healthy controls. Moreover, this study also aimed at suggesting new potential targets for personalized tES interventions. The results encourage the fMRI-guided montage stimulation and hint at future studies applications to enhance WM in clinical cohorts, stressing the use of multichannel approach to stimulate other brain regions functionally more activated in these patients instead of the common dlPFC. Mapping the functional network associated with a specific cognitive function is not the only way to lead biophysical modeling. For example, several studies have recently suggested the use of rs-fcMRI maps as the perfect targets for stimulation. Consequently, the mixed results obtained in literature by stimulating through NIBS patients affected by Disorder of Consciousness (DoC) led us to investigate the neural correlates of this disease. Considering this as crucial landmark for the conceptualization and application of effective therapeutic interventions, we also investigated their functional connectivity and used the network mapping approach in order to better understand the topography of this disease. Network mapping performed on brain regions resulting from our metanalysis suggested a link between brain regions altered in DoC patients and two sets of brain networks representing internal mentation/cognitive control and sensory/salience processing, respectively. Based on biophysical modeling of network alterations, two different neuromodulation approaches have been presented. The results suggested that the most effective brain stimulation solution for patients with DoC involves stimulation of a network resembling the DMN and FPCN, promoting the value of network mapping and personalized montage optimization in future DoC studies. Overall, Chapter 3 has shed light into the utility and possibility of using brain networks as target for future neuromodulation studies in healthy and clinical cohorts. Since the human brain is organized in functional networks composed of multiple regions, brain stimulation solution allowing to modulate network activity are needed. Nowadays, the network stimulation approach has been investigated in few studies, confirming its success

from a physiological point of view on sensorimotor network (Fisher et al., 2017), but no one has demonstrated the effects at neuroimaging level. Therefore, considering the motor cortex as one of the most examined area in the brain, we decided to test the network specificity of multichannel stimulation approach in modulating the functional connectivity of the sensorimotor network. Consequently, in the Chapter 4 we proved that network stimulation approach, leveraging through multifocal tDCS solution informed by resting-state fMRI connectivity patterns of M1, can increase the precision of brain networks targeting in humans. In particular, we provided evidence of the efficacy of network-targeted electrical stimulation, showing an increase of the spontaneous activity of the targeted sensorimotor network, as well as a possible modulation of its interplay with other brain networks. The possibility of inducing functional effects on multiple network nodes at the same time while affecting both local and network-to-network connectivity dynamics might be relevant for the optimization of brain stimulation in clinical populations where alterations of network connectivity rather than single brain areas have been documented, as well as for cognitive enhancement purposes. Following the just mentioned aims, in the Chapter 5 we used the images-guided targeting approaches determining the feasibility and safety of ten 1-hour-long sessions of gamma induction via 40 Hz transcranial alternating current stimulation (tACS) in patients with mild to moderate Alzheimer's disease (AD). Based on the recent literature showing the decrease of amyloid-β plaques and the improvement of cognitive benefits after the induction of gamma frequency through sensory stimulation on animals (Iaccarino et al., 2016; Rajji, 2019, Adaikkan et al., 2019), multifocal tACS protocols have been optimized based on combined T1-weighted MRI and amyloid-beta (Aβ) PET images targeting regions with maximal Aß burden. Considering this was the first study addressing the effects of 40Hz tACS on individuals with AD during a 10-days long intervention, the results proved the safety and feasibility of this procedure. Moreover, a cumulative increase in gamma power throughout tACS intervention, spatially localized in the regions predicted by biophysical modeling, demonstrated the frequency and spatial specificity of this treatment. Additionally, the significant improvement in working memory processing revealed by a reduction of P200 latency normally associated with dementia-related cognitive decline, suggests personalized 40 Hz tACS gamma-induction as a potential therapeutic intervention for AD.

This dissertation has some limits and some questions that remain unanswered, every study we have presented has its specific limitations due to the research implementation. However, considering the general work, I can affirm that using information from neuroimaging to obtain

patient- or function- specific brain stimulation protocols, taking into account the network-to-network connectivity, might decrease the inter-individual variability and potentially also increase the overall clinical effectiveness.

In this thesis, neuroimaging techniques have been used to investigate the effect of NIBS but also to lead the targeting optimization by using biophysical modeling. However, in future studies also the stimulation intensity, timing and frequency might be subjects for personalization of tES protocols. The individual stimulation frequency, for example, might be derived from off-line EEG recording, whereas optimizing timing of the stimulation might require real time EEG or MEG recording during every stimulation procedure through a closed-loop system. Furthermore, simultaneous TMS-fMRI or TMS-EEG might help to optimized subject-specific stimulation intensity recording the effects of stimulation in terms of BOLD activity or TEPs. Nevertheless, future studies need to be performed to investigate if these patient's specific stimulation parameters improve the clinical efficacy. Moreover, considering the clinical cohort, it will be equally important to learn about the patient and the pathology that needs to be treated. Overall improvement of the clinical efficacy of brain stimulation techniques is an iterative process: more knowledge about stimulation techniques can improve the knowledge about pathology and vice versa. Besides, efficiency of brain stimulation might be increased by combining stimulation treatment with other types of treatment, such as for example psychotherapy or cognitive therapies.

REFERENCES

Achard, S., Salvador, R., Whitcher, B., Suckling, J., & Bullmore, E. (2006). A Resilient, Low-Frequency, Small-World Human Brain Functional Network with Highly Connected Association Cortical Hubs. *Journal of Neuroscience*, *26*(1), 63–72. https://doi.org/10.1523/JNEUROSCI.3874-05.2006

Ackermann, H. (2008). Cerebellar contributions to speech production and speech perception: Psycholinguistic and neurobiological perspectives. *Trends in Neurosciences*, *31*(6), 265–272. https://doi.org/10.1016/j.tins.2008.02.011

Adaikkan, C., Middleton, S. J., Marco, A., Pao, P.-C., Mathys, H., Kim, D. N.-W., Gao, F., Young, J. Z., Suk, H.-J., Boyden, E. S., McHugh, T. J., & Tsai, L.-H. (2019). Gamma Entrainment Binds Higher-Order Brain Regions and Offers Neuroprotection. *Neuron*, *102*(5), 929-943.e8. https://doi.org/10.1016/j.neuron.2019.04.011

Adaikkan, C., & Tsai, L.-H. (2020a). Gamma Entrainment: Impact on Neurocircuits, Glia, and Therapeutic Opportunities. *Trends in Neurosciences*, *43*(1), 24–41. https://doi.org/10.1016/j.tins.2019.11.001

Adaikkan, C., & Tsai, L.-H. (2020b). Gamma Entrainment: Impact on Neurocircuits, Glia, and Therapeutic Opportunities. *Trends in Neurosciences*, *43*(1), 24–41. https://doi.org/10.1016/j.tins.2019.11.001

Adler, C. M., Holland, S. K., Schmithorst, V., Tuchfarber, M. J., & Strakowski, S. M. (2004). Changes in neuronal activation in patients with bipolar disorder during performance of a working memory task. *Bipolar Disorders*, *6*(6), 540–549. https://doi.org/10.1111/j.1399-5618.2004.00117.x

Alekseichuk, I., Falchier, A. Y., Linn, G., Xu, T., Milham, M. P., Schroeder, C. E., & Opitz, A. (2019). Electric field dynamics in the brain during multi-electrode transcranial electric stimulation. *Nature Communications*, *10*(1), 2573. https://doi.org/10.1038/s41467-019-10581-7

Alekseichuk, I., Turi, Z., Amador de Lara, G., Antal, A., & Paulus, W. (2016). Spatial Working Memory in Humans Depends on Theta and High Gamma Synchronization in the Prefrontal Cortex. *Current Biology*, *26*(12), 1513–1521. https://doi.org/10.1016/j.cub.2016.04.035

Amadi, U., Ilie, A., Johansen-Berg, H., & Stagg, C. J. (2014). Polarity-specific effects of motor transcranial direct current stimulation on fMRI resting state networks. *NeuroImage*, *88*, 155–161. https://doi.org/10.1016/j.neuroimage.2013.11.037

Andrews-Hanna, J. R., Smallwood, J., & Spreng, R. N. (2014). The default network and self-generated thought: Component processes, dynamic control, and clinical relevance. *Annals of the New York Academy of Sciences*, *1316*(1), 29–52. https://doi.org/10.1111/nyas.12360

Angelakis, E., Liouta, E., Andreadis, N., Korfias, S., Ktonas, P., Stranjalis, G., & Sakas, D. E. (2014). Transcranial Direct Current Stimulation Effects in Disorders of Consciousness. *Archives of Physical Medicine and Rehabilitation*, *95*(2), 283–289. https://doi.org/10.1016/j.apmr.2013.09.002

Antal, A., Alekseichuk, I., Bikson, M., Brockmöller, J., Brunoni, A. R., Chen, R., Cohen, L. G., Dowthwaite, G., Ellrich, J., Flöel, A., Fregni, F., George, M. S., Hamilton, R., Haueisen, J., Herrmann, C. S., Hummel, F. C., Lefaucheur, J. P., Liebetanz, D., Loo, C. K., … Paulus, W. (2017). Low intensity transcranial electric stimulation: Safety, ethical, legal regulatory and application guidelines. *Clinical Neurophysiology: Official Journal of the International Federation of Clinical Neurophysiology*, *128*(9), 1774–1809. https://doi.org/10.1016/j.clinph.2017.06.001

Antal, Andrea, & Paulus, W. (2013). Transcranial alternating current stimulation (tACS). *Frontiers in Human Neuroscience*, *7*. https://doi.org/10.3389/fnhum.2013.00317

Antal, Andrea, Polania, R., Schmidt-Samoa, C., Dechent, P., & Paulus, W. (2011). Transcranial direct current stimulation over the primary motor cortex during fMRI. *NeuroImage*, *55*(2), 590–596. https://doi.org/10.1016/j.neuroimage.2010.11.085

Antal, Andrea, Terney, D., Poreisz, C., & Paulus, W. (2007). Towards unravelling task-related modulations of neuroplastic changes induced in the human motor cortex. *European Journal of Neuroscience*, *26*(9), 2687–2691. https://doi.org/10.1111/j.1460-9568.2007.05896.x

Argyelan, M., Ikuta, T., DeRosse, P., Braga, R. J., Burdick, K. E., John, M., Kingsley, P. B., Malhotra, A. K., & Szeszko, P. R. (2014). Resting-State fMRI Connectivity Impairment in Schizophrenia and Bipolar Disorder. *Schizophrenia Bulletin*, *40*(1), 100–110. https://doi.org/10.1093/schbul/sbt092

Arnone, D., McIntosh, A. M., Ebmeier, K. P., Munafò, M. R., & Anderson, I. M. (2012). Magnetic resonance imaging studies in unipolar depression: Systematic review and meta-regression analyses. *European Neuropsychopharmacology*, *22*(1), 1–16. https://doi.org/10.1016/j.euroneuro.2011.05.003

Ashburner, J. (2007). A fast diffeomorphic image registration algorithm. *NeuroImage*, *38*(1), 95–113. https://doi.org/10.1016/j.neuroimage.2007.07.007

Awh, E., Jonides, J., Smith, E. E., Schumacher, E. H., Koeppe, R. A., & Katz, S. (1996). Dissociation of Storage and Rehearsal in Verbal Working Memory: Evidence from Positron Emission Tomography. *Psychological Science*, *7*(1), 25–31.

Aydin-Abidin, S., Trippe, J., Funke, K., Eysel, U. T., & Benali, A. (2008). High- and low-frequency repetitive transcranial magnetic stimulation differentially activates c-Fos and zif268 protein expression in the rat brain. *Experimental Brain Research*, *188*(2), 249–261. https://doi.org/10.1007/s00221-008-1356-2

Bachtiar, V., Near, J., Johansen-Berg, H., & Stagg, C. J. (2015, September 18). *Modulation of GABA and resting state functional connectivity by transcranial direct current stimulation*. ELife; eLife Sciences Publications Limited. https://doi.org/10.7554/eLife.08789

Baddeley, A. (1992). Working memory. *Science*, *255*(5044), 556–559. https://doi.org/10.1126/science.1736359

Baddeley, A. D., Bressi, S., Della Sala, S., Logie, R., & Spinnler, H. (1991a). The decline of working memory in Alzheimer's disease. A longitudinal study. *Brain: A Journal of Neurology*, *114 (Pt 6)*, 2521–2542. https://doi.org/10.1093/brain/114.6.2521

Baddeley, A. D., Bressi, S., Della Sala, S., Logie, R., & Spinnler, H. (1991b). THE DECLINE OF WORKING MEMORY IN ALZHEIMER'S DISEASEA LONGITUDINAL STUDY. *Brain*, *114*(6), 2521–2542. https://doi.org/10.1093/brain/114.6.2521

Baddeley, Alan, Della Sala, S., Robbins, T. W., & Baddeley, A. (1996). Working Memory and Executive Control [and Discussion]. *Philosophical Transactions: Biological Sciences*, *351*(1346), 1397–1404.

Baeken, C., Remue, J., Vanderhasselt, M.-A., Brunoni, A. R., De Witte, S., Duprat, R., Koster, E. H. W., De Raedt, R., & Wu, G.-R. (2017). Increased left prefrontal brain perfusion after MRI compatible tDCS attenuates momentary ruminative self-referential thoughts. *Brain Stimulation*, *10*(6), 1088–1095. https://doi.org/10.1016/j.brs.2017.09.005

Bagherzadeh, Y., Khorrami, A., Zarrindast, M. R., Shariat, S. V., & Pantazis, D. (2016). Repetitive transcranial magnetic stimulation of the dorsolateral prefrontal cortex enhances working memory. *Experimental Brain Research*, *234*(7), 1807–1818. https://doi.org/10.1007/s00221-016-4580-1

Baillet, S. (2017). Magnetoencephalography for brain electrophysiology and imaging. *Nature Neuroscience*, *20*(3), 327–339. https://doi.org/10.1038/nn.4504

Baranski, M. F. S., & Was, C. A. (2018). A More Rigorous Examination of the Effects of Mindfulness Meditation on Working Memory Capacity. *Journal of Cognitive Enhancement*, *2*(3), 225–239. https://doi.org/10.1007/s41465-018-0064-5

Barch, D. M., Sheline, Y. I., Csernansky, J. G., & Snyder, A. Z. (2003). Working memory and prefrontal cortex dysfunction: Specificity to schizophrenia compared with major depression. *Biological Psychiatry*, *53*(5), 376–384.

Barker, A. T. (1991). An introduction to the basic principles of magnetic nerve stimulation. *Journal of Clinical Neurophysiology : Official Publication of the American Electroencephalographic Society*, *8*(1), 26–37. https://doi.org/10.1097/00004691-199101000-00005

Barker, A. T., Jalinous, R., & Freeston, I. L. (1985). Non-invasive magnetic stimulation of human motor cortex. *The Lancet*, *325(8437)*, 1106–1107.

Battleday, R. M., Muller, T., Clayton, M. S., & Cohen Kadosh, R. (2014). Mapping the Mechanisms of Transcranial Alternating Current Stimulation: A Pathway from Network Effects to Cognition. *Frontiers in Psychiatry*, *5*. https://doi.org/10.3389/fpsyt.2014.00162

Baxter, L. R., Schwartz, J. M., Phelps, M. E., Mazziotta, J. C., Guze, B. H., Selin, C. E., Gerner, R. H., & Sumida, R. M. (1989). Reduction of Prefrontal Cortex Glucose Metabolism Common to Three Types of Depression. *Archives of General Psychiatry*, *46*(3), 243–250. https://doi.org/10.1001/archpsyc.1989.01810030049007

Bayerl, M., Dielentheis, T. F., Vucurevic, G., Gesierich, T., Vogel, F., Fehr, C., Stoeter, P., Huss, M., & Konrad, A. (2010). Disturbed brain activation during a working memory task in drug-naive adult patients with ADHD. *NeuroReport*, *21*(6), 442–446. https://doi.org/10.1097/WNR.0b013e328338b9be

Beckmann, C.F., & Smith, S. M. (2005a). Tensorial extensions of independent component analysis for multisubject FMRI analysis. *NeuroImage*, *25*(1), 294–311. https://doi.org/10.1016/j.neuroimage.2004.10.043

Beckmann, C.F., & Smith, S. M. (2005b). Tensorial extensions of independent component analysis for multisubject FMRI analysis. *NeuroImage*, *25*(1), 294–311. https://doi.org/10.1016/j.neuroimage.2004.10.043

Beckmann, Christian F, DeLuca, M., Devlin, J. T., & Smith, S. M. (2005). Investigations into resting-state connectivity using independent component analysis. *Philosophical Transactions of the Royal Society B: Biological Sciences*, *360*(1457), 1001–1013. https://doi.org/10.1098/rstb.2005.1634

Behzadi, Y., Restom, K., Liau, J., & Liu, T. T. (2007). A component based noise correction method (CompCor) for BOLD and perfusion based fMRI. *NeuroImage*, *37*(1), 90–101. https://doi.org/10.1016/j.neuroimage.2007.04.042

Bench, C. J., Friston, K. J., Brown, R. G., Scott, L. C., Frackowiak, R. S., & Dolan, R. J. (1992). The anatomy of melancholia—Focal abnormalities of cerebral blood flow in major depression. *Psychological Medicine*, *22*(3), 607–615. https://doi.org/10.1017/s003329170003806x

Berlingeri, M., Magnani, F. G., Salvato, G., Rosanova, M., & Bottini, G. (2019). Neuroimaging Studies on Disorders of Consciousness: A Meta-Analytic Evaluation. *Journal of Clinical Medicine*, *8*(4), 516. https://doi.org/10.3390/jcm8040516

Berman, K. F., Doran, A. R., Pickar, D., & Weinberger, D. R. (1993). Is the Mechanism of Prefrontal Hypofunction in Depression the Same as in Schizophrenia?: Regional Cerebral Blood Flow During Cognitive Activation. *The British Journal of Psychiatry*, *162*(2), 183–192. https://doi.org/10.1192/bjp.162.2.183

Berryhill, M. E., & Jones, K. T. (2012). TDCS selectively improves working memory in older adults with more education. *Neuroscience Letters*, *521*(2), 148–151. https://doi.org/10.1016/j.neulet.2012.05.074

Bestmann, S., de Berker, A. O., & Bonaiuto, J. (2015). Understanding the behavioural consequences of noninvasive brain stimulation. *Trends in Cognitive Sciences*, *19*(1), 13–20. https://doi.org/10.1016/j.tics.2014.10.003

Bikson, M., Datta, A., Rahman, A., & Scaturro, J. (2010). Electrode montages for tDCS and weak transcranial electrical stimulation: Role of "return" electrode's position and size. *Clin. Neurophysiol*, *121*(12), 1976–1978. https://doi.org/10.1016/j.clinph.2010.05.020

Biswal, B. B., Mennes, M., Zuo, X.-N., Gohel, S., Kelly, C., Smith, S. M., Beckmann, C. F., Adelstein, J. S., Buckner, R. L., Colcombe, S., Dogonowski, A.-M., Ernst, M., Fair, D., Hampson, M., Hoptman, M. J., Hyde, J. S., Kiviniemi, V. J., Kötter, R., Li, S.-J., … Milham, M. P. (2010). Toward discovery science of human brain function. *Proceedings of the National Academy of Sciences*, *107*(10), 4734–4739. https://doi.org/10.1073/pnas.0911855107

Biswal, B., Yetkin, F. Z., Haughton, V. M., & Hyde, J. S. (1995). Functional connectivity in the motor cortex of resting human brain using echo-planar mri. *Magnetic Resonance in Medicine*, *34*(4), 537–541. https://doi.org/10.1002/mrm.1910340409

Bloom, J. S., & Hynd, G. W. (2005). The Role of the Corpus Callosum in Interhemispheric Transfer of Information: Excitation or Inhibition? *Neuropsychology Review*, *15*(2), 59–71. https://doi.org/10.1007/s11065-005-6252-y

Bodart, O., Gosseries, O., Wannez, S., Thibaut, A., Annen, J., Boly, M., Rosanova, M., Casali, A. G., Casarotto, S., Tononi, G., Massimini, M., & Laureys, S. (2017). Measures of metabolism and complexity in the brain of patients with disorders of consciousness. *NeuroImage: Clinical*, *14*, 354–362. https://doi.org/10.1016/j.nicl.2017.02.002

Boly, M., Tshibanda, L., Vanhaudenhuyse, A., Noirhomme, Q., Schnakers, C., Ledoux, D., Boveroux, P., Garweg, C., Lambermont, B., Phillips, C., Luxen, A., Moonen, G., Bassetti, C., Maquet, P., & Laureys, S. (2009). Functional connectivity in the default network during resting state is preserved in a vegetative but not in a brain dead patient. *Human Brain Mapping*, *30*(8), 2393–2400. https://doi.org/10.1002/hbm.20672

Bora, E., Fornito, A., Pantelis, C., & Yücel, M. (2012). Gray matter abnormalities in Major Depressive Disorder: A meta-analysis of voxel based morphometry studies. *Journal of Affective Disorders*, *138*(1), 9–18. https://doi.org/10.1016/j.jad.2011.03.049

Boros, K., Poreisz, C., Münchau, A., Paulus, W., & Nitsche, M. A. (2008). Premotor transcranial direct current stimulation (tDCS) affects primary motor excitability in humans. *European Journal of Neuroscience*, *27*(5), 1292–1300. https://doi.org/10.1111/j.1460-9568.2008.06090.x

Botvinick, M. M., Carter, C. S., Braver, T. S., Carter, C. S., & Cohen, J. D. (2001). Conflict monitoring and cognitive control. *Psychological Review*, *108*(3), 624–652. https://doi.org/10.1037//0033-295X.108.3.624

Botvinick, M. M., Cohen, J. D., & Carter, C. S. (2004). Conflict monitoring and anterior cingulate cortex: An update. *Trends in Cognitive Sciences*, *8*(12), 539–546. https://doi.org/10.1016/j.tics.2004.10.003

Bourdillon, P., Hermann, B., Sitt, J. D., & Naccache, L. (2019). Electromagnetic Brain Stimulation in Patients With Disorders of Consciousness. *Frontiers in Neuroscience*, *13*, 223. https://doi.org/10.3389/fnins.2019.00223

Bouyer, J. J., Montaron, M. F., & Rougeul, A. (1981). Fast fronto-parietal rhythms during combined focused attentive behaviour and immobility in cat: Cortical and thalamic localizations. *Electroencephalography and Clinical Neurophysiology*, *51*(3), 244–252. https://doi.org/10.1016/0013-4694(81)90138-3

Brem, A.-K., Almquist, J. N.-F., Mansfield, K., Plessow, F., Sella, F., Santarnecchi, E., Orhan, U., McKanna, J., Pavel, M., Mathan, S., Yeung, N., Pascual-Leone, A., Kadosh, R. C., & authors, H. S. T. (2018). Modulating fluid intelligence performance through combined cognitive training and brain stimulation. *Neuropsychologia*, *118*(Pt A), 107–114. https://doi.org/10.1016/j.neuropsychologia.2018.04.008

Brem, A.-K., Almquist, J. N.-F., Mansfield, K., Plessow, F., Sella, F., Santarnecchi, E., Orhan, U., McKanna, J., Pavel, M., Mathan, S., Yeung, N., Pascual-Leone, A., Kadosh, R. C., & Honeywell SHARP Team authors. (2018). Modulating fluid intelligence performance through combined cognitive training and brain stimulation. *Neuropsychologia*, *118*(Pt A), 107–114. https://doi.org/10.1016/j.neuropsychologia.2018.04.008

Britz, J., Van De Ville, D., & Michel, C. M. (2010). BOLD correlates of EEG topography reveal rapid resting-state network dynamics. *NeuroImage*, *52*(4), 1162–1170. https://doi.org/10.1016/j.neuroimage.2010.02.052

Bruno, Marie-Aurélie, Majerus, S., Boly, M., Vanhaudenhuyse, A., Schnakers, C., Gosseries, O., Boveroux, P., Kirsch, M., Demertzi, A., Bernard, C., Hustinx, R., Moonen, G., & Laureys, S. (2012). Functional neuroanatomy underlying the clinical subcategorization of minimally conscious state patients. *Journal of Neurology*, *259*(6), 1087–1098. https://doi.org/10.1007/s00415-011-6303-7

Bruno, Marie-Aurelie, Vanhaudenhuyse, A., Schnakers, C., Boly, M., Gosseries, O., Demertzi, A., Majerus, S., Moonen, G., Hustinx, R., & Laureys, S. (2010). *Visual fixation in the vegetative state: An observational case series PET study*. https://www.ncbi.nlm.nih.gov/pmc/articles/PMC2895583/

Brunoni, A. R., Boggio, P. S., De Raedt, R., Benseñor, I. M., Lotufo, P. A., Namur, V., Valiengo, L. C. L., & Vanderhasselt, M. A. (2014). Cognitive control therapy and transcranial direct current stimulation for depression: A randomized, double-blinded, controlled trial. *Journal of Affective Disorders*, *162*, 43–49. https://doi.org/10.1016/j.jad.2014.03.026

Brunoni, André Russowsky, & Vanderhasselt, M.-A. (2014a). Working memory improvement with non-invasive brain stimulation of the dorsolateral prefrontal cortex: A systematic review and meta-analysis. *Brain and Cognition*, *86*, 1–9. https://doi.org/10.1016/j.bandc.2014.01.008

Brunoni, André Russowsky, & Vanderhasselt, M.-A. (2014b). Working memory improvement with non-invasive brain stimulation of the dorsolateral prefrontal cortex: A systematic review and meta-analysis. *Brain and Cognition*, *86*, 1–9. https://doi.org/10.1016/j.bandc.2014.01.008

Buccino, G., Binkofski, F., Fink, G. R., Fadiga, L., Fogassi, L., Gallese, V., Seitz, R. J., Zilles, K., Rizzolatti, G., & Freund, H. J. (2001). Action observation activates premotor and parietal areas in a somatotopic manner: An fMRI study. *The European Journal of Neuroscience*, *13*(2), 400–404.

Buckner, R. L., & DiNicola, L. M. (2019). The brain's default network: Updated anatomy, physiology and evolving insights. *Nature Reviews Neuroscience*, *20*(10), 593–608. https://doi.org/10.1038/s41583-019-0212-7

Buckner, R. L., Krienen, F. M., Castellanos, A., Diaz, J. C., & Yeo, B. T. T. (2011). The organization of the human cerebellum estimated by intrinsic functional connectivity. *Journal of Neurophysiology*, *106*(5), 2322–2345. https://doi.org/10.1152/jn.00339.2011

Buckner, R. L., & Vincent, J. L. (2007). Unrest at rest: Default activity and spontaneous network correlations. *NeuroImage*, *37*(4), 1091–1096. https://doi.org/10.1016/j.neuroimage.2007.01.010

Burns, S. P., Xing, D., & Shapley, R. M. (2011). Is Gamma-Band Activity in the Local Field Potential of V1 Cortex a "Clock" or Filtered Noise? *Journal of Neuroscience*, *31*(26), 9658–9664. https://doi.org/10.1523/JNEUROSCI.0660-11.2011

Buzsáki, G. (2015). Hippocampal sharp wave-ripple: A cognitive biomarker for episodic memory and planning. *Hippocampus*, *25*(10), 1073–1188. https://doi.org/10.1002/hipo.22488

Buzsáki, G., & Draguhn, A. (2004). Neuronal Oscillations in Cortical Networks. *Science*, *304*(5679), 1926–1929. https://doi.org/10.1126/science.1099745

Cabeza, R., & Nyberg, L. (2000). Imaging Cognition II: An Empirical Review of 275 PET and fMRI Studies. *Journal of Cognitive Neuroscience*, *12*(1), 1–47. https://doi.org/10.1162/08989290051137585

Calhoun, V. D., Adali, T., Pearlson, G. D., & Pekar, J. J. (2001). A method for making group inferences from functional MRI data using independent component analysis. *Human Brain Mapping*, *14*(3), 140–151. https://doi.org/10.1002/hbm.1048

Cardin, J. A., Carlén, M., Meletis, K., Knoblich, U., Zhang, F., Deisseroth, K., Tsai, L.-H., & Moore, C. I. (2009a). Driving fast-spiking cells induces gamma rhythm and controls sensory responses. *Nature*, *459*(7247), 663–667. https://doi.org/10.1038/nature08002

Cardin, J. A., Carlén, M., Meletis, K., Knoblich, U., Zhang, F., Deisseroth, K., Tsai, L.-H., & Moore, C. I. (2009b). Driving fast-spiking cells induces gamma rhythm and controls sensory responses. *Nature*, *459*(7247), 663–667. https://doi.org/10.1038/nature08002

Carr, M. F., Jadhav, S. P., & Frank, L. M. (2011). Hippocampal replay in the awake state: A potential substrate for memory consolidation and retrieval. *Nature Neuroscience*, *14*(2), 147–153. https://doi.org/10.1038/nn.2732

Carr, M. F., Karlsson, M. P., & Frank, L. M. (2012). Transient Slow Gamma Synchrony Underlies Hippocampal Memory Replay. *Neuron*, *75*(4), 700–713. https://doi.org/10.1016/j.neuron.2012.06.014

Casarotto, S., Comanducci, A., Rosanova, M., Sarasso, S., Fecchio, M., Napolitani, M., Pigorini, A., G Casali, A., Trimarchi, P. D., Boly, M., Gosseries, O., Bodart, O., Curto, F., Landi, C., Mariotti, M., Devalle, G., Laureys, S., Tononi, G., & Massimini, M. (2016). Stratification of unresponsive patients by an independently validated index of brain complexity. *Annals of Neurology*, *80*(5), 718–729. https://doi.org/10.1002/ana.24779

Castaigne, P., Lhermitte, F., Buge, A., Escourolle, R., Hauw, J. J., & Lyon-Caen, O. (1981). Paramedian thalamic and midbrain infarcts: Clinical and neuropathological study. *Annals of Neurology*, *10*(2), 127–148. https://doi.org/10.1002/ana.410100204

Castellano, M., Ibanez-Soria, D., Kroupi, E., Acedo, J., Campolo, M., Martinez, X., Soria-Frisch, A., Valls-Sole, J., Verma, A., & Ruffini, G. (2017). Occipital tACS bursts during a visual task impact ongoing neural oscillation power, coherence and LZW complexity. *BioRxiv*, 198788. https://doi.org/10.1101/198788

Cavanna, A. E., & Trimble, M. R. (2006). The precuneus: A review of its functional anatomy and behavioural correlates. *Brain: A Journal of Neurology*, *129*(Pt 3), 564–583. https://doi.org/10.1093/brain/awl004

Chaieb, L., Antal, A., & Paulus, W. (2011). Transcranial alternating current stimulation in the low kHz range increases motor cortex excitability. *Restorative Neurology and Neuroscience*, *29*(3), 167–175. https://doi.org/10.3233/RNN-2011-0589

Chaieb, L., Antal, A., & Paulus, W. (2015). Transcranial random noise stimulation-induced plasticity is NMDA-receptor independent but sodium-channel blocker and benzodiazepines sensitive. *Frontiers in Neuroscience*, *9*. https://doi.org/10.3389/fnins.2015.00125

Chan, H.-N., Alonzo, A., Martin, D. M., Player, M., Mitchell, P. B., Sachdev, P., & Loo, C. K. (2012). Treatment of major depressive disorder by transcranial random noise stimulation: Case report of a novel treatment. *Biological Psychiatry*, *72*(4), e9–e10. https://doi.org/10.1016/j.biopsych.2012.02.009

Chang, C., Liu, Z., Chen, M. C., Liu, X., & Duyn, J. H. (2013). EEG correlates of time-varying BOLD functional connectivity. *NeuroImage*, *72*, 227–236. https://doi.org/10.1016/j.neuroimage.2013.01.049

Chao, L. L., & Martin, A. (2000). Representation of manipulable man-made objects in the dorsal stream. *NeuroImage*, *12*(4), 478–484. https://doi.org/10.1006/nimg.2000.0635

Chen, A. C. N., Feng, W., Zhao, H., Yin, Y., & Wang, P. (2008). EEG default mode network in the human brain: Spectral regional field powers. *NeuroImage*, *41*(2), 561–574. https://doi.org/10.1016/j.neuroimage.2007.12.064

Chen, C.-M. A., Stanford, A. D., Mao, X., Abi-Dargham, A., Shungu, D. C., Lisanby, S. H., Schroeder, C. E., & Kegeles, L. S. (2014). GABA level, gamma oscillation, and working memory performance in schizophrenia. *NeuroImage: Clinical*, *4*, 531–539. https://doi.org/10.1016/j.nicl.2014.03.007

Cheyne, D. O., & Ferrari, P. (2013). MEG studies of motor cortex gamma oscillations: Evidence for a gamma "fingerprint" in the brain? *Frontiers in Human Neuroscience*, *7*. https://doi.org/10.3389/fnhum.2013.00575

Chou, T.-L., Booth, J. R., Burman, D. D., Bitan, T., Bigio, J. D., Lu, D., & Cone, N. E. (2006). Developmental changes in the neural correlates of semantic processing. *NeuroImage*, *29*(4), 1141–1149. https://doi.org/10.1016/j.neuroimage.2005.09.064

Cieslik, E. C., Zilles, K., Kurth, F., & Eickhoff, S. B. (2010). Dissociating bottom-up and top-down processes in a manual stimulus-response compatibility task. *Journal of Neurophysiology*, *104*(3), 1472–1483. https://doi.org/10.1152/jn.00261.2010

Cincotta, M., Giovannelli, F., Chiaramonti, R., Bianco, G., Godone, M., Battista, D., Cardinali, C., Borgheresi, A., Sighinolfi, A., D'Avanzo, A. M., Breschi, M., Dine, Y., Lino, M., Zaccara, G., Viggiano, M. P., & Rossi, S. (2015). No effects of 20 Hz-rTMS of the primary motor cortex in vegetative state: A randomised, sham-controlled study. *Cortex*, *71*, 368–376. https://doi.org/10.1016/j.cortex.2015.07.027

Cocchini, G., Logie, R. H., Sala, S. D., MacPherson, S. E., & Baddeley, A. D. (2002). Concurrent performance of two memory tasks: Evidence for domain-specific working memory systems. *Memory & Cognition*, *30*(7), 1086–1095. https://doi.org/10.3758/BF03194326

Cohen, J. D., Perlstein, W. M., Braver, T. S., Nystrom, L. E., Noll, D. C., Jonides, J., & Smith, E. E. (1997). Temporal dynamics of brain activation during a working memory task. *Nature*, *386*(6625), 604–608. https://doi.org/10.1038/386604a0

Cohen, M. X. (2017). Where Does EEG Come From and What Does It Mean? *Trends in Neurosciences*, *40*(4), 208–218. https://doi.org/10.1016/j.tins.2017.02.004

Cohen, T. E., Kaplan, S. W., Kandel, E. R., & Hawkins, R. D. (1997). A Simplified Preparation for Relating Cellular Events to Behavior: Mechanisms Contributing to Habituation, Dishabituation, and Sensitization of the Aplysia Gill-Withdrawal Reflex. *Journal of Neuroscience*, *17*(8), 2886–2899. https://doi.org/10.1523/JNEUROSCI.17-08-02886.1997

Colgin, L. L. (2016). Rhythms of the hippocampal network. *Nature Reviews Neuroscience*, *17*(4), 239–249. https://doi.org/10.1038/nrn.2016.21

Cooke, S. F., & Bliss, T. V. P. (2006). Plasticity in the human central nervous system. *Brain*, *129*(7), 1659–1673. https://doi.org/10.1093/brain/awl082

Corbetta, M., Shulman, G. L., Miezin, F. M., & Petersen, S. E. (1995). Superior parietal cortex activation during spatial attention shifts and visual feature conjunction. *Science (New York, N.Y.)*, *270*(5237), 802–805.

Corbetta, Maurizio. (1998). Frontoparietal cortical networks for directing attention and the eye to visual locations: Identical, independent, or overlapping neural systems? *Proceedings of the National Academy of Sciences*, *95*(3), 831–838. https://doi.org/10.1073/pnas.95.3.831

Corbetta, Maurizio, Kincade, J. M., & Shulman, G. L. (2002). Neural Systems for Visual Orienting and Their Relationships to Spatial Working Memory. *Journal of Cognitive Neuroscience*, *14*(3), 508–523. https://doi.org/10.1162/089892902317362029

Corbetta, Maurizio, Patel, G., & Shulman, G. L. (2008). The Reorienting System of the Human Brain: From Environment to Theory of Mind. *Neuron*, *58*(3), 306–324. https://doi.org/10.1016/j.neuron.2008.04.017

Corbetta, Maurizio, & Shulman, G. L. (2002a). Control of goal-directed and stimulus-driven attention in the brain. *Nature Reviews Neuroscience*, *3*(3), 201–215. https://doi.org/10.1038/nrn755

Corbetta, Maurizio, & Shulman, G. L. (2002b). Control of goal-directed and stimulus-driven attention in the brain. *Nature Reviews. Neuroscience*, *3*(3), 201–215. https://doi.org/10.1038/nrn755

Cordes, D., Haughton, V. M., Arfanakis, K., Wendt, G. J., Turski, P. A., Moritz, C. H., Quigley, M. A., & Meyerand, M. E. (2000). Mapping Functionally Related Regions of Brain with Functional Connectivity MR Imaging. *American Journal of Neuroradiology*, *21*(9), 1636–1644.

Craft, S., Newcomer, J., Kanne, S., Dagogo-Jack, S., Cryer, P., Sheline, Y., Luby, J., Dagogo-Jack, A., & Alderson, A. (1996). Memory improvement following induced hyperinsulinemia in Alzheimer's disease. *Neurobiology of Aging*, *17*(1), 123–130. https://doi.org/10.1016/0197-4580(95)02002-0

Cremaschi, L., Penzo, B., Palazzo, M., Dobrea, C., Cristoffanini, M., Dell'Osso, B., & Altamura, A. C. (2013). Assessing Working Memory via N-Back Task in Euthymic Bipolar I Disorder Patients: A Review of Functional Magnetic Resonance Imaging Studies. *Neuropsychobiology*, *68*(2), 63–70. https://doi.org/10.1159/000352011

Crone, J. S., Soddu, A., Höller, Y., Vanhaudenhuyse, A., Schurz, M., Bergmann, J., Schmid, E., Trinka, E., Laureys, S., & Kronbichler, M. (2013). Altered network properties of the fronto-parietal network and the thalamus in impaired consciousness. *NeuroImage : Clinical*, *4*, 240–248. https://doi.org/10.1016/j.nicl.2013.12.005

Crossley, N. A., Mechelli, A., Fusar-Poli, P., Broome, M. R., Matthiasson, P., Johns, L. C., Bramon, E., Valmaggia, L., Williams, S. C. R., & McGuire, P. K. (2009). Superior temporal lobe dysfunction and frontotemporal dysconnectivity in subjects at risk of psychosis and in first-episode psychosis. *Human Brain Mapping*, *30*(12), 4129–4137. https://doi.org/10.1002/hbm.20834

Crottaz-Herbette, S., & Menon, V. (2006). Where and When the Anterior Cingulate Cortex Modulates Attentional Response: Combined fMRI and ERP Evidence. *Journal of Cognitive Neuroscience*, *18*(5), 766–780. https://doi.org/10.1162/jocn.2006.18.5.766

Dagan, M., Herman, T., Harrison, R., Zhou, J., Giladi, N., Ruffini, G., Manor, B., & Hausdorff, J. M. (2018a). Multitarget transcranial direct current stimulation for freezing of gait in Parkinson's disease. *Movement Disorders: Official Journal of the Movement Disorder Society*, *33*(4), 642–646. https://doi.org/10.1002/mds.27300

Dagan, M., Herman, T., Harrison, R., Zhou, J., Giladi, N., Ruffini, G., Manor, B., & Hausdorff, J. M. (2018b). Multitarget transcranial direct current stimulation for freezing of gait in Parkinson's disease. *Movement Disorders: Official Journal of the Movement Disorder Society*, *33*(4), 642–646. https://doi.org/10.1002/mds.27300

D'Agata, F., Peila, E., Cicerale, A., Caglio, M. M., Caroppo, P., Vighetti, S., Piedimonte, A., Minuto, A., Campagnoli, M., Salatino, A., Molo, M. T., Mortara, P., Pinessi, L., & Massazza, G. (2016). Cognitive and Neurophysiological Effects of Non-invasive Brain Stimulation in Stroke Patients after Motor Rehabilitation. *Frontiers in Behavioral Neuroscience*, *10*, 135. https://doi.org/10.3389/fnbeh.2016.00135

Damoiseaux, J. S., Rombouts, S. a. R. B., Barkhof, F., Scheltens, P., Stam, C. J., Smith, S. M., & Beckmann, C. F. (2006a). Consistent resting-state networks across healthy subjects. *Proceedings of the National Academy of Sciences*, *103*(37), 13848–13853. https://doi.org/10.1073/pnas.0601417103

Damoiseaux, J. S., Rombouts, S. a. R. B., Barkhof, F., Scheltens, P., Stam, C. J., Smith, S. M., & Beckmann, C. F. (2006b). Consistent resting-state networks across healthy subjects. *Proceedings of the National Academy of Sciences*, *103*(37), 13848–13853. https://doi.org/10.1073/pnas.0601417103

Daskalakis, Z. J., Farzan, F., Radhu, N., & Fitzgerald, P. B. (2012). Combined transcranial magnetic stimulation and electroencephalography: Its past, present and future. *Brain Research*, *1463*, 93–107. https://doi.org/10.1016/j.brainres.2012.04.045

De Luca, M., Smith, S., De Stefano, N., Federico, A., & Matthews, P. M. (2005). Blood oxygenation level dependent contrast resting state networks are relevant to functional activity in the neocortical sensorimotor system. *Experimental Brain Research*, *167*(4), 587–594. https://doi.org/10.1007/s00221-005-0059-1

Dell'Osso, B., & Di Lorenzo, G. (Eds.). (2020). *Non Invasive Brain Stimulation in Psychiatry and Clinical Neurosciences*. Springer International Publishing. https://doi.org/10.1007/978-3-030-43356-7

Delorme, A., & Makeig, S. (2004). EEGLAB: An open source toolbox for analysis of single-trial EEG dynamics including independent component analysis. *Journal of Neuroscience Methods*, *134*(1), 9–21. https://doi.org/10.1016/j.jneumeth.2003.10.009

Delvecchio, G., Fossati, P., Boyer, P., Brambilla, P., Falkai, P., Gruber, O., Hietala, J., Lawrie, S. M., Martinot, J.-L., McIntosh, A. M., Meisenzahl, E., & Frangou, S. (2012). Common and distinct neural correlates of emotional processing in Bipolar Disorder and Major Depressive Disorder: A voxel-based meta-analysis of functional magnetic resonance imaging studies. *European Neuropsychopharmacology*, *22*(2), 100–113. https://doi.org/10.1016/j.euroneuro.2011.07.003

Demertzi, A., Gómez, F., Crone, J. S., Vanhaudenhuyse, A., Tshibanda, L., Noirhomme, Q., Thonnard, M., Charland-Verville, V., Kirsch, M., Laureys, S., & Soddu, A. (2014). Multiple fMRI system-level baseline connectivity is disrupted in patients with consciousness alterations. *Cortex*, *52*, 35–46. https://doi.org/10.1016/j.cortex.2013.11.005

Démonet, J. F., Price, C., Wise, R., & Frackowiak, R. S. (1994). Differential activation of right and left posterior sylvian regions by semantic and phonological tasks: A positron-emission tomography study in normal human subjects. *Neuroscience Letters*, *182*(1), 25–28.

Deserno, L., Sterzer, P., Wüstenberg, T., Heinz, A., & Schlagenhauf, F. (2012). Reduced Prefrontal-Parietal Effective Connectivity and Working Memory Deficits in Schizophrenia. *Journal of Neuroscience*, *32*(1), 12–20. https://doi.org/10.1523/JNEUROSCI.3405-11.2012

D'Esposito, M., Aguirre, G. K., Zarahn, E., Ballard, D., Shin, R. K., & Lease, J. (1998). Functional MRI studies of spatial and nonspatial working memory. *Brain Research. Cognitive Brain Research*, *7*(1), 1–13.

D'Esposito, M., Detre, J. A., Alsop, D. C., Shin, R. K., Atlas, S., & Grossman, M. (1995). The neural basis of the central executive system of working memory. *Nature*, *378*(6554), 279–281. https://doi.org/10.1038/378279a0

D'Esposito, M., Postle, B. R., & Rypma, B. (2000). Prefrontal cortical contributions to working memory: Evidence from event-related fMRI studies. *Experimental Brain Research*, *133*(1), 3–11. https://doi.org/10.1007/s002210000395

Devlin, J. T., Jamison, H. L., Gonnerman, L. M., & Matthews, P. M. (2006). The role of the posterior fusiform gyrus in reading. *Journal of Cognitive Neuroscience*, *18*(6), 911–922. https://doi.org/10.1162/jocn.2006.18.6.911

Di Lorenzo, F., Ponzo, V., Motta, C., Bonnì, S., Picazio, S., Caltagirone, C., Bozzali, M., Martorana, A., & Koch, G. (2018). Impaired Spike Timing Dependent Cortico-Cortical Plasticity in Alzheimer's Disease Patients. *Journal of Alzheimer's Disease*, *66*(3), 983–991. https://doi.org/10.3233/JAD-180503

Dice, L. R. (1945). Measures of the Amount of Ecologic Association Between Species. *Ecology*, *26*(3), 297–302. https://doi.org/10.2307/1932409

Dmochowski, J. P., Datta, A., Bikson, M., Su, Y., & Parra, L. C. (2011a). Optimized multi-electrode stimulation increases focality and intensity at target. *J. Neural Eng*, *8*(4), 046011. https://doi.org/10.1088/1741-2560/8/4/046011

Dmochowski, J. P., Datta, A., Bikson, M., Su, Y., & Parra, L. C. (2011b). Optimized multi-electrode stimulation increases focality and intensity at target. *J. Neural Eng*, *8*(4), 046011. https://doi.org/10.1088/1741-2560/8/4/046011

Dosenbach, N. U. F., Fair, D. A., Cohen, A. L., Schlaggar, B. L., & Petersen, S. E. (2008). A dual-networks architecture of top-down control. *Trends in Cognitive Sciences*, *12*(3), 99–105. https://doi.org/10.1016/j.tics.2008.01.001

Dosenbach, N. U. F., Fair, D. A., Miezin, F. M., Cohen, A. L., Wenger, K. K., Dosenbach, R. A. T., Fox, M. D., Snyder, A. Z., Vincent, J. L., Raichle, M. E., Schlaggar, B. L., & Petersen, S. E. (2007). Distinct brain networks for adaptive and stable task control in humans. *Proceedings of the National Academy of Sciences*, *104*(26), 11073–11078. https://doi.org/10.1073/pnas.0704320104

Drysdale, A. T., Grosenick, L., Downar, J., Dunlop, K., Mansouri, F., Meng, Y., Fetcho, R. N., Zebley, B., Oathes, D. J., Etkin, A., Schatzberg, A. F., Sudheimer, K., Keller, J., Mayberg, H. S., Gunning, F. M., Alexopoulos, G. S., Fox, M. D., Pascual-Leone, A., Voss, H. U., … Liston, C. (2017). Resting-state connectivity biomarkers define neurophysiological subtypes of depression. *Nature Medicine*, *23*(1), 28–38. https://doi.org/10.1038/nm.4246

Eckert, M., Vinod, M., Adam, W., Jayne, A., Stewart, D., Amy, H., & R, D. J. (2009). At the heart of the ventral attention system: The right anterior insula. *Human Brain Mapping*, *30*(8), 2530–2541. https://doi.org/10.1002/hbm.20688

Eickhoff, S. B., Bzdok, D., Laird, A. R., Kurth, F., & Fox, P. T. (2012). Activation likelihood estimation meta-analysis revisited. *NeuroImage*, *59*(3), 2349–2361. https://doi.org/10.1016/j.neuroimage.2011.09.017

Eickhoff, S. B., Laird, A. R., Grefkes, C., Wang, L. E., Zilles, K., & Fox, P. T. (2009). Coordinate-based activation likelihood estimation meta-analysis of neuroimaging data: A random-effects approach based on empirical estimates of spatial uncertainty. *Human Brain Mapping*, *30*(9), 2907–2926. https://doi.org/10.1002/hbm.20718

Eickhoff, S. B., Nichols, T. E., Laird, A. R., Hoffstaedter, F., Amunts, K., Fox, P. T., Bzdok, D., & Eickhoff, C. R. (2016). Behavior, sensitivity, and power of activation likelihood estimation characterized by massive empirical simulation. *NeuroImage*, *137*, 70–85. https://doi.org/10.1016/j.neuroimage.2016.04.072

Engel, A. K., & Fries, P. (2010). Beta-band oscillations—Signalling the status quo? *Current Opinion in Neurobiology*, *20*(2), 156–165. https://doi.org/10.1016/j.conb.2010.02.015

Estraneo, A., Pascarella, A., Moretta, P., Masotta, O., Fiorenza, S., Chirico, G., Crispino, E., Loreto, V., & Trojano, L. (2017). Repeated transcranial direct current stimulation in prolonged disorders of consciousness: A double-blind cross-over study. *Journal of the Neurological Sciences*, *375*, 464–470. https://doi.org/10.1016/j.jns.2017.02.036

Etkin, A., Egner, T., Peraza, D. M., Kandel, E. R., & Hirsch, J. (2006). Resolving Emotional Conflict: A Role for the Rostral Anterior Cingulate Cortex in Modulating Activity in the Amygdala. *Neuron*, *51*(6), 871–882. https://doi.org/10.1016/j.neuron.2006.07.029

Evers, A. W. M., Kraaimaat, F. W., van Lankveld, W., Jongen, P. J. H., Jacobs, J. W. G., & Bijlsma, J. W. J. (2001). Beyond unfavorable thinking: The Illness Cognition Questionnaire for chronic diseases. *Journal of Consulting and Clinical Psychology*, *69*(6), 1026–1036. https://doi.org/10.1037/0022-006X.69.6.1026

Feige, B., Spiegelhalder, K., Kiemen, A., Bosch, O. G., Tebartz van Elst, L., Hennig, J., Seifritz, E., & Riemann, D. (2017). Distinctive time-lagged resting-state networks revealed by simultaneous EEG-fMRI. *NeuroImage*, *145*, 1–10. https://doi.org/10.1016/j.neuroimage.2016.09.027

Ferbert, A., Priori, A., Rothwell, J. C., Day, B. L., Colebatch, J. G., & Marsden, C. D. (1992). Interhemispheric inhibition of the human motor cortex. *The Journal of Physiology*, *453*(1), 525–546. https://doi.org/10.1113/jphysiol.1992.sp019243

Fernández-Espejo, D., Junque, C., Cruse, D., Bernabeu, M., Roig-Rovira, T., Fábregas, N., Rivas, E., & Mercader, J. M. (2010). Combination of diffusion tensor and functional magnetic resonance imaging during recovery from the vegetative state. *BMC Neurology*, *10*(1), 77. https://doi.org/10.1186/1471-2377-10-77

Fertonani, A., Ferrari, C., & Miniussi, C. (2015). What do you feel if I apply transcranial electric stimulation? Safety, sensations and secondary induced effects. *Clinical Neurophysiology: Official Journal of the International Federation of Clinical Neurophysiology*, *126*(11), 2181–2188. https://doi.org/10.1016/j.clinph.2015.03.015

Fertonani, A., Rosini, S., Cotelli, M., Rossini, P. M., & Miniussi, C. (2010a). Naming facilitation induced by transcranial direct current stimulation. *Behavioural Brain Research*, *208*(2), 311–318. https://doi.org/10.1016/j.bbr.2009.10.030

Fertonani, A., Rosini, S., Cotelli, M., Rossini, P. M., & Miniussi, C. (2010b). Naming facilitation induced by transcranial direct current stimulation. *Behavioural Brain Research*, *208*(2), 311–318. https://doi.org/10.1016/j.bbr.2009.10.030

Feurra, M., Bianco, G., Santarnecchi, E., Testa, M. D., Rossi, A., & Rossi, S. (2011). Frequency-Dependent Tuning of the Human Motor System Induced by Transcranial Oscillatory Potentials. *Journal of Neuroscience*, *31*(34), 12165–12170. https://doi.org/10.1523/JNEUROSCI.0978-11.2011

Feurra, M., Galli, G., Pavone, E. F., Rossi, A., & Rossi, S. (2016). Frequency-specific insight into short-term memory capacity. *Journal of Neurophysiology*, *116*(1), 153–158. https://doi.org/10.1152/jn.01080.2015

Feurra, M., Pasqualetti, P., Bianco, G., Santarnecchi, E., Rossi, A., & Rossi, S. (2013). State-Dependent Effects of Transcranial Oscillatory Currents on the Motor System: What You Think Matters. *Journal of Neuroscience*, *33*(44), 17483–17489. https://doi.org/10.1523/JNEUROSCI.1414-13.2013

Fiori, F., Chiappini, E., & Avenanti, A. (2018). Enhanced action performance following TMS manipulation of associative plasticity in ventral premotor-motor pathway. *NeuroImage*, *183*, 847–858. https://doi.org/10.1016/j.neuroimage.2018.09.002

Fischer, D. B., Fried, P. J., Ruffini, G., Ripolles, O., Salvador, R., Banus, J., Ketchabaw, W. T., Santarnecchi, E., Pascual-Leone, A., & Fox, M. D. (2017a). Multifocal tDCS targeting the resting state motor network increases cortical excitability beyond traditional tDCS targeting unilateral motor cortex. *NeuroImage*, *157*, 34–44. https://doi.org/10.1016/j.neuroimage.2017.05.060

Fischer, D. B., Fried, P. J., Ruffini, G., Ripolles, O., Salvador, R., Banus, J., Ketchabaw, W. T., Santarnecchi, E., Pascual-Leone, A., & Fox, M. D. (2017b). Multifocal tDCS targeting the resting state motor network increases cortical excitability beyond traditional tDCS targeting unilateral motor cortex. *NeuroImage*, *157*, 34–44. https://doi.org/10.1016/j.neuroimage.2017.05.060

Fischer, D. B., Fried, P. J., Ruffini, G., Ripolles, O., Salvador, R., Banus, J., Ketchabaw, W. T., Santarnecchi, E., Pascual-Leone, A., & Fox, M. D. (2017c). Multifocal tDCS targeting the resting state motor network increases cortical excitability beyond traditional tDCS targeting unilateral motor cortex. *NeuroImage*, *157*, 34–44. https://doi.org/10.1016/j.neuroimage.2017.05.060

Fitzgerald, P. B. (2010). TMS-EEG: A technique that has come of age? *Clinical Neurophysiology*, *121*(3), 265–267. https://doi.org/10.1016/j.clinph.2009.11.012

Fitzgibbon, S. P., Pope, K. J., Mackenzie, L., Clark, C. R., & Willoughby, J. O. (2004). Cognitive tasks augment gamma EEG power. *Clinical Neurophysiology*, *115*(8), 1802–1809. https://doi.org/10.1016/j.clinph.2004.03.009

Fornito, A., Zalesky, A., & Breakspear, M. (2015). The connectomics of brain disorders. *Nature Reviews Neuroscience*, *16*(3), 159–172. https://doi.org/10.1038/nrn3901

Fox, M.D., Buckner, R. L., Liu, H., Chakravarty, M. M., Lozano, A. M., & Pascual-Leone, A. (2014a). Resting-state networks link invasive and noninvasive brain stimulation across diverse psychiatric and neurological diseases. *Proc.Natl.Acad.Sci.U.S.A*, *111*(1091-6490 (Electronic)), E4367–E4375. https://doi.org/10.1073/pnas.1405003111

Fox, M.D., Buckner, R. L., Liu, H., Chakravarty, M. M., Lozano, A. M., & Pascual-Leone, A. (2014b). Resting-state networks link invasive and noninvasive brain stimulation across diverse psychiatric and neurological diseases. *Proc.Natl.Acad.Sci.U.S.A*, *111*(1091-6490 (Electronic)), E4367–E4375. https://doi.org/10.1073/pnas.1405003111

Fox, Michael D. (2018). Mapping Symptoms to Brain Networks with the Human Connectome. *New England Journal of Medicine*, *379*(23), 2237–2245. https://doi.org/10.1056/NEJMra1706158

Fox, Michael D., Buckner, R. L., White, M. P., Greicius, M. D., & Pascual-Leone, A. (2012). Efficacy of Transcranial Magnetic Stimulation Targets for Depression Is Related to Intrinsic Functional Connectivity with the Subgenual Cingulate. *Biological Psychiatry*, *72*(7), 595–603. https://doi.org/10.1016/j.biopsych.2012.04.028

Fox, Michael D., & Greicius, M. (2010). Clinical applications of resting state functional connectivity. *Frontiers in Systems Neuroscience*, *4*. https://doi.org/10.3389/fnsys.2010.00019

Fox, Michael D., Halko, M. A., Eldaief, M. C., & Pascual-Leone, A. (2012). Measuring and manipulating brain connectivity with resting state functional connectivity magnetic resonance imaging (fcMRI) and transcranial magnetic stimulation (TMS). *NeuroImage*, *62*(4), 2232–2243. https://doi.org/10.1016/j.neuroimage.2012.03.035

Fox, Michael D., Snyder, A. Z., Vincent, J. L., Corbetta, M., Essen, D. C. V., & Raichle, M. E. (2005a). The human brain is intrinsically organized into dynamic, anticorrelated functional networks. *Proceedings of the National Academy of Sciences*, *102*(27), 9673–9678. https://doi.org/10.1073/pnas.0504136102

Fox, Michael D., Snyder, A. Z., Vincent, J. L., Corbetta, M., Essen, D. C. V., & Raichle, M. E. (2005b). The human brain is intrinsically organized into dynamic, anticorrelated functional networks. *Proceedings of the National Academy of Sciences*, *102*(27), 9673–9678. https://doi.org/10.1073/pnas.0504136102

Fox, Michael D., Zhang, D., Snyder, A. Z., & Raichle, M. E. (2009). The Global Signal and Observed Anticorrelated Resting State Brain Networks. *Journal of Neurophysiology*, *101*(6), 3270–3283. https://doi.org/10.1152/jn.90777.2008

Frangou, S., Kington, J., Raymont, V., & Shergill, S. S. (2008). Examining ventral and dorsal prefrontal function in bipolar disorder: A functional magnetic resonance imaging study. *European Psychiatry*, *23*(4), 300–308. https://doi.org/10.1016/j.eurpsy.2007.05.002

Fregni, F., Boggio, P. S., Nitsche, M., Bermpohl, F., Antal, A., Feredoes, E., Marcolin, M. A., Rigonatti, S. P., Silva, M. T. A., Paulus, W., & Pascual-Leone, A. (2005). Anodal transcranial direct current stimulation of prefrontal cortex enhances working memory. *Experimental Brain Research*, *166*(1), 23–30. https://doi.org/10.1007/s00221-005-2334-6

Friedman, N. P., Miyake, A., Corley, R. P., Young, S. E., DeFries, J. C., & Hewitt, J. K. (2006). Not All Executive Functions Are Related to Intelligence. *Psychological Science*, *17*(2), 172–179.

Friston, K. J., Frith, C. D., Liddle, P. F., & Frackowiak, R. S. J. (1993). Functional Connectivity: The Principal-Component Analysis of Large (PET) Data Sets. *Journal of Cerebral Blood Flow & Metabolism*, *13*(1), 5–14. https://doi.org/10.1038/jcbfm.1993.4

Fritsch, B., Reis, J., Martinowich, K., Schambra, H. M., Ji, Y., Cohen, L. G., & Lu, B. (2010a). Direct Current Stimulation Promotes BDNF-Dependent Synaptic Plasticity: Potential Implications for Motor Learning. *Neuron*, *66*(2), 198–204. https://doi.org/10.1016/j.neuron.2010.03.035

Fritsch, B., Reis, J., Martinowich, K., Schambra, H. M., Ji, Y., Cohen, L. G., & Lu, B. (2010b). Direct Current Stimulation Promotes BDNF-Dependent Synaptic Plasticity: Potential Implications for Motor Learning. *Neuron*, *66*(2), 198–204. https://doi.org/10.1016/j.neuron.2010.03.035

Fröhlich, F., & McCormick, D. A. (2010). Endogenous Electric Fields May Guide Neocortical Network Activity. *Neuron*, *67*(1), 129–143. https://doi.org/10.1016/j.neuron.2010.06.005

Furubayashi, T., Terao, Y., Arai, N., Okabe, S., Mochizuki, H., Hanajima, R., Hamada, M., Yugeta, A., Inomata-Terada, S., & Ugawa, Y. (2008). Short and long duration transcranial direct current stimulation (tDCS) over the human hand motor area. *Experimental Brain Research*, *185*(2), 279–286. https://doi.org/10.1007/s00221-007-1149-z

Galli, G., Vadillo, M. A., Sirota, M., Feurra, M., & Medvedeva, A. (2019). A systematic review and meta-analysis of the effects of transcranial direct current stimulation (tDCS) on episodic memory. *Brain Stimulation*, *12*(2), 231–241. https://doi.org/10.1016/j.brs.2018.11.008

Galynker, I. I., Cai, J., Ongseng, F., Finestone, H., Dutta, E., & Serseni, D. (1998). Hypofrontality and negative symptoms in major depressive disorder. *Journal of Nuclear Medicine: Official Publication, Society of Nuclear Medicine*, *39*(4), 608–612.

Gamboa, O. L., Antal, A., Moliadze, V., & Paulus, W. (2010). Simply longer is not better: Reversal of theta burst after-effect with prolonged stimulation. *Experimental Brain Research*, *204*(2), 181–187. https://doi.org/10.1007/s00221-010-2293-4

Gelfand, J. R., & Bookheimer, S. Y. (2003). Dissociating neural mechanisms of temporal sequencing and processing phonemes. *Neuron*, *38*(5), 831–842.

Gevins, A., Smith, M. E., McEvoy, L., & Yu, D. (1997). High-resolution EEG mapping of cortical activation related to working memory: Effects of task difficulty, type of processing, and practice. *Cerebral Cortex*, *7*(4), 374–385. https://doi.org/10.1093/cercor/7.4.374

Giacino, J. T., Ashwal, S., Childs, N., Cranford, R., Jennett, B., Katz, D. I., Kelly, J. P., Rosenberg, J. H., Whyte, J., Zafonte, R. D., & Zasler, N. D. (2002). The minimally conscious state: Definition and diagnostic criteria. *Neurology*, *58*(3), 349–353. https://doi.org/10.1212/wnl.58.3.349

Giacino, J. T., Fins, J. J., Laureys, S., & Schiff, N. D. (2014). Disorders of consciousness after acquired brain injury: The state of the science. *Nature Reviews. Neurology*, *10*(2), 99–114. https://doi.org/10.1038/nrneurol.2013.279

Glahn, D. C., Ragland, J. D., Abramoff, A., Barrett, J., Laird, A. R., Bearden, C. E., & Velligan, D. I. (2005). Beyond hypofrontality: A quantitative meta-analysis of functional neuroimaging studies of working memory in schizophrenia. *Human Brain Mapping*, *25*(1), 60–69. https://doi.org/10.1002/hbm.20138

Göbel, S. M., & Rushworth, M. F. S. (2004). Cognitive neuroscience: Acting on numbers. *Current Biology: CB*, *14*(13), R517-519. https://doi.org/10.1016/j.cub.2004.06.042

Goethals, I., Audenaert, K., Jacobs, F., Van de Wiele, C., Ham, H., Pyck, H., Vandierendonck, A., Van Heeringen, C., & Dierckx, R. (2005). Blunted prefrontal perfusion in depressed patients performing the Tower of London task. *Psychiatry Research: Neuroimaging*, *139*(1), 31–40. https://doi.org/10.1016/j.pscychresns.2004.09.007

Goldberg, I. I., Harel, M., & Malach, R. (2006). When the brain loses its self: Prefrontal inactivation during sensorimotor processing. *Neuron*, *50*(2), 329–339. https://doi.org/10.1016/j.neuron.2006.03.015

Gonzalez-Burgos, G., & Lewis, D. A. (2012). NMDA Receptor Hypofunction, Parvalbumin-Positive Neurons, and Cortical Gamma Oscillations in Schizophrenia. *Schizophrenia Bulletin*, *38*(5), 950–957. https://doi.org/10.1093/schbul/sbs010

Grady, C. L., McIntosh, A. R., Bookstein, F., Horwitz, B., Rapoport, S. I., & Haxby, J. V. (1998). Age-Related Changes in Regional Cerebral Blood Flow during Working Memory for Faces. *NeuroImage*, *8*(4), 409–425. https://doi.org/10.1006/nimg.1998.0376

Greicius, M. D., Krasnow, B., Reiss, A. L., & Menon, V. (2003). Functional connectivity in the resting brain: A network analysis of the default mode hypothesis. *Proceedings of the National Academy of Sciences*, *100*(1), 253–258. https://doi.org/10.1073/pnas.0135058100

Guerra, A., Suppa, A., Bologna, M., D'Onofrio, V., Bianchini, E., Brown, P., Di Lazzaro, V., & Berardelli, A. (2018). Boosting the LTP-like plasticity effect of intermittent theta-burst stimulation using gamma transcranial alternating current stimulation. *Brain Stimulation*, *11*(4), 734–742. https://doi.org/10.1016/j.brs.2018.03.015

Guse, B., Falkai, P., & Wobrock, T. (2010). Cognitive effects of high-frequency repetitive transcranial magnetic stimulation: A systematic review. *Journal of Neural Transmission*, *117*(1), 105–122. https://doi.org/10.1007/s00702-009-0333-7

Gusnard, D. A., Akbudak, E., Shulman, G. L., & Raichle, M. E. (2001). Medial prefrontal cortex and self-referential mental activity: Relation to a default mode of brain function. *Proceedings of the National Academy of Sciences*, *98*(7), 4259–4264. https://doi.org/10.1073/pnas.071043098

Hallett, M. (2000). Transcranial magnetic stimulation and the human brain. *Nature*, *406*(6792), 147–150. https://doi.org/10.1038/35018000

Hampson, M., Peterson, B. S., Skudlarski, P., Gatenby, J. C., & Gore, J. C. (2002). Detection of functional connectivity using temporal correlations in MR images. *Human Brain Mapping*, *15*(4), 247–262. https://doi.org/10.1002/hbm.10022

Hannawi, Y., & Lindquist, M. A. (2015). *Resting brain activity in disorders of consciousness*. 9.

Harrington, A., & Hammond-Tooke, G. D. (2015). Theta Burst Stimulation of the Cerebellum Modifies the TMS-Evoked N100 Potential, a Marker of GABA Inhibition. *PLOS ONE*, *10*(11), e0141284. https://doi.org/10.1371/journal.pone.0141284

Hart, H., Radua, J., Nakao, T., Mataix-Cols, D., & Rubia, K. (2013). Meta-analysis of functional magnetic resonance imaging studies of inhibition and attention in attention-deficit/hyperactivity disorder: Exploring task-specific, stimulant medication, and age effects. *JAMA Psychiatry*, *70*(2), 185–198. https://doi.org/10.1001/jamapsychiatry.2013.277

Harvey, P.-O., Fossati, P., Pochon, J.-B., Levy, R., LeBastard, G., Lehéricy, S., Allilaire, J.-F., & Dubois, B. (2005). Cognitive control and brain resources in major depression: An fMRI study using the n-back task. *NeuroImage*, *26*(3), 860–869. https://doi.org/10.1016/j.neuroimage.2005.02.048

Haxby, J. V., Petit, L., Ungerleider, L. G., & Courtney, S. M. (2000). Distinguishing the functional roles of multiple regions in distributed neural systems for visual working memory. *NeuroImage*, *11*(2), 145–156. https://doi.org/10.1006/nimg.1999.0527

He, B. J., Zempel, J. M., Snyder, A. Z., & Raichle, M. E. (2010). The Temporal Structures and Functional Significance of Scale-free Brain Activity. *Neuron*, *66*(3), 353–369. https://doi.org/10.1016/j.neuron.2010.04.020

He, J.-H., Yang, Y., Zhang, Y., Qiu, S.-Y., Zhou, Z.-Y., Dang, Y.-Y., Dai, Y.-W., Liu, Y.-J., & Xu, R.-X. (2014). Hyperactive external awareness against hypoactive internal awareness in disorders of consciousness using resting-state functional MRI: highlighting the involvement of visuo-motor modulation: IMBALANCED INTERNAL AND EXTERNAL AWARENESS IN DISORDERS OF CONSCIOUSNESS. *NMR in Biomedicine*, *27*(8), 880–886. https://doi.org/10.1002/nbm.3130

Helfrich, R. F., Schneider, T. R., Rach, S., Trautmann-Lengsfeld, S. A., Engel, A. K., & Herrmann, C. S. (2014a). Entrainment of brain oscillations by transcranial alternating current stimulation. *Current Biology: CB*, *24*(3), 333–339. https://doi.org/10.1016/j.cub.2013.12.041

Helfrich, R. F., Schneider, T. R., Rach, S., Trautmann-Lengsfeld, S. A., Engel, A. K., & Herrmann, C. S. (2014b). Entrainment of brain oscillations by transcranial alternating current stimulation. *Current Biology: CB*, *24*(3), 333–339. https://doi.org/10.1016/j.cub.2013.12.041

Henson, R. N. A., Burgess, N., & Frith, C. D. (2000). Recoding, storage, rehearsal and grouping in verbal short-term memory: An fMRI study. *Neuropsychologia*, *38*(4), 426–440. https://doi.org/10.1016/S0028-3932(99)00098-6

Herrmann, C. S., Rach, S., Neuling, T., & Strüber, D. (2013a). Transcranial alternating current stimulation: A review of the underlying mechanisms and modulation of cognitive processes. *Frontiers in Human Neuroscience*, *7*, 279. https://doi.org/10.3389/fnhum.2013.00279

Herrmann, C. S., Rach, S., Neuling, T., & Strüber, D. (2013b). Transcranial alternating current stimulation: A review of the underlying mechanisms and modulation of cognitive processes. *Frontiers in Human Neuroscience*, *7*, 279. https://doi.org/10.3389/fnhum.2013.00279

Herwig, U., Satrapi, P., & Schönfeldt-Lecuona, C. (2003). Using the International 10-20 EEG System for Positioning of Transcranial Magnetic Stimulation. *Brain Topography*, *16*(2), 95–99. https://doi.org/10.1023/B:BRAT.0000006333.93597.9d

Heuvel, M. P. van den, Mandl, R. C. W., Kahn, R. S., & Pol, H. E. H. (2009). Functionally linked resting-state networks reflect the underlying structural connectivity architecture of the human brain. *Human Brain Mapping*, *30*(10), 3127–3141. https://doi.org/10.1002/hbm.20737

Hill, A. T., Fitzgerald, P. B., & Hoy, K. E. (2016a). Effects of Anodal Transcranial Direct Current Stimulation on Working Memory: A Systematic Review and Meta-Analysis of Findings From Healthy and Neuropsychiatric Populations. *Brain Stimulation*, *9*(2), 197–208. https://doi.org/10.1016/j.brs.2015.10.006

Hill, A. T., Fitzgerald, P. B., & Hoy, K. E. (2016b). Effects of Anodal Transcranial Direct Current Stimulation on Working Memory: A Systematic Review and Meta-Analysis of Findings From Healthy and Neuropsychiatric Populations. *Brain Stimulation*, *9*(2), 197–208. https://doi.org/10.1016/j.brs.2015.10.006

Hoffman, B. M., Blumenthal, J. A., Babyak, M. A., Smith, P. J., Rogers, S. D., Doraiswamy, P. M., & Sherwood, A. (2008). Exercise Fails to Improve Neurocognition in Depressed Middle-Aged and Older Adults. *Medicine and Science in Sports and Exercise*, *40*(7), 1344–1352. https://doi.org/10.1249/MSS.0b013e31816b877c

Hong, X., Lu, Z. K., Teh, I., Nasrallah, F. A., Teo, W. P., Ang, K. K., Phua, K. S., Guan, C., Chew, E., & Chuang, K.-H. (2017). Brain plasticity following MI-BCI training combined with tDCS in a randomized trial in chronic subcortical

stroke subjects: A preliminary study. *Scientific Reports*, *7*(1), 1–12. https://doi.org/10.1038/s41598-017-08928-5

Honkanen, R., Rouhinen, S., Wang, S. H., Palva, J. M., & Palva, S. (2015). Gamma Oscillations Underlie the Maintenance of Feature-Specific Information and the Contents of Visual Working Memory. *Cerebral Cortex*, *25*(10), 3788–3801. https://doi.org/10.1093/cercor/bhu263

Horvath, J. C., Forte, J. D., & Carter, O. (2015). Quantitative Review Finds No Evidence of Cognitive Effects in Healthy Populations From Single-session Transcranial Direct Current Stimulation (tDCS). *Brain Stimulation*, *8*(3), 535–550. https://doi.org/10.1016/j.brs.2015.01.400

Howard, M. W., Rizzuto, D. S., Caplan, J. B., Madsen, J. R., Lisman, J., Aschenbrenner-Scheibe, R., Schulze-Bonhage, A., & Kahana, M. J. (2003). Gamma Oscillations Correlate with Working Memory Load in Humans. *Cerebral Cortex*, *13*(12), 1369–1374. https://doi.org/10.1093/cercor/bhg084

Hoy, K. E., Bailey, N., Arnold, S., Windsor, K., John, J., Daskalakis, Z. J., & Fitzgerald, P. B. (2015). The effect of γ-tACS on working memory performance in healthy controls. *Brain and Cognition*, *101*, 51–56. https://doi.org/10.1016/j.bandc.2015.11.002

Hsu, W.-Y., Ku, Y., Zanto, T. P., & Gazzaley, A. (2015). Effects of noninvasive brain stimulation on cognitive function in healthy aging and Alzheimer's disease: A systematic review and meta-analysis. *Neurobiology of Aging*, *36*(8), 2348–2359. https://doi.org/10.1016/j.neurobiolaging.2015.04.016

Huang, Y., Dmochowski, J. P., Su, Y., Datta, A., Rorden, C., & Parra, L. C. (2013). Automated MRI segmentation for individualized modeling of current flow in the human head. *Journal of Neural Engineering*, *10*(6), 066004. https://doi.org/10.1088/1741-2560/10/6/066004

Huang, Y.-Z., Edwards, M. J., Rounis, E., Bhatia, K. P., & Rothwell, J. C. (2005). Theta Burst Stimulation of the Human Motor Cortex. *Neuron*, *45*(2), 201–206. https://doi.org/10.1016/j.neuron.2004.12.033

Huang, Y.-Z., Lu, M.-K., Antal, A., Classen, J., Nitsche, M., Ziemann, U., Ridding, M., Hamada, M., Ugawa, Y., Jaberzadeh, S., Suppa, A., Paulus, W., & Rothwell, J. (2017a). Plasticity induced by non-invasive transcranial brain stimulation: A position paper. *Clinical Neurophysiology*, *128*(11), 2318–2329. https://doi.org/10.1016/j.clinph.2017.09.007

Huang, Y.-Z., Lu, M.-K., Antal, A., Classen, J., Nitsche, M., Ziemann, U., Ridding, M., Hamada, M., Ugawa, Y., Jaberzadeh, S., Suppa, A., Paulus, W., & Rothwell, J. (2017b). Plasticity induced by non-invasive transcranial brain stimulation: A position paper. *Clinical Neurophysiology*, *128*(11), 2318–2329. https://doi.org/10.1016/j.clinph.2017.09.007

Huang, Y.-Z., Rothwell, J. C., Chen, R.-S., Lu, C.-S., & Chuang, W.-L. (2011). The theoretical model of theta burst form of repetitive transcranial magnetic stimulation. *Clinical Neurophysiology*, *122*(5), 1011–1018. https://doi.org/10.1016/j.clinph.2010.08.016

Huang, Z., Dai, R., Wu, X., Yang, Z., Liu, D., Hu, J., Gao, L., Tang, W., Mao, Y., Jin, Y., Wu, X., Liu, B., Zhang, Y., Lu, L., Laureys, S., Weng, X., & Northoff, G. (2014). The self and its resting state in consciousness: An investigation of the vegetative state: Self and Resting State in Consciousness. *Human Brain Mapping*, *35*(5), 1997–2008. https://doi.org/10.1002/hbm.22308

Hubbard, E. M., Piazza, M., Pinel, P., & Dehaene, S. (2005). Interactions between number and space in parietal cortex. *Nature Reviews. Neuroscience*, *6*(6), 435–448. https://doi.org/10.1038/nrn1684

Hunter, T., Sacco, P., Nitsche, M. A., & Turner, D. L. (2009). Modulation of internal model formation during force field-induced motor learning by anodal transcranial direct current stimulation of primary motor cortex. *The Journal of Physiology*, *587*(12), 2949–2961. https://doi.org/10.1113/jphysiol.2009.169284

Hurley, R., & Machado, L. (2018). Using transcranial direct current stimulation to improve verbal working memory: A detailed review of the methodology. *Journal of Clinical and Experimental Neuropsychology*, *40*(8), 790–804. https://doi.org/10.1080/13803395.2018.1434133

Iaccarino, H. F., Singer, A. C., Martorell, A. J., Rudenko, A., Gao, F., Gillingham, T. Z., Mathys, H., Seo, J., Kritskiy, O., Abdurrob, F., Adaikkan, C., Canter, R. G., Rueda, R., Brown, E. N., Boyden, E. S., & Tsai, L.-H. (2016a). Gamma frequency entrainment attenuates amyloid load and modifies microglia. *Nature*, *540*(7632), 230–235. https://doi.org/10.1038/nature20587

Iaccarino, H. F., Singer, A. C., Martorell, A. J., Rudenko, A., Gao, F., Gillingham, T. Z., Mathys, H., Seo, J., Kritskiy, O., Abdurrob, F., Adaikkan, C., Canter, R. G., Rueda, R., Brown, E. N., Boyden, E. S., & Tsai, L.-H. (2016b). Gamma

frequency entrainment attenuates amyloid load and modifies microglia. *Nature*, *540*(7632), 230–235. https://doi.org/10.1038/nature20587

Ilmoniemi Rj, J, V., J, R., J, K., Hj, A., R, N., & T, K. (1997, October 11). *Neuronal responses to magnetic stimulation reveal cortical reactivity and connectivity*. Neuroreport; Neuroreport. https://doi.org/10.1097/00001756-199711100-00024

Ingvar, D. H. (1979). "Hyperfrontal" distribution of the cerebral grey matter flow in resting wakefulness; on the functional anatomy of the conscious state. *Acta Neurologica Scandinavica*, *60*(1), 12–25. https://doi.org/10.1111/j.1600-0404.1979.tb02947.x

Innes, K. E., Selfe, T. K., Khalsa, D. S., & Kandati, S. (2017). Meditation and Music Improve Memory and Cognitive Function in Adults with Subjective Cognitive Decline: A Pilot Randomized Controlled Trial. *Journal of Alzheimer's Disease*, *56*(3), 899–916. https://doi.org/10.3233/JAD-160867

Inui, T., Otsu, Y., Tanaka, S., Okada, T., Nishizawa, S., & Konishi, J. (1998). A functional MRI analysis of comprehension processes of Japanese sentences. *Neuroreport*, *9*(14), 3325–3328.

Jacquemot, C., Pallier, C., LeBihan, D., Dehaene, S., & Dupoux, E. (2003). Phonological grammar shapes the auditory cortex: A functional magnetic resonance imaging study. *The Journal of Neuroscience: The Official Journal of the Society for Neuroscience*, *23*(29), 9541–9546.

Jak, A. J. (2012). The Impact of Physical and Mental Activity on Cognitive Aging. In M.-C. Pardon & M. W. Bondi (Eds.), *Behavioral Neurobiology of Aging* (pp. 273–291). Springer. https://doi.org/10.1007/7854_2011_141

JASPER, H. H. (1958). The ten-twenty electrode system of the international federation. *Electroencephalogr. Clin. Neurophysiol.*, *10*, 370–375.

Jaušovec, N., & Jaušovec, K. (2014a). Increasing working memory capacity with theta transcranial alternating current stimulation (tACS). *Biological Psychology*, *96*, 42–47. https://doi.org/10.1016/j.biopsycho.2013.11.006

Jaušovec, N., & Jaušovec, K. (2014b). Increasing working memory capacity with theta transcranial alternating current stimulation (tACS). *Biological Psychology*, *96*, 42–47. https://doi.org/10.1016/j.biopsycho.2013.11.006

Jellinger, K. A. (2009). Plum and Posner's—Diagnosis of Stupor and Coma, Fourth Edition. *European Journal of Neurology*, *16*(2), e29–e29. https://doi.org/10.1111/j.1468-1331.2008.02454.x

Jennett, B., & Plum, F. (1972). Persistent vegetative state after brain damage. A syndrome in search of a name. *Lancet (London, England)*, *1*(7753), 734–737. https://doi.org/10.1016/s0140-6736(72)90242-5

Jensen, O., & Tesche, C. D. (2002). Frontal theta activity in humans increases with memory load in a working memory task. *European Journal of Neuroscience*, *15*(8), 1395–1399. https://doi.org/10.1046/j.1460-9568.2002.01975.x

Jones, K. T., Stephens, J. A., Alam, M., Bikson, M., & Berryhill, M. E. (2015). Longitudinal Neurostimulation in Older Adults Improves Working Memory. *PLOS ONE*, *10*(4), e0121904. https://doi.org/10.1371/journal.pone.0121904

Jonides, J., Schumacher, E. H., Smith, E. E., Koeppe, R. A., Awh, E., Reuter-Lorenz, P. A., Marshuetz, C., & Willis, C. R. (1998). The role of parietal cortex in verbal working memory. *The Journal of Neuroscience: The Official Journal of the Society for Neuroscience*, *18*(13), 5026–5034.

Jonides, J., Schumacher, E. H., Smith, E. E., Lauber, E. J., Awh, E., Minoshima, S., & Koeppe, R. A. (1997). Verbal Working Memory Load Affects Regional Brain Activation as Measured by PET. *Journal of Cognitive Neuroscience*, *9*(4), 462–475. https://doi.org/10.1162/jocn.1997.9.4.462

Kanai, R., Chaieb, L., Antal, A., Walsh, V., & Paulus, W. (2008). Frequency-Dependent Electrical Stimulation of the Visual Cortex. *Current Biology*, *18*(23), 1839–1843. https://doi.org/10.1016/j.cub.2008.10.027

Kanai, R., Paulus, W., & Walsh, V. (2010). Transcranial alternating current stimulation (tACS) modulates cortical excitability as assessed by TMS-induced phosphene thresholds. *Clinical Neurophysiology*, *121*(9), 1551–1554. https://doi.org/10.1016/j.clinph.2010.03.022

Kane, M. J., Conway, A. R. A., Miura, T. K., & Colflesh, G. J. H. (2007). Working memory, attention control, and the N-back task: A question of construct validity. *Journal of Experimental Psychology. Learning, Memory, and Cognition*, *33*(3), 615–622. https://doi.org/10.1037/0278-7393.33.3.615

Kemere, C., Carr, M. F., Karlsson, M. P., & Frank, L. M. (2013). Rapid and Continuous Modulation of Hippocampal Network State during Exploration of New Places. *PLOS ONE*, *8*(9), e73114. https://doi.org/10.1371/journal.pone.0073114

Kerestes, R., Ladouceur, C. D., Meda, S., Nathan, P. J., Blumberg, H. P., Maloney, K., Ruf, B., Saricicek, A., Pearlson, G. D., Bhagwagar, Z., & Phillips, M. L. (2012). Abnormal prefrontal activity subserving attentional control of emotion in remitted depressed patients during a working memory task with emotional distracters. *Psychological Medicine*, *42*(1), 29–40. https://doi.org/10.1017/S0033291711001097

Khader, P. H., Jost, K., Ranganath, C., & Rösler, F. (2010). Theta and alpha oscillations during working-memory maintenance predict successful long-term memory encoding. *Neuroscience Letters*, *468*(3), 339–343. https://doi.org/10.1016/j.neulet.2009.11.028

Kim, K. K., Karunanayaka, P., Privitera, M. D., Holland, S. K., & Szaflarski, J. P. (2011). Semantic association investigated with fMRI and independent component analysis. *Epilepsy & Behavior : E&B*, *20*(4), 613–622. https://doi.org/10.1016/j.yebeh.2010.11.010

Kim, Y. W., Kim, H. S., & An, Y.-S. (2013). Brain metabolism in patients with vegetative state after post-resuscitated hypoxic-ischemic brain injury: Statistical parametric mapping analysis of F-18 fluorodeoxyglucose positron emission tomography. *Chinese Medical Journal*, 7.

Kim, Y. W., Kim, H. S., An, Y.-S., & Im, S. H. (2010). Voxel-based statistical analysis of cerebral glucose metabolism in patients with permanent vegetative state after acquired brain injury. *Chinese Medical Journal*, 5.

Kirchner, W. K. (1958). Age differences in short-term retention of rapidly changing information. *Journal of Experimental Psychology*, *55*(4), 352–358.

Klimesch, W., Sauseng, P., & Gerloff, C. (2003). Enhancing cognitive performance with repetitive transcranial magnetic stimulation at human individual alpha frequency. *European Journal of Neuroscience*, *17*(5), 1129–1133. https://doi.org/10.1046/j.1460-9568.2003.02517.x

Knyazev, G. G., Slobodskoj-Plusnin, J. Y., & Bocharov, A. V. (2009). Event-related delta and theta synchronization during explicit and implicit emotion processing. *Neuroscience*, *164*(4), 1588–1600. https://doi.org/10.1016/j.neuroscience.2009.09.057

Kobayashi, C., Glover, G. H., & Temple, E. (2008). Switching language switches mind: Linguistic effects on developmental neural bases of 'Theory of Mind.' *Social Cognitive and Affective Neuroscience*, *3*(1), 62–70. https://doi.org/10.1093/scan/nsm039

Kobayashi, M., Hutchinson, S., Schlaug, G., & Pascual-Leone, A. (2003). Ipsilateral motor cortex activation on functional magnetic resonance imaging during unilateral hand movements is related to interhemispheric interactions. *NeuroImage*, *20*(4), 2259–2270. https://doi.org/10.1016/S1053-8119(03)00220-9

Kobayashi, M., & Pascual-Leone, A. (2003). Transcranial magnetic stimulation in neurology. *The Lancet Neurology*, *2*(3), 145–156. https://doi.org/10.1016/S1474-4422(03)00321-1

Kobel, M., Bechtel, N., Weber, P., Specht, K., Klarhöfer, M., Scheffler, K., Opwis, K., & Penner, I.-K. (2009). Effects of methylphenidate on working memory functioning in children with attention deficit/hyperactivity disorder. *European Journal of Paediatric Neurology*, *13*(6), 516–523. https://doi.org/10.1016/j.ejpn.2008.10.008

Koch, G. (2020). Cortico-cortical connectivity: The road from basic neurophysiological interactions to therapeutic applications. *Experimental Brain Research*, *238*(7), 1677–1684. https://doi.org/10.1007/s00221-020-05844-5

Koch, G., Ponzo, V., Lorenzo, F. D., Caltagirone, C., & Veniero, D. (2013). Hebbian and Anti-Hebbian Spike-Timing-Dependent Plasticity of Human Cortico-Cortical Connections. *Journal of Neuroscience*, *33*(23), 9725–9733. https://doi.org/10.1523/JNEUROSCI.4988-12.2013

Koenig, M. A., Holt, J. L., Ernst, T., Buchthal, S. D., Nakagawa, K., Stenger, V. A., & Chang, L. (2014). MRI Default Mode Network Connectivity is Associated with Functional Outcome After Cardiopulmonary Arrest. *Neurocritical Care*, *20*(3), 348–357. https://doi.org/10.1007/s12028-014-9953-3

Koziol, L. F., Budding, D., Andreasen, N., D'Arrigo, S., Bulgheroni, S., Imamizu, H., Ito, M., Manto, M., Marvel, C., Parker, K., Pezzulo, G., Ramnani, N., Riva, D., Schmahmann, J., Vandervert, L., & Yamazaki, T. (2014). Consensus paper: The cerebellum's role in movement and cognition. *Cerebellum (London, England)*, *13*(1), 151–177. https://doi.org/10.1007/s12311-013-0511-x

Kramer, A. F., Hahn, S., Cohen, N. J., Banich, M. T., McAuley, E., Harrison, C. R., Chason, J., Vakil, E., Bardell, L., Boileau, R. A., & Colcombe, A. (1999). Ageing, fitness and neurocognitive function. *Nature*, *400*(6743), 418–419. https://doi.org/10.1038/22682

Krause, B., & Cohen Kadosh, R. (2014). Not all brains are created equal: The relevance of individual differences in responsiveness to transcranial electrical stimulation. *Frontiers in Systems Neuroscience*, *8*. https://doi.org/10.3389/fnsys.2014.00025

Krause, M. R., Vieira, P. G., Csorba, B. A., Pilly, P. K., & Pack, C. C. (2019a). Transcranial alternating current stimulation entrains single-neuron activity in the primate brain. *Proceedings of the National Academy of Sciences*, *116*(12), 5747–5755. https://doi.org/10.1073/pnas.1815958116

Krause, M. R., Vieira, P. G., Csorba, B. A., Pilly, P. K., & Pack, C. C. (2019b). Transcranial alternating current stimulation entrains single-neuron activity in the primate brain. *Proceedings of the National Academy of Sciences*, *116*(12), 5747–5755. https://doi.org/10.1073/pnas.1815958116

Kumari, V., Aasen, I., Taylor, P., Ffytche, D. H., Das, M., Barkataki, I., Goswami, S., O'Connell, P., Howlett, M., Williams, S. C. R., & Sharma, T. (2006). Neural dysfunction and violence in schizophrenia: An fMRI investigation. *Schizophrenia Research*, *84*(1), 144–164. https://doi.org/10.1016/j.schres.2006.02.017

Laakso, I., Tanaka, S., Koyama, S., De Santis, V., & Hirata, A. (2015). Inter-subject Variability in Electric Fields of Motor Cortical tDCS. *Brain Stimulation*, *8*(5), 906–913. https://doi.org/10.1016/j.brs.2015.05.002

Lafon, B., Rahman, A., Bikson, M., & Parra, L. C. (2017). Direct Current Stimulation Alters Neuronal Input/Output Function. *Brain Stimulation*, *10*(1), 36–45. https://doi.org/10.1016/j.brs.2016.08.014

Langlois, J. A., Rutland-Brown, W., & Wald, M. M. (2006). The epidemiology and impact of traumatic brain injury: A brief overview. *The Journal of Head Trauma Rehabilitation*, *21*(5), 375–378.

Latalova, K., Prasko, J., Diveky, T., & Velartova, H. (2011). Cognitive impairment in bipolar disorder. *Biomedical Papers of the Medical Faculty of the University Palacky, Olomouc, Czechoslovakia*, *155*(1), 19–26.

Laufs, H. (2008). Endogenous brain oscillations and related networks detected by surface EEG-combined fMRI. *Human Brain Mapping*, *29*(7), 762–769. https://doi.org/10.1002/hbm.20600

Laureys, S., Faymonville, M. E., Luxen, A., Lamy, M., Franck, G., & Maquet, P. (2000). Restoration of thalamocortical connectivity after recovery from persistent vegetative state. *The Lancet*, *355*(9217), 1790–1791. https://doi.org/10.1016/S0140-6736(00)02271-6

Laureys, Steven, Celesia, G. G., Cohadon, F., Lavrijsen, J., León-Carrión, J., Sannita, W. G., Sazbon, L., Schmutzhard, E., von Wild, K. R., Zeman, A., Dolce, G., & Consciousness, E. T. F. on D. of. (2010). Unresponsive wakefulness syndrome: A new name for the vegetative state or apallic syndrome. *BMC Medicine*, *8*, 68. https://doi.org/10.1186/1741-7015-8-68

Laureys, Steven, & Tononi, G. (2011). *The Neurology of Consciousness: Cognitive Neuroscience and Neuropathology*. Academic Press.

Lefaucheur, J.-P., Antal, A., Ayache, S. S., Benninger, D. H., Brunelin, J., Cogiamanian, F., Cotelli, M., De Ridder, D., Ferrucci, R., Langguth, B., Marangolo, P., Mylius, V., Nitsche, M. A., Padberg, F., Palm, U., Poulet, E., Priori, A., Rossi, S., Schecklmann, M., … Paulus, W. (2017a). Evidence-based guidelines on the therapeutic use of transcranial direct current stimulation (tDCS). *Clinical Neurophysiology*, *128*(1), 56–92. https://doi.org/10.1016/j.clinph.2016.10.087

Lefaucheur, J.-P., Antal, A., Ayache, S. S., Benninger, D. H., Brunelin, J., Cogiamanian, F., Cotelli, M., De Ridder, D., Ferrucci, R., Langguth, B., Marangolo, P., Mylius, V., Nitsche, M. A., Padberg, F., Palm, U., Poulet, E., Priori, A., Rossi, S., Schecklmann, M., … Paulus, W. (2017b). Evidence-based guidelines on the therapeutic use of transcranial direct current stimulation (tDCS). *Clinical Neurophysiology*, *128*(1), 56–92. https://doi.org/10.1016/j.clinph.2016.10.087

Liang, X., Kuhlmann, L., Johnston, L. A., Grayden, D. B., Vogrin, S., Crossley, R., Fuller, K., Lourensz, M., & Cook, M. J. (2014). Extending Communication for Patients with Disorders of Consciousness: FMRI of Disorders of Consciousness. *Journal of Neuroimaging*, *24*(1), 31–38. https://doi.org/10.1111/j.1552-6569.2012.00744.x

Liberati, A., Altman, D. G., Tetzlaff, J., Mulrow, C., Gøtzsche, P. C., Ioannidis, J. P. A., Clarke, M., Devereaux, P. J., Kleijnen, J., & Moher, D. (2009a). The PRISMA Statement for Reporting Systematic Reviews and Meta-Analyses of Studies That Evaluate Health Care Interventions: Explanation and Elaboration. *PLoS Medicine*, *6*(7), e1000100. https://doi.org/10.1371/journal.pmed.1000100

Liberati, A., Altman, D. G., Tetzlaff, J., Mulrow, C., Gøtzsche, P. C., Ioannidis, J. P. A., Clarke, M., Devereaux, P. J., Kleijnen, J., & Moher, D. (2009b). The PRISMA Statement for Reporting Systematic Reviews and Meta-Analyses of Studies That Evaluate Health Care Interventions: Explanation and Elaboration. *PLoS Medicine*, *6*(7), e1000100. https://doi.org/10.1371/journal.pmed.1000100

Liebetanz, D., Nitsche, M. A., Tergau, F., & Paulus, W. (2002). Pharmacological approach to the mechanisms of transcranial DC-stimulation-induced after-effects of human motor cortex excitability. *Brain*, *125*(10), 2238–2247. https://doi.org/10.1093/brain/awf238

Liew, S. L., Santarnecchi, E., Buch, E. R., & Cohen, L. G. (2014). Non-invasive brain stimulation in neurorehabilitation: Local and distant effects for motor recovery. *Front Hum.Neurosci.*, *8*(1662-5161 (Electronic)), 378. https://doi.org/10.3389/fnhum.2014.00378

Lindenberg, R., Nachtigall, L., Meinzer, M., Sieg, M. M., & Floel, A. (2013). Differential Effects of Dual and Unihemispheric Motor Cortex Stimulation in Older Adults. *Journal of Neuroscience*, *33*(21), 9176–9183. https://doi.org/10.1523/JNEUROSCI.0055-13.2013

Lindgren, L., Westling, G., Brulin, C., Lehtipalo, S., Andersson, M., & Nyberg, L. (2012). Pleasant human touch is represented in pregenual anterior cingulate cortex. *NeuroImage*, *59*(4), 3427–3432. https://doi.org/10.1016/j.neuroimage.2011.11.013

Liu, Q., Ganzetti, M., Wenderoth, N., & Mantini, D. (2018). Detecting Large-Scale Brain Networks Using EEG: Impact of Electrode Density, Head Modeling and Source Localization. *Frontiers in Neuroinformatics*, *12*, 4. https://doi.org/10.3389/fninf.2018.00004

Lopes da Silva, F. (2013). EEG and MEG: Relevance to Neuroscience. *Neuron*, *80*(5), 1112–1128. https://doi.org/10.1016/j.neuron.2013.10.017

López Zunini, R. A., Knoefel, F., Lord, C., Dzuali, F., Breau, M., Sweet, L., Goubran, R., & Taler, V. (2016). Event-related potentials elicited during working memory are altered in mild cognitive impairment. *International Journal of Psychophysiology*, *109*, 1–8. https://doi.org/10.1016/j.ijpsycho.2016.09.012

Lou, H. C., Luber, B., Crupain, M., Keenan, J. P., Nowak, M., Kjaer, T. W., Sackeim, H. A., & Lisanby, S. H. (2004). Parietal cortex and representation of the mental Self. *Proceedings of the National Academy of Sciences of the United States of America*, *101*(17), 6827–6832. https://doi.org/10.1073/pnas.0400049101

Lowe, M. J., Dzemidzic, M., Lurito, J. T., Mathews, V. P., & Phillips, M. D. (2000). *RAPID COMMUNICATION Correlations in Low-Frequency BOLD Fluctuations Reflect Cortico-Cortical Connections*.

Mably, A. J., & Colgin, L. L. (2018a). Gamma oscillations in cognitive disorders. *Current Opinion in Neurobiology*, *52*, 182–187. https://doi.org/10.1016/j.conb.2018.07.009

Mably, A. J., & Colgin, L. L. (2018b). Gamma oscillations in cognitive disorders. *Current Opinion in Neurobiology*, *52*, 182–187. https://doi.org/10.1016/j.conb.2018.07.009

Maguire, E. A., Woollett, K., & Spiers, H. J. (2006). London taxi drivers and bus drivers: A structural MRI and neuropsychological analysis. *Hippocampus*, *16*(12), 1091–1101. https://doi.org/10.1002/hipo.20233

Mancuso, M., Abbruzzese, L., Canova, S., Landi, G., Rossi, S., & Santarnecchi, E. (2017). Transcranial Random Noise Stimulation Does Not Improve Behavioral and Neurophysiological Measures in Patients with Subacute Vegetative-Unresponsive Wakefulness State (VS-UWS). *Frontiers in Human Neuroscience*, *11*, 524. https://doi.org/10.3389/fnhum.2017.00524

Mander, B. A., Winer, J. R., Jagust, W. J., & Walker, M. P. (2016). Sleep: A Novel Mechanistic Pathway, Biomarker, and Treatment Target in the Pathology of Alzheimer's Disease? *Trends in Neurosciences*, *39*(8), 552–566. https://doi.org/10.1016/j.tins.2016.05.002

Mansouri, F. A., Tanaka, K., & Buckley, M. J. (2009). Conflict-induced behavioural adjustment: A clue to the executive functions of the prefrontal cortex. *Nature Reviews. Neuroscience*, *10*(2), 141–152. https://doi.org/10.1038/nrn2538

Mantovani, A., Neri, F., D'Urso, G., Mencarelli, L., Tatti, E., Momi, D., Menardi, A., Sprugnoli, G., Santarnecchi, E., & Rossi, S. (2020). Functional connectivity changes and symptoms improvement after personalized, double-daily dosing, repetitive transcranial magnetic stimulation in obsessive-compulsive disorder: A pilot study. *Journal of Psychiatric Research*. https://doi.org/10.1016/j.jpsychires.2020.10.030

Marek, S., & Dosenbach, N. U. F. (2018). The frontoparietal network: Function, electrophysiology, and importance of individual precision mapping. *Dialogues in Clinical Neuroscience*, *20*(2), 133–140.

Marek, S., Hwang, K., Foran, W., Hallquist, M. N., & Luna, B. (2015). The Contribution of Network Organization and Integration to the Development of Cognitive Control. *PLOS Biology*, *13*(12), e1002328. https://doi.org/10.1371/journal.pbio.1002328

Marino, S., Bonanno, L., Ciurleo, R., Baglieri, A., Morabito, R., Guerrera, S., Rifici, C., Giorgio, A., Bramanti, P., & De Stefano, N. (2017). Functional Evaluation of Awareness in Vegetative and Minimally Conscious State. *The Open Neuroimaging Journal*, *11*(1), 17–25. https://doi.org/10.2174/1874440001711010017

Martinussen, R., Hayden, J., Hogg-Johnson, S., & Tannock, R. (2005). A Meta-Analysis of Working Memory Impairments in Children With Attention-Deficit/Hyperactivity Disorder. *Journal of the American Academy of Child & Adolescent Psychiatry*, *44*(4), 377–384. https://doi.org/10.1097/01.chi.0000153228.72591.73

Martorell, A. J., Paulson, A. L., Suk, H.-J., Abdurrob, F., Drummond, G. T., Guan, W., Young, J. Z., Kim, D. N.-W., Kritskiy, O., Barker, S. J., Mangena, V., Prince, S. M., Brown, E. N., Chung, K., Boyden, E. S., Singer, A. C., & Tsai, L.-H. (2019). Multi-sensory Gamma Stimulation Ameliorates Alzheimer's-Associated Pathology and Improves Cognition. *Cell*, *177*(2), 256-271.e22. https://doi.org/10.1016/j.cell.2019.02.014

Marvel, C. L., & Desmond, J. E. (2010). Functional Topography of the Cerebellum in Verbal Working Memory. *Neuropsychology Review*, *20*(3), 271–279. https://doi.org/10.1007/s11065-010-9137-7

Mason, M. F., Norton, M. I., Van Horn, J. D., Wegner, D. M., Grafton, S. T., & Macrae, C. N. (2007). Wandering Minds: The Default Network and Stimulus-Independent Thought. *Science (New York, N.Y.)*, *315*(5810), 393–395. https://doi.org/10.1126/science.1131295

Massimini, M., Ferrarelli, F., Sarasso, S., & Tononi, G. (2012). Cortical mechanisms of loss of consciousness: Insight from TMS/EEG studies. *Archives Italiennes De Biologie*, *150*(2–3), 44–55. https://doi.org/10.4449/aib.v150i2.1361

Massimini, Marcello, Boly, M., Casali, A., Rosanova, M., & Tononi, G. (2009). A perturbational approach for evaluating the brain's capacity for consciousness. In Steven Laureys, N. D. Schiff, & A. M. Owen (Eds.), *Progress in Brain Research* (Vol. 177, pp. 201–214). Elsevier. https://doi.org/10.1016/S0079-6123(09)17714-2

Massimini, Marcello, Ferrarelli, F., Huber, R., Esser, S. K., Singh, H., & Tononi, G. (2005). Breakdown of Cortical Effective Connectivity During Sleep. *Science*, *309*(5744), 2228–2232. https://doi.org/10.1126/science.1117256

Matsuo, K., Glahn, D. C., Peluso, M. a. M., Hatch, J. P., Monkul, E. S., Najt, P., Sanches, M., Zamarripa, F., Li, J., Lancaster, J. L., Fox, P. T., Gao, J.-H., & Soares, J. C. (2007). Prefrontal hyperactivation during working memory task in untreated individuals with major depressive disorder. *Molecular Psychiatry*, *12*(2), 158–166. https://doi.org/10.1038/sj.mp.4001894

Mattfeld, A. T., Whitfield-Gabrieli, S., Biederman, J., Spencer, T., Brown, A., Fried, R., & Gabrieli, J. D. E. (2016). Dissociation of working memory impairments and attention-deficit/hyperactivity disorder in the brain. *NeuroImage: Clinical*, *10*, 274–282. https://doi.org/10.1016/j.nicl.2015.12.003

Maurer, U., Brem, S., Liechti, M., Maurizio, S., Michels, L., & Brandeis, D. (2015). Frontal Midline Theta Reflects Individual Task Performance in a Working Memory Task. *Brain Topography*, *28*(1), 127–134. https://doi.org/10.1007/s10548-014-0361-y

McCarthy, G., Blamire, A. M., Puce, A., Nobre, A. C., Bloch, G., Hyder, F., Goldman-Rakic, P., & Shulman, R. G. (1994). Functional magnetic resonance imaging of human prefrontal cortex activation during a spatial working memory task. *Proceedings of the National Academy of Sciences*, *91*(18), 8690–8694.

McCarthy, H., Skokauskas, N., & Frodl, T. (2014). Identifying a consistent pattern of neural function in attention deficit hyperactivity disorder: A meta-analysis. *Psychological Medicine*, *44*(4), 869–880. https://doi.org/10.1017/S0033291713001037

McDermott, B., Porter, E., Hughes, D., McGinley, B., Lang, M., O'Halloran, M., & Jones, M. (2018). Gamma Band Neural Stimulation in Humans and the Promise of a New Modality to Prevent and Treat Alzheimer's Disease. *Journal of Alzheimer's Disease*, *65*(2), 363–392. https://doi.org/10.3233/JAD-180391

McDonnell, M. D., & Abbott, D. (2009). What Is Stochastic Resonance? Definitions, Misconceptions, Debates, and Its Relevance to Biology. *PLOS Computational Biology*, *5*(5), e1000348. https://doi.org/10.1371/journal.pcbi.1000348

McKiernan, K. A., D'Angelo, B. R., Kaufman, J. N., & Binder, J. R. (2006). Interrupting the "stream of consciousness": An fMRI investigation. *NeuroImage*, *29*(4), 1185–1191. https://doi.org/10.1016/j.neuroimage.2005.09.030

McKiernan, K. A., Kaufman, J. N., Kucera-Thompson, J., & Binder, J. R. (2003). A Parametric Manipulation of Factors Affecting Task-induced Deactivation in Functional Neuroimaging. *Journal of Cognitive Neuroscience*, *15*(3), 394–408. https://doi.org/10.1162/089892903321593117

Meinzer, M., Antonenko, D., Lindenberg, R., Hetzer, S., Ulm, L., Avirame, K., Flaisch, T., & Flöel, A. (2012). Electrical Brain Stimulation Improves Cognitive Performance by Modulating Functional Connectivity and Task-Specific Activation. *Journal of Neuroscience*, *32*(5), 1859–1866. https://doi.org/10.1523/JNEUROSCI.4812-11.2012

Meinzer, M., Lindenberg, R., Antonenko, D., Flaisch, T., & Flöel, A. (2013). Anodal Transcranial Direct Current Stimulation Temporarily Reverses Age-Associated Cognitive Decline and Functional Brain Activity Changes. *Journal of Neuroscience*, *33*(30), 12470–12478. https://doi.org/10.1523/JNEUROSCI.5743-12.2013

Melby-Lervåg, M., & Hulme, C. (2013). Is working memory training effective? A meta-analytic review. *Developmental Psychology*, *49*(2), 270–291. https://doi.org/10.1037/a0028228

Mencarelli, L., Menardi, A., Neri, F., Monti, L., Ruffini, G., Salvador, R., Pascual-Leone, A., Momi, D., Sprugnoli, G., Rossi, A., Rossi, S., & Santarnecchi, E. (2020). Impact of network-targeted multichannel transcranial direct current stimulation on intrinsic and network-to-network functional connectivity. *Journal of Neuroscience Research*, *98*(10), 1843–1856. https://doi.org/10.1002/jnr.24690

Mencarelli, M., Neri, N., Davide, M., Menardi, Simone, R., Alessandro, R., & Emiliano, S. (2019). Stimuli, presentation modality, and load-specific brain activity patterns during n-back task. *Human Brain Mapping*, hbm.24633. https://doi.org/10.1002/hbm.24633

Menon, V., & Uddin, L. Q. (2010). Saliency, switching, attention and control: A network model of insula function. *Brain Structure and Function*, *214*(5), 655–667. https://doi.org/10.1007/s00429-010-0262-0

Milani, S. A., Marsiske, M., Cottler, L. B., Chen, X., & Striley, C. W. (2018). Optimal cutoffs for the Montreal Cognitive Assessment vary by race and ethnicity. *Alzheimer's & Dementia : Diagnosis, Assessment & Disease Monitoring*, *10*, 773–781. https://doi.org/10.1016/j.dadm.2018.09.003

Miller, E. K., & Cohen, J. D. (2001). An integrative theory of prefrontal cortex function. *Annual Review of Neuroscience*, *24*, 167–202. https://doi.org/10.1146/annurev.neuro.24.1.167

Miniussi, C., Cappa, S. F., Cohen, L. G., Floel, A., Fregni, F., Nitsche, M. A., Oliveri, M., Pascual-Leone, A., Paulus, W., Priori, A., & Walsh, V. (2008). Efficacy of repetitive transcranial magnetic stimulation/transcranial direct current stimulation in cognitive neurorehabilitation. *Brain Stimulation*, *1*(4), 326–336. https://doi.org/10.1016/j.brs.2008.07.002

Miniussi, C., Harris, J. A., & Ruzzoli, M. (2013). Modelling non-invasive brain stimulation in cognitive neuroscience. *Neuroscience & Biobehavioral Reviews*, *37*(8), 1702–1712. https://doi.org/10.1016/j.neubiorev.2013.06.014

Miniussi, C., Ruzzoli, M., & Walsh, V. (2010). The mechanism of transcranial magnetic stimulation in cognition. *Cortex*, *46*(1), 128–130. https://doi.org/10.1016/j.cortex.2009.03.004

Minzenberg, M. J., Laird, A. R., Thelen, S., Carter, C. S., & Glahn, D. C. (2009). Meta-analysis of 41 Functional Neuroimaging Studies of Executive Function in Schizophrenia. *Archives of General Psychiatry*, *66*(8), 811. https://doi.org/10.1001/archgenpsychiatry.2009.91

Miranda, Pedro C., Callejón-Leblic, M. A., Salvador, R., & Ruffini, G. (2018). Realistic modeling of transcranial current stimulation: The electric field in the brain. *Current Opinion in Biomedical Engineering*, *8*, 20–27. https://doi.org/10.1016/j.cobme.2018.09.002

Miranda, Pedro Cavaleiro, Faria, P., & Hallett, M. (2009). What does the ratio of injected current to electrode area tell us about current density in the brain during tDCS? *Clinical Neurophysiology*, *120*(6), 1183–1187. https://doi.org/10.1016/j.clinph.2009.03.023

Miranda, Pedro Cavaleiro, Mekonnen, A., Salvador, R., & Ruffini, G. (2013a). The electric field in the cortex during transcranial current stimulation. *NeuroImage*, *70*, 48–58. https://doi.org/10.1016/j.neuroimage.2012.12.034

Miranda, Pedro Cavaleiro, Mekonnen, A., Salvador, R., & Ruffini, G. (2013b). The electric field in the cortex during transcranial current stimulation. *NeuroImage*, *70*, 48–58. https://doi.org/10.1016/j.neuroimage.2012.12.034

Missonnier, P., Deiber, M.-P., Gold, G., Herrmann, F. R., Millet, P., Michon, A., Fazio-Costa, L., Ibañez, V., & Giannakopoulos, P. (2007a). Working memory load-related electroencephalographic parameters can differentiate progressive from stable mild cognitive impairment. *Neuroscience*, *150*(2), 346–356. https://doi.org/10.1016/j.neuroscience.2007.09.009

Missonnier, P., Deiber, M.-P., Gold, G., Herrmann, F. R., Millet, P., Michon, A., Fazio-Costa, L., Ibañez, V., & Giannakopoulos, P. (2007b). Working memory load-related electroencephalographic parameters can differentiate progressive from stable mild cognitive impairment. *Neuroscience*, *150*(2), 346–356. https://doi.org/10.1016/j.neuroscience.2007.09.009

Miyake, A., Friedman, N. P., Emerson, M. J., Witzki, A. H., Howerter, A., & Wager, T. D. (2000a). The Unity and Diversity of Executive Functions and Their Contributions to Complex "Frontal Lobe" Tasks: A Latent Variable Analysis. *Cognitive Psychology*, *41*(1), 49–100. https://doi.org/10.1006/cogp.1999.0734

Miyake, A., Friedman, N. P., Emerson, M. J., Witzki, A. H., Howerter, A., & Wager, T. D. (2000b). The Unity and Diversity of Executive Functions and Their Contributions to Complex "Frontal Lobe" Tasks: A Latent Variable Analysis. *Cognitive Psychology*, *41*(1), 49–100. https://doi.org/10.1006/cogp.1999.0734

Miyauchi, E., Kitajo, K., & Kawasaki, M. (2016). TMS-induced theta phase synchrony reveals a bottom-up network in working memory. *Neuroscience Letters*, *622*, 10–14. https://doi.org/10.1016/j.neulet.2016.04.008

Moliadze, V., Antal, A., & Paulus, W. (2010). Electrode-distance dependent after-effects of transcranial direct and random noise stimulation with extracephalic reference electrodes. *Clinical Neurophysiology*, *121*(12), 2165–2171. https://doi.org/10.1016/j.clinph.2010.04.033

Moliadze, V., Atalay, D., Antal, A., & Paulus, W. (2012). Close to threshold transcranial electrical stimulation preferentially activates inhibitory networks before switching to excitation with higher intensities. *Brain Stimulation*, *5*(4), 505–511. https://doi.org/10.1016/j.brs.2011.11.004

Monks, P. J., Thompson, J. M., Bullmore, E. T., Suckling, J., Brammer, M. J., Williams, S. C., Simmons, A., Giles, N., Lloyd, A. J., Harrison, C. L., Seal, M., Murray, R. M., Ferrier, I. N., Young, A. H., & Curtis, V. A. (2004). A functional MRI study of working memory task in euthymic bipolar disorder: Evidence for task-specific dysfunction. *Bipolar Disorders*, *6*(6), 550–564. https://doi.org/10.1111/j.1399-5618.2004.00147.x

Monti, M. M., Pickard, J. D., & Owen, A. M. (2013). Visual cognition in disorders of consciousness: From V1 to top-down attention. *Human Brain Mapping*, *34*(6), 1245–1253. https://doi.org/10.1002/hbm.21507

Moret, B., Donato, R., Nucci, M., Cona, G., & Campana, G. (2019). Transcranial random noise stimulation (tRNS): A wide range of frequencies is needed for increasing cortical excitability. *Scientific Reports*, *9*(1), 1–8. https://doi.org/10.1038/s41598-019-51553-7

Motter, J. N., Pimontel, M. A., Rindskopf, D., Devanand, D. P., Doraiswamy, P. M., & Sneed, J. R. (2016). Computerized cognitive training and functional recovery in major depressive disorder: A meta-analysis. *Journal of Affective Disorders*, *189*, 184–191. https://doi.org/10.1016/j.jad.2015.09.022

Müller, V. I., Cieslik, E. C., Laird, A. R., Fox, P. T., Radua, J., Mataix-Cols, D., Tench, C. R., Yarkoni, T., Nichols, T. E., Turkeltaub, P. E., Wager, T. D., & Eickhoff, S. B. (2018). Ten simple rules for neuroimaging meta-analysis. *Neuroscience & Biobehavioral Reviews*, *84*, 151–161. https://doi.org/10.1016/j.neubiorev.2017.11.012

Müller, V. I., Cieslik, E. C., Serbanescu, I., Laird, A. R., Fox, P. T., & Eickhoff, S. B. (2017). Altered Brain Activity in Unipolar Depression Revisited: Meta-analyses of Neuroimaging Studies. *JAMA Psychiatry*, *74*(1), 47. https://doi.org/10.1001/jamapsychiatry.2016.2783

Mulquiney, P. G., Hoy, K. E., Daskalakis, Z. J., & Fitzgerald, P. B. (2011). Improving working memory: Exploring the effect of transcranial random noise stimulation and transcranial direct current stimulation on the dorsolateral prefrontal cortex. *Clinical Neurophysiology*, *122*(12), 2384–2389. https://doi.org/10.1016/j.clinph.2011.05.009

Mummery, C. J., Patterson, K., Hodges, J. R., & Price, C. J. (1998). Functional neuroanatomy of the semantic system: Divisible by what? *Journal of Cognitive Neuroscience*, *10*(6), 766–777.

Nakase-Thompson, R., Sherer, M., Yablon, S. A., Nick, T. G., & Trzepacz, P. T. (2004). Acute confusion following traumatic brain injury. *Brain Injury*, *18*(2), 131–142. https://doi.org/10.1080/0269905031000149542

Nakayama, N. (2006). Relationship between regional cerebral metabolism and consciousness disturbance in traumatic diffuse brain injury without large focal lesions: An FDG-PET study with statistical parametric mapping analysis. *Journal of Neurology, Neurosurgery & Psychiatry*, *77*(7), 856–862. https://doi.org/10.1136/jnnp.2005.080523

Naro, A., Corallo, F., De Salvo, S., Marra, A., Di Lorenzo, G., Muscarà, N., Russo, M., Marino, S., De Luca, R., Bramanti, P., & Calabrò, R. S. (2016). Promising Role of Neuromodulation in Predicting the Progression of Mild Cognitive Impairment to Dementia. *Journal of Alzheimer's Disease: JAD*, *53*(4), 1375–1388. https://doi.org/10.3233/JAD-160305

Neri, F., Mencarelli, L., Menardi, A., Giovannelli, F., Rossi, S., Sprugnoli, G., Rossi, A., Pascual-Leone, A., Salvador, R., Ruffini, G., & Santarnecchi, E. (2019a). A Novel tDCS Sham Approach Based on Model-Driven Controlled Shunting. *Brain Stimulation*. https://doi.org/10.1016/j.brs.2019.11.004

Neri, F., Mencarelli, L., Menardi, A., Giovannelli, F., Rossi, S., Sprugnoli, G., Rossi, A., Pascual-Leone, A., Salvador, R., Ruffini, G., & Santarnecchi, E. (2019b). A Novel tDCS Sham Approach Based on Model-Driven Controlled Shunting. *Brain Stimulation*. https://doi.org/10.1016/j.brs.2019.11.004

Neubert, F.-X., Mars, R. B., Sallet, J., & Rushworth, M. F. S. (2015). Connectivity reveals relationship of brain areas for reward-guided learning and decision making in human and monkey frontal cortex. *Proceedings of the National Academy of Sciences of the United States of America*, *112*(20), E2695-2704. https://doi.org/10.1073/pnas.1410767112

Nielsen, J. D., Madsen, K. H., Wang, Z., Liu, Z., Friston, K. J., & Zhou, Y. (2017). Working Memory Modulation of Frontoparietal Network Connectivity in First-Episode Schizophrenia. *Cerebral Cortex*, *27*(7), 3832–3841. https://doi.org/10.1093/cercor/bhx050

Nitsche, M. A., & Paulus, W. (2000a). Excitability changes induced in the human motor cortex by weak transcranial direct current stimulation. *The Journal of Physiology*, *527*(3), 633–639. https://doi.org/10.1111/j.1469-7793.2000.t01-1-00633.x

Nitsche, M. A., & Paulus, W. (2000b). Excitability changes induced in the human motor cortex by weak transcranial direct current stimulation. *The Journal of Physiology*, *527*(3), 633–639. https://doi.org/10.1111/j.1469-7793.2000.t01-1-00633.x

Nitsche, M. A., & Paulus, W. (2001). Sustained excitability elevations induced by transcranial DC motor cortex stimulation in humans. *Neurology*, *57*(10), 1899–1901. https://doi.org/10.1212/WNL.57.10.1899

Nitsche, Michael A., Cohen, L. G., Wassermann, E. M., Priori, A., Lang, N., Antal, A., Paulus, W., Hummel, F., Boggio, P. S., Fregni, F., & Pascual-Leone, A. (2008). Transcranial direct current stimulation: State of the art 2008. *Brain Stimulation*, *1*(3), 206–223. https://doi.org/10.1016/j.brs.2008.06.004

Nitsche, Michael A., Schauenburg, A., Lang, N., Liebetanz, D., Exner, C., Paulus, W., & Tergau, F. (2003a). Facilitation of Implicit Motor Learning by Weak Transcranial Direct Current Stimulation of the Primary Motor Cortex in the Human. *Journal of Cognitive Neuroscience*, *15*(4), 619–626. https://doi.org/10.1162/089892903321662994

Nitsche, Michael A., Schauenburg, A., Lang, N., Liebetanz, D., Exner, C., Paulus, W., & Tergau, F. (2003b). Facilitation of Implicit Motor Learning by Weak Transcranial Direct Current Stimulation of the Primary Motor Cortex in the Human. *Journal of Cognitive Neuroscience*, *15*(4), 619–626. https://doi.org/10.1162/089892903321662994

Nitsche, Michael A., Seeber, A., Frommann, K., Klein, C. C., Rochford, C., Nitsche, M. S., Fricke, K., Liebetanz, D., Lang, N., Antal, A., Paulus, W., & Tergau, F. (2005). Modulating parameters of excitability during and after transcranial direct current stimulation of the human motor cortex. *The Journal of Physiology*, *568*(1), 291–303. https://doi.org/10.1113/jphysiol.2005.092429

Nord, C. L., Popa, T., Smith, E., Hannah, R., Doñamayor, N., Weidacker, K., Bays, P. M., Rothwell, J., & Voon, V. (2019). The effect of frontoparietal paired associative stimulation on decision-making and working memory. *Cortex*, *117*, 266–276. https://doi.org/10.1016/j.cortex.2019.03.015

Norton, L., Hutchison, R. M., Young, G. B., Lee, D. H., Sharpe, M. D., & Mirsattari, S. M. (2012). Disruptions of functional connectivity in the default mode network of comatose patients. *Neurology*, *78*(3), 175–181. https://doi.org/10.1212/WNL.0b013e31823fcd61

Nystrom, L. E., Braver, T. S., Sabb, F. W., Delgado, M. R., Noll, D. C., & Cohen, J. D. (2000). Working memory for letters, shapes, and locations: FMRI evidence against stimulus-based regional organization in human prefrontal cortex. *NeuroImage*, *11*(5 Pt 1), 424–446. https://doi.org/10.1006/nimg.2000.0572

Onton, J., Delorme, A., & Makeig, S. (2005). Frontal midline EEG dynamics during working memory. *NeuroImage*, *27*(2), 341–356. https://doi.org/10.1016/j.neuroimage.2005.04.014

Opitz, A., Fox, M. D., Craddock, R. C., Colcombe, S., & Milham, M. P. (2016). An integrated framework for targeting functional networks via transcranial magnetic stimulation. *NeuroImage*, *127*, 86–96. https://doi.org/10.1016/j.neuroimage.2015.11.040

Ovadia-Caro, S., Nir, Y., Soddu, A., Ramot, M., Hesselmann, G., Vanhaudenhuyse, A., Dinstein, I., Tshibanda, J.-F. L., Boly, M., Harel, M., Laureys, S., & Malach, R. (2012). Reduction in Inter-Hemispheric Connectivity in Disorders of Consciousness. *PLoS ONE*, *7*(5), e37238. https://doi.org/10.1371/journal.pone.0037238

Owen, A. M. (1997). The functional organization of working memory processes within human lateral frontal cortex: The contribution of functional neuroimaging. *The European Journal of Neuroscience*, *9*(7), 1329–1339.

Owen, Adrian M., McMillan, K. M., Laird, A. R., & Bullmore, E. (2005a). N-back working memory paradigm: A meta-analysis of normative functional neuroimaging studies. *Human Brain Mapping*, *25*(1), 46–59. https://doi.org/10.1002/hbm.20131

Owen, Adrian M., McMillan, K. M., Laird, A. R., & Bullmore, E. (2005b). N-back working memory paradigm: A meta-analysis of normative functional neuroimaging studies. *Human Brain Mapping*, *25*(1), 46–59. https://doi.org/10.1002/hbm.20131

Owen, Adrian M., Menon, D. K., Johnsrude, I. S., Bor, D., Scott, S. K., Manly, T., Williams, E. J., Mummery, C., & Pickard, J. D. (2002). Detecting Residual Cognitive Function in Persistent Vegetative State. *Neurocase*, *8*(5), 394–403. https://doi.org/10.1076/neur.8.4.394.16184

Ozdemir, R. A., Tadayon, E., Boucher, P., Momi, D., Karakhanyan, K. A., Fox, M. D., Halko, M. A., Pascual-Leone, A., Shafi, M. M., & Santarnecchi, E. (2020a). Individualized perturbation of the human connectome reveals reproducible biomarkers of network dynamics relevant to cognition. *Proceedings of the National Academy of Sciences*. https://doi.org/10.1073/pnas.1911240117

Ozdemir, R. A., Tadayon, E., Boucher, P., Momi, D., Karakhanyan, K. A., Fox, M. D., Halko, M. A., Pascual-Leone, A., Shafi, M. M., & Santarnecchi, E. (2020b). Individualized perturbation of the human connectome reveals reproducible biomarkers of network dynamics relevant to cognition. *Proceedings of the National Academy of Sciences*. https://doi.org/10.1073/pnas.1911240117

Ozen, S., Sirota, A., Belluscio, M. A., Anastassiou, C. A., Stark, E., Koch, C., & Buzsáki, G. (2010). Transcranial Electric Stimulation Entrains Cortical Neuronal Populations in Rats. *Journal of Neuroscience*, *30*(34), 11476–11485. https://doi.org/10.1523/JNEUROSCI.5252-09.2010

Pahor, A., & Jaušovec, N. (2018). The Effects of Theta and Gamma tACS on Working Memory and Electrophysiology. *Frontiers in Human Neuroscience*, *11*. https://doi.org/10.3389/fnhum.2017.00651

Palm, U., Chalah, M. A., Padberg, F., Al-Ani, T., Abdellaoui, M., Sorel, M., Dimitri, D., Créange, A., Lefaucheur, J.-P., & Ayache, S. S. (2016). Effects of transcranial random noise stimulation (tRNS) on affect, pain and attention in multiple sclerosis. *Restorative Neurology and Neuroscience*, *34*(2), 189–199. https://doi.org/10.3233/RNN-150557

Palm, U., Hasan, A., Keeser, D., Falkai, P., & Padberg, F. (2013). Transcranial random noise stimulation for the treatment of negative symptoms in schizophrenia. *Schizophrenia Research*, *146*(1–3), 372–373. https://doi.org/10.1016/j.schres.2013.03.003

Palop, J. J., & Mucke, L. (2010). Amyloid-beta-induced neuronal dysfunction in Alzheimer's disease: From synapses toward neural networks. *Nature Neuroscience*, *13*(7), 812–818. https://doi.org/10.1038/nn.2583

Palop, J. J., & Mucke, L. (2016a). Network abnormalities and interneuron dysfunction in Alzheimer disease. *Nature Reviews Neuroscience*, *17*(12), 777–792. https://doi.org/10.1038/nrn.2016.141

Palop, J. J., & Mucke, L. (2016b). Network abnormalities and interneuron dysfunction in Alzheimer disease. *Nature Reviews Neuroscience*, *17*(12), 777–792. https://doi.org/10.1038/nrn.2016.141

Palva, S., & Palva, J. M. (2007). New vistas for α-frequency band oscillations. *Trends in Neurosciences*, *30*(4), 150–158. https://doi.org/10.1016/j.tins.2007.02.001

Pasqualotto, A. (2016). Transcranial random noise stimulation benefits arithmetic skills. *Neurobiology of Learning and Memory*, *133*, 7–12. https://doi.org/10.1016/j.nlm.2016.05.004

Paulesu, E., Frith, C. D., & Frackowiak, R. S. (1993). The neural correlates of the verbal component of working memory. *Nature*, *362*(6418), 342–345. https://doi.org/10.1038/362342a0

Paulus, W. (2003). Chapter 26 Transcranial direct current stimulation (tDCS). In W. Paulus, F. Tergau, M. A. Nitsche, J. G. Rothwell, U. Ziemann, & M. Hallett (Eds.), *Supplements to Clinical Neurophysiology* (Vol. 56, pp. 249–254). Elsevier. https://doi.org/10.1016/S1567-424X(09)70229-6

Paulus, Walter. (2011). Transcranial electrical stimulation (tES – tDCS; tRNS, tACS) methods. *Neuropsychological Rehabilitation*, *21*(5), 602–617. https://doi.org/10.1080/09602011.2011.557292

Pellicciari, M. C., Brignani, D., & Miniussi, C. (2013). Excitability modulation of the motor system induced by transcranial direct current stimulation: A multimodal approach. *NeuroImage*, *83*, 569–580. https://doi.org/10.1016/j.neuroimage.2013.06.076

Picard, N., & Strick, P. L. (1996). Motor Areas of the Medial Wall: A Review of Their Location and Functional Activation. *Cerebral Cortex*, *6*(3), 342–353.

Picazio, S., Ponzo, V., & Koch, G. (2016). Cerebellar Control on Prefrontal-Motor Connectivity During Movement Inhibition. *The Cerebellum*, *15*(6), 680–687. https://doi.org/10.1007/s12311-015-0731-3

Pisa, F. E., Biasutti, E., Drigo, D., & Barbone, F. (2014). The Prevalence of Vegetative and Minimally Conscious States: A Systematic Review and Methodological Appraisal. *Journal of Head Trauma Rehabilitation*, *29*(4), E23–E30. https://doi.org/10.1097/HTR.0b013e3182a4469f

Pisoni, A., Mattavelli, G., Papagno, C., Rosanova, M., Casali, A. G., & Romero Lauro, L. J. (2018). Cognitive Enhancement Induced by Anodal tDCS Drives Circuit-Specific Cortical Plasticity. *Cerebral Cortex*, *28*(4), 1132–1140. https://doi.org/10.1093/cercor/bhx021

Polanía, R., Nitsche, M. A., Korman, C., Batsikadze, G., & Paulus, W. (2012). The Importance of Timing in Segregated Theta Phase-Coupling for Cognitive Performance. *Current Biology*, *22*(14), 1314–1318. https://doi.org/10.1016/j.cub.2012.05.021

Polanía, R., Nitsche, M. A., & Paulus, W. (2011). Modulating functional connectivity patterns and topological functional organization of the human brain with transcranial direct current stimulation. *Human Brain Mapping*, *32*(8), 1236–1249. https://doi.org/10.1002/hbm.21104

Polanía, R., Paulus, W., & Nitsche, M. A. (2011). Noninvasively Decoding the Contents of Visual Working Memory in the Human Prefrontal Cortex within High-gamma Oscillatory Patterns. *Journal of Cognitive Neuroscience*, *24*(2), 304–314. https://doi.org/10.1162/jocn_a_00151

Polanía, R., Paulus, W., & Nitsche, M. A. (2012a). Modulating cortico-striatal and thalamo-cortical functional connectivity with transcranial direct current stimulation. *Human Brain Mapping*, *33*(10), 2499–2508. https://doi.org/10.1002/hbm.21380

Polanía, R., Paulus, W., & Nitsche, M. A. (2012b). Reorganizing the Intrinsic Functional Architecture of the Human Primary Motor Cortex during Rest with Non-Invasive Cortical Stimulation. *PLOS ONE*, *7*(1), e30971. https://doi.org/10.1371/journal.pone.0030971

Popescu, T., Krause, B., Terhune, D. B., Twose, O., Page, T., Humphreys, G., & Cohen Kadosh, R. (2016). Transcranial random noise stimulation mitigates increased difficulty in an arithmetic learning task. *Neuropsychologia*, *81*, 255–264. https://doi.org/10.1016/j.neuropsychologia.2015.12.028

Posner, M. I. (1994). Attention: The mechanisms of consciousness. *Proceedings of the National Academy of Sciences of the United States of America*, *91*(16), 7398–7403.

Power, J. D., Cohen, A. L., Nelson, S. M., Wig, G. S., Barnes, K. A., Church, J. A., Vogel, A. C., Laumann, T. O., Miezin, F. M., Schlaggar, B. L., & Petersen, S. E. (2011). Functional Network Organization of the Human Brain. *Neuron*, *72*(4), 665–678. https://doi.org/10.1016/j.neuron.2011.09.006

Power, J. D., Schlaggar, B. L., Lessov-Schlaggar, C. N., & Petersen, S. E. (2013). Evidence for Hubs in Human Functional Brain Networks. *Neuron*, *79*(4), 798–813. https://doi.org/10.1016/j.neuron.2013.07.035

Pozdniakov, I., Gorina, E., & Feurra, M. (2019). Transcranial alternating current stimulation of the primary motor cortex: Intensity effects. *Brain Stimulation: Basic, Translational, and Clinical Research in Neuromodulation*, *12*(2), 492. https://doi.org/10.1016/j.brs.2018.12.610

Prince, M., Comas-Herrera, A., Knapp, M., Guerchet, M., & Karagiannidou, M. (2016, September). *World Alzheimer report 2016: Improving healthcare for people living with dementia: coverage, quality and costs now and in the future* [Monograph]. Alzheimer's Disease International (ADI). http://www.alz.co.uk/

Pu, S., Yamada, T., Yokoyama, K., Matsumura, H., Kobayashi, H., Sasaki, N., Mitani, H., Adachi, A., Kaneko, K., & Nakagome, K. (2011). A multi-channel near-infrared spectroscopy study of prefrontal cortex activation during working memory task in major depressive disorder. *Neuroscience Research*, *70*(1), 91–97. https://doi.org/10.1016/j.neures.2011.01.001

Qianqian Fang, & Boas, D. A. (2009). Tetrahedral mesh generation from volumetric binary and grayscale images. *2009 IEEE International Symposium on Biomedical Imaging: From Nano to Macro*, 1142–1145. https://doi.org/10.1109/ISBI.2009.5193259

Radman, T., Ramos, R. L., Brumberg, J. C., & Bikson, M. (2009). Role of cortical cell type and morphology in subthreshold and suprathreshold uniform electric field stimulation in vitro. *Brain Stimulation*, *2*(4), 215-228.e3. https://doi.org/10.1016/j.brs.2009.03.007

Ragazzoni, A., Cincotta, M., Giovannelli, F., Cruse, D., Young, G. B., Miniussi, C., & Rossi, S. (2017). Clinical neurophysiology of prolonged disorders of consciousness: From diagnostic stimulation to therapeutic

neuromodulation. *Clinical Neurophysiology: Official Journal of the International Federation of Clinical Neurophysiology*, *128*(9), 1629–1646. https://doi.org/10.1016/j.clinph.2017.06.037

Ragland, J. D., Turetsky, B. I., Gur, R. C., Gunning-Dixon, F., Turner, T., Schroeder, L., Chan, R., & Gur, R. E. (2002). Working memory for complex figures: An fMRI comparison of letter and fractal n-back tasks. *Neuropsychology*, *16*(3), 370–379.

Raichle, M. E., MacLeod, A. M., Snyder, A. Z., Powers, W. J., Gusnard, D. A., & Shulman, G. L. (2001a). A default mode of brain function. *Proceedings of the National Academy of Sciences*, *98*(2), 676–682. https://doi.org/10.1073/pnas.98.2.676

Raichle, M. E., MacLeod, A. M., Snyder, A. Z., Powers, W. J., Gusnard, D. A., & Shulman, G. L. (2001b). A default mode of brain function. *Proceedings of the National Academy of Sciences*, *98*(2), 676–682. https://doi.org/10.1073/pnas.98.2.676

Rajji, T. K. (2019). Impaired brain plasticity as a potential therapeutic target for treatment and prevention of dementia. *Expert Opinion on Therapeutic Targets*, *23*(1), 21–28. https://doi.org/10.1080/14728222.2019.1550074

Rand, D., Eng, J. J., Liu-Ambrose, T., & Tawashy, A. E. (2010). Feasibility of a 6-Month Exercise and Recreation Program to Improve Executive Functioning and Memory in Individuals With Chronic Stroke. *Neurorehabilitation and Neural Repair*, *24*(8), 722–729. https://doi.org/10.1177/1545968310368684

Rankin, C. H., Abrams, T., Barry, R. J., Bhatnagar, S., Clayton, D., Colombo, J., Coppola, G., Geyer, M. A., Glanzman, D. L., Marsland, S., McSweeney, F., Wilson, D. A., Wu, C.-F., & Thompson, R. F. (2009). Habituation Revisited: An Updated and Revised Description of the Behavioral Characteristics of Habituation. *Neurobiology of Learning and Memory*, *92*(2), 135–138. https://doi.org/10.1016/j.nlm.2008.09.012

Raposo, A., Moss, H. E., Stamatakis, E. A., & Tyler, L. K. (2006). Repetition suppression and semantic enhancement: An investigation of the neural correlates of priming. *Neuropsychologia*, *44*(12), 2284–2295. https://doi.org/10.1016/j.neuropsychologia.2006.05.017

Ravizza, S. M., Delgado, M. R., Chein, J. M., Becker, J. T., & Fiez, J. A. (2004). Functional dissociations within the inferior parietal cortex in verbal working memory. *NeuroImage*, *22*(2), 562–573. https://doi.org/10.1016/j.neuroimage.2004.01.039

Ray, S., & Maunsell, J. H. R. (2011). Different Origins of Gamma Rhythm and High-Gamma Activity in Macaque Visual Cortex. *PLOS Biology*, *9*(4), e1000610. https://doi.org/10.1371/journal.pbio.1000610

Reis, J., Schambra, H. M., Cohen, L. G., Buch, E. R., Fritsch, B., Zarahn, E., Celnik, P. A., & Krakauer, J. W. (2009). Noninvasive cortical stimulation enhances motor skill acquisition over multiple days through an effect on consolidation. *Proceedings of the National Academy of Sciences*, *106*(5), 1590–1595. https://doi.org/10.1073/pnas.0805413106

Revill, K. P., Haut, M. W., Belagaje, S. R., Nahab, F., Drake, D., & Buetefisch, C. M. (2020). Hebbian-Type Primary Motor Cortex Stimulation: A Potential Treatment of Impaired Hand Function in Chronic Stroke Patients. *Neurorehabilitation and Neural Repair*, *34*(2), 159–171. https://doi.org/10.1177/1545968319899911

Ridding, M. C., & Rothwell, J. C. (2007). Is there a future for therapeutic use of transcranial magnetic stimulation? *Nature Reviews Neuroscience*, *8*(7), 559–567. https://doi.org/10.1038/nrn2169

Robinson, L. J., & Ferrier, I. N. (2006). Evolution of cognitive impairment in bipolar disorder: A systematic review of cross-sectional evidence. *Bipolar Disorders*, *8*(2), 103–116. https://doi.org/10.1111/j.1399-5618.2006.00277.x

Rogasch, N. C., & Fitzgerald, P. B. (2013). Assessing cortical network properties using TMS–EEG. *Human Brain Mapping*, *34*(7), 1652–1669. https://doi.org/10.1002/hbm.22016

Roh, T., Song, K., Cho, H., Shin, D., & Yoo, H. (2014). A Wearable Neuro-Feedback System With EEG-Based Mental Status Monitoring and Transcranial Electrical Stimulation. *IEEE Transactions on Biomedical Circuits and Systems*, *8*(6), 755–764. https://doi.org/10.1109/TBCAS.2014.2384017

Röhner, F., Breitling, C., Rufener, K. S., Heinze, H.-J., Hinrichs, H., Krauel, K., & Sweeney-Reed, C. M. (2018). Modulation of Working Memory Using Transcranial Electrical Stimulation: A Direct Comparison Between TACS and TDCS. *Frontiers in Neuroscience*, *12*. https://doi.org/10.3389/fnins.2018.00761

Romero Lauro, L. J., Rosanova, M., Mattavelli, G., Convento, S., Pisoni, A., Opitz, A., Bolognini, N., & Vallar, G. (2014a). TDCS increases cortical excitability: Direct evidence from TMS–EEG. *Cortex*, *58*, 99–111. https://doi.org/10.1016/j.cortex.2014.05.003

Romero Lauro, L. J., Rosanova, M., Mattavelli, G., Convento, S., Pisoni, A., Opitz, A., Bolognini, N., & Vallar, G. (2014b). TDCS increases cortical excitability: Direct evidence from TMS–EEG. *Cortex*, *58*, 99–111. https://doi.org/10.1016/j.cortex.2014.05.003

Rose, E. J., Simonotto, E., & Ebmeier, K. P. (2006). Limbic over-activity in depression during preserved performance on the n-back task. *NeuroImage*, *29*(1), 203–215. https://doi.org/10.1016/j.neuroimage.2005.07.002

Rossi, S., Antal, A., Bestmann, S., Bikson, M., Brewer, C., Brockmöller, J., Carpenter, L. L., Cincotta, M., Chen, R., Daskalakis, J. D., Di Lazzaro, V., Fox, M. D., George, M. S., Gilbert, D., Kimiskidis, V. K., Koch, G., Ilmoniemi, R. J., Pascal Lefaucheur, J., Leocani, L., … Hallett, M. (2020). Safety and recommendations for TMS use in healthy subjects and patient populations, with updates on training, ethical and regulatory issues: Expert Guidelines. *(2020) (In Press).* https://doi.org/10.1016/j.clinph.2020.10.003

Rossi, Simone, Hallett, M., Rossini, P. M., & Pascual-Leone, A. (2009). Safety, ethical considerations, and application guidelines for the use of transcranial magnetic stimulation in clinical practice and research. *Clinical Neurophysiology*, *120*(12), 2008–2039. https://doi.org/10.1016/j.clinph.2009.08.016

Rossini, D., Lucca, A., Magri, L., Malaguti, A., Smeraldi, E., Colombo, C., & Zanardi, R. (2010). A Symptom-Specific Analysis of the Effect of High-Frequency Left or Low-Frequency Right Transcranial Magnetic Stimulation over the Dorsolateral Prefrontal Cortex in Major Depression. *Neuropsychobiology*, *62*(2), 91–97. https://doi.org/10.1159/000315439

Rossini, P. M., & Rossi, S. (2007). Transcranial magnetic stimulation: Diagnostic, therapeutic, and research potential. *Neurology*, *68*(7), 484–488. https://doi.org/10.1212/01.wnl.0000250268.13789.b2

Rottschy, C., Langner, R., Dogan, I., Reetz, K., Laird, A. R., Schulz, J. B., Fox, P. T., & Eickhoff, S. B. (2012). Modelling neural correlates of working memory: A coordinate-based meta-analysis. *NeuroImage*, *60*(1), 830–846. https://doi.org/10.1016/j.neuroimage.2011.11.050

Roux, F., Wibral, M., Mohr, H. M., Singer, W., & Uhlhaas, P. J. (2012). Gamma-Band Activity in Human Prefrontal Cortex Codes for the Number of Relevant Items Maintained in Working Memory. *Journal of Neuroscience*, *32*(36), 12411–12420. https://doi.org/10.1523/JNEUROSCI.0421-12.2012

Rubia, K., Smith, A. B., Taylor, E., & Brammer, M. (2007). Linear age-correlated functional development of right inferior fronto-striato-cerebellar networks during response inhibition and anterior cingulate during error-related processes. *Human Brain Mapping*, *28*(11), 1163–1177. https://doi.org/10.1002/hbm.20347

Ruffini, G., Wendling, F., Merlet, I., Molaee-Ardekani, B., Mekonnen, A., Salvador, R., Soria-Frisch, A., Grau, C., Dunne, S., & Miranda, P. C. (2013). Transcranial Current Brain Stimulation (tCS): Models and Technologies. *IEEE Transactions on Neural Systems and Rehabilitation Engineering*, *21*(3), 333–345. https://doi.org/10.1109/TNSRE.2012.2200046

Ruffini, Giulio, Fox, M. D., Ripolles, O., Miranda, P. C., & Pascual-Leone, A. (2014a). Optimization of multifocal transcranial current stimulation for weighted cortical pattern targeting from realistic modeling of electric fields. *NeuroImage*, *89*, 216–225. https://doi.org/10.1016/j.neuroimage.2013.12.002

Ruffini, Giulio, Fox, M. D., Ripolles, O., Miranda, P. C., & Pascual-Leone, A. (2014b). Optimization of multifocal transcranial current stimulation for weighted cortical pattern targeting from realistic modeling of electric fields. *NeuroImage*, *89*, 216–225. https://doi.org/10.1016/j.neuroimage.2013.12.002

Ruffini, Giulio, Fox, M. D., Ripolles, O., Miranda, P. C., & Pascual-Leone, A. (2014c). Optimization of multifocal transcranial current stimulation for weighted cortical pattern targeting from realistic modeling of electric fields. *NeuroImage*, *89*, 216–225. https://doi.org/10.1016/j.neuroimage.2013.12.002

Ruffini, Giulio, Wendling, F., Sanchez-Todo, R., & Santarnecchi, E. (2018a). Targeting brain networks with multichannel transcranial current stimulation (tCS). *Current Opinion in Biomedical Engineering*, *8*, 70–77. https://doi.org/10.1016/j.cobme.2018.11.001

Ruffini, Giulio, Wendling, F., Sanchez-Todo, R., & Santarnecchi, E. (2018b). Targeting brain networks with multichannel transcranial current stimulation (tCS). *Current Opinion in Biomedical Engineering*, *8*, 70–77. https://doi.org/10.1016/j.cobme.2018.11.001

Ruffini, Giulio, Wendling, F., Sanchez-Todo, R., & Santarnecchi, E. (in press). Targeting brain networks with multichannel transcranial current stimulation (tCS). *BioMedical Engineering*.

Sackeim, H. A., Prohovnik, I., Moeller, J. R., Brown, R. P., Apter, S., Prudic, J., Devanand, D. P., & Mukherjee, S. (1990). Regional Cerebral Blood Flow in Mood Disorders: I. Comparison of Major Depressives and Normal Controls at Rest. *Archives of General Psychiatry*, *47*(1), 60–70. https://doi.org/10.1001/archpsyc.1990.01810130062009

Sadaghiani, S., Scheeringa, R., Lehongre, K., Morillon, B., Giraud, A.-L., & Kleinschmidt, A. (2010). Intrinsic Connectivity Networks, Alpha Oscillations, and Tonic Alertness: A Simultaneous Electroencephalography/Functional Magnetic Resonance Imaging Study. *Journal of Neuroscience*, *30*(30), 10243–10250. https://doi.org/10.1523/JNEUROSCI.1004-10.2010

Salmon, E., Van der Linden, M., Collette, F., Delfiore, G., Maquet, P., Degueldre, C., Luxen, A., & Franck, G. (1996). Regional brain activity during working memory tasks. *Brain*, *119*(5), 1617–1625. https://doi.org/10.1093/brain/119.5.1617

Sánchez-Kuhn, A., Pérez-Fernández, C., Cánovas, R., Flores, P., & Sánchez-Santed, F. (2017). Transcranial direct current stimulation as a motor neurorehabilitation tool: An empirical review. *BioMedical Engineering OnLine*, *16*(1), 76. https://doi.org/10.1186/s12938-017-0361-8

Sandström, A., Säll, R., Peterson, J., Salami, A., Larsson, A., Olsson, T., & Nyberg, L. (2012). Brain activation patterns in major depressive disorder and work stress-related long-term sick leave among Swedish females. *Stress*, *15*(5), 503–513. https://doi.org/10.3109/10253890.2011.646347

Santarnecchi, E., Biasella, A., Tatti, E., Rossi, A., Prattichizzo, D., & Rossi, S. (2017a). High-gamma oscillations in the motor cortex during visuo-motor coordination: A tACS interferential study. *Brain Research Bulletin*, *131*, 47–54. https://doi.org/10.1016/j.brainresbull.2017.03.006

Santarnecchi, E., Biasella, A., Tatti, E., Rossi, A., Prattichizzo, D., & Rossi, S. (2017b). High-gamma oscillations in the motor cortex during visuo-motor coordination: A tACS interferential study. *Brain Research Bulletin*, *131*, 47–54. https://doi.org/10.1016/j.brainresbull.2017.03.006

Santarnecchi, Emiliano, Brem, A.-K., Levenbaum, E., Thompson, T., Kadosh, R. C., & Pascual-Leone, A. (2015a). Enhancing cognition using transcranial electrical stimulation. *Current Opinion in Behavioral Sciences*, *4*, 171–178. https://doi.org/10.1016/j.cobeha.2015.06.003

Santarnecchi, Emiliano, Brem, A.-K., Levenbaum, E., Thompson, T., Kadosh, R. C., & Pascual-Leone, A. (2015b). Enhancing cognition using transcranial electrical stimulation. *Current Opinion in Behavioral Sciences*, *4*, 171–178. https://doi.org/10.1016/j.cobeha.2015.06.003

Santarnecchi, Emiliano, Emmendorfer, A., & Pascual-Leone, A. (2017a). Dissecting the parieto-frontal correlates of fluid intelligence: A comprehensive ALE meta-analysis study. *Intelligence*, *63*, 9–28. https://doi.org/10.1016/j.intell.2017.04.008

Santarnecchi, Emiliano, Emmendorfer, A., & Pascual-Leone, A. (2017b). Dissecting the parieto-frontal correlates of fluid intelligence: A comprehensive ALE meta-analysis study. *Intelligence*, *63*, 9–28. https://doi.org/10.1016/j.intell.2017.04.008

Santarnecchi, Emiliano, Emmendorfer, A., Tadayon, S., Rossi, S., Rossi, A., & Pascual-Leone, A. (2017c). Network connectivity correlates of variability in fluid intelligence performance. *Intelligence*, *65*, 35–47. https://doi.org/10.1016/j.intell.2017.10.002

Santarnecchi, Emiliano, Emmendorfer, A., Tadayon, S., Rossi, S., Rossi, A., & Pascual-Leone, A. (2017d). Network connectivity correlates of variability in fluid intelligence performance. *Intelligence*, *65*, 35–47. https://doi.org/10.1016/j.intell.2017.10.002

Santarnecchi, Emiliano, Khanna, A. R., Musaeus, C. S., Benwell, C. S. Y., Davila, P., Farzan, F., Matham, S., Pascual-Leone, A., Shafi, M. M., & Authors, on behalf of H. S. T. (2017). EEG Microstate Correlates of Fluid Intelligence and Response to Cognitive Training. *Brain Topography*, *30*(4), 502–520. https://doi.org/10.1007/s10548-017-0565-z

Santarnecchi, Emiliano, Momi, D., Sprugnoli, G., Neri, F., Pascual-Leone, A., Rossi, A., & Rossi, S. (2018a). Modulation of network-to-network connectivity via spike-timing-dependent noninvasive brain stimulation. *Human Brain Mapping*. https://doi.org/10.1002/hbm.24329

Santarnecchi, Emiliano, Momi, D., Sprugnoli, G., Neri, F., Pascual-Leone, A., Rossi, A., & Rossi, S. (2018b). Modulation of network-to-network connectivity via spike-timing-dependent noninvasive brain stimulation. *Human Brain Mapping*, *39*(12), 4870–4883. https://doi.org/10.1002/hbm.24329

Santarnecchi, Emiliano, Sprugnoli, G., Bricolo, E., Costantini, G., Liew, S.-L., Musaeus, C. S., Salvi, C., Pascual-Leone, A., Rossi, A., & Rossi, S. (2019a). Gamma tACS over the temporal lobe increases the occurrence of Eureka! Moments. *Scientific Reports*, *9*(1), 1–12. https://doi.org/10.1038/s41598-019-42192-z

Santarnecchi, Emiliano, Sprugnoli, G., Bricolo, E., Costantini, G., Liew, S.-L., Musaeus, C. S., Salvi, C., Pascual-Leone, A., Rossi, A., & Rossi, S. (2019b). Gamma tACS over the temporal lobe increases the occurrence of Eureka! Moments. *Scientific Reports*, *9*. https://doi.org/10.1038/s41598-019-42192-z

Santarnecchi, Emiliano, Sprugnoli, G., Tatti, E., Mencarelli, L., Neri, F., Momi, D., Di Lorenzo, G., Pascual-Leone, A., Rossi, S., & Rossi, A. (2018). Brain functional connectivity correlates of coping styles. *Cognitive, Affective, & Behavioral Neuroscience*, *18*(3), 495–508. https://doi.org/10.3758/s13415-018-0583-7

Santarnecchi, Polizzotto, N. R., Godone, M., Giovannelli, F., Feurra, M., Matzen, L., Rossi, A., & Rossi, S. (2013). Frequency-Dependent Enhancement of Fluid Intelligence Induced by Transcranial Oscillatory Potentials. *Current Biology*, *23*(15), 1449–1453. https://doi.org/10.1016/j.cub.2013.06.022

Sathappan, A. V., Luber, B. M., & Lisanby, S. H. (2019). The Dynamic Duo: Combining noninvasive brain stimulation with cognitive interventions. *Progress in Neuro-Psychopharmacology and Biological Psychiatry*, *89*, 347–360. https://doi.org/10.1016/j.pnpbp.2018.10.006

Schaefer, A., Kong, R., Gordon, E. M., Laumann, T. O., Zuo, X.-N., Holmes, A. J., Eickhoff, S. B., & Yeo, B. T. T. (2018). Local-Global Parcellation of the Human Cerebral Cortex from Intrinsic Functional Connectivity MRI. *Cerebral Cortex*, *28*(9), 3095–3114. https://doi.org/10.1093/cercor/bhx179

Schiff, N. D., Giacino, J. T., Kalmar, K., Victor, J. D., Baker, K., Gerber, M., Fritz, B., Eisenberg, B., O'Connor, J., Kobylarz, E. J., Farris, S., Machado, A., McCagg, C., Plum, F., Fins, J. J., & Rezai, A. R. (2007). Behavioural improvements with thalamic stimulation after severe traumatic brain injury. *Nature*, *448*(7153), 600–603. https://doi.org/10.1038/nature06041

Schilbach, L., Eickhoff, S. B., Rotarska-Jagiela, A., Fink, G. R., & Vogeley, K. (2008). Minds at rest? Social cognition as the default mode of cognizing and its putative relationship to the "default system" of the brain. *Consciousness and Cognition*, *17*(2), 457–467. https://doi.org/10.1016/j.concog.2008.03.013

Schmahmann, J. D., & Sherman, J. C. (1998). The cerebellar cognitive affective syndrome. *Brain: A Journal of Neurology*, *121 (Pt 4)*, 561–579.

Schulz, K. P., Bédard, A.-C. V., Czarnecki, R., & Fan, J. (2011). Preparatory Activity and Connectivity in Dorsal Anterior Cingulate Cortex for Cognitive Control. *NeuroImage*, *57*(1), 242–250. https://doi.org/10.1016/j.neuroimage.2011.04.023

Schumacher, E. H., Lauber, E., Awh, E., Jonides, J., Smith, E. E., & Koeppe, R. A. (1996). PET evidence for an amodal verbal working memory system. *NeuroImage*, *3*(2), 79–88. https://doi.org/10.1006/nimg.1996.0009

Sehm, B., Kipping, J., Schäfer, A., Villringer, A., & Ragert, P. (2013). A Comparison between Uni- and Bilateral tDCS Effects on Functional Connectivity of the Human Motor Cortex. *Frontiers in Human Neuroscience*, *7*. https://doi.org/10.3389/fnhum.2013.00183

Selvaraj, S., Arnone, D., Job, D., Stanfield, A., Farrow, T. F., Nugent, A. C., Scherk, H., Gruber, O., Chen, X., Sachdev, P. S., Dickstein, D. P., Malhi, G. S., Ha, T. H., Ha, K., Phillips, M. L., & McIntosh, A. M. (2012). Grey matter differences in bipolar disorder: A meta-analysis of voxel-based morphometry studies. *Bipolar Disorders*, *14*(2), 135–145. https://doi.org/10.1111/j.1399-5618.2012.01000.x

Shafi, M. M., Westover, M. B., Fox, M. D., & Pascual-Leone, A. (2012). Exploration and modulation of brain network interactions with noninvasive brain stimulation in combination with neuroimaging. *European Journal of Neuroscience*, *35*(6), 805–825. https://doi.org/10.1111/j.1460-9568.2012.08035.x

Shallice, T., Fletcher, P., Frith, C. D., Grasby, P., Frackowiak, R. S. J., & Dolan, R. J. (1994). Brain regions associated with acquisition and retrieval of verbal episodic memory. *Nature*, *368*(6472), 633–635. https://doi.org/10.1038/368633a0

Shallice, Tim. (1988). *From Neuropsychology to Mental Structure*. Cambridge University Press.

Sheffield, J. M., & Barch, D. M. (2016a). Cognition and resting-state functional connectivity in schizophrenia. *Neuroscience & Biobehavioral Reviews*, *61*, 108–120. https://doi.org/10.1016/j.neubiorev.2015.12.007

Sheffield, J. M., & Barch, D. M. (2016b). Cognition and resting-state functional connectivity in schizophrenia. *Neuroscience & Biobehavioral Reviews*, *61*, 108–120. https://doi.org/10.1016/j.neubiorev.2015.12.007

Sheffield, J. M., Repovs, G., Harms, M. P., Carter, C. S., Gold, J. M., MacDonald III, A. W., Daniel Ragland, J., Silverstein, S. M., Godwin, D., & Barch, D. M. (2015). Fronto-parietal and cingulo-opercular network integrity and cognition in health and schizophrenia. *Neuropsychologia*, *73*, 82–93. https://doi.org/10.1016/j.neuropsychologia.2015.05.006

Sheline, Y. I., Barch, D. M., Price, J. L., Rundle, M. M., Vaishnavi, S. N., Snyder, A. Z., Mintun, M. A., Wang, S., Coalson, R. S., & Raichle, M. E. (2009). The default mode network and self-referential processes in depression. *Proceedings of the National Academy of Sciences*, *106*(6), 1942–1947. https://doi.org/10.1073/pnas.0812686106

Shipstead, Z., Harrison, T. L., & Engle, R. W. (2015). Working memory capacity and the scope and control of attention. *Attention, Perception, & Psychophysics*, *77*(6), 1863–1880. https://doi.org/10.3758/s13414-015-0899-0

Shirer, W. R., Ryali, S., Rykhlevskaia, E., Menon, V., & Greicius, M. D. (2012a). Decoding subject-driven cognitive states with whole-brain connectivity patterns. *Cerebral Cortex (New York, N.Y.: 1991)*, *22*(1), 158–165. https://doi.org/10.1093/cercor/bhr099

Shirer, W. R., Ryali, S., Rykhlevskaia, E., Menon, V., & Greicius, M. D. (2012b). Decoding subject-driven cognitive states with whole-brain connectivity patterns. *Cerebral Cortex (New York, N.Y.: 1991)*, *22*(1), 158–165. https://doi.org/10.1093/cercor/bhr099

Shokri-Kojori, E., Wang, G.-J., Wiers, C. E., Demiral, S. B., Guo, M., Kim, S. W., Lindgren, E., Ramirez, V., Zehra, A., Freeman, C., Miller, G., Manza, P., Srivastava, T., Santi, S. D., Tomasi, D., Benveniste, H., & Volkow, N. D. (2018). β-Amyloid accumulation in the human brain after one night of sleep deprivation. *Proceedings of the National Academy of Sciences*, *115*(17), 4483–4488. https://doi.org/10.1073/pnas.1721694115

Shpektor, A., Nazarova, M., & Feurra, M. (2017). Effects of Transcranial Alternating Current Stimulation on the Primary Motor Cortex by Online Combined Approach with Transcranial Magnetic Stimulation. *JoVE (Journal of Visualized Experiments)*, *127*, e55839. https://doi.org/10.3791/55839

Shulman, G. L., Corbetta, M., Buckner, R. L., Raichle, M. E., Fiez, J. A., Miezin, F. M., & Petersen, S. E. (1997). Top-down modulation of early sensory cortex. *Cerebral Cortex*, *7*(3), 193–206. https://doi.org/10.1093/cercor/7.3.193

Shulman, Gordon L., Ollinger, J. M., Linenweber, M., Petersen, S. E., & Corbetta, M. (2001). Multiple neural correlates of detection in the human brain. *Proceedings of the National Academy of Sciences of the United States of America*, *98*(1), 313–318.

Siebner, H. R., Bergmann, T. O., Bestmann, S., Massimini, M., Johansen-Berg, H., Mochizuki, H., Bohning, D. E., Boorman, E. D., Groppa, S., Miniussi, C., Pascual-Leone, A., Huber, R., Taylor, P. C. J., Ilmoniemi, R. J., De Gennaro, L., Strafella, A. P., Kähkönen, S., Klöppel, S., Frisoni, G. B., … Rossini, P. M. (2009). Consensus paper: Combining transcranial stimulation with neuroimaging. *Brain Stimulation*, *2*(2), 58–80. https://doi.org/10.1016/j.brs.2008.11.002

Siegel, J. S., Ramsey, L. E., Snyder, A. Z., Metcalf, N. V., Chacko, R. V., Weinberger, K., Baldassarre, A., Hacker, C. D., Shulman, G. L., & Corbetta, M. (2016). Disruptions of network connectivity predict impairment in multiple behavioral domains after stroke. *Proceedings of the National Academy of Sciences*, *113*(30), E4367–E4376. https://doi.org/10.1073/pnas.1521083113

Silvanto, J., & Pascual-Leone, A. (2008). State-Dependency of Transcranial Magnetic Stimulation. *Brain Topography*, *21*(1), 1. https://doi.org/10.1007/s10548-008-0067-0

Smith, E. E., & Jonides, J. (1997). Working memory: A view from neuroimaging. *Cognitive Psychology*, *33*(1), 5–42.

Smith, E. E., & Jonides, J. (1999). Storage and Executive Processes in the Frontal Lobes. *Science*, *283*(5408), 1657–1661. https://doi.org/10.1126/science.283.5408.1657

Smith, S. M., Fox, P. T., Miller, K. L., Glahn, D. C., Fox, P. M., Mackay, C. E., Filippini, N., Watkins, K. E., Toro, R., Laird, A. R., & Beckmann, C. F. (2009). Correspondence of the brain's functional architecture during activation and rest. *Proceedings of the National Academy of Sciences*, *106*(31), 13040–13045. https://doi.org/10.1073/pnas.0905267106

Snowball, A., Tachtsidis, I., Popescu, T., Thompson, J., Delazer, M., Zamarian, L., Zhu, T., & Cohen Kadosh, R. (2013). Long-Term Enhancement of Brain Function and Cognition Using Cognitive Training and Brain Stimulation. *Current Biology*, *23*(11), 987–992. https://doi.org/10.1016/j.cub.2013.04.045

Soddu, A., Gómez, F., Heine, L., Di Perri, C., Bahri, M. A., Voss, H. U., Bruno, M.-A., Vanhaudenhuyse, A., Phillips, C., Demertzi, A., Chatelle, C., Schrouff, J., Thibaut, A., Charland-Verville, V., Noirhomme, Q., Salmon, E., Tshibanda, J.-F. L., Schiff, N. D., & Laureys, S. (2016). Correlation between resting state fMRI total neuronal activity and PET metabolism in healthy controls and patients with disorders of consciousness. *Brain and Behavior*, *6*(1), n/a-n/a. https://doi.org/10.1002/brb3.424

Sohal, V. S., Zhang, F., Yizhar, O., & Deisseroth, K. (2009). Parvalbumin neurons and gamma rhythms enhance cortical circuit performance. *Nature*, *459*(7247), 698–702. https://doi.org/10.1038/nature07991

Sohn, M.-H., Ursu, S., Anderson, J. R., Stenger, V. A., & Carter, C. S. (2000). The role of prefrontal cortex and posterior parietal cortex in task switching. *Proceedings of the National Academy of Sciences*, *97*(24), 13448–13453. https://doi.org/10.1073/pnas.240460497

Sporns, O. (2011, April). *The human connectome: A complex network*. Annals of the New York Academy of Sciences; Ann N Y Acad Sci. https://doi.org/10.1111/j.1749-6632.2010.05888.x

Spreng, R. Nathan, & Schacter, D. L. (2012). Default Network Modulation and Large-Scale Network Interactivity in Healthy Young and Old Adults. *Cerebral Cortex (New York, NY)*, *22*(11), 2610–2621. https://doi.org/10.1093/cercor/bhr339

Spreng, R. Nathan, Sepulcre, J., Turner, G. R., Stevens, W. D., & Schacter, D. L. (2012). Intrinsic Architecture Underlying the Relations among the Default, Dorsal Attention, and Frontoparietal Control Networks of the Human Brain. *Journal of Cognitive Neuroscience*, *25*(1), 74–86. https://doi.org/10.1162/jocn_a_00281

Spreng, R. Nathan, Stevens, W. D., Viviano, J. D., & Schacter, D. L. (2016). Attenuated anticorrelation between the default and dorsal attention networks with aging: Evidence from task and rest. *Neurobiology of Aging*, *45*, 149–160. https://doi.org/10.1016/j.neurobiolaging.2016.05.020

Spreng, R.N., Stevens, W. D., Viviano, J. D., & Schacter, D. L. (2016). Attenuated anticorrelation between the default and dorsal attention networks with aging: Evidence from task and rest. *Neurobiol. Aging*, *45*(1558-1497 (Electronic)), 149–160. https://doi.org/10.1016/j.neurobiolaging.2016.05.020

Sprugnoli, G., Monti, L., Lippa, L., Neri, F., Mencarelli, L., Ruffini, G., Salvador, R., Oliveri, G., Batani, B., Momi, D., Cerase, A., Pascual-Leone, A., Rossi, A., Rossi, S., & Santarnecchi, E. (2019a). Reduction of intratumoral brain perfusion by noninvasive transcranial electrical stimulation. *Science Advances*, *5*(8), eaau9309. https://doi.org/10.1126/sciadv.aau9309

Sprugnoli, G., Monti, L., Lippa, L., Neri, F., Mencarelli, L., Ruffini, G., Salvador, R., Oliveri, G., Batani, B., Momi, D., Cerase, A., Pascual-Leone, A., Rossi, A., Rossi, S., & Santarnecchi, E. (2019b). Reduction of intratumoral brain perfusion by noninvasive transcranial electrical stimulation. *Science Advances*, *5*(8), eaau9309. https://doi.org/10.1126/sciadv.aau9309

Stagg, C. J., Jayaram, G., Pastor, D., Kincses, Z. T., Matthews, P. M., & Johansen-Berg, H. (2011). Polarity and timing-dependent effects of transcranial direct current stimulation in explicit motor learning. *Neuropsychologia*, *49*(5), 800–804. https://doi.org/10.1016/j.neuropsychologia.2011.02.009

Stagg, Charlotte J., Lin, R. L., Mezue, M., Segerdahl, A., Kong, Y., Xie, J., & Tracey, I. (2013). Widespread Modulation of Cerebral Perfusion Induced during and after Transcranial Direct Current Stimulation Applied to the Left Dorsolateral Prefrontal Cortex. *Journal of Neuroscience*, *33*(28), 11425–11431. https://doi.org/10.1523/JNEUROSCI.3887-12.2013

Stephani, C., Nitsche, M. A., Sommer, M., & Paulus, W. (2011). Impairment of motor cortex plasticity in Parkinson's disease, as revealed by theta-burst-transcranial magnetic stimulation and transcranial random noise stimulation. *Parkinsonism & Related Disorders*, *17*(4), 297–298. https://doi.org/10.1016/j.parkreldis.2011.01.006

Stomrud, E., Hansson, O., Minthon, L., Blennow, K., Rosén, I., & Londos, E. (2010). Slowing of EEG correlates with CSF biomarkers and reduced cognitive speed in elderly with normal cognition over 4 years. *Neurobiology of Aging*, *31*(2), 215–223. https://doi.org/10.1016/j.neurobiolaging.2008.03.025

Stoodley, C. J., & Schmahmann, J. D. (2009). Functional topography in the human cerebellum: A meta-analysis of neuroimaging studies. *NeuroImage*, *44*(2), 489–501. https://doi.org/10.1016/j.neuroimage.2008.08.039

Suppa, A., Huang, Y.-Z., Funke, K., Ridding, M. C., Cheeran, B., Di Lazzaro, V., Ziemann, U., & Rothwell, J. C. (2016). Ten Years of Theta Burst Stimulation in Humans: Established Knowledge, Unknowns and Prospects. *Brain Stimulation*, *9*(3), 323–335. https://doi.org/10.1016/j.brs.2016.01.006

Tagliazucchi, E., von Wegner, F., Morzelewski, A., Brodbeck, V., & Laufs, H. (2012). Dynamic BOLD functional connectivity in humans and its electrophysiological correlates. *Frontiers in Human Neuroscience*, *6*. https://doi.org/10.3389/fnhum.2012.00339

Tan, H.-R. M., Gross, J., & Uhlhaas, P. J. (2016). MEG sensor and source measures of visually induced gamma-band oscillations are highly reliable. *NeuroImage*, *137*, 34–44. https://doi.org/10.1016/j.neuroimage.2016.05.006

Tatti, E., Rossi, S., Innocenti, I., Rossi, A., & Santarnecchi, E. (2016a). Non-invasive brain stimulation of the aging brain: State of the art and future perspectives. *Ageing Research Reviews*, *29*, 66–89. https://doi.org/10.1016/j.arr.2016.05.006

Tatti, E., Rossi, S., Innocenti, I., Rossi, A., & Santarnecchi, E. (2016b). Non-invasive brain stimulation of the aging brain: State of the art and future perspectives. *Ageing Research Reviews*, *29*, 66–89. https://doi.org/10.1016/j.arr.2016.05.006

Tavakoli, A. V., & Yun, K. (2017). Transcranial Alternating Current Stimulation (tACS) Mechanisms and Protocols. *Frontiers in Cellular Neuroscience*, *11*. https://doi.org/10.3389/fncel.2017.00214

Tecchio, F., Cancelli, A., Cottone, C., Tomasevic, L., Devigus, B., Zito, G., Ercolani, M., & Carducci, F. (2013). Regional Personalized Electrodes to Select Transcranial Current Stimulation Target. *Frontiers in Human Neuroscience*, *7*. https://doi.org/10.3389/fnhum.2013.00131

Terney, D., Chaieb, L., Moliadze, V., Antal, A., & Paulus, W. (2008). Increasing Human Brain Excitability by Transcranial High-Frequency Random Noise Stimulation. *Journal of Neuroscience*, *28*(52), 14147–14155. https://doi.org/10.1523/JNEUROSCI.4248-08.2008

Thermenos, H. W., Goldstein, J. M., Milanovic, S. M., Whitfield-Gabrieli, S., Makris, N., LaViolette, P., Koch, J. K., Faraone, S. V., Tsuang, M. T., Buka, S. L., & Seidman, L. J. (2010). An fMRI study of working memory in persons with bipolar disorder or at genetic risk for bipolar disorder. *American Journal of Medical Genetics Part B: Neuropsychiatric Genetics*, *153B*(1), 120–131. https://doi.org/10.1002/ajmg.b.30964

Thibaut, A, Bruno, M., Chatelle, C., Gosseries, O., Vanhaudenhuyse, A., Demertzi, A., Schnakers, C., Thonnard, M., Charland-Verville, V., Bernard, C., Bahri, M., Phillips, C., Boly, M., Hustinx, R., & Laureys, S. (2012). Metabolic activity in external and internal awareness networks in severely brain-damaged patients. *Journal of Rehabilitation Medicine*, *44*(6), 487–494. https://doi.org/10.2340/16501977-0940

Thibaut, A., Bruno, M.-A., Ledoux, D., Demertzi, A., & Laureys, S. (2014). tDCS in patients with disorders of consciousness: Sham-controlled randomized double-blind study. *Neurology*, *82*(13), 1112–1118. https://doi.org/10.1212/WNL.0000000000000260

Thibaut, Aurore, Russo, C., Hurtado-Puerto, A. M., Morales-Quezada, J. L., Deitos, A., Petrozza, J. C., Freedman, S., & Fregni, F. (2017a). Effects of Transcranial Direct Current Stimulation, Transcranial Pulsed Current Stimulation, and Their Combination on Brain Oscillations in Patients with Chronic Visceral Pain: A Pilot Crossover Randomized Controlled Study. *Frontiers in Neurology*, *8*. https://doi.org/10.3389/fneur.2017.00576

Thibaut, Aurore, Russo, C., Hurtado-Puerto, A. M., Morales-Quezada, J. L., Deitos, A., Petrozza, J. C., Freedman, S., & Fregni, F. (2017b). Effects of Transcranial Direct Current Stimulation, Transcranial Pulsed Current Stimulation, and Their Combination on Brain Oscillations in Patients with Chronic Visceral Pain: A Pilot Crossover Randomized Controlled Study. *Frontiers in Neurology*, *8*. https://doi.org/10.3389/fneur.2017.00576

Thibaut, Aurore, Schiff, N., Giacino, J., Laureys, S., & Gosseries, O. (2019). Therapeutic interventions in patients with prolonged disorders of consciousness. *The Lancet Neurology*, *18*(6), 600–614. https://doi.org/10.1016/S1474-4422(19)30031-6

Thickbroom, G. W. (2007). Transcranial magnetic stimulation and synaptic plasticity: Experimental framework and human models. *Experimental Brain Research*, *180*(4), 583–593. https://doi.org/10.1007/s00221-007-0991-3

Thompson, J. M., Gray, J. M., Hughes, J. H., Watson, S., Young, A. H., & Ferrier, I. N. (2007). Impaired working memory monitoring in euthymic bipolar patients. *Bipolar Disorders*, *9*(5), 478–489. https://doi.org/10.1111/j.1399-5618.2007.00470.x

Thut, G., & Miniussi, C. (2009). New insights into rhythmic brain activity from TMS–EEG studies. *Trends in Cognitive Sciences*, *13*(4), 182–189. https://doi.org/10.1016/j.tics.2009.01.004

Thut, G., & Pascual-Leone, A. (2009). A Review of Combined TMS-EEG Studies to Characterize Lasting Effects of Repetitive TMS and Assess Their Usefulness in Cognitive and Clinical Neuroscience. *Brain Topography*, *22*(4), 219. https://doi.org/10.1007/s10548-009-0115-4

Thut, G., Schyns, P., & Gross, J. (2011). Entrainment of Perceptually Relevant Brain Oscillations by Non-Invasive Rhythmic Stimulation of the Human Brain. *Frontiers in Psychology*, *2*. https://doi.org/10.3389/fpsyg.2011.00170

Töpper, R., Mottaghy, F. M., Brügmann, M., Noth, J., & Huber, W. (1998). Facilitation of picture naming by focal transcranial magnetic stimulation of Wernicke's area. *Experimental Brain Research*, *121*(4), 371–378. https://doi.org/10.1007/s002210050471

Tremblay, S., Rogasch, N. C., Premoli, I., Blumberger, D. M., Casarotto, S., Chen, R., Di Lazzaro, V., Farzan, F., Ferrarelli, F., Fitzgerald, P. B., Hui, J., Ilmoniemi, R. J., Kimiskidis, V. K., Kugiumtzis, D., Lioumis, P., Pascual-Leone, A.,

Pellicciari, M. C., Rajji, T., Thut, G., … Daskalakis, Z. J. (2019). Clinical utility and prospective of TMS–EEG. *Clinical Neurophysiology*, *130*(5), 802–844. https://doi.org/10.1016/j.clinph.2019.01.001

Tsai, Y.-H., Yuan, R., Huang, Y.-C., Yeh, M.-Y., Lin, C.-P., & Biswal, B. B. (2014). Disruption of brain connectivity in acute stroke patients with early impairment in consciousness. *Frontiers in Psychology*, *4*. https://doi.org/10.3389/fpsyg.2013.00956

Turkeltaub, P. E., Eden, G. F., Jones, K. M., & Zeffiro, T. A. (2002). Meta-analysis of the functional neuroanatomy of single-word reading: Method and validation. *NeuroImage*, *16*(3 Pt 1), 765–780.

Turkeltaub, P. E., Eickhoff, S. B., Laird, A. R., Fox, M., Wiener, M., & Fox, P. (2012). Minimizing within-experiment and within-group effects in Activation Likelihood Estimation meta-analyses. *Human Brain Mapping*, *33*(1), 1–13. https://doi.org/10.1002/hbm.21186

Uddin, L. Q. (2015). Salience processing and insular cortical function and dysfunction. *Nature Reviews Neuroscience*, *16*(1), 55–61. https://doi.org/10.1038/nrn3857

Uy, J., Ridding, M. C., Hillier, S., Thompson, P. D., & Miles, T. S. (2003). Does induction of plastic change in motor cortex improve leg function after stroke? *Neurology*, *61*(7), 982–984.

V. Di Lazzaro, Pilato, F., Dileone, M., Profice, P., Oliviero, A., Mazzone, P., Insola, A., Ranieri, F., Meglio, M., Tonali, P. A., & Rothwell, J. C. (2008). The physiological basis of the effects of intermittent theta burst stimulation of the human motor cortex. *The Journal of Physiology*, *586*(16), 3871–3879. https://doi.org/10.1113/jphysiol.2008.152736

Valderrama, M., Crépon, B., Botella-Soler, V., Martinerie, J., Hasboun, D., Alvarado-Rojas, C., Baulac, M., Adam, C., Navarro, V., & Quyen, M. L. V. (2012). Human Gamma Oscillations during Slow Wave Sleep. *PLOS ONE*, *7*(4), e33477. https://doi.org/10.1371/journal.pone.0033477

Valera, E. M., Faraone, S. V., Biederman, J., Poldrack, R. A., & Seidman, L. J. (2005). Functional neuroanatomy of working memory in adults with attention-deficit/hyperactivity disorder. *Biological Psychiatry*, *57*(5), 439–447. https://doi.org/10.1016/j.biopsych.2004.11.034

Valero-Cabré, A., Amengual, J. L., Stengel, C., Pascual-Leone, A., & Coubard, O. A. (2017). Transcranial magnetic stimulation in basic and clinical neuroscience: A comprehensive review of fundamental principles and novel insights. *Neuroscience & Biobehavioral Reviews*, *83*, 381–404. https://doi.org/10.1016/j.neubiorev.2017.10.006

van Asseldonk, E. H. F., & Boonstra, T. A. (2016). Transcranial Direct Current Stimulation of the Leg Motor Cortex Enhances Coordinated Motor Output During Walking With a Large Inter-Individual Variability. *Brain Stimulation*, *9*(2), 182–190. https://doi.org/10.1016/j.brs.2015.10.001

Vanhaudenhuyse, A., Demertzi, A., Schabus, M., Noirhomme, Q., Bredart, S., Boly, M., Phillips, C., Soddu, A., Luxen, A., Moonen, G., & Laureys, S. (2011). Two distinct neuronal networks mediate the awareness of environment and of self. *Journal of Cognitive Neuroscience*, *23*(3), 570–578. https://doi.org/10.1162/jocn.2010.21488

Vanhaudenhuyse, A., Noirhomme, Q., Tshibanda, L. J.-F., Bruno, M.-A., Boveroux, P., Schnakers, C., Soddu, A., Perlbarg, V., Ledoux, D., Brichant, J.-F., Moonen, G., Maquet, P., Greicius, M. D., Laureys, S., & Boly, M. (2010). Default network connectivity reflects the level of consciousness in non-communicative brain-damaged patients. *Brain*, *133*(1), 161–171. https://doi.org/10.1093/brain/awp313

Varoli, E., Pisoni, A., Mattavelli, G. C., Vergallito, A., Gallucci, A., Mauro, L. D., Rosanova, M., Bolognini, N., Vallar, G., & Romero Lauro, L. J. (2018). Tracking the Effect of Cathodal Transcranial Direct Current Stimulation on Cortical Excitability and Connectivity by Means of TMS-EEG. *Frontiers in Neuroscience*, *12*, 319. https://doi.org/10.3389/fnins.2018.00319

Vasic, N., Walter, H., Sambataro, F., & Wolf, R. C. (2009). Aberrant functional connectivity of dorsolateral prefrontal and cingulate networks in patients with major depression during working memory processing. *Psychological Medicine*, *39*(6), 977–987. https://doi.org/10.1017/S0033291708004443

Veniero, D., Ponzo, V., & Koch, G. (2013). Paired Associative Stimulation Enforces the Communication between Interconnected Areas. *Journal of Neuroscience*, *33*(34), 13773–13783. https://doi.org/10.1523/JNEUROSCI.1777-13.2013

Vines, B. W., Nair, D. G., & Schlaug, G. (2006). Contralateral and ipsilateral motor effects after transcranial direct current stimulation. *Neuroreport*, *17*(6), 671–674.

Violante, I. R., Li, L. M., Carmichael, D. W., Lorenz, R., Leech, R., Hampshire, A., Rothwell, J. C., & Sharp, D. J. (2017, March 14). *Externally induced frontoparietal synchronization modulates network dynamics and enhances working memory performance*. ELife; eLife Sciences Publications Limited. https://doi.org/10.7554/eLife.22001

Vugt, B. van, Dagnino, B., Vartak, D., Safaai, H., Panzeri, S., Dehaene, S., & Roelfsema, P. R. (2018). The threshold for conscious report: Signal loss and response bias in visual and frontal cortex. *Science*, *360*(6388), 537–542. https://doi.org/10.1126/science.aar7186

Wach, C., Krause, V., Moliadze, V., Paulus, W., Schnitzler, A., & Pollok, B. (2013). Effects of 10Hz and 20Hz transcranial alternating current stimulation (tACS) on motor functions and motor cortical excitability. *Behavioural Brain Research*, *241*, 1–6. https://doi.org/10.1016/j.bbr.2012.11.038

Wager, T. D., & Smith, E. E. (2003). Neuroimaging studies of working memory: A meta-analysis. *Cognitive, Affective & Behavioral Neuroscience*, *3*(4), 255–274.

Wagner, T., Fregni, F., Fecteau, S., Grodzinsky, A., Zahn, M., & Pascual-Leone, A. (2007). Transcranial direct current stimulation: A computer-based human model study. *NeuroImage*, *35*(3), 1113–1124. https://doi.org/10.1016/j.neuroimage.2007.01.027

Walter, H., Vasic, N., Höse, A., Spitzer, M., & Wolf, R. C. (2007). Working memory dysfunction in schizophrenia compared to healthy controls and patients with depression: Evidence from event-related fMRI. *NeuroImage*, *35*(4), 1551–1561. https://doi.org/10.1016/j.neuroimage.2007.01.041

Walton, M. E., Devlin, J. T., & Rushworth, M. F. S. (2004). Interactions between decision making and performance monitoring within prefrontal cortex. *Nature Neuroscience*, *7*(11), 1259–1265. https://doi.org/10.1038/nn1339

Wang, X.-L., Du, M.-Y., Chen, T.-L., Chen, Z.-Q., Huang, X.-Q., Luo, Y., Zhao, Y.-J., Kumar, P., & Gong, Q.-Y. (2015). Neural correlates during working memory processing in major depressive disorder. *Progress in Neuro-Psychopharmacology and Biological Psychiatry*, *56*, 101–108. https://doi.org/10.1016/j.pnpbp.2014.08.011

Weinberger, D. R., Berman, K. F., & Zec, R. F. (1986). Physiologic Dysfunction of Dorsolateral Prefrontal Cortex in Schizophrenia: I. Regional Cerebral Blood Flow Evidence. *Archives of General Psychiatry*, *43*(2), 114–124. https://doi.org/10.1001/archpsyc.1986.01800020020004

Whitfield-Gabrieli, S., & Nieto-Castanon, A. (2012). Conn: A functional connectivity toolbox for correlated and anticorrelated brain networks. *Brain Connect*, *2*(3), 125–141. https://doi.org/10.1089/brain.2012.0073

Whittington, M. A., Traub, R. D., Kopell, N., Ermentrout, B., & Buhl, E. H. (2000). Inhibition-based rhythms: Experimental and mathematical observations on network dynamics. *International Journal of Psychophysiology*, *38*(3), 315–336. https://doi.org/10.1016/S0167-8760(00)00173-2

Williams, D. L., Goldstein, G., Carpenter, P. A., & Minshew, N. J. (2005). Verbal and Spatial Working Memory in Autism. *Journal of Autism and Developmental Disorders*, *35*(6), 747. https://doi.org/10.1007/s10803-005-0021-x

Winker, C., Rehbein, M. A., Sabatinelli, D., & Junghofer, M. (2020). Repeated noninvasive stimulation of the ventromedial prefrontal cortex reveals cumulative amplification of pleasant compared to unpleasant scene processing: A single subject pilot study. *PloS One*, *15*(1), e0222057. https://doi.org/10.1371/journal.pone.0222057

Wise, T., Radua, J., Nortje, G., Cleare, A. J., Young, A. H., & Arnone, D. (2016). Voxel-Based Meta-Analytical Evidence of Structural Disconnectivity in Major Depression and Bipolar Disorder. *Biological Psychiatry*, *79*(4), 293–302. https://doi.org/10.1016/j.biopsych.2015.03.004

Witkowski, M., Garcia-Cossio, E., Chander, B. S., Braun, C., Birbaumer, N., Robinson, S. E., & Soekadar, S. R. (2016). Mapping entrained brain oscillations during transcranial alternating current stimulation (tACS). *NeuroImage*, *140*, 89–98. https://doi.org/10.1016/j.neuroimage.2015.10.024

Yamamoto, J., Suh, J., Takeuchi, D., & Tonegawa, S. (2014). Successful Execution of Working Memory Linked to Synchronized High-Frequency Gamma Oscillations. *Cell*, *157*(4), 845–857. https://doi.org/10.1016/j.cell.2014.04.009

Yaple, Z. A., Stevens, W. D., & Arsalidou, M. (2019). Meta-analyses of the n-back working memory task: FMRI evidence of age-related changes in prefrontal cortex involvement across the adult lifespan. *NeuroImage*, *196*, 16–31. https://doi.org/10.1016/j.neuroimage.2019.03.074

Yeo, B. T. T., Krienen, F. M., Sepulcre, J., Sabuncu, M. R., Lashkari, D., Hollinshead, M., Roffman, J. L., Smoller, J. W., Zöllei, L., Polimeni, J. R., Fischl, B., Liu, H., & Buckner, R. L. (2011a). The organization of the human cerebral

cortex estimated by intrinsic functional connectivity. *Journal of Neurophysiology*, *106*(3), 1125–1165. https://doi.org/10.1152/jn.00338.2011

Yeo, B. T. T., Krienen, F. M., Sepulcre, J., Sabuncu, M. R., Lashkari, D., Hollinshead, M., Roffman, J. L., Smoller, J. W., Zöllei, L., Polimeni, J. R., Fischl, B., Liu, H., & Buckner, R. L. (2011b). The organization of the human cerebral cortex estimated by intrinsic functional connectivity. *Journal of Neurophysiology*, *106*(3), 1125–1165. https://doi.org/10.1152/jn.00338.2011

Zaehle, T., Rach, S., & Herrmann, C. S. (2010). Transcranial Alternating Current Stimulation Enhances Individual Alpha Activity in Human EEG. *PLOS ONE*, *5*(11), e13766. https://doi.org/10.1371/journal.pone.0013766

Zeman, A. (2001). Consciousness. *Brain*, *124*(7), 1263–1289. https://doi.org/10.1093/brain/124.7.1263

Zhang, H., Wei, X., Tao, H., Mwansisya, T. E., Pu, W., He, Z., Hu, A., Xu, L., Liu, Z., Shan, B., & Xue, Z. (2013). Opposite Effective Connectivity in the Posterior Cingulate and Medial Prefrontal Cortex between First-Episode Schizophrenic Patients with Suicide Risk and Healthy Controls. *PLOS ONE*, *8*(5), e63477. https://doi.org/10.1371/journal.pone.0063477

Zheng, X., Alsop, D. C., & Schlaug, G. (2011a). Effects of transcranial direct current stimulation (tDCS) on human regional cerebral blood flow. *NeuroImage*, *58*(1), 26–33. https://doi.org/10.1016/j.neuroimage.2011.06.018

Zheng, X., Alsop, D. C., & Schlaug, G. (2011b). Effects of transcranial direct current stimulation (tDCS) on human regional cerebral blood flow. *NeuroImage*, *58*(1), 26–33. https://doi.org/10.1016/j.neuroimage.2011.06.018

Zhou, J., Greicius, M. D., Gennatas, E. D., Growdon, M. E., Jang, J. Y., Rabinovici, G. D., Kramer, J. H., Weiner, M., Miller, B. L., & Seeley, W. W. (2010). Divergent network connectivity changes in behavioural variant frontotemporal dementia and Alzheimer's disease. *Brain*, *133*(Pt 5), 1352–1367. https://doi.org/10.1093/brain/awq075

Zimerman, M., Nitsch, M., Giraux, P., Gerloff, C., Cohen, L. G., & Hummel, F. C. (2013). Neuroenhancement of the Aging Brain: Restoring Skill Acquisition in Old Subjects. *Annals of Neurology*, *73*(1), 10–15. https://doi.org/10.1002/ana.23761

Zuo, X.-N., Kelly, C., Adelstein, J. S., Klein, D. F., Castellanos, F. X., & Milham, M. P. (2010). Reliable intrinsic connectivity networks: Test–retest evaluation using ICA and dual regression approach. *NeuroImage*, *49*(3), 2163–2177. https://doi.org/10.1016/j.neuroimage.2009.10.080

Ringraziamenti

La fine di questo viaggio arriva in un momento molto particolare della mia vita, e per questo ringraziare le persone che ho incontrato nel mio cammino è ancora più doveroso.

Primo fra tutti vorrei dire grazie al prof. Rossi, che con la sua allegria e schiettezza ha reso questo percorso di dottorato, che per molti è un percorso tortuoso, una bellissima opportunità di crescita. Nel suo laboratorio ho avuto la possibilità di mettere in pratica molte cose che avevo conosciuto solo sui libri, e molto di più. Ho imparato l'umiltà e la pazienza, due virtù che purtroppo spesso sono accantonate nel mondo scientifico, ma che se presenti ti permettono di essere uno scienziato migliore. Grazie prof! La aspetto per un giro in bici tra le colline Umbre.

In seconda battuta devo ringraziare Emiliano, che mi ha offerto l'opportunità più incredibile della mia vita, spingendomi a fare sempre di più e mi ha insegnato che spesso, al di là di quella che viene chiamata 'comfort zone' c'è un mondo che non bisogna aver paura di scoprire. Grazie anche per le conoscenze che mi hai donato, per le chiacchiere che mi hanno insegnato a pensare come uno scienziato, per avermi resa scientificamente critica e curiosa.

Ringrazio tutti i colleghi che ho incontrato lungo la via, che hanno reso questi tre anni davvero divertenti, oltre che scientificamente stimolanti. A Francesco un ringraziamento in particolare, per avermi 'coccolata' e protetta come una sorella minore, per aver reso leggeri anche i momenti più pesanti, per avermi spronato a non mollare mai! Sei e sarai un meraviglioso ricercatore!

Ai miei genitori che mi hanno sempre supportata e a Giulia a cui è toccato invece l'arduo compito di sopportarmi, voglio dire Grazie per aver assecondato tutti i miei sproloqui sulle Neuroscienze durante le cene familiari, senza probabilmente capirci niente. Sappiate che ho apprezzato ogni silenzio e accenno di comprensione, e so che siete fieri di me anche se non sapete spiegare ai parenti cosa faccio nella vita. Grazie, soprattutto, per avermi resa libera!

Un grazie speciale va alle mie sorelle acquisite, tutte le mie amiche senza le quali non potrei immaginarmi una vita. Amo stare da sola, ma con voi è sempre meglio! Grazie per avermi resa partecipe della vostra vita sempre, nonostante la lontananza fisica. Non c'è posto migliore del cuore per accogliere le persone che ami, questo mi permetterà di avervi sempre con me, ovunque andrò.

Grazie a chi ha camminato al mio fianco per molto tempo e mi ha resa quella che sono, regalandomi momenti indimenticabili.

E infine grazie soprattutto alla mia perseveranza, alla mia testardaggine, alla mia dedizione e passione, senza le quali non avrei mai raggiunto questo meraviglioso traguardo.

The best is yet to come.